FROM MOUSE TO HUMAN:

METABOLIC TARGETING OF CANCER WITH TEG-BASED IMMUNOTHERAPY

Inez Johanna Gan

From mouse to human: Metabolic targeting of cancer
with TEG-based immunotherapy

Inez Johanna Gan

From mouse to human: Metabolic targeting of cancer with TEG-based immunotherapy
Thesis with a summary in Dutch, Utrecht University
© Inez Johanna Gan, 2021

From mouse to human: Metabolic targeting of cancer with TEG-based immunotherapy

**Van muis naar mens:
TEG als nieuwe immunotherapie gericht tegen
metabolische veranderingen in tumorcellen**
(met een samenvatting in het Nederlands)

Proefschrift

ter verkrijging van de graad van doctor aan de
Universiteit Utrecht
op gezag van de
rector magnificus, prof.dr. H.R.B.M. Kummeling,
ingevolge het besluit van het college voor promoties
in het openbaar te verdedigen op

woensdag 9 februari 2022 des middags te 2.15 uur

door

Inez Johanna Gan

geboren op 10 oktober 1988
te Jakarta, Indonesië

Promotor

Prof.dr. J.H.E. Kuball

Copromotors

Dr. Z. Sebestyén

Dr. G.C.M. Straetemans

CONTENTS

CHAPTER 1

General Introduction

The human immune system functions to monitor tissue homeostasis, protect cells from foreign infection and eliminate damaged or stress-induced cells (1). In recent decades, the role of immune cells has been uncovered as one of the defense mechanisms against cancerous/neoplastic cells. Thus, cancer immunotherapy has been widely applied as one of the therapeutic options against different malignancies.

T cells play an important role in cellular immunity with antigen-specific effector function and able to develop long-term immunity from memory responses (2). The main subset of T cells carries T-cell receptor (TCR) consisting of α- and β-chain heterodimer, known as αβT cells, that recognize their cognate antigen in specific peptide-major histocompatibility complex (pMHC) dependent manner.

Ideally, target antigens for αβT cell therapies should be selectively expressed on tumor cells but not in healthy tissues (3). Also, target antigens should elicit immune responses, in this context, specifically evoke αβT cell response. Following target antigen selection, another critical factor is to obtain antigen-specific TCR with good functionality. αβT cell function is determined by its αβTCR affinity and avidity. TCR affinity affects the binding strength of the receptor to its cognate antigen, while TCR avidity governs the ability of receptor clustering between cells.

Adoptive T cell therapy (ACT)
The first known cancer immunotherapy approach is adoptive T cell therapy (ACT), in which tumor-infiltrating T lymphocytes (TILs), consisting of mainly αβT cells, found in the tumor are isolated, ex vivo expanded, and subsequently re-infused back to patients after lymphodepletion (Figure 1A) (4). Despite their potential, the translational effort of tumor-specific αβT cells is rather challenging as the number of TILs that could be isolated from cancer patients is limited. On the other hand, most tumor-associated antigens (TAAs) are "self-antigens" that generate low-affinity αβTCRs and render and incompetent immune response against cancer due to the elimination of self-reactive immune cells during central and peripheral tolerance mechanisms (5, 6). Furthermore, neoantigens derived from somatic mutation of cancer cells mainly found in tumor with higher tumor mutational load and limiting potential immunogenic target(s) in several tumor types, such as acute myeloid leukemia (AML) (7). As alternatives, αβTCR-engineered αβT cell and chimeric antigen receptor (CAR) therapies are developed methodologies to circumvent the limitation of TILs therapy by introducing highly-tumor reactive αβTCR that recognize antigens expressed by tumor cells (3, 5).

αβTCR-engineered αβT cell therapy
αβTCR-engineered αβT cell therapy allows the introduction of allogenic αβTCR into patient's αβT cells, follows by *ex vivo* expansion prior to re-infusion, and thereby circumvent the limited amount of autologous tumor-reactive T cells (Figure 1B). Clinical studies collectively demonstrate significantly favorable outcomes, including tumor regression (8), in the majority of patients with several malignancies, such as multiple myeloma (9), metastatic melanoma (10), and colorectal carcinoma (11).

Despite their clinical benefits, αβTCR-engineered therapies only benefit for a certain percentage of patients who express targetable tumor antigen in an MHC-restricted manner. This also holds through for ACT with allogeneic T cells, where HLA-match donor becomes a limiting factor to avoid possible graft-versus-host-disease (GvHD) (12). Moreover, tumor cells could develop resistance by downregulation of MHC molecules or antigens expression, leading to unsustainable clinical responses in patients (3).
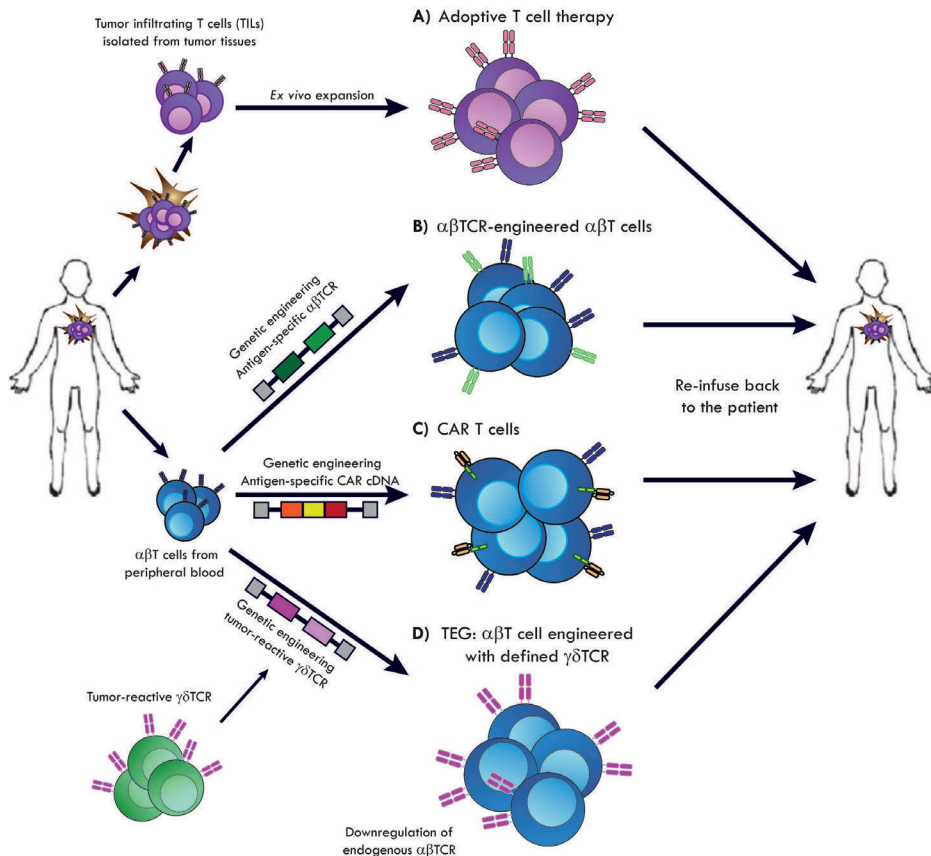
Figure 1 Cellular T cell immunotherapy approaches for cancer patients. (A) Tumor-infiltrating T cells (TILs) found on tumor biopsy of cancer patients can be ex vivo expanded prior to reinfusion to patients to elicit better T cell response against tumor cells. **(B)** Alternatively, gene transfer of identified antigen-specific αβTCR into αβT cells could be used as therapeutic approach to circumvent the limited TILs in patients. **(C)** Chimeric antigen receptor (CAR) introduced into αβT cells redirect their tumor reactivity in antigen-specific and pMHC-independent manner. **(D)** Introduction of highly tumor-reactive γδTCR into αβT cells redirect tumor-reactivity against early metabolic changes occur in tumor cells, overcoming the proficient deficiency of unmodified γδT cells as well as their broad diversity repertoires.

Chimeric antigen receptor (CAR)

An alternative approach for cellular therapy is the introduction of chimeric antigen receptor (CAR) to T cells to redirect αßT cell anti-tumor specificity and enhance the efficacy of adoptive T cells in patients (Figure 1C) (13). CAR T cells are designed with extracellular domain of single-chain variable fragment (scFv) from immunoglobulin molecules, hinge region that important for flexibility and CAR dimerization, transmembrane domain, and intracellular signaling domain consisting of CD3ζ (1st generation CARs) and co-stimulatory molecules (2nd and 3rd generation CARs) that are important for T cell activation and persistence (13-15).

Studies with CAR T cells directed towards CD19/CD20 antigens have shown remarkable clinical responses in patients with hematological malignancies (16-18); subsequently leads to FDA- and EMA-approved products, including Axicabtagene ciloleucel (19, 20) and Tisagenlecleucel (21-23). Nevertheless, there are still some concerns regarding the side effects of CAR T cell therapy, including tumor lysis syndrome, on-target off-tumor toxicity, cytokine release syndrome (CRS), neurotoxicity, and lymphopenia. CAR T cells induce tonic signaling leading to high risk for CRS and promoting T cell exhaustion, hence the ineffective anti-tumor efficacy and possible off-target toxicity (15).

Following the unprecedented success of CAR T cell therapy for hematological malignancies, clinical studies with CAR T cells directed towards antigens express in solid malignancies have been initiated (24-30). Unlike hematological malignancies that are dispersed, solid tumor masses developed in specific organs and resulted in the growth of immunosuppressive cells that causes lower penetration of CAR T cells into solid tumor masses (31, 32). Furthermore, the high heterogeneity of solid malignancies hampers the therapeutic effect of cancer immunotherapy, including CAR T cells.

γδT cells-based cellular therapy

Up to 1-10% of circulating CD3$^+$ human T cells carry a TCR heterodimer with γ-chain and δ-chain and known as γδT cells. The unconventional γδT cells share the property of innate and adaptive immunity that allows recognition of infected, stress-induced, and malignantly-transformed cells and undergo clonal expansion and memory formation (33, 34). The role of γδT cells in cancer immunosurveillance first observed in γδT cell-deficient mice that increased the chance of cutaneous tumor development (35, 36) and spontaneous adenocarcinoma growth (37) compared to wild-type mice. The potential application of unconventional γδT cells in cancer immunotherapy increases as intratumoral γδT cells have been associated with favorable prognosis for patients across different malignancies (38, 39).

Similar to αßT cells, γδT cells able to exert cytotoxic capacity against their target antigens and elicit immune responses, either directly via perforin and granzyme or indirectly via cytokines production (40). γδT cells do not require antigen presentation in pMHC complex for their target recognition, and also do not require CD4 and CD8 co-receptor binding for proper γδTCR signaling (41), which allow antigen recognition

1

across a broad range of malignancies, also irrespective of their tumor mutational load. γδT cells could recognize its target in a γδTCR-independent manner via natural cytotoxicity receptors, such as NKG2D, DNAM-1, NKp30, and NKp44, contributing to their diverse repertoire (42, 43).

γδT cells are classified into two major subsets, Vδ2$^+$ and Vδ2$^-$ T cells. Vδ2$^+$ cells exclusively interact with Vγ9$^+$ chain and subsequently known Vγ9δ2$^+$ T cells mainly reside in peripheral blood, whereas the Vδ2$^-$ subset, i.e., Vδ1$^+$, Vδ3$^+$ cells, primarily reside in epithelial tissues or mucosal membranes (44, 45). Vδ2$^+$ cells recognize metabolic changes in infected or malignantly-transformed cells by sensing accumulation of intracellular metabolite antigens, known as phosphoantigens (pAgs). pAgs are produced by bacterial pathogens with the non-mevalonate pathway for isoprenoid synthesis (46, 47). In malignantly-transformed cells, dysregulated mevalonate pathway is associated with high accumulation of intracellular isopentenyl pyrophosphate (IPP) compared to healthy cells, promoting the recognition by Vδ2$^+$ T cells (48, 49).

Vδ2$^-$ cells are known for their diverse stress-induced ligands, including MHC-associated antigens MICA/B protein (50-52), lipid antigens presented by CD1d molecules (53), UL16-binding protein (ULBP) family members (54-56), endothelial protein C receptor (EPCR; (57)), and Annexin A2 (58). However, the exact ligands and their mode-of-activation are yet to be elucidated. Vδ1$^+$ cells, one of the major Vδ2$^-$ subsets, also exert cytotoxic capacity against infected and tumor cells, yet their activation is phosphoantigen-independent. Recent studies have shown the antitumor efficacy of Vδ1$^+$ cells against hematological and solid malignances (59-62), suggesting their promising potential in cancer immunotherapy alongside Vδ2$^+$ cells.

γδT cells have a diverse repertoire in function and receptor expression, complex biology, and tissue-specific tropism that may impede their application in adoptive cellular therapy (63-65). Therapeutic application of γδT cells in cancer immunotherapy mainly focuses on Vδ2$^+$ cells, for which clinical studies are conducted against different types of cancer (39, 66-70). These studies are mainly executed with adoptive transfers of *ex vivo* expanded unmodified γδT cell, either autologous or allogeneic. Unfortunately, naturally elevated IPP levels in cancer cells does not promote sufficient antitumor response of Vδ2$^+$ cells (71). Therefore, most clinical studies are performed together with the administration of aminobiphosphonates (i.e., Zoledronate, pamidronate), which increase the accumulation of IPP, and interleukin-2 (IL-2) to promote tumor recognition by VD2$^+$ cells. These clinical studies showed a favorable safety profile of γδT cell-based therapy, including the absence of GvHDs in MHC mismatch background (72). Yet, clinical responses are still marginal.

New kid on the block: αßT cells Engineered to express defined γδTCR (TEGs)
Considering the major downsides of autologous γδT cell therapy, our group developed the concept of metabolic targeting of cancer with TEGs: αßT cell engineered to express a defined γδTCR, which utilizes the superior proliferative capacity of αßT cells while

retaining antitumor efficacy of γδTCR (Figure 1D) (73-75). Introduction of highly tumor-specific γδTCR into αßT cells bypasses the needs of MHC-restricted αßT cell recognition and could efficiently target a broad range of hematological and solid malignancies (73, 74, 76, 77). Additionally, TEGs uncouple γδTCR from its innate-like environment, such as the interplay of NK receptors, that are not present in αßT cells (78). In this way, TEGs also mitigates the underestimated diversity of γδTCR, both in function and receptor expression (63, 64).

One of the main advantages of TEG cells is the absence of TCR mispairing between γδTCR and αßTCR chains and do not produce unwanted TCRs with unknown specificities. In addition, the successful gene transfer of γδTCR into αßT cells leads to downregulation of the endogenous αßTCRs on the cell surface and thus decreases alloreactivity and facilitates the depletion of non-engineered T cells (73, 74). Our group successfully develop an untouched GMP-ready strategy using clinical-grade anti-human αßTCR antibody to purify TEG cells without cross-reactivity against γδTCR chains and therefore able to segregate between engineered- and non-engineered cells by negative selection procedures. This production process allows expansion of sufficient TEG-based cellular therapy from apheresis products from cancer patients and readily translated for clinical use (75, 79). TEG format allows efficient production of αßT cells expressing a highly tumor-specific γδTCR, either from Vδ2$^+$ or Vδ2$^-$ subsets. Moreover, TEGs also retain CD4$^+$ and CD8$^+$ effector cell functions.

OUTLINE OF THE THESIS

Before clinical implementation, efficacy and safety profiles of cellular therapy, including TEGs, have to be evaluated carefully. The efficacy profile of T cells could be determined by *in vitro* co-culture with tumor target, both cell lines and primary patient materials, and assessed for their cytotoxicity by cytokines production and direct killing capacity. The safety profile of T cells is evaluated with the same method with the co-culture of healthy cell lines or hematopoietic compartments to assess possible off-target toxicity (80). Furthermore, 3D models can be used to evaluate efficacy and toxicity profile in a closer physiologically-relevant tumor microenvironment, such as interplay with stromal and epithelial cells in the bone marrow (81). The major limitation for γδT cells translational research is the evolutionary difference between humans and mice, commonly used as preclinical model for cellular therapy. Distinct γδT cell repertoire exclusively presents in human and non-human primates, but not in their mice counterparts (82, 83). Thus, preclinical assessment of efficacy and safety profile of cellular therapy is mainly performed *in vivo* using transgenic mice or immunodeficient mice model transplanted with human tumor cells followed by adoptive transfer of human T cell therapy. Therefore, this thesis aims to evaluate efficacy and safety profiles of TEG products, particularly TEG001 and TEG011, in relevant preclinical models and thereby highlighting their therapeutic potential prior to further clinical testing.

Chapter 2, published in *J ImmunoTher Cancer* 2019;7:69 (doi:10.1186/s40425-019-0558-4), describes the efficacy-safety balance of TEG001 in more physiological relevant environments, with primary tumor tissues as well as primary healthy cells. Using a humanized mouse model, we were able to assess the activity of TEG001 against established leukemia in patient-derived xenograft (PD-X) mice and toxicity against complete hematopoietic compartment by engrafting healthy cord blood-derived CD34^{+} progenitor cells in healthy donor-derived (HD-X) mice. We provide supporting evidence for TEG001 *in vivo* therapeutic potential against primary AML without harming healthy hematopoietic compartments and bestow a rationale for the first-in-human study.

Chapter 3, published in *Blood Adv.* 2019;3(19):2870-2882 (doi: 10.1182/bloodadvances.2019032409), elucidates the antitumor reactivity of an allo-HLA-A*24:02-restricted Vγ5Vδ1TCR and CD8α-dependent (derived from clone FE11) against both solid and hematological tumor cells, while sparring their healthy counterparts. When applied into TEG format, subsequently referred to as TEG011, this TCR retains the tumor-specific activity and the ability to differentiate between healthy and malignant cells in HLA-A*24:02-restricted manner. Importantly, we focused on the *in vivo* assessment of TEG011 efficacy in a transgenic mouse model expressing human HLA-A*24:02 and highlighting its promising therapeutic application.

Chapter 4, published in *J Leukoc Biol*. 2020;1–11 (doi: 10.1002/JLB.5MA0120-228R), extends the assessment of TEG011 safety profile *in vivo* as well as its pharmacokinetics in non-tumor bearing and tumor-bearing humanized HLA-A*24:02 transgenic NSG (NSG-A24:02) mice, where no off-target toxicity observed. Furthermore, we describe the association between TEG011 persistence and tumor control, emphasizing that the kinetics of adoptive transferred TEG011 is crucial to sustain long-term efficacy.

Chapter 5 describes the introduction of transgenic CD8α receptor to improve TEG011 efficacy further. As shown in Chapter 3, TEG011 is critically dependent on CD8α co-receptor and lacks support by antigen-specific CD4^{+} T cells. Thus, co-expression of both FE11 γδTCR and CD8α receptor on T cells (referred to as TEG011_CD8α) is deemed a good strategy to enhance TEG011 antitumor efficacy and T cell infiltration. This chapter was submitted for publication to *Frontiers in Immunology*, August 2021.

Chapter 6 summarizes the major findings in chapters mentioned earlier and puts the crucial aspects of preclinical model development within the context of γδTCR-engineered T cell immunotherapy, specifically for TEG-based therapy, and in comparison to other immunotherapeutic platforms.

REFERENCES

1. de Visser KE, Eichten A, Coussens LM. Paradoxical roles of the immune system during cancer development. *Nat Rev Cancer*. 2006;6(1):24-37.

2. Sharpe ME. T-cell Immunotherapies and the Role of Nonclinical Assessment: The Balance between Efficacy and Pathology. *Toxicol Pathol*. 2018;46(2):131-46.

3. Debets R, Donnadieu E, Chouaib S, Coukos G. TCR-engineered T cells to treat tumors: Seeing but not touching? *Semin Immunol*. 2016;28(1):10-21.

4. Stevanovic S, Draper LM, Langhan MM, Campbell TE, Kwong ML, Wunderlich JR, *et al*. Complete regression of metastatic cervical cancer after treatment with human papillomavirus-targeted tumor-infiltrating T cells. *J Clin Oncol*. 2015;33(14):1543-50.

5. Chandran SS, Klebanoff CA. T cell receptor-based cancer immunotherapy: Emerging efficacy and pathways of resistance. *Immunol Rev*. 2019;290(1):127-47.

6. Bonini C, Mondino A. Adoptive T-cell therapy for cancer: The era of engineered T cells. *Eur J Immunol*. 2015;45(9):2457-69.

7. Lee JB, Chen B, Vasic D, Law AD, Zhang L. Cellular immunotherapy for acute myeloid leukemia: How specific should it be? *Blood Rev*. 2019;35:18-31.

8. Morgan RA, Dudley ME, Wunderlich JR, Hughes MS, Yang JC, Sherry RM, *et al*. Cancer regression in patients after transfer of genetically engineered lymphocytes. *Science*. 2006;314(5796):126-9.

9. Rapoport AP, Stadtmauer EA, Binder-Scholl GK, Goloubeva O, Vogl DT, Lacey SF, *et al*. NY-ESO-1-specific TCR-engineered T cells mediate sustained antigen-specific antitumor effects in myeloma. *Nat Med*. 2015;21(8):914-21.

10. Johnson LA, Morgan RA, Dudley ME, Cassard L, Yang JC, Hughes MS, *et al*. Gene therapy with human and mouse T-cell receptors mediates cancer regression and targets normal tissues expressing cognate antigen. *Blood*. 2009;114(3):535-46.

11. Parkhurst MR, Yang JC, Langan RC, Dudley ME, Nathan DA, Feldman SA, *et al*. T cells targeting carcinoembryonic antigen can mediate regression of metastatic colorectal cancer but induce severe transient colitis. *Mol Ther*. 2011;19(3):620-6.

12. Bendle GM, Linnemann C, Hooijkaas AI, Bies L, de Witte MA, Jorritsma A, *et al*. Lethal graft-versus-host disease in mouse models of T cell receptor gene therapy. *Nat Med*. 2010; 16(5): 565-70.

13. Srivastava S, Riddell SR. Engineering CAR-T cells: Design concepts. *Trends Immunol*. 2015; 36(8): 494-502.

14. Eisenberg V, Hoogi S, Shamul A, Barliya T, Cohen CJ. T-cells "a la CAR-T(e)" - Genetically engineering T-cell response against cancer. *Adv Drug Deliv Rev*. 2019;141:23-40.

15. Resetca D, Neschadim A, Medin JA. Engineering Hematopoietic Cells for Cancer Immunotherapy: Strategies to Address Safety and Toxicity Concerns. *J Immunother*. 2016;39(7):249-59.

16. Enblad G, Karlsson H, Gammelgard G, Wenthe J, Lovgren T, Amini RM, *et al*. A Phase I/IIa Trial Using CD19-Targeted Third-Generation CAR T Cells for Lymphoma and Leukemia. *Clin Cancer Res*. 2018;24(24):6185-94.

17. Ramos CA, Rouce R, Robertson CS, Reyna A, Narala N, Vyas G, *et al*. In Vivo Fate and Activity of Second- versus Third-Generation CD19-Specific CAR-T Cells in B Cell Non-Hodgkin's Lymphomas. *Mol Ther*. 2018;26(12):2727-37.

18. Mikkilineni L, Kochenderfer JN. Chimeric antigen receptor T-cell therapies for multiple myeloma. *Blood*. 2017;130(24):2594-602.

1

19. Kochenderfer JN, Feldman SA, Zhao Y, Xu H, Black MA, Morgan RA, *et al*. Construction and preclinical evaluation of an anti-CD19 chimeric antigen receptor. *J Immunother*. 2009;32(7):689-702.

20. Neelapu SS, Locke FL, Bartlett NL, Lekakis LJ, Miklos DB, Jacobson CA, *et al*. Axicabtagene Ciloleucel CAR T-Cell Therapy in Refractory Large B-Cell Lymphoma. *N Engl J Med*. 2017; 377(26): 2531-44.

21. Maude SL, Laetsch TW, Buechner J, Rives S, Boyer M, Bittencourt H, *et al*. Tisagenlecleucel in Children and Young Adults with B-Cell Lymphoblastic Leukemia. *N Engl J Med*. 2018;378(5):439-48.

22. Turtle CJ, Maloney DG. Clinical trials of CD19-targeted CAR-modified T cell therapy; a complex and varied landscape. *Expert Rev Hematol*. 2016;9(8):719-21.

23. Lee DW, Kochenderfer JN, Stetler-Stevenson M, Cui YK, Delbrook C, Feldman SA, *et al*. T cells expressing CD19 chimeric antigen receptors for acute lymphoblastic leukaemia in children and young adults: a phase 1 dose-escalation trial. *Lancet*. 2015;385(9967):517-28.

24. Katz SC, Burga RA, McCormack E, Wang LJ, Mooring W, Point GR, *et al*. Phase I Hepatic Immunotherapy for Metastases Study of Intra-Arterial Chimeric Antigen Receptor-Modified T-cell Therapy for CEA+ Liver Metastases. *Clin Cancer Res*. 2015;21(14):3149-59.

25. Brown CE, Alizadeh D, Starr R, Weng L, Wagner JR, Naranjo A, *et al*. Regression of Glioblastoma after Chimeric Antigen Receptor T-Cell Therapy. *N Engl J Med*. 2016;375(26):2561-9.

26. Lamers CH, Sleijfer S, van Steenbergen S, van Elzakker P, van Krimpen B, Groot C, *et al*. Treatment of metastatic renal cell carcinoma with CAIX CAR-engineered T cells: clinical evaluation and management of on-target toxicity. *Mol Ther*. 2013;21(4):904-12.

27. Park JR, Digiusto DL, Slovak M, Wright C, Naranjo A, Wagner J, *et al*. Adoptive transfer of chimeric antigen receptor re-directed cytolytic T lymphocyte clones in patients with neuroblastoma. *Mol Ther*. 2007;15(4):825-33.

28. Wilkie S, van Schalkwyk MC, Hobbs S, Davies DM, van der Stegen SJ, Pereira AC, *et al*. Dual targeting of ErbB2 and MUC1 in breast cancer using chimeric antigen receptors engineered to provide complementary signaling. *J Clin Immunol*. 2012;32(5):1059-70.

29. Louis CU, Savoldo B, Dotti G, Pule M, Yvon E, Myers GD, *et al*. Antitumor activity and long-term fate of chimeric antigen receptor-positive T cells in patients with neuroblastoma. *Blood*. 2011;118(23):6050-6.

30. van Schalkwyk MC, Papa SE, Jeannon JP, Guerrero Urbano T, Spicer JF, Maher J. Design of a phase I clinical trial to evaluate intratumoral delivery of ErbB-targeted chimeric antigen receptor T-cells in locally advanced or recurrent head and neck cancer. *Hum Gene Ther Clin Dev*. 2013; 24(3):134-42.

31. Newick K, O'Brien S, Moon E, Albelda SM. CAR T Cell Therapy for Solid Tumors. *Annu Rev Med*. 2017;68:139-52.

32. Garber K. Driving T-cell immunotherapy to solid tumors. *Nat Biotechnol*. 2018;36(3):215-9.

33. Tanaka Y, Morita CT, Tanaka Y, Nieves E, Brenner MB, Bloom BR. Natural and synthetic non-peptide antigens recognized by human γδT cells. *Nature*. 1995;375(6527):155-8.

34. Melandri D, Zlatareva I, Chaleil RAG, Dart RJ, Chancellor A, Nussbaumer O, *et al*. The γδTCR combines innate immunity with adaptive immunity by utilizing spatially distinct regions for agonist selection and antigen responsiveness. *Nat Immunol*. 2018;19(12):1352-65.

35. Gao Y, Yang W, Pan M, Scully E, Girardi M, Augenlicht LH, *et al*. γδT cells provide an early source of interferon gamma in tumor immunity. *J Exp Med*. 2003;198(3):433-42.

36. Girardi M, Oppenheim DE, Steele CR, Lewis JM, Glusac E, Filler R, Regulation of cutaneous malignancy by γδT cells. *Science*. 2001;294(5542):605-9.

37. Liu Z, Eltoum IE, Guo B, Beck BH, Cloud GA, Lopez RD. Protective immunosurveillance and therapeutic antitumor activity of γδ T cells demonstrated in a mouse model of prostate cancer. *J Immunol*. 2008;180(9):6044-53.

38. Gentles AJ, Newman AM, Liu CL, Bratman SV, Feng W, Kim D, *et al*. The prognostic landscape of genes and infiltrating immune cells across human cancers. *Nat Med*. 2015;21(8):938-45.

39. Payne KK, Mine JA, Biswas S, Chaurio RA, Perales-Puchalt A, Anadon CM, *et al*. BTN3A1 governs antitumor responses by coordinating αß and γδT cells. *Science*. 2020;369(6506):942-9.

40. Silva-Santos B, Serre K, Norell H. γδT cells in cancer. *Nat Rev Immunol*. 2015;15(11):683-91.

41. Muro R, Takayanagi H, Nitta T. T cell receptor signaling for γδT cell development. *Inflamm Regen*. 2019;39:6.

42. Lo Presti E, Corsale AM, Dieli F, Meraviglia S. γδ cell-based immunotherapy for cancer. *Expert Opin Biol Ther*. 2019;19(9):887-95.

43. Hudspeth K, Silva-Santos B, Mavilio D. Natural cytotoxicity receptors: broader expression patterns and functions in innate and adaptive immune cells. *Front Immunol*. 2013;4:69.

44. Chien YH, Meyer C, Bonneville M. γδT cells: first line of defense and beyond. *Annu Rev Immunol*. 2014;32:121-55.

45. Godfrey DI, Le Nours J, Andrews DM, Uldrich AP, Rossjohn J. Unconventional T Cell Targets for Cancer Immunotherapy. *Immunity*. 2018;48(3):453-73.

46. Perera MK, Carter R, Goonewardene R, Mendis KN. Transient increase in circulating γδT cells during Plasmodium vivax malarial paroxysms. *J Exp Med*. 1994;179(1):311-5.

47. Kabelitz D, Bender A, Prospero T, Wesselborg S, Janssen O, Pechhold K. The primary response of human γδ⁺ T cells to Mycobacterium tuberculosis is restricted to Vγ9-bearing cells. *J Exp Med*. 1991;173(6):1331-8.

48. Gober HJ, Kistowska M, Angman L, Jeno P, Mori L, De Libero G. Human T cell receptor γδ cells recognize endogenous mevalonate metabolites in tumor cells. *J Exp Med*. 2003;197(2):163-8.

49. Simoes AE, Di Lorenzo B, Silva-Santos B. Molecular Determinants of Target Cell Recognition by Human γδT Cells. *Front Immunol*. 2018;9:929.

50. Groh V, Steinle A, Bauer S, Spies T. Recognition of stress-induced MHC molecules by intestinal epithelial γδT cells. *Science*. 1998;279(5357):1737-40.

51. Xu B, Pizarro JC, Holmes MA, McBeth C, Groh V, Spies T, *et al*. Crystal structure of a gammadelta T-cell receptor specific for the human MHC class I homolog MICA. *Proc Natl Acad Sci USA*. 2011; 108(6):2414-9.

52. Wu J, Groh V, Spies T. T cell antigen receptor engagement and specificity in the recognition of stress-inducible MHC class I-related chains by human epithelial γδT cells. *J Immunol*. 2002; 169(3): 1236-40.

53. Luoma AM, Castro CD, Mayassi T, Bembinster LA, Bai L, Picard D, *et al*. Crystal structure of Vδ1 T cell receptor in complex with CD1d-sulfatide shows MHC-like recognition of a self-lipid by human γδT cells. *Immunity*. 2013;39(6):1032-42.

54. Lanca T, Correia DV, Moita CF, Raquel H, Neves-Costa A, Ferreira C, *et al*. The MHC class Ib protein ULBP1 is a nonredundant determinant of leukemia/lymphoma susceptibility to γδT-cell cytotoxicity. *Blood*. 2010;115(12):2407-11.

55. Catellani S, Poggi A, Bruzzone A, Dadati P, Ravetti JL, Gobbi M, *et al*. Expansion of Vδ1 T lymphocytes producing IL-4 in low-grade non-Hodgkin lymphomas expressing UL-16-binding proteins. *Blood*. 2007;109(5):2078-85.

56. Poggi A, Venturino C, Catellani S, Clavio M, Miglino M, Gobbi M, *et al*. Vδ1 T lymphocytes from B-CLL patients recognize ULBP3 expressed on leukemic B cells and up-regulated by trans-retinoic acid. *Cancer Res*. 2004;64(24):9172-9.

1

57. Willcox CR, Pitard V, Netzer S, Couzi L, Salim M, Silberzahn T, *et al*. Cytomegalovirus and tumor stress surveillance by binding of a human γδT cell antigen receptor to endothelial protein C receptor. *Nat Immunol*. 2012;13(9):872-9.

58. Marlin R, Pappalardo A, Kaminski H, Willcox CR, Pitard V, Netzer S, *et al*. Sensing of cell stress by human γδTCR-dependent recognition of annexin A2. *Proc Natl Acad Sci USA*. 2017; 114(12): 3163-8.

59. Schilbach K, Frommer K, Meier S, Handgretinger R, Eyrich M. Immune response of human propagated γδ-T-cells to neuroblastoma recommend the Vδ1+ subset for γδ-T-cell-based immunotherapy. *J Immunother*. 2008;31(9):896-905.

60. Devaud C, Rousseau B, Netzer S, Pitard V, Paroissin C, Khairallah C, *et al*. Anti-metastatic potential of human Vδ1+ γδT cells in an orthotopic mouse xenograft model of colon carcinoma. *Cancer Immunol Immunother*. 2013;62(7):1199-210.

61. Almeida AR, Correia DV, Fernandes-Platzgummer A, da Silva CL, da Silva MG, Anjos DR, *et al*. Delta One T Cells for Immunotherapy of Chronic Lymphocytic Leukemia: Clinical-Grade Expansion/Differentiation and Preclinical Proof of Concept. *Clin Cancer Res*. 2016;22(23):5795-804.

62. Di Lorenzo B, Ravens S, Silva-Santos B. High-throughput analysis of the human thymic Vδ1+ T cell receptor repertoire. *Sci Data*. 2019;6(1):115.

63. Scheper W, Grunder C, Straetemans T, Sebestyen Z, Kuball J. Hunting for clinical translation with innate-like immune cells and their receptors. *Leukemia*. 2014;28(6):1181-90.

64. Sebestyen Z, Prinz I, Dechanet-Merville J, Silva-Santos B, Kuball J. Translating gammadelta (γδ) T cells and their receptors into cancer cell therapies. *Nat Rev Drug Discov*. 2020;19(3):169-84.

65. Yazdanifar M, Barbarito G, Bertaina A, Airoldi I. γδT Cells: The Ideal Tool for Cancer Immunotherapy. *Cells*. 2020;9(5).

66. Sakamoto M, Nakajima J, Murakawa T, Fukami T, Yoshida Y, Murayama T, *et al*. Adoptive immunotherapy for advanced non-small cell lung cancer using zoledronate-expanded γδTcells: a phase I clinical study. *J Immunother*. 2011;34(2):202-11.

67. Nicol AJ, Tokuyama H, Mattarollo SR, Hagi T, Suzuki K, Yokokawa K, *et al*. Clinical evaluation of autologous γδT cell-based immunotherapy for metastatic solid tumors. *Br J Cancer*. 2011; 105(6): 778-86.

68. Kobayashi H, Tanaka Y, Yagi J, Minato N, Tanabe K. Phase I/II study of adoptive transfer of γδT cells in combination with zoledronic acid and IL-2 to patients with advanced renal cell carcinoma. *Cancer Immunol Immunother*. 2011;60(8):1075-84.

69. Davey MS, Willcox CR, Hunter S, Kasatskaya SA, Remmerswaal EBM, Salim M, *et al*. The human Vδ2+ T-cell compartment comprises distinct innate-like Vγ9+ and adaptive Vγ9- subsets. *Nat Commun*. 2018;9(1):1760.

70. Bertaina A, Zorzoli A, Petretto A, Barbarito G, Inglese E, Merli P, *et al*. Zoledronic acid boosts γδT-cell activity in children receiving αß+ T and CD19+ cell-depleted grafts from an HLA-haplo-identical donor. *Oncoimmunology*. 2017;6(2):e1216291.

71. Kunkele KP, Wesch D, Oberg HH, Aichinger M, Supper V, Baumann C. Vγ9Vδ2 T Cells: Can We Re-Purpose a Potent Anti-Infection Mechanism for Cancer Therapy? *Cells*. 2020;9(4).

72. Godder KT, Henslee-Downey PJ, Mehta J, Park BS, Chiang KY, Abhyankar S, *et al*. Long term disease-free survival in acute leukemia patients recovering with increased γδT cells after partially mismatched related donor bone marrow transplantation. *Bone Marrow Transplant*. 2007;39(12):751-7.

73. Marcu-Malina V, Heijhuurs S, van Buuren M, Hartkamp L, Strand S, Sebestyen Z, *et al*. Redirecting αßT cells against cancer cells by transfer of a broadly tumor-reactive γδT-cell receptor. *Blood*. 2011;118(1):50-9.

74. Grunder C, van Dorp S, Hol S, Drent E, Straetemans T, Heijhuurs S, *et al*. γ9 and δ2CDR3 domains regulate functional avidity of T cells harboring γ9δ2TCRs. *Blood*. 2012;120(26):5153-62.

75. Straetemans T, Grunder C, Heijhuurs S, Hol S, Slaper-Cortenbach I, Bonig H, *et al*. Untouched GMP-Ready Purified Engineered Immune Cells to Treat Cancer. *Clin Cancer Res*. 2015;21(17):3957-68.

76. Scheper W, van Dorp S, Kersting S, Pietersma F, Lindemans C, Hol S, *et al*. γδT cells elicited by CMV reactivation after allo-SCT cross-recognize CMV and leukemia. *Leukemia*. 2013;27(6):1328-38.

77. Kierkels GJJ, Scheper W, Meringa AD, Johanna I, Beringer DX, Janssen A, *et al*. Identification of a tumor-specific allo-HLA-restricted γδTCR. *Blood Adv*. 2019;3(19):2870-82.

78. Das H, Wang L, Kamath A, Bukowski JF. Vγ2Vδ2 T-cell receptor-mediated recognition of aminobis-phosphonates. *Blood*. 2001;98(5):1616-8.

79. Straetemans T, Kierkels GJJ, Doorn R, Jansen K, Heijhuurs S, Dos Santos JM, *et al*. GMP-Grade Manufacturing of T Cells Engineered to Express a Defined γδTCR. *Front Immunol*. 2018;9:1062.

80. Chen H, Zou M, Teng D, Hu Y, Zhang J, He W. Profiling the pattern of the human T-cell receptor γδ complementary determinant region 3 repertoire in patients with lung carcinoma via high-throughput sequencing analysis. *Cell Mol Immunol*. 2019;16(3):250-9.

81. Braham MVJ, Minnema MC, Aarts T, Sebestyen Z, Straetemans T, Vyborova A, *et al*. Cellular immunotherapy on primary multiple myeloma expanded in a 3D bone marrow niche model. *Oncoimmunology*. 2018;7(6):e1434465.

82. Hayday AC. γδ cells: a right time and a right place for a conserved third way of protection. *Annu Rev Immunol*. 2000;18:975-1026.

83. Rakasz E, MacDougall AV, Zayas MT, Helgelund JL, Ruckward TJ, Hatfield G, *et al*. γδT cell receptor repertoire in blood and colonic mucosa of rhesus macaques. *J Med Primatol*. 2000;29(6):387-96.

1

CHAPTER 2

Evaluating *in vivo* efficacy – toxicity profile of TEG001 in humanized mice xenografts against primary human AML disease and healthy hematopoietic cells

Inez Johanna[1,*], Trudy Straetemans[1,*], Sabine Heijhuurs[1], Tineke Aarts-Riemens[1], Håkan Norell[2], Laura Bongiovanni[3], Alain de Bruin[3], Zsolt Sebestyen[1,**], and Jürgen Kuball[1,**]

[1] Department of Hematology and Laboratory of Translational Immunology, University Medical Center Utrecht, Utrecht, The Netherlands
[2] Instituto de Medicina Molecular, Faculdade de Medicina, Universidade de Lisboa, Lisbon, Portugal
[3] Department of Pathobiology, Faculty of Veterinary Medicine, Dutch Molecular Pathology Center, Utrecht University, Utrecht, The Netherlands

* These authors contributed equally to this work
** Senior authors

ABSTRACT

γ9δ2T cells, which express Vγ9 and Vδ2 chains of the T cell receptor (TCR), mediate cancer immune surveillance by sensing early metabolic changes in malignant leukemic blast and not their healthy hematopoietic stem counterparts via the γ9δ2TCR targeting joined conformational and spatial changes of CD277 at the cell membrane (CD277J). This concept led to the development of next generation CAR-T cells, so called TEGs: αßT cells Engineered to express a defined γδTCR. The high affinity γ9δ2TCR clone 5 has recently been selected within the TEG format as a clinical candidate (TEG001). However, exploring safety and efficacy against a target, which reflects an early metabolic change in tumor cells, remains challenging given the lack of appropriate tools. Therefore, we tested whether TEG001 is able to eliminate established leukemia in a primary disease model, without harming other parts of the healthy hematopoiesis *in vivo*.

Separate sets of NSG mice were respectively injected with primary human acute myeloid leukemia (AML) blasts and cord blood-derived human progenitor cells from healthy donors. These mice were then treated with TEG001 and mock cells. Tumor burden and human cells engraftment were measured in peripheral blood and followed up over time by quantifying for absolute cell number by flow cytometry. Statistical analysis was performed using non-parametric 2-tailed Mann-Whitney t-test. We successfully engrafted primary AML blasts and healthy hematopoietic cells after 6-8 weeks. Here we report that metabolic cancer targeting through TEG001 eradicated established primary leukemic blasts *in vivo*, while healthy hematopoietic compartments derived from human cord-blood remained unharmed in spite of TEGs persistence up to 50 days after infusion. No additional signs of off-target toxicity were observed in any other tissues. Within the limitations of humanized PD-X models, targeting CD277J by TEG001 is safe and efficient. Therefore, we have initiated clinical testing of TEG001 in a phase I first-in-human clinical trial (NTR6541; date of registration 25 July 2017).

INTRODUCTION

Adoptive cell therapy with engineered immune cells targeting hematological malignancies entered clinical practice (1). Reprogramming immune cells has been achieved so far with chimeric antigen-reactive receptors (2) and tumor-specific αßT cell receptors (TCRs) (3, 4). However, the CAR-T concept frequently targets ubiquitously expressed antigens like CD19 for B cell malignancies (5), or FLT-3 (6) for acute myeloid leukemia (AML), as well as stress antigens like NKG2D (natural-killer group 2, member D) for a broader range of cancers (7), raising the question of whether such strategies result as collateral damage in either the long-term deletion of essential hematopoietic subsets or within the context of physiological or therapeutic stress like irradiation to self-reactivity. Given the low mutational load of AML (8), the targeting of neo-antigens has not been successful, and targeting of minor antigens like HA-1 allows only the inclusion of a minority of patients (9). Thus, novel strategies are needed to attack myeloid malignancies within the context of engineered immune cells.

One very attractive and so far, not well-explored alternative to mediate tumor-specific TCR derives from unconventional γ9δ2T cells subsets (10). γ9δ2T cells sense molecular stress signatures via the accumulation of intracellular phosphoantigens level on infected and malignant cells (11). This cell subset has the ability to kill tumor cells originating from hematological and solid malignancies *in vitro*, making it a promising immunotherapeutic option (10, 12). While several clinical trials have been conducted using *ex vivo* expanded and adoptively transferred autologous γ9δ2T cells in patients with advanced malignancies including AML, the results showed scarce activity (13). One major obstacle has been the limited proliferative capacity of γ9δ2T cells in advanced cancer patients (14), as well as the underestimation of the substantial molecular and functional diversity within this subset (15, 16). Therefore, alternative strategies are needed for the clinical translation of the strong antitumor reactivity of receptors expressed on γ9δ2T cells (15).

To override the major weakness of γ9δ2T cells for its defective proliferative capacity and underestimated diversity, our group demonstrated that αßT cells engineered to express a defined γδTCR, so-called TEGs, solves the proliferation deficiency and diversity of γ9δ2T cells by utilizing one defined γ9δ2TCR with strong antitumor reactivity and the strong proliferative capacity of αßT cells. Furthermore, by utilizing αßT properties, we retain both CD4^{+} and CD8^{+} effector cell functions in our TEGs. The first clinical candidate of TEGs derived from clone 5 (TEG001) has been shown to mediate the highest antitumor reactivity against a broader panel of tumor cells *in vitro* and in cell line-derived xenograft mouse models and to outperform natural γ9δ2T cells (10, 12, 17, 18). However, the assessment of the true activity of TEG001 against primary leukemia as well as potential toxicity in physiologically more relevant models has not been assessed so far, but is essential prior to entering a first-in-human clinical trial. Low toxicity of natural γ9δ2T cells in many clinical trials (13) cannot be used as an argument for safety, given also their lack of activity in men, mainly orchestrated through many NK-like immune inhibitory receptors expressed at the cell surface of natural γ9δ2T cells (16). The major

driver of the activity of TEG001, but also its potential risk of toxicity, is derived from the concept of utilizing a highly active γ9δ2TCR out of the context of the natural brakes of a γ9δ2T cells, which have been also the pitfalls for their successful clinical translation to date. Thus, the key obstacle of clinical translation of TEG001 remains the assessment of its bare activity against primary leukemia as well as potential side effects against e.g. healthy hematopoietic compartments. Classical concept of efficacy and safety testing fail for this novel type of tumor-specific antigen, given that a joint conformational and spatial change of CD277 (later referred to as CD277J) mediated through early metabolic changes in cancer cells is recognized by the utilized γ9δ2TCR (12, 19, 20) and no tools are available to directly assess CD277J. To date, only cellular re-localization of RhoB can serve as a surrogate marker of CD277J (12). Antibodies used for detecting CD277 rather induce or inhibit the conformational and spatial changes of CD277J (21, 22), thus they do not have the intrinsic ability to sense these alterations. Soluble γδTCR have been suggested to sense CD277J (23), however a more comprehensive analysis of such tools could not confirm their suitability, most likely due to the low affinity of the γ9δ2TCR (J Kuball unpublished observation). To remove these obstacles before clinical testing, we developed models which allow us to assess efficacy and toxicity of TEG001 in more physiological relevant environments, with primary tumor tissues as well as primary healthy cells. One example is the recently established 3D bone marrow model which enabled us to determine the efficacy of TEG001 against primary multiple myeloma cells, and to simultaneously exclude toxicity against stroma and endothelial cells in the bone marrow niche (24). However, limited information is available when assessing activity of TEG001 against established leukemia, and toxicity against the complete hematopoietic compartment. Therefore, we utilized in this report an *in vivo* patient-derived xenograft (PD-X), and a healthy donor-derived xenograft (HD-X) model for assessing the efficacy of TEG001 against primary leukemic blasts and toxicity against the complete hematopoietic compartment, to provide a rationale for first-in-human testing of TEG001.

MATERIALS & METHODS

Functional T cell assay

IFNγ ELISPOT was performed using anti-human IFNγ mAb1-D1K(I) and mAb7-B6-1 (II) (Mabtech) in accordance with the manufacturer's protocol. Effector and target cells (E:T 1:3) were incubated for 24 hours with or without pamidronate (10 or 100 μM; Calbiochem) as indicated. Pamidronate was added in all our *in vitro* experiment in order to enhance TEGs activation as previously reported (10).

RhoB distribution analysis using confocal microscopy

Human CD34^{+} progenitor cells from a healthy donor were subjected to different conditions as follows: **1)** untreated; **2)** overnight stimulation with 50 IU/ml IL-2 or **3)** 1000 IU/ml IFNγ; **4)** overnight incubation in the presence of 5mM Cyclophosphamide (Cy, Sigma-Aldrich Chemie NV, South Holland), or **5)** 20μM Fludarabine-phosphate (Flu, Sigma-Aldrich Chemie NV, South Holland), or **6)** Cy/Flu combination. Primary AML, B

cells, T cells, and monocytes were exposed to 100 μM pamidronate and all cells were subsequently loaded to poly-L-lysine-coated coverslips. Attached cells were fixed, permeabilized and stained with a rabbit polyclonal anti-RhoB antibody (AbCam) followed by a secondary Goat anti-Rabbit IgG AlexaFluor488-conjugated antibody (Jackson ImmunoResearch). Cells were also stained with DAPI for nuclear staining. Intracellular RhoB distribution was visualized by confocal microscopy. RhoB signal ratios between intra-nuclear and extra-nuclear compartments were quantified using ImageJ software as described previously (12).

Animal models

NOD.Cg-Prkdc^{scid}Il2rg$^{tm1Wjl/SzJ}$ (NSG) and NOD.Cg-Prkdc^{scid}Il2rg^{tm1Wjl} Tg(CMVIL3,CSF2,KITL-G)1Eav/ MloySzJ (NSG-SGM3) mice originally obtained from Jackson Laboratory (Bar Harbor, ME, USA) were bred and housed in the specific pathogen-free (SPF) breeding unit of the Central Animal Facility of Utrecht University. Experiments were conducted according to Institutional Guidelines under acquired permission from the local Ethical Committee and per current Dutch laws on Animal Experimentation. Mice were housed in sterile conditions using an individually ventilated cage (IVC) system and fed with sterile food and water. Irradiated mice were given sterile water with antibiotic ciproxin for the duration of the experiment. Mice were randomized with equal distribution by sex and divided into 5 mice/group (for efficacy study) or 10 mice/group (for safety study).

Adult mice (10-14 weeks old) received sublethal total body irradiation (1.75 Gy) on Day 0. On Day 1, NSG mice were injected intravenously with 5×10^6 CD3-depleted primary AML blast from donor p25 (efficacy study as PD-X model) or 0.25×10^6 healthy human CD34$^+$ cells from six different donors (safety study as HD-X model). Engraftment and tumor burden were followed up in the peripheral blood as described in the subsection below. When the arbitrary threshold of 500 cells/ml was reached, treatment was initiated. Mice received 2 injections of 10^7 therapeutic TEG001 cells or TEG-LM1 mock cells (non-functional γδTCR-transduced T cells that carries length mutation of on the complementary determining region 3 (CDR3) region of the δ2-chain (18)). For second PD-X model for efficacy study, adult NSG-SGM3 mice received 2 injections of 10^7 therapeutic TEG001 cells or TEG-LM1 mock cells at Days 8 and 16. All mice received 0.6×10^6 IU of IL-2 (Proleukin; Novartis) in IFA subcutaneously together with the first T cell injection and every 21 days until the end of the experiment. Pamidronate (10 mg/kg body weight) was injected intravenously together with the first T cell injection, and every 21 days until the end of the experiment. Pamidronate was added in all our *in vivo* experiment in order to enhance TEGs activation as previously reported (10). Mice were routinely monitored at least twice a week for weight loss and symptoms of disease (sign of paralysis, weakness, and reduced motility).

Cytology staining and analysis

Cytopathologic evaluation of mouse bone marrow cytospin was performed by May-Grünwald Giemsa staining. Each sample was qualitatively and semi-quantitatively evaluated based on the following criteria: 1) cellularity (1= high; 2= moderate; 3= low); 2) pres-

ence of megakaryocytes; 3) presence of all cell lineages; 4) presence of all stages of maturation for each cell lineage; 5) description of the cell types present for each cell lineage.

Histology staining and analysis

Histopathologic evaluation was performed by hematoxylin and eosin (H&E) staining for the following mouse tissues: liver, spleen, small (duodenum, jejunum, ileum) intestine. Each organ was semi-quantitatively evaluated based on the following criteria: 1) histologic lesions were semi-quantitatively assessed (grade: 0=absent; 1=minimal; 2=mild; 3=moderate; 4=marked); 2) the inflammation was evaluated considering the distribution (focal, multifocal, multifocal to coalescing, diffuse), severity (grade 1-4) and cell type (lymphocytes, plasma cells, macrophages, neutrophils); 3) the presence of leukemic cell infiltrate.

Statistical analysis

Data were analyzed using GraphPad Prism (GraphPad Software Inc.) and represented as mean ± standard deviation (SD) or standard error of mean (SEM) with * $P<0.05$; ** $P < 0.01$; and *** $P < 0.001$. Differences between groups were assessed using a two-way ANOVA, non-parametric 2-tailed Mann-Whitney t-test or Kruskal-Wallis test and Dunn's multiple comparison test where indicated. Cell lines, primary human materials, retroviral transduction and depletion of non-engineered T cells, CFU assays, flow cytometry analysis, assessment for human cell engraftment and preparation of single cell suspensions are described in Supplementary Methods.

RESULTS

***In vitro* and *in vivo* activity of TEG001 against primary AML**

Approximately 50% of the primary AML blasts tested so far are susceptible to TEG001 ((17) and unpublished observation). We first confirmed activity of TEG001 against the primary AML blasts from multiple donors (Supplementary Table 1) by performing an IFNγ ELIspot assay in the presence or absence of 10μM pamidronate (PAM) while the negative control (healthy T cells) was not recognized. Aminobiphosphonate compounds, including clinically used pamidronate, further accumulate intracellular phosphoantigens level (11). Based on our previous study (10), the application of therapeutic concentrations of PAM enhances γ9δ2TCR recognition, including TEG001. Daudi served as a positive control. Most of the primary AML blasts could induce significant IFNγ production by TEG001 in the presence of PAM (Figure 1A). Furthermore, we tested the cytolytic activity of TEG001 against primary AML blasts from donor p2. Primary AML blasts were incubated with either bulk αßT cells (as mock control) or with TEG001 cells in the presence of PAM on the methylcellulose matrix for the colony formation assay. Colonies were counted 8 days later. TEG001 showed a superior reduction of AML blast as shown by less colony formation in comparison to mock T cells (Figure 1B). This result aligns with our previous data in which γ9δ2TCR-transduced αßT cells inhibited colony forming unit (CFU) of primary AML blast (10).
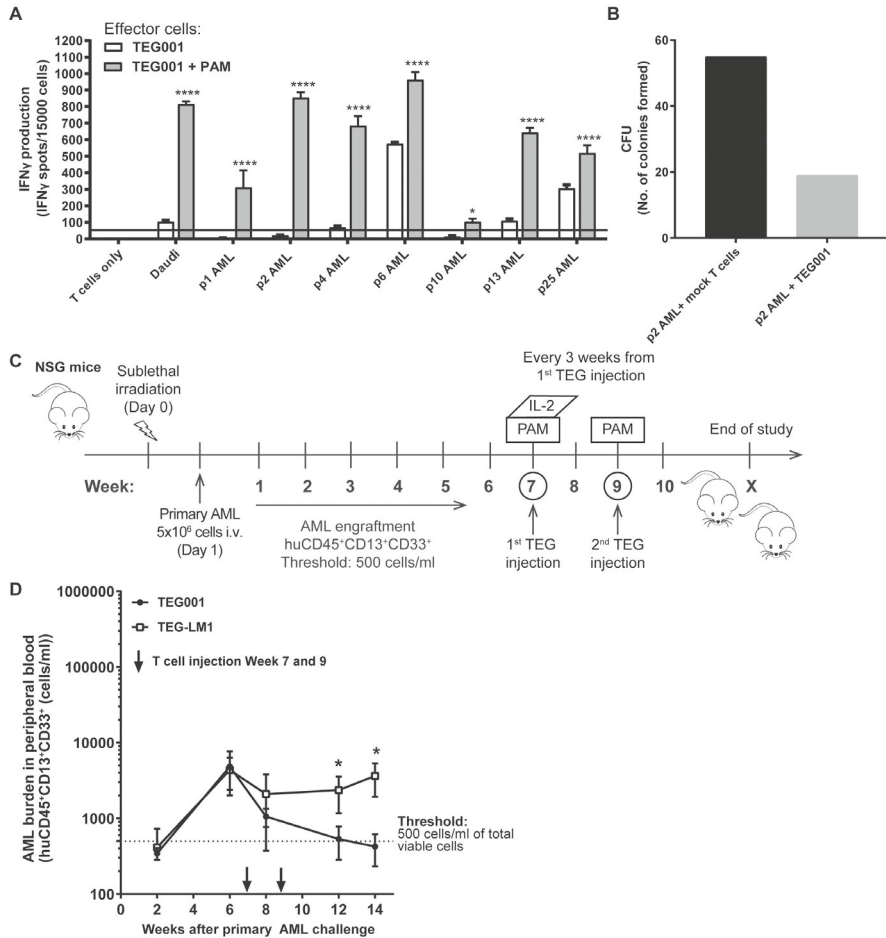
Figure 1 In vitro and in vivo efficacy profile of TEG001. (A) Antitumor reactivity of TEG001 towards patient-derived primary AML blasts in vitro. Effector cells TEG001 and primary AML blasts from multiple donors (E:T ratio is 1:3) were incubated for 24 hours with or without 10 µM PAM as indicated. Daudi and healthy T cells were included as positive and negative target controls, respectively. IFNγ secretion was measured by ELISPOT. IFNγ spots per 15,000 T cells are shown as mean ± SD of at least 3 independent replicates for each target. Fifty spots/15,000 cells were considered as a positive antitumor response and indicated by the black horizontal line. Statistical significances were calculated by two-way ANOVA; *, P < 0.05; **, P < 0.01; ***, P < 0.001; ****, P < 0.0001; **(B)** Bulk αßT cells (as mock T cells) or TEG001 cells were incubated with primary AML blast from donor p2 for 5 hours at E:T ratio 10:1. Then cells were plated in methylcellulose-based medium and, after 8 days, colony formation was quantified using an inverted microscope. Shown is the number of CFU formed. Data is the result of a single experiment from single primary AML donor; **(C)** Schematic overview of in vivo experiment. NSG mice were irradiated at day 0 and engrafted with primary AML cells at day 1. AML cells were followed-up in the peripheral blood by flow cytometry. When the average AML cells were >500 cells/ml, treatment was initiated. Mice received 2 injections of therapeutic TEG001 or TEG-LM1 mock in the presence of PAM (at week 7 and 9) and IL-2 (at week 7); **(D)** Tumor burden for primary AML was measured in peripheral blood by quantifying for absolute cell number by flow cytometry. Data represent mean ± SD of all mice per group (n = 5). Statistical significances were calculated by non-parametric 2-tailed Mann-Whitney t test; *, P < 0.05; **, P < 0.01; ***, P < 0.001; ****, P < 0.0001.

From this screening, we selected AML blasts from patient 25 (p25) because of its initial susceptibility to TEG001, as well as its availability in sufficient numbers for further testing in mice. Next, we injected CD3-depleted primary AML blasts from p25 into irradiated mice intravenously (Figure 1C). Engraftment and leukemia outgrowth were detected by measuring specific AML markers huCD45$^+$CD13$^+$CD33$^+$ in peripheral blood by flow cytometry (Figure S2). When 500 AML cells/ml were detected in peripheral blood, treatment was initiated. Mice received two injections of TEG001 or TEG-LM1 mock in the presence of PAM and IL-2 (for the first TEGs injection) to support TEGs activation and proliferation *in vivo*.

TEG-LM1 carries γ9δ2TCR with length mutation of on the CDR3 of the δ2-chain, which abrogates its function (18) and therefore chosen as a suitable mock control. γδTCR expression for both TEG001 and TEG-LM1 mock is comparable, which subsequently infused into the mice (Figure S1). In the peripheral blood of the TEG001-treated mice, primary AML cells were no longer detectable five weeks after TEGs infusion, but remained measurable in mock-treated mice (Figure 1D), suggesting that in the described PD-X model TEG001 specifically eliminates primary AML blasts over time. We further addressed the influence of microenvironment to TEG001 recognition against primary AML blasts and developed a separate PD-X model using the same p25 AML in NSG-SGM3 mice that express human cytokines (i.e. IL-3, granulocyte/macrophage colony-stimulating factor (GM-CSF), and stem cell factor (SCF)) that support better engraftment of AML blast *in vivo* (25). Similarly, mice received two injections of TEG001 or TEG-LM1 mock in the presence of PAM and IL-2 (for the first TEGs injection) at Day 8 and Day 16 (Figure S3A). While we did not see elimination primary AML blasts over time, TEG001-treated mice consistently showed lower AML burden in comparison to mock-treated mice as measured in peripheral blood (Figure S3B). This result demonstrates antitumor activity of TEG001 against primary AML blasts *in vivo* as shown in two independent PD-X models.

Assessing the activity of TEG001 against healthy hematopoiesis *in vitro*

Next, we aimed to assess the toxicity of TEG001 against the hematopoietic compartment *in vitro*. Therefore, TEG001 and mock transduced T cells were incubated with the physiological hematopoietic target of γδT cells, namely CD14$^+$ monocytes, activated T cells as well as non-activated and activated B cells in the absence and presence of PAM. Similar to the efficacy study, we include the presence of PAM to enhance TEG001 recognition as previously shown (10). Daudi served again as a positive control. In an IFNγ ELIspot assay cytokine secretion was only observed against the positive control and CD14$^+$ monocytes in the presence of PAM, while other T and B cells did not induce IFNγ production (Figure 2A).
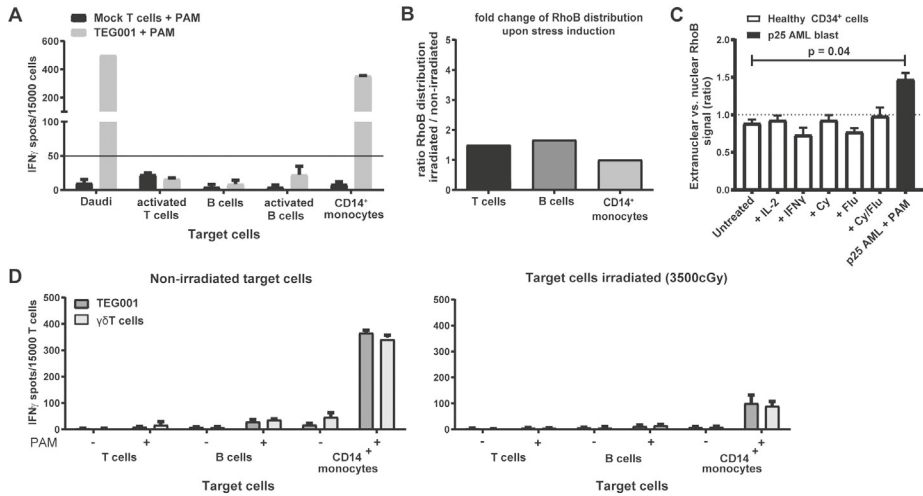
Figure 2 In vitro safety profile of TEG001. (A) Comparable recognition profile of Daudi tumor cells versus healthy hematopoietic cells. Effector cells TEG001 and target cells (E:T ratio 1:3) were incubated for 24 hours in the presence of 10 µM PAM. IFNγ secretion was measured by ELISPOT. IFNγ spots per 15,000 T cells are shown as mean±SD of at least 3 independent replicates for each target. Fifty spots/15,000 cells were considered as a positive recognition response and indicated by the black horizontal line. **(B)** RhoB distribution for healthy hematopoietic cells upon irradiation as analyzed by confocal microscopy in the presence of 10 µM PAM. Data is shown as fold-changed of RhoB distribution between irradiated cells (cellular stress condition) compared to non-irradiated cells from average ratio of at least ten different cells; **(C)** CD34+ progenitor cells from a healthy donor were treated with either 50 IU/ml IL-2, 1000 IU/ml IFNγ, 5mM Cy, 20µM Flu or combination of Cy/Flu. As positive control primary AML blast from donor p25 was treated with PAM. All cells were analyzed for intracellular distribution of RhoB using confocal microscopy. White bars represent healthy CD34+ progenitor cells, while black bar indicate primary AML blast (p25 AML). The RhoB signal ratio between nuclear and extranuclear cellular compartments was measured using ImageJ image analysis software. Graphs show average ratios of at least ten different cells ±SEM. Statistical significance compared to untreated CD34+ progenitor cells was determined by using Kruskal-Wallis test and Dunn's multiple comparison test; **(D)** Comparable recognition profile of healthy hematopoietic cells in non-stressed (left panel) and stressed (irradiated, right panel) conditions. Effector cells TEG001 and target cells (E:T ratio 1:3) were incubated for 24 hours in the presence of 100 µM PAM. IFNγ secretion was measured by ELISPOT. IFNγ spots per 15,000 T cells are shown as mean ± SD of at least 3 independent replicates for each target.

Translocation of RhoB towards the cell membrane has been described as a key step for the recognition of a potential target by a γ9δ2TCR (12). This insight allowed us to test whether an additional stress of hematopoietic cells would activate this key step in the mode of action and thereby facilitate recognition of healthy compartments. As "stress" we have chosen irradiation, which is well known to activate many innate danger signals like MHC-like molecules (26), and is frequently used as preconditioning before the transfer of immune cells (27). Therefore, we assessed the translocation of RhoB towards the cell membrane in T cells, B cells and CD14+ monocytes in the absence and presence of irradiation. No significant increase in translocation of RhoB to the cell membrane could be observed (Figure 2B) for the tested healthy hematopoietic cells. We also assessed the RhoB localization in healthy CD34+ progenitor cells upon stimulation

with cytokines, such as IL-2 and IFNγ, as well as the presence of chemotherapy agents Cy/Flu and compared to primary AML blast from donor p25. While there is a significant increase in RhoB localization towards cell membrane in p25 AML blast, there are no significant increased for the healthy CD34^{+} progenitor cells in all conditions (Figure 2C). Furthermore, the recognition profile by TEG001 of the same cell subsets after irradiation was assessed by cytokine secretion. Recognition of a *priori* non-recognized cells was not induced and recognition of CD14^{+} monocytes was slightly reduced after irradiation (Figure 2D). Overall, our results suggest that TEG001 does not attack subsets of healthy hematopoiesis in the absence or presence of stress. Only CD14^{+} monocytes can be recognized in the presence of PAM as reported also for natural γ9δ2T cells (10).

In vivo pharmacology and toxicology of TEG001

Assessment of different hematopoietic subsets by TEGs *in vitro* is very restricted due to the limited sub-fractions available for testing. In addition, it does not allow for assessment of whether early precursors are affected. Therefore, we established a HD-X model with human cord-blood derived CD34^{+} progenitor cells from six healthy donors repopulated in irradiated mice to further assess the safety profile of TEG001 against the hematopoietic compartment (Figure 3A). Engraftment of human leukocytes (huCD45^{+}) and other hematopoietic cellular subsets in peripheral blood was measured by flow cytometry (Figure S4A and S4B). When 500 huCD45^{+} cells/ml were detected in peripheral blood, treatment was initiated with either TEG001 or TEG-LM1 mock in the presence of PAM and IL-2 (for the first TEGs injection) to support TEGs activation and proliferation *in vivo*. While we observed a reduction of tumor burden by TEG001 (Figure 1D), no significant differences in engraftment of healthy hematopoietic cells between treatment groups were observed up to 50 days after infusion when assessed by huCD45^{+} (Figure 3B). TEG001 as well as TEG-LM1 cells could be detected after injection until the end of the study period in the peripheral blood of mice (Figure 3C).

Next, we investigated the reconstitution of diverse hematopoietic cellular subsets *in vivo* in more detail in the peripheral blood of mice. In particular, we were interested in the impact on monocytes given that *in vitro* natural γ9δ2T cells as well as TEG001 can recognize primary monocytes. Interestingly, neither CD14^{+} monocytes, nor CD19^{+} B cells, CD3^{+} T cells, or CD34^{+} progenitor cells were impaired in outgrowth when comparing mice injected with TEG001 or TEG-LM1 (Figure 4A-D). At the end of study period, we also obtained single cell suspension from spleen and bone marrow from three mice for both the TEG001 and TEG-LM1 mock group to analyze the reconstitution of similar cell subsets in more detail in primary tissues (Figure 5A-E). In line with our observations in peripheral blood, we could observe all relevant subsets, namely CD14^{+} monocytes, CD19^{+} B cells, CD3^{+} T cells, and CD34^{+} progenitor cells.

We next collected bone marrow cytospin samples from the same mice for a more detailed cytopathology analyses. All of the bone marrow samples from both treatment groups showed a pleomorphic population of cells derived from erythroid and myeloid lineages, with all the maturation stages (Figure 6A). In almost all samples (5/6) eosin-

ophilic differentiation was also evident. Beside normal blasts, an immature population with altered morphology (dysplastic immune cells), consistent with granular blasts was detected in both TEG001 and TEG-LM1 treated mice as well as cells with blast-like phenotypes with an indented nucleous, consistent with promonocytes (4/6), but no leukemic features were observed. Importantly, we did not observe any apparent differences in their outgrowth between treatment groups indicating that TEG001 do not harm the reconstitution of healthy hematopoietic compartments *in vivo*.
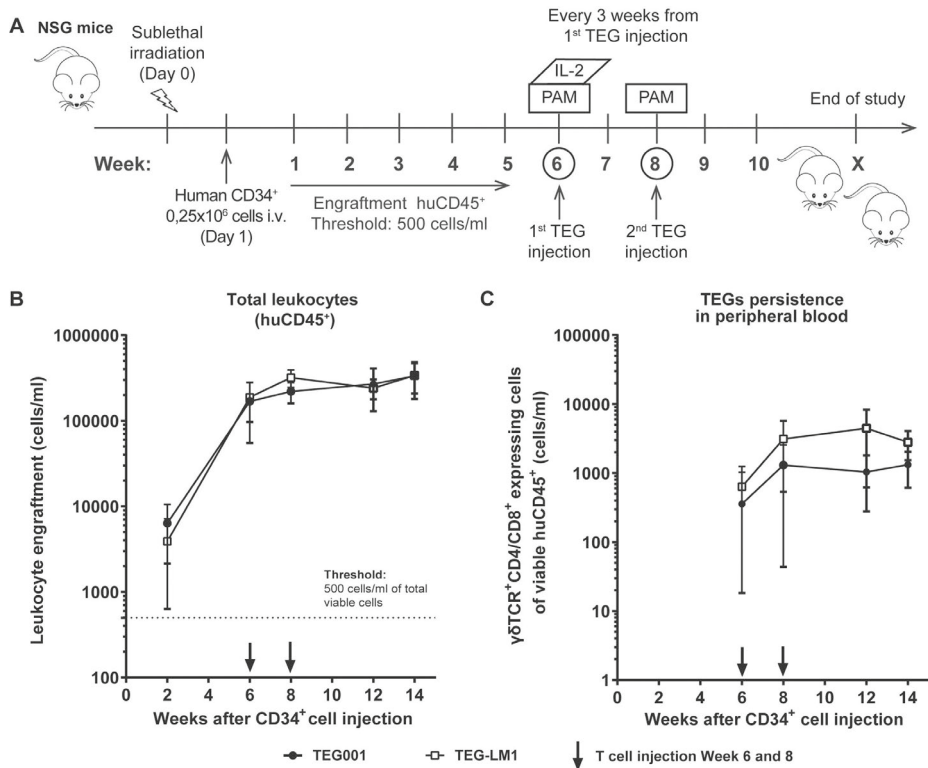

Figure 3 In vivo safety profile of TEG001. (A) Schematic overview of the safety experiment in healthy donor-derived xenograft (H DX) model. NSG mice were irradiated at day 0 and engrafted with healthy cord blood-derived CD34+ progenitor cells on day 1. Engraftment was followed up in peripheral blood by flow cytometry and when >500 huCD45+ cells/ml were present, mice received 2 injections of therapeutic TEG001 or TEG-LM1 mock in the presence of PAM (at week 6 and 8) and IL-2 (at week 6); **(B-C)** In vivo safety profile of TEG001 towards healthy human hematopoietic cells. Healthy human cells engrafted in NSG mice (B) with long term persistence of TEGs in peripheral blood (C). Data represent mean ± SD of all mice per group (n = 10).
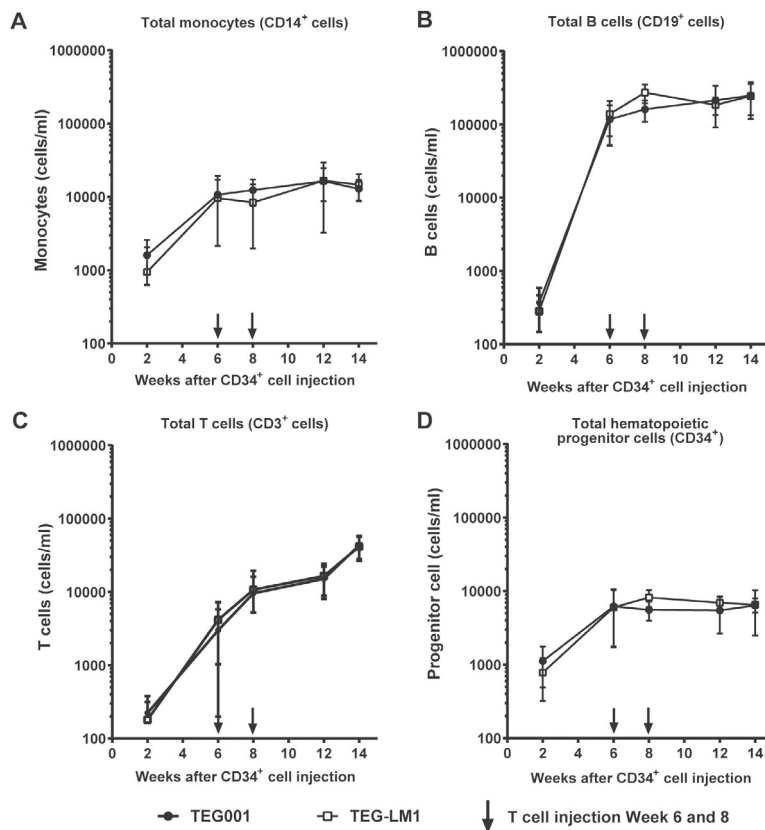
Figure 4 In vivo reconstitution of healthy human hematopoietic compartments in peripheral blood. Comparable profile between TEG001 and TEG-LM1 mock group of reconstituted healthy human hematopoietic cellular subsets, including CD14+ monocytes (A) B cells (B), T cells (C), and CD34+ progenitor cells (D) as measured by flow cytometry. Data represent mean ± SD of all mice per group (n = 10).

To evaluate off-target toxicity of TEG001 towards healthy tissues not related to the known mode of action which is absent in mice (21), we collected further mouse spleen, liver and intestine from three mice for each TEG001 and TEG-LM1 mock group and performed histopathology analyses. Spleen tissues showed non-neoplastic, lympho/histiocytic proliferative lesions in all the examined samples, of both treatment groups (Figure 6B). Similarly, no significant histological features of toxicity or other relevant abnormalities were observed in liver or intestine in all samples (Figure 6C-D). Most of the samples showed extramedullary hematopoiesis, mainly involving the erythroid lineage (extramedullary erythropoiesis) with scattered megakaryocytes sometimes evident, as a possible consequence of the engrafted human CD34+ progenitor cells in this mouse model. Overall, our data indicate there are no significant differences in histology features and notably, there are no off-target toxicities observed in all healthy tissues upon TEG001 treatment.

DISCUSSION

TEG001 has been selected as the first candidate for clinical testing (NTR6541) based on its superior recognition of hematological malignancies against both cell lines and primary AML *in vitro* and its ability to limit the tumor outgrowth in cell line-derived xenograft mouse models (10, 17, 18). Within this study, we have been able, for the very first time, to assess therapeutic efficacy towards primary AML blasts in a clinically relevant model with established leukemic load *in vivo*, while excluding toxicity against other hematopoietic stem cell compartments. Our current observation that primary AML can be eliminated in an *in vivo* model by TEG001, without affecting the hematopoietic compartment, is in line with our previous observation that an alteration in the RhoB-CD277J axis, the putative ligand of γ9δ2TCR, is selectively observed in the leukemic but not healthy hematopoietic stem cell (12).

A major challenge a *priori* clinical testing of novel cell-based and gene therapy products remains to assess efficacy and toxicity in relevant pre-clinical models in order to avoid unwanted toxicities like those reported for different CAR-T (28) or αβTCR gene therapy programs (29). This reflects the quite different characteristics of cell-based gene therapy medicinal products in comparison to conventional synthetic drugs. Thus, classical clinical considerations of therapeutic efficacy and safety assessments might no longer apply for these 'living' medicinal products.
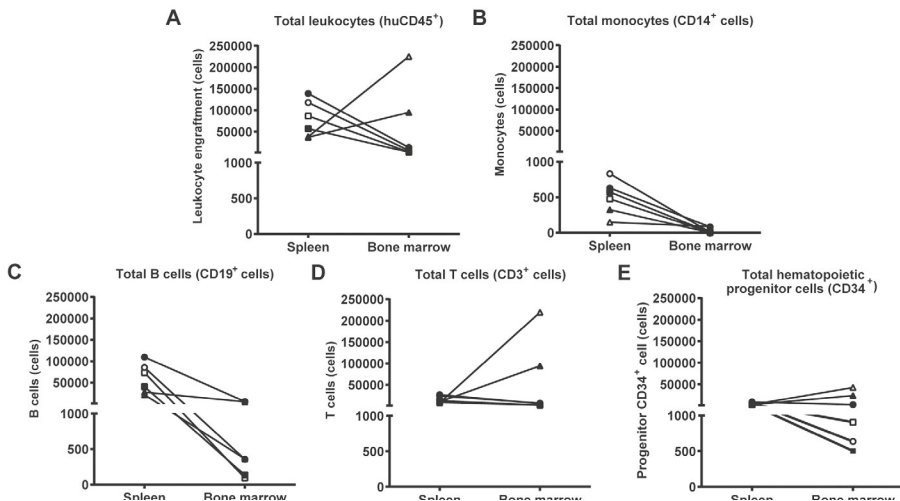

Figure 5 In vivo reconstitution of healthy human hematopoietic compartments in tissues. Comparable profile between TEG001 and TEG-LM1 mock group of reconstituted healthy human hematopoietic cellular subsets in spleen and bone marrow, including total human CD45+ leukocytes (A), CD14+ monocytes (B), B cells (C), T cells (D) and CD34+ progenitor cells (E) as measured by flow cytometry. Shown in the data from individual mouse (represented by different symbols) of both TEG001 (filled symbol) and TEG-LM1 mock (open symbol) group (n = 3 mice/group).
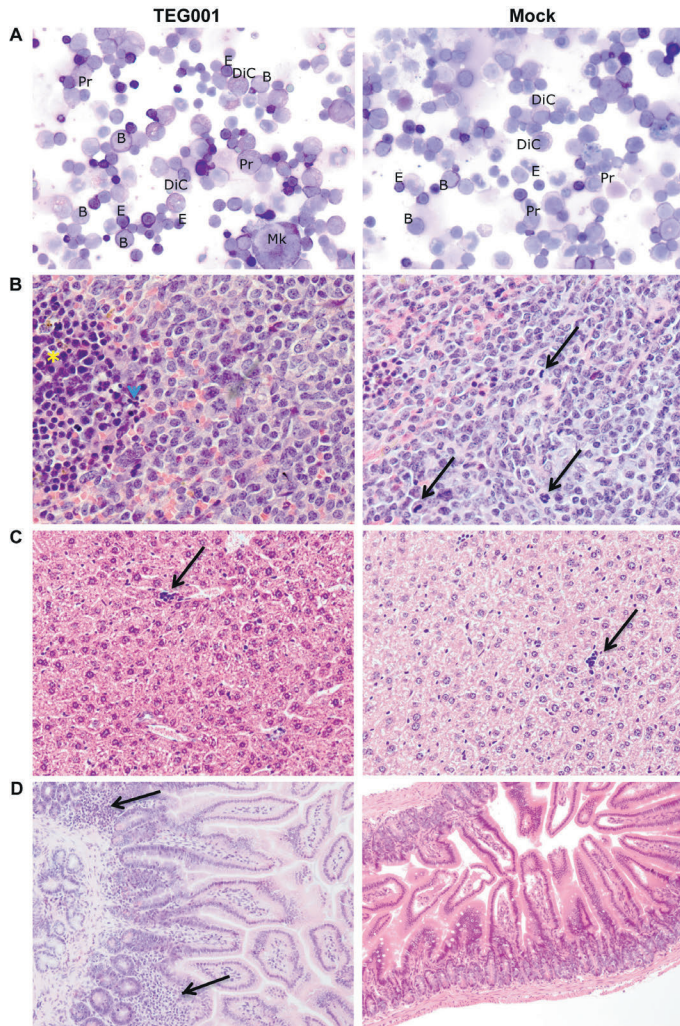
Figure 6 Cytopathology analysis of bone marrow and histopathology analysis of mouse vital organs (spleen, liver, intestine). (A) Representative picture of May-Grünwald Giemsa staining for bone marrow cytospin from both treatment groups (TEG001 and TEG-LM1 mock) with pleomorphic population of cells with all maturation stages including numerous blasts (B), promyelocytes (Pr), dysplastic immature cells (DiC), megakaryocytes (Mk) and a mixed population of myeloid and erythroid (E) lineages; **(B)** Representative pictures for H&E staining of mouse spleen for both treatment group (TEG001 and TEG-LM1 mock) with non-neoplastic, lympho/histiocytic hyperplastic lesion with mitotic figure (arrows), apoptotic bodies (arrowhead) and erythroid precursors (*). Magnification: 40X; **(C)** Representative pictures for H&E staining of mouse liver for both treatment group (TEG001 and TEG-LM1 mock) with small focus of extramedullary hematopoiesis (arrows) in all samples, which could be due to the mouse model with engraftment of human CD34+ progenitor cells. Magnification: 20X; **(D)** Representative pictures for H&E staining of mouse intestine for TEG001 treated group (left) showing multifocal lymphocytic infiltration of lymphoid cells (arrows) in a small tract of the small intestine (background lesion) and TEG-LM1 mock-treated group (right) with normal jejunum. Magnification: 10X. Shown are representative pictures from an individual mouse of both TEG001 and TEG-LM1 mock group (n = 3 mice/group) with no significant differences in overall cytopathology and histology features between treatment groups.

With TEG001, a next level of complexity is introduced due to the nature of the target. In contrast to, e.g., CD19-directed CAR T gene therapy, which targets a very well-defined protein expressed on cancer cells and B cells (5), TEG001 is targeting metabolic changes in stressed and malignant cells, driven by a dysregulated mevalonate pathway (11). Although transfer of conventional γ9δ2T cells has not been reported to associate with substantial toxicity (13), the TEG concepts express an activating γ9δ2TCR outside the context of its natural brakes, through a plethora of killer immunoglobulin-like receptor (KIR) inhibitory receptors usually operational in natural γ9δ2T cells. Therefore, Dutch authorities have required additional safety tests for TEG001 prior to clinical testing. However, dysregulated metabolic pathways do not allow for high throughput evaluations of the ligand in all tissues through, e.g., gene expression or transcriptome analyses (30). Consequently, following the advice of the Dutch authorities, our group developed different strategies to test the efficacy and safety of TEG001 in models where healthy and malignant cells are present either simultaneously or sequentially. One such model is a 3D bone marrow model where primary multiple myeloma cells grow out along with healthy stromal cells into an artificial bone marrow niche. Upon TEG001 injection, this model confirmed the activity of TEG001 against the malignant fraction, but not healthy bystander cells present in the bone marrow niche (24). However, the 3D bone marrow niche is also limited, as it does not allow for engrafting of the complex hematopoietic system and or assessing toxicity against all cellular compartments usually generated from a hematopoietic stem cell.

To study the interaction between tumor and immune cells, we have to consider also their interaction within the same microenvironment. Xia and colleagues (31) develop humanized mice model with human hematopoietic system and autologous leukemia in the same individual mouse. This model is developed by transducing CD34+ fetal liver cells with retroviral vector containing mixed-lineage leukemia MLL-AF9 fusion gene, which allows recapitulation of human leukemic diseases (31, 32). Although it would be interesting to develop a similar humanized mouse model in which healthy human hematopoietic cells and primary leukemic blasts presence in the same individual mouse, the availability of healthy human CD34+ progenitor cells from the very same leukemia patient is a limiting factor. Hence, we develop two separate mice models and thereby avoiding limiting criteria of HLA-matching between healthy CD34+ progenitor cells and primary AML donors.

In order to test the efficacy of TEG001, we utilized a mouse xenograft model, which has been widely used to study therapeutic responses in heterogeneous diseases such as cancer. PD-X models, considered to closely mimic human diseases, are established by engrafting primary patient material into immunodeficient mice (33). Assessment of AML burden in mouse xenograft models is commonly performed by measuring the percentage of human leukemic cells in bone marrow at the end of study period. In this study, we developed a stringent treatment model where we infused TEG001 upon the onset of the disease (represented by an arbitrary threshold of 500 AML cells/ml detected in peripheral blood). Moreover, we developed an elegant method that allowed us to

follow the disease progression for a longer period as well as the treatment effect to reduce tumor burden over time by measuring AML cells in peripheral blood. Nonetheless, we acknowledged some limitations in our method, such as variable engraftment rates commonly observed in PD-X model (34) and a low level of AML engraftment in peripheral blood of adult NSG mice as reported previously (35). In spite of these limitations, we were able to detect a significant reduction of AML cells in peripheral blood of TEG001-treated mice in comparison to the mock-treated group. Furthermore, we developed a separate PD-X model using NSG-SGM3 mice using the same primary AML blast from donor p25 to assess the influence of microenvironment towards TEG001 efficacy profile. NSG-SGM3 mice express human cytokines, including IL-3, GM-SCF, and SCF, and thereby supporting primary AML engraftment and their survival *in vivo* (25). Here we demonstrate that TEG001-treated group showed significantly lower AML burden in comparison to mock-treated group, despite the lack of tumor clearance. This could be due to the more protective microenvironment poses by NSG-SSGM3 mice, which could hamper T cell access to target cells and therefore limit the ability of TEG001 to clear primary AML burden over time. Based on the overall data and thus as proof-of-principle we have demonstrated the efficacy profile of TEG001 against primary human AML in two independent models.

In order to assess the toxicity of TEG001 against the hematopoietic compartment in the very same model we engrafted NSG mice with CD34^{+} progenitor cells derived from healthy human cord blood donors. Reconstitution of hematopoietic cellular compartments when assessed in the peripheral blood occurred at different stages, in which CD14^{+} monocytes and CD19^{+} B cells significantly increased two weeks after progenitor cell injection, whereas CD3^{+} T cells reconstituted relatively slower, however no differences could be observed between TEG001 and mock-treated mice. Furthermore, we investigated whether TEG001 does affect hematopoietic compartments in different tissues, specifically spleen and bone marrow, at which progenitor cells should reside (36, 37). While we could find all equivalent cell subsets with comparable reconstitution for both treatment groups also in spleen and bone marrow, there were differences in the prevalence for CD14^{+} monocytes and CD19^{+} B cells in different tissues, however again with no difference between TEG001 and mock treated mice. Monocytes were found in higher numbers in the peripheral blood when compared to bone marrow and spleen, whereas B cells were prevalently observed in the periphery and spleen. This observation is in line with previous studies showing that the reconstitution of human hematopoietic stem cells in host mice is commences predominantly with erythroid and myeloid cells, followed by lymphoid progenitor and lastly mature lymphocytes (38). Also, neither induction of cellular stress by irradiation nor exposure to inflammatory cytokines (i.e., IL-2 and IFNγ), or the presence of chemotherapy agent Cy/Flu alter RhoB translocation towards the cell membrane for healthy CD34^{+} progenitor cells, and thus no alteration of TEG001 recognition pattern. In addition, our data confirm that different tissue compartments are comprised of different types of immune cells; and show that TEG001 treatment did not influence this pattern. Thus TEG001 most likely does not affect homing of hematological subsets nor mediate hematopoietic toxicity, as suggested by our previous work

demonstrating that the mode of action is mainly observed in tumor cells and not in the healthy hematopoietic compartment (12, 19). The only physiological target of γ9δ2TCRs are professional antigen presenting cells (APC) like monocytes and dendritic cells in the presence of PAM (18), as also demonstrated in this study in the *in vitro* experiments. However, as reported previously, this recognition apparently fosters the maturation of APC and potentially broadens an adaptive immune response through epitope spreading (39) rather than promoting elimination of APC. In line with this assumption, we could still detect CD14+ monocytes reconstitution *in vivo* after transfer of TEG001.

CONCLUSION

In conclusion, our data suggest antitumor reactivity of TEG001 against primary AML blasts *in vivo*. While we concur that the absence of evidence is not equal to the evidence of absence and within the limitation of our current models where off-target activities cannot be excluded entirely, there are no data indicating an increased safety risk specific for TEG001. A GMP-compliant production of TEG001 has now been established (17, 40), and will be used in an ongoing phase I open-label dose escalation study to explore toxicity and activity of TEG001 in patients with primary refractory or relapsed acute myeloid leukemia, as well as patients with multiple myeloma.

REFERENCES

1. Chabannon C, Kuball J, Bondanza A, Dazzi F, Pedrazzoli P, Toubert A, *et al*. Hematopoietic stem cell transplantation in its 60s: A platform for cellular therapies. *Sci Transl Med*. 2018;10(436).

2. Srivastava S, Riddell SR. Engineering CAR-T cells: Design concepts. *Trends Immunol*. 2015;36(8):494-502.

3. Kuball J, Hauptrock B, Malina V, Antunes E, Voss RH, Wolfl M, *et al*. Increasing functional avidity of TCR-redirected T cells by removing defined N-glycosylation sites in the TCR constant domain. *J Exp Med*. 2009;206(2):463-75.

4. Kuball J, Dossett ML, Wolfl M, Ho WY, Voss RH, Fowler C, *et al*. Facilitating matched pairing and expression of TCR chains introduced into human T cells. *Blood*. 2007;109(6):2331-8.

5. Turtle CJ, Maloney DG. Clinical trials of CD19-targeted CAR-modified T cell therapy; a complex and varied landscape. *Expert Rev Hematol*. 2016;9(8):719-21.

6. Jetani H, Garcia-Cadenas I, Nerreter T, Thomas S, Rydzek J, Meijide JB, *et al*. CAR T-cells targeting FLT3 have potent activity against FLT3-ITD+ AML and act synergistically with the FLT3-inhibitor crenolanib. *Leukemia*. 2018;32(5):1168-79.

7. Lonez C, Verma B, Hendlisz A, Aftimos P, Awada A, Van Den Neste E, *et al*. Study protocol for THINK: a multinational open-label phase I study to assess the safety and clinical activity of multiple administrations of NKR-2 in patients with different metastatic tumour types. *BMJ Open*. 2017;7(11):e017075.

8. Alexandrov LB, Nik-Zainal S, Wedge DC, Aparicio SA, Behjati S, Biankin AV, *et al*. Signatures of mutational processes in human cancer. *Nature*. 2013;500(7463):415-21.

9. van Loenen MM, de Boer R, Hagedoorn RS, van Egmond EH, Falkenburg JH, Heemskerk MH. Optimization of the HA-1-specific T-cell receptor for gene therapy of hematologic malignancies. *Haematologica*. 2011;96(3):477-81.

10. Marcu-Malina V, Heijhuurs S, van BM, Hartkamp L, Strand S, Sebestyen Z, *et al*. Redirecting αβT cells against cancer cells by transfer of a broadly tumor-reactive γδT-cell receptor. *Blood*. 2011; 118(1):50-9.

11. Gober HJ, Kistowska M, Angman L, Jeno P, Mori L, De LG. Human T cell receptor γδ cells recognize endogenous mevalonate metabolites in tumor cells. *J Exp Med*. 2003;197(2):163-8.

12. Sebestyen Z, Scheper W, Vyborova A, Gu S, Rychnavska Z, Schiffler M, *et al*. RhoB Mediates Phosphoantigen Recognition by Vγ9Vδ2 T Cell Receptor. *Cell Rep*. 2016;15(9):1973-85.

13. Deniger DC, Moyes JS, Cooper LJ. Clinical applications of γδT cells with multivalent immunity. *Front Immunol*. 2014;5:636.

14. Kunzmann V, Bauer E, Feurle J, Weissinger F, Tony HP, Wilhelm M. Stimulation of γδT cells by aminobisphosphonates and induction of antiplasma cell activity in multiple myeloma. *Blood*. 2000;96(2):384-92.

15. Scheper W, Grunder C, Straetemans T, Sebestyen Z, Kuball J. Hunting for clinical translation with innate-like immune cells and their receptors. *Leukemia*. 2014;28(6):1181-90.

16. Scheper W, Sebestyen Z, Kuball J. Cancer Immunotherapy Using γδT Cells: Dealing with Diversity. *Frontiers in immunology*. 2014;5:601.

17. Straetemans T, Grunder C, Heijhuurs S, Hol S, Slaper-Cortenbach I, Bonig H, *et al*. Untouched GMP-Ready Purified Engineered Immune Cells to Treat Cancer. *Clin Cancer Res*. 2015; 21(17): 3957-68.

18. Grunder C, van DS, Hol S, Drent E, Straetemans T, Heijhuurs S, *et al*. γ9 and δ2CDR3 domains regulate functional avidity of T cells harboring γ9δ2TCRs. *Blood*. 2012;120(26):5153-62.

19. Gu S, Borowska MT, Boughter CT, Adams EJ. Butyrophilin3A proteins and Vγ9Vδ2T cell activation. *Semin Cell Dev Biol*. 2018.

20. Gu S, Sachleben JR, Boughter CT, Nawrocka WI, Borowska MT, Tarrasch JT, *et al*. Phosphoantigen-induced conformational change of butyrophilin 3A1 (BTN3A1) and its implication on Vγ9Vδ2 T cell activation. *Proc Natl Acad Sci USA*. 2017;114(35):E7311-E20.

21. Harly C, Guillaume Y, Nedellec S, Peigne CM, Monkkonen H, Monkkonen J, *et al*. Key implication of CD277/butyrophilin-3 (BTN3A) in cellular stress sensing by a major human γδT-cell subset. *Blood*. 2012;120(11):2269-79.

22. Palakodeti A, Sandstrom A, Sundaresan L, Harly C, Nedellec S, Olive D, *et al*. The molecular basis for modulation of human Vγ9Vδ2 T cell responses by CD277/butyrophilin-3 (BTN3A)-specific antibodies. *J Biol Chem*. 2012;287(39):32780-90.

23. Vavassori S, Kumar A, Wan GS, Ramanjaneyulu GS, Cavallari M, El Daker S, *et al*. Butyrophilin 3A1 binds phosphorylated antigens and stimulates human γδT cells. *Nat Immunol*. 2013; 14(9): 908-16.

24. Braham MVJ, Minnema MC, Aarts T, Sebestyen Z, Straetemans T, Vyborova A, *et al*. Cellular immunotherapy on primary multiple myeloma expanded in a 3D bone marrow niche model. *Oncoimmunology*. 2018:e1434465.

25. Wunderlich M, Chou FS, Link KA, Mizukawa B, Perry RL, Carroll M, *et al*. AML xenograft efficiency is significantly improved in NOD/SCID-IL2RG mice constitutively expressing human SCF, GM-CSF and IL-3. *Leukemia*. 2010;24(10):1785-8.

26. Gleimer M, Parham P. Stress management: MHC class I and class I-like molecules as reporters of cellular stress. *Immunity*. 2003;19(4):469-77.

27. Dudley ME, Yang JC, Sherry R, Hughes MS, Royal R, Kammula U, *et al*. Adoptive cell therapy for patients with metastatic melanoma: evaluation of intensive myeloablative chemoradiation preparative regimens. *J Clin Oncol*. 2008;26(32):5233-9.

28. Neelapu SS, Tummala S, Kebriaei P, Wierda W, Gutierrez C, Locke FL, *et al*. Chimeric antigen receptor T-cell therapy - assessment and management of toxicities. *Nat Rev Clin Oncol*. 2018; 15(1):47-62.

29. Linette GP, Stadtmauer EA, Maus MV, Rapoport AP, Levine BL, Emery L, *et al*. Cardiovascular toxicity and titin cross-reactivity of affinity-enhanced T cells in myeloma and melanoma. *Blood*. 2013;122(6):863-71.

30. Novosiadly R, Kalos M. High-content molecular profiling of T-cell therapy in oncology. *Mol Ther Oncolytics*. 2016;3:16009.

31. Xia J, Hu Z, Yoshihara S, Li Y, Jin CH, Tan S, *et al*. Modeling Human Leukemia Immunotherapy in Humanized Mice. *EBioMedicine*. 2016;10:101-8.

32. Barabe F, Kennedy JA, Hope KJ, Dick JE. Modeling the initiation and progression of human acute leukemia in mice. *Science*. 2007;316(5824):600-4.

33. Lai Y, Wei X, Lin S, Qin L, Cheng L, Li P. Current status and perspectives of patient-derived xenograft models in cancer research. *J Hematol Oncol*. 2017;10(1):106.

34. Siolas D, Hannon GJ. Patient-derived tumor xenografts: transforming clinical samples into mouse models. *Cancer Res*. 2013;73(17):5315-9.

35. Sanchez PV, Perry RL, Sarry JE, Perl AE, Murphy K, Swider CR, *et al*. A robust xenotransplantation model for acute myeloid leukemia. *Leukemia*. 2009;23(11):2109-17.

36. Frasca D, Guidi F, Arbitrio M, Pioli C, Poccia F, Cicconi R, *et al*. Hematopoietic reconstitution after lethal irradiation and bone marrow transplantation: effects of different hematopoietic cytokines on the recovery of thymus, spleen and blood cells. *Bone Marrow Transplant*. 2000;25(4):427-33.

2

37. Serafini M, Dylla SJ, Oki M, Heremans Y, Tolar J, Jiang Y, *et al*. Hematopoietic reconstitution by multipotent adult progenitor cells: precursors to long-term hematopoietic stem cells. *J Exp Med*. 2007;204(1):129-39.

38. Miller SC. Hematopoietic reconstitution of irradiated, stem cell-injected mice: early dynamics of restoration of the cell lineages of the spleen and bone marrow. *J Hematother Stem Cell Res*. 2002;11(6):965-70.

39. Gulley JL, Madan RA, Pachynski R, Mulders P, Sheikh NA, Trager J, *et al*. Role of Antigen Spread and Distinctive Characteristics of Immunotherapy in Cancer Treatment. *J Natl Cancer Inst*. 2017;109(4).

40. Straetemans T, Kierkels G, Doorn R, Jansen K, Heijhuurs S, dos Santos J, *et al*. GMP-Grade Manufacturing of T Cells Engineered to Express a Defined γδTCR. *Frontier in Immunology*. 2018;9:1062.

SUPPLEMENTARY MATERIALS AND METHODS

Cells and cell lines

Daudi and Phoenix-Ampho were obtained from ATCC (authenticated by short tandem repeat profiling/karyotyping/isoenzyme analysis). Daudi cells were cultured in RPMI media supplemented with 10% fetal calf serum (FCS) and 1% Pen/Strep. Phoenix-Ampho cells were cultured in DMEM media supplemented with 10% FCS and 1% Pen/Strep. All cells were passaged for a maximum of 2 months, after which new seed stocks were thawed for experimental use. Furthermore, all cell lines were routinely verified by growth rate, morphology, and/or flow cytometry and tested negative for mycoplasma using MycoAlert Mycoplasma Kit. Peripheral blood mononuclear cells (PBMCs) were isolated using Ficoll gradient centrifugation methods from buffy coats obtained from Sanquin Blood bank (Amsterdam, The Netherlands).

Primary materials

Primary AML blasts were obtained from biobank of University Medical Center Utrecht in accordance with good clinical practice and Declaration of Helsinki regulations. All patients gave their consent prior to storage in the biobank (TCBio 16-088). For *in vivo* experiments, apheresis material from primary AML material from donor p25 was depleted for $CD3^+$ cells using human CD3 Microbeads (Miltenyi Biotech) per the manufacturer's protocol. Human $CD34^+$ derived from cord blood of six healthy donors were isolated using anti-CD34 magnetic beads separation (Miltenyi Biotec), and are obtained as a kind gift from Dr. Maud Platinga (University Medical Center Utrecht).

Retroviral transductions of T cells

TEGs were produced as previously described (10). Briefly, packaging cells (Phoenix-Ampho) were transfected with helper constructs gag-pol (pHIT60), env (pCOLT-GALV) and pMP71 retroviral vectors containing both γδTCR chains separated by a ribosomal skipping T2A sequence, using FugeneHD reagent (Promega). Human PBMCs from a healthy donor were pre-activated with anti-CD3 (30 ng/mL; Orthoclone OKT3; Janssen-Cilag) and IL-2 (50 IU/mL; Proleukin, Novartis) and subsequently transduced twice with viral supernatant within 48 hours in the presence of 50 IU/mL IL-2 and 6 mg/mL polybrene (Sigma-Aldrich). TCR-transduced T cells were expanded by stimulation with anti-CD3/CD28 Dynabeads (500,000 beads/10^6 cells; Life Technologies) and IL-2 (50 IU/mL). Thereafter, TCR-transduced T cells were depleted of the non-engineered T cells.

Depletion of non-engineered T cells

Depletion of non-engineered T cells was performed as previously described (17). Briefly, γδTCRs transduced αβT cells were incubated with a biotin-labeled anti-αβTCR antibody (clone BW242/412; Miltenyi Biotec) and subsequently incubated with an anti-biotin antibody coupled to magnetic beads (anti-biotin MicroBeads; Miltenyi Biotec). Thereafter, the cell suspension was loaded onto an LD column and αβTCR$^+$ T cells were depleted by MACS cell separation per the manufacturer's protocol (Miltenyi Biotec). After depletion, TEGs were expanded using T cell REP.

2

CFU assay

Colony formation unit assay: 0,125 × 10⁶ primary AML blasts from donor p2 were pre-incubated with medium only with 1,25 × 10⁶ TEG001 or bulk αβT cells (as mock T cells) in the presence of 100 μM pamidronate (PAM) for 5 hours at 37°C prior to plating in Methylcellulose-based medium with recombinant cytokines (MethoCult™ H4434 Classic, StemCell Technologies). Cultures were incubated in 37° at 5% CO_2 for 8 days and colonies were counted using an inverted microscope.

Flow cytometry analysis

The following antibodies were used for flow cytometry analysis: huCD45-PB (clone HI30, Sony Biotechnology), mCD45-APC (clone 30-F11, Sony Biotechnology), CD13-PECy7 (clone WM15, Sony Biotechnology), CD33-BV711 (clone WM33, Sony Biotechnology), pan-γδTCR-PE (clone IMMU510, Beckman-Coulter), CD3-AF700 (clone UCHT1, Biolegend), CD8-PerCPCy5.5 (clone RPA-T8, Biolegend), CD8-FITC (clone TPA-T8, BD Biosciences), CD4-FITC (clone TPA-R4, Biolegend), CD34-BV650 (clone 581, BD Biosciences), CD19-PerCPCy5.5 (clone HIB19, BD Biosciences), CD14-APCeFluor780 (clone 61D3, eBioscience). To exclude non-viable cells from the analysis, Fixable Viability Dye eFluor506 was used (eBioscience). All samples were analyzed on BD LSRFortessa using FACSDiva Software (BD Biosciences).

Assessment for human cell engraftment

Peripheral blood samples were obtained via cheek vein (max. 100-200μl/mouse) every 1-2 weeks. Human cells in peripheral blood were quantified using Flow-count Fluorospheres (Beckman Coulter). Red blood cell lysis was performed for blood samples using 1X RBC lysis buffer (Biolegend) before cell staining. Blood samples were stained with a mixed of antibody panels as listed above. Engraftment and tumor burden was measured in peripheral blood by quantifying for absolute cell number by flow cytometry using specific markers huCD45⁺CD13⁺CD33⁺ for primary AML blasts and huCD45⁺ for healthy progenitor cells, respectively. An arbitrary threshold of 500 cells/ml was chosen to represent established human cell engraftment.

Preparation of single cell suspensions

At the end of the study, bone marrow (mixed from tibia and femur) and spleen sections were isolated and processed into single cell suspension. Femur and tibia from the hind legs were collected; bone marrow cells were collected by centrifugation of the bones at 10,000 rpm for 15 seconds and resuspension of the cells in RPMI media. Bone marrow cells were also used to make cytospin slides (1 million cells per slide per mouse) for further cytopathology analysis. A small section of the spleen was minced and passed through a 70μm cell strainer (BD); cells were washed in PBS and resuspended in RPMI media. A total of 500,000 cells were stained and analyzed for human hematopoietic cellular compartments by flow cytometry analysis (BD LSRFortessa). Human cells from spleen and bone marrow were measured by quantifying absolute cell number from total 500,000 cells using Flow-count Fluorospheres (Beckman Coulter) for each hematopoietic cellular compartment.

Table S1. Characterization of primary AML-patient samples

| Donor	Classification [1]	% blast [2]	Major phenotype	Cytogenetic	Risk classification
p1	Transformation of CML to myeloid blast crisis	80%	CD34+, CD117+, CD13+, CD36+, CD33+, CD45low, HLA-DR+, MPO+, CD19+, CD22-, cTdT+, CD79a+	BCR-ABL1 fusion mRNA type Major (~t(9;22) (q34;q1))	N/A [3]
p2	M5	47% blasts, 18% monocytic cells	Blasts: CD34+, CD117+, HDL-DR+, CD13+, CD7+, CD11c+, CD56+, cCD3low, cMPOlow. Monocytic cells: CD36+, CD14+, CD11b+, CD13+, CD33+, HLA-DR+, CD3low, CD56+	Monosomy chromosome 7	Poor
p4	M4eo	46%	CD34+, CD117+, CD45low, CD33+, CD13+, HLA-DR+, CD38low, CD65+, cMPO+, cTDTlow	Inversion chromosome 16 (inv(16)(p13q22))	Good
p6	AML with monocytic maturation	88%	CD45low, CD33+, CD11blow, CD11c+, CD15+, CD36low, CD65+, CD4low, CD117+, HLA-DR+, CD38+, CD56+, CD113+, CD79a+	Complex karyotype	Very poor
p10	M4/M5 with extramedullary manifestations	50%	CD45low, CD117low, cMPOlow, CD13+, CD33+, CD38+, HLA-DR+, CD11blow, CD36+, CD65+, CD4low	Normal karyotype No abnormalities detected	Poor
p13	M5	85%	CD45low, CD33+, CD38+, CD4low, CD11c+, cCD79a+, cMPO+, CD14+, CD13+, CD36+, HLA-DR+, CD11b+, CD65+	MLL-MLLT3 fusion mRNA, 46XY, (t(9;11)(p21;q23))	Poor
p25	M5A	96%	CD45low, cMPO+, CD34+, CD117+, CD33+, CD13+, CD38+, HLA-DR+, CD36+, CD14+, CD15+ and CD11b+	Extra chromosome 8 No other abnormalities	Poor

[1] Based on the French-American-British (FAB) classification in accordance to WHO 2008

[2] Measured in the blood at the moment of diagnosis

[3] Not applicable, data is not available for this patient
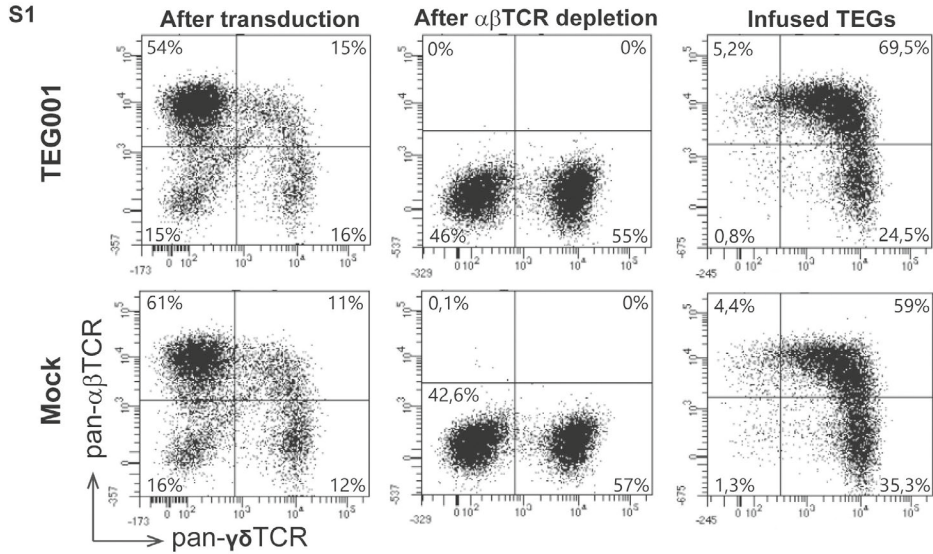
2

S1

Supplementary Figure S1 γδTCR expression of TEG001 and TEG-LM1 mock. A representative flow cytometry plot γδTCR expression of TEG001 and TEG-LM1 mock after transductions, after aβTCR depletion and prior to infusion into mice after 2 weeks expansion.

S2
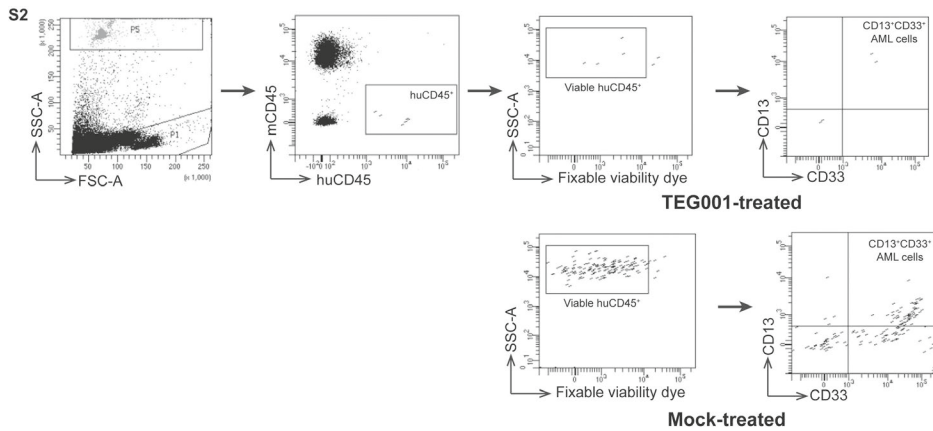
Supplementary Figure S2 Gating strategy for flow cytometry analysis of primary AML burden. A representative flow cytometry plot of murine peripheral blood. Tumor load was measured by quantifying absolute cell number of viable huCD45+CD13+CD33+ of the primary AML blast and representative plot for TEG001 and TEG-LM1 mock group.
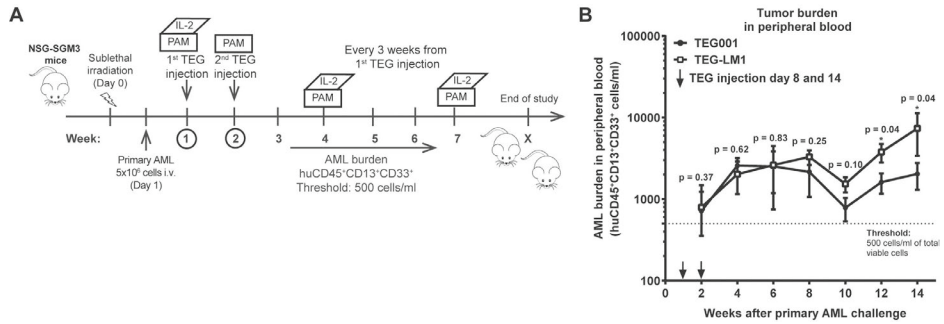
Supplementary Figure S3 In vivo efficacy profile of TEG001 in PD-X model of primary blast in NSG-SGM3 mice. (A) Schematic overview of in vivo experiment. NSG-SGM3 mice were irradiated at day 0 and engrafted with primary AML cells at day 1. AML cells were followed-up in the peripheral blood by flow cytometry. Mice received 2 injections of therapeutic TEG001 or TEG-LM1 mock in the presence of PAM (at Day 8 and 16) and IL-2 (at Day 8); (B) Tumor burden for primary AML was measured in peripheral blood by quantifying for absolute cell number by flow cytometry. Data represent mean ± SD of all mice per group (n = 5 mice/group). Statistical significances were calculated by non-parametric 2-tailed Mann-Whitney t test; *, $P < 0.05$; **, $P < 0.01$; ***, $P < 0.001$; ****, $P < 0.0001$.
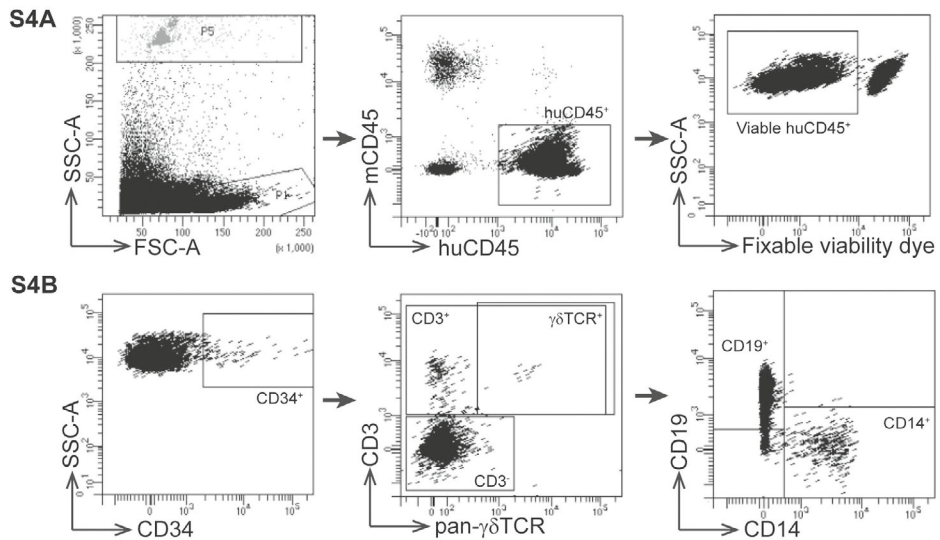
Supplementary Figure S4 Gating strategy for flow cytometry analysis of healthy hematopoietic compartments. A representative flow cytometry plot of murine peripheral blood. (A) Engraftment was determined by quantifying absolute cell number of viable huCD45+ of healthy stem cells; (B) Hematopoietic cellular compartments outgrowth were determined by quantifying absolute cell number for CD19+ B cells, CD3+ T cells, and CD14+ monocytes. Also, persistence of TEGs were determined by quantifying absolute cell number for γδTCR+ cells.

CHAPTER 3

Identification of a tumor-specific allo-HLA-restricted γδTCR

G.J.J. Kierkels[1#], W. Scheper[1#], A.D. Meringa[1#], I. Johanna[1#], D.X. Beringer[1] A. Janssen[1], M. Schiffler[1], T. Aarts-Riemens[1], L. Kramer[1], T. Straetemans[1], S. Heijhuurs[1], J.H.W. Leusen[1], E. San José[2], K. Fuchs[3], M. Griffioen[3], J.H. Falkenburg[3], L. Bongiovanni[4], A. de Bruin[4], D. Vargas-Diaz[5], M. Altelaar[5], A.J.R. Heck[5], L.D. Shultz[6], F. Ishikawa[7], M. I. Nishimura[8], Z. Sebestyén[1##], J. Kuball[1,9*##]

[1] Laboratory of Translational Immunology, University Medical Center Utrecht, Utrecht University, The Netherlands
[2] Universidad Europea de Madrid, Spain
[3] Department of Hematology, Leiden University Medical Center, Leiden, the Netherlands
[4] Department of Pathobiology, Faculty of Veterinary Medicine, Dutch Molecular Pathology Center, Utrecht University, Utrecht, The Netherlands.
[5] Biomolecular Mass Spectrometry and Proteomics, Bijvoet Center for Biomolecular Research and Utrecht Institute for Pharmaceutical Sciences, Utrecht University, Padualaan 8, 3584 CH Utrecht, The Netherlands
[6] Department of Immunology, The Jackson Laboratory, Bar Harbor, Maine, USA
[7] Laboratory for Human Disease Models, RIKEN Center for Integrative Medical Sciences, Yokohama 230-0045, Japan
[8] Department of Surgery, Cardinal Bernardin Cancer Center, Loyola University Chicago, Maywood, IL, USA.
[9] Department of Hematology, University Medical Center Utrecht, The Netherlands

[#] These authors contributed equally to this work
[##] Shared senior authors

ABSTRACT

γδT-cells are key players in cancer immune surveillance due to their ability to recognize malignant transformed cells, which makes them promising therapeutic tools in the treatment of cancer. However, the biological mechanisms of how γδT-cell receptors (TCR) interact with their ligands are poorly understood. Within this context we describe a novel allo-HLA-restricted and CD8α-dependent Vγ5Vδ1TCR. In contrast to the previous assumption of the general allo-HLA reactivity of a minor fraction of γδTCRs, we show that classical anti-HLA-directed γδTCR mediated reactivity can selectively act towards hematological and solid tumor cells, while not harming healthy tissues *in vitro* and *in vivo*. We identified the molecular interface with close proximity to the peptide-binding groove of HLA-A*24:02 as the essential determinant for recognition and describe the critical role of CD8 as co-receptor. We conclude that allo-reactive γδT-cell repertoires provide therapeutic opportunities either within the context of haplo-transplantation or as individual γδTCRs for genetic engineering of tumor reactive T-cells.

INTRODUCTION

Human immunity is organized by interacting innate and adaptive immune subsystems that elicit a fast or durable response respectively. γδT-cells are situated between the innate and adaptive immune systems as they share properties of both systems, illustrated by their ability to recognize malignant transformed (1), or infected (2) cells, to clonally expand, and to form memory (3). Recently, the important biological role of γδT-cells in cancer immune surveillance has been further highlighted by the fact that γδT-cells infiltrate various tumors (4, 5). However, the biological understanding of cancer immune surveillance and potential clinical applicability of γδT-cells, or their individual receptors, is substantially hampered by the lack of well-defined γδT-cell receptor (TCR) ligands as well as their precise molecular requirements for recognition (6). γδT-cell ligands that have been identified so far are mostly associated with metabolic changes in stressed cells, e.g. Vγ9Vδ2 T-cells, the major subset of γδT-cells in the periphery, are activated by cells with an increase of intracellular phosphoantigens caused by a dysregulated mevalonate pathway due to transformation or infection (7, 8). γδT-cell that do not express a Vδ2-chain, collectively called Vδ2-negative γδT-cells, are mainly found in tissues and are activated by stress-related ligands such as EPCR (9), MICA (10), and Annexin A2 (11). Furthermore, CD1c and CD1d can present self and foreign lipid antigens to Vδ2-negative γδT-cells in a classical αβT-cell HLA-like fashion (12). Since ligands of both Vδ2-positive and Vδ2-negative γδT-cells are to some extend constitutively expressed on healthy cells, it remains unclear how exactly the balance between self and tumor or infection is orchestrated. Recent data suggests that receptors, such as Vγ9Vδ2TCRs, modulate the delicate line between healthy and diseased tissue by sensing spatial and conformational changes of membrane expressed CD277, which occurs in transformed cells (8, 13). To exploit γδT-cells or their receptors as therapeutical tools, the understanding of the localization and structure of the ligands during stress or transformation needs to be understood. Furthermore, identifying new γδTCR ligands restricted to stressed or transformed cells is valuable for developing therapies for unmet medical needs. Within this context, we aimed to identify a potential ligand of a Vδ1-positive γδT-cell clone, which has been classified as reactive against different tumor cell types, as well as to understand the molecular interaction of this receptor with its ligand (2).

3

MATERIALS AND METHODS

Cells lines and Flow cytometry (see supplementary methods)

Generation of γδT-cell clone FE11
Clone FE11 was generated as described in a previous publication (2).

Cloning NEF134-144 and WT1126-134 -specific αBTCRs

The HLA-A*02:01 restricted WT1$_{126\text{-}134}$-specific αBTCR (14) and HLA-A*24:02 restricted NEF$_{134\text{-}144}$ αBTCR (Clone C1-28 (15)) were codon-optimized, synthesized at BaseClear (Leiden, The Netherlands) and subcloned into the retroviral pBullet vector.

Retroviral transduction of TCRs

Details are provided in supplementary methods and our previous publication (16).

Retroviral transduction of HLA

Phoenix-ampho retroviral packaging cells were transduced with pLZRS-A*02:01-IRES-NG-FR or pLZRS-A*24:02-IRES-NGFR and the retroviral packaging plasmids gag-pol (pHIT60) and env (pCOLT-GALV) using Fugene-HD. The HLA plasmids were kindly provided by Marieke Griffioen (Leiden University Medical Centre, the Netherlands).

CRISPR/Cas genome editing

The ß2m gene-specific regions of the gRNA sequence (GAGTAGCGCGAGCACAGCTA) was designed by the CRISPR design tool from the Zhang lab (http://crispr.mit.edu/). As control gRNA, the eGFP gene was targeted (GGAGCGCACCATCTTCTTCA). The pSicoR-CRIS-PR-Cas9 vector used was a kind gift from Robert Jan Lebbink (University Medical Center Utrecht, The Netherlands). LCL-TM cells were transduced with the viral supernatants, knockdown of ß2M was confirmed by flow cytometry.

Functional T cell assays

IFNγ ELISA and ELISPOT were performed as previously described (2, 16) and in supplementary methods.

Flow cytometry FRET

To study dimerization of HLA, cells were labelled with Alexa594-conjugated α-HLA-A (donor) and Alexa647-conjugated α-HLA-A (acceptor), respectively. The donor fluorescence was measured using a FACS LSRFortessa flow cytometer (BD) where donor fluorescence of the double-labeled healthy samples was compared with that of the double-labeled malignant samples. FRET efficiency was calculated from the fractional decrease of the donor fluorescence in the presence of the acceptor, using the equations as described by Sebestyen and colleagues (17). Correction factors for the spectral overlap between the different fluorescence channels were obtained from data measured on unlabeled and single-labeled cells.

Animal model

The NOD.Cg-$Prkdc^{scid}Il2rg^{tm1Wjl}$Tg(HLA-A24)3Dvs/Sz (NSG-A24) mice (18) were kindly provided by Leonard D. Shultz (The Jackson Laboratory, Bar Harbor, ME, USA). C57BL/6 mice were purchased from Janvier (Le Genest-Saint-Isle, France). All mice were bred and housed in the specific pathogen-free breeding unit of the Central Animal Facility of Utrecht University. Experiments were conducted according to institutional guidelines after acquiring permission from the local ethical committee and in accordance with

current Dutch laws on animal experimentation. NSG-A24 mice received sublethal total body irradiation on day -1 followed by intravenous injection of $0{,}1 \times 10^6$ K562-HLA-A*24:02 luciferase tumor cells on day 0, after which they were treated with 1×10^7 TEG011 or Mock TCR transduced T-cells on days 1 and 6. IL-2 (6×10^5 IU in 100μl incomplete Freund's adjuvant) was administered subcutaneously once every 3 weeks.

Statistical Analyses

Differences were analyzed using indicated statistical tests in GraphPad Prism 7 for Windows (GraphPad Software Inc., La Jolla, CA, USA).

RESULTS

Tumor specificity of Vγ5Vδ1T-cell clone can be transferred to αβT-cell by transfer of the γδTCR only.

To confirm the tumor reactivity of the recently identified tumor specific γδT clone FE11 (2), the clone was co-incubated with SW480 (colorectal adenocarcinoma), EBV-LCL (Epstein-Barr virus-transformed lymphoblastoid cell line), and healthy PBMCs, leading to recognition, as measured by interferon (IFN)γ ELISpot, of the 2 tumor cells lines but not the healthy PBMCs (Figure 1A). Next, both the γ and δ chain of γδT-cell clone FE11 were sequenced, identified as a Vγ5Vδ1 TCR, and cloned into pBullet retroviral vector and subsequently introduced into αβT-cells as previously described (16). Taking the γδTCR out of the innate-like environment enabled us to study the functioning of the receptor without interference of NK-receptors, which are not present on αβT-cells (19, 20). This strategy we have recently described as TEGs (T-cells engineered to express a defined γδT-cell receptor (19, 21, 22)). Introduction of FE11 γδTCR in αβT-cells (later referred to as TEG011) resulted as reported in a strong expression of the introduced FE11 γδTCR and a substantial downregulation of the endogenous αβTCR with many cells becoming single positive for the expression of the introduced γδTCR (Supplementary Figure 1). This led to a comparable recognition of target-cells when comparing TEG011 to the original clone FE11 (Figure 1B), indicating that tumor-reactivity is mediated by the γδTCR and independent of (epi)genetic factors exclusively present in the original T cell clone.
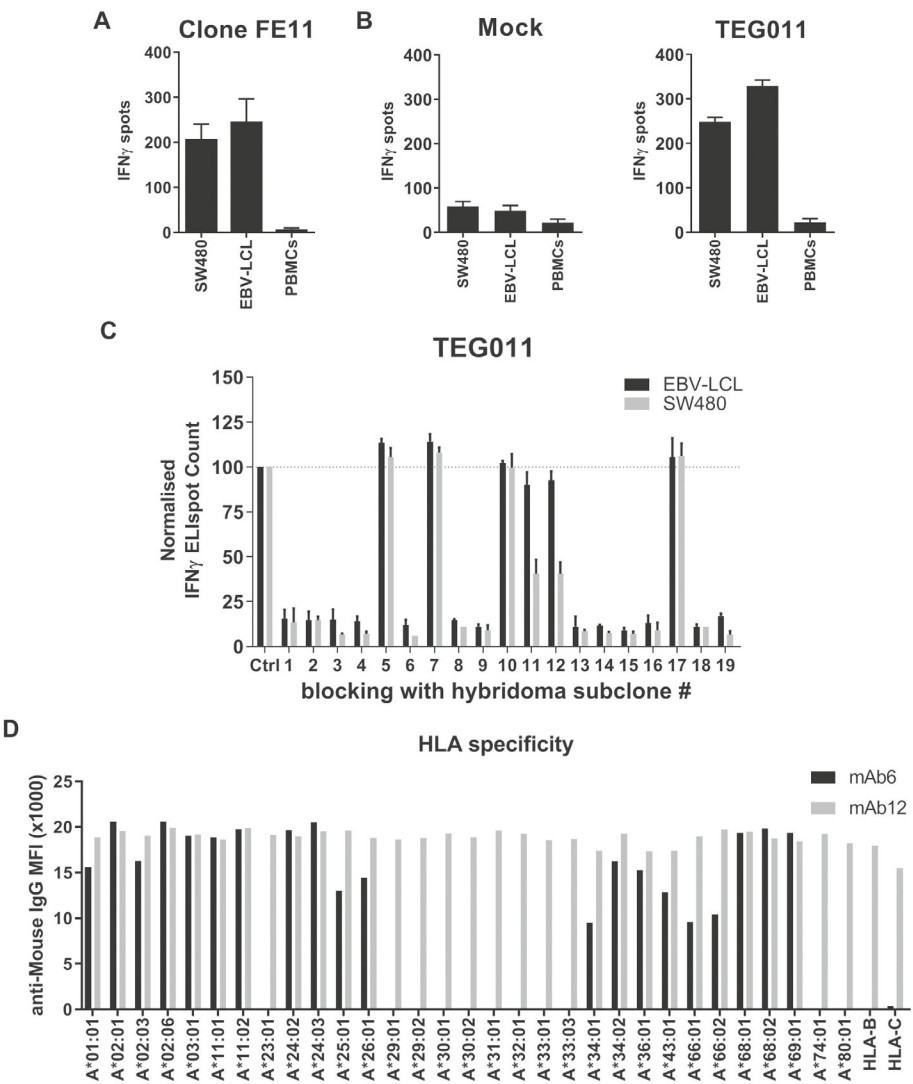
3

Figure 1 Introduction of FE11 γδTCR in αßT-cells can re-establish tumor cell recognition of clone FE11. (A) To assess tumor reactivity, FE11 cells were incubated with SW480 or EBV-LCL tumor targets. IFNγ secretion was measured by ELISPOT. Healthy PBMCs served as negative control targets. **(B)** The TCR γ and δ chains of clone FE11 were sequenced and retrovirally transduced into αßT-cells. Transfer of γδTCR-mediated tumor-reactivity was tested by co-incubating γδTCR- or mock-transduced T-cells with indicated target-cells in an IFNγ ELIspot. **(C)** The effect of blocking with FE-11 like hybridoma supernatant on the recognition of SW480 and LCL-TM by FE11 γδTCR transduced T cells. **(D)** LABScreen Single Antigen HLA class I beads were incubated with antibodies purified from hybridoma 6 (mAb 6) or antibodies purified from hybridoma 12 (mAb 12) and secondary α-mIgG-PE and measured using Luminex. Error bars represent SD (n≥1).

Hybridoma-derived antibodies indicate a role for classical HLA molecules.

The observation that the FE11 γδTCR by itself recognizes multiple tumor cell lines but not healthy PBMCs, was highly interesting. We aimed to identify the ligand of the FE11 γδTCR by generating TCR-like antibodies by the immunization of C57BL/6 mice with complete tumor cell lines SW480 and LCL-TM that were recognized *in vitro* by TEG011. From the hybridomas generated, 19 clones were isolated that produced antibodies that specifically bound FE11 γδTCR reactive tumor cells in an antibody binding screen. To further determine the ligand specificity of the antibodies, the FE11 targets SW480 and LCL-TM were pre-incubated with supernatants from these hybridomas and subsequently used in co-cultures to stimulate TEG011. 13 out of the 19 antibodies (i.e. hybridoma supernatants) blocked the activation of the TEG011 substantially, as measured by IFNγ ELISpot (Figure 1C). These data suggest that the majority of the raised antibodies were able to partially or completely prevent the binding of the FE11 γδTCR to its ligand. In contrast, none of the 19 hybridomas produced an antibody that could block the recognition of WT1$_{126\text{-}134}$ (HLA-A*02:01) peptide loaded SW480 by αβT-cells engineered with a WT1$_{126\text{-}134}$-specific αβTCR (Supplementary Figure 2A), suggesting that the blocking was not induced via binding to other molecules expressed on an αβT-cell than the introduced γδTCR (23). From the 19 hybridomas, one antibody that completely blocked activity (clone 6) and one that partially blocked activity (clone 12) (from here on named mAb6 and mAb12) were arbitrarily selected for the array of options for antibody production and purification. These purified antibodies were coupled to streptavidin beads and subsequently used for ligand-immunoprecipitation in cell lysates of either SW480 or LCL-TM cells. Mass spectrometry analysis resulted in the identification of a panel of mostly classical HLA molecules (Supplementary Table 1) suggesting that, in contrast to the general assumption, classical HLA molecules may be involved in recognition of tumor cells by this particular γδTCR. To confirm that raised antibodies are specific for classical HLA, we incubated LABScreen Single Antigen HLA class I beads (24) with mAb6 and mAb12 and measured the beads by Luminex to determine HLA-specificity. Figure 1D shows that mAb6 has a reactivity to a defined subgroup of HLA-A alleles, while mAb12 displayed no specificity, reacting towards all HLA class I alleles, including HLA-B and HLA-C, present on the LABScreen beads.

Target cell recognition by the FE11 γδTCR is critically dependent on HLA-A*24:02.

The raised antibodies were able to bind a broad range of different HLA types. To further narrow down the type of HLA recognized by γδTCR-FE11, we made use of the library of cell lines from the Centre d'Etude du Polymorphisme Human (CEPH), which contains a large collection of EBV-transformed B-cell lines (EBV-LCLs) obtained from several family pedigrees with a large variety of HLA haplotypes (25). TEG011 was co-incubated with 7 different CEPH EBV-LCLs, covering multiple possible HLA molecules as suggested by the LABScreen beads (Figure 1D), Daudi and LCL-TM, and reactivity was assessed by measuring IFNγ-release. Correlating reactivity of TEG011 to the different HLA types from a large panel of LCL line covering many frequent HLA types suggested that uniquely the HLA-A*24:02 haplotype, but not HLA-A*02:01 or HLA-A*03:01 (Figure 2A and Supplementary Table 2), was involved in the recognition. To formally confirm HLA-A*24:02

mediated recognition we retrovirally introduced either HLA-A*24:02 or HLA-A*02:01 (as control) into the HLA negative cell lines COS-7 and K562. In both cell lines, introduction of HLA-A*24:02, but not HLA-A*02:01, resulted in strong activation of TEG011 (Figure 2B). Additionally, we found that the density of the ligand HLA-A*24:02 on target-cells was associated with the activity of TEG011, since reactivity of TEG011 was higher against cell lines homozygous for HLA-A*24:02 than against heterozygous cell lines (Figure 2C).
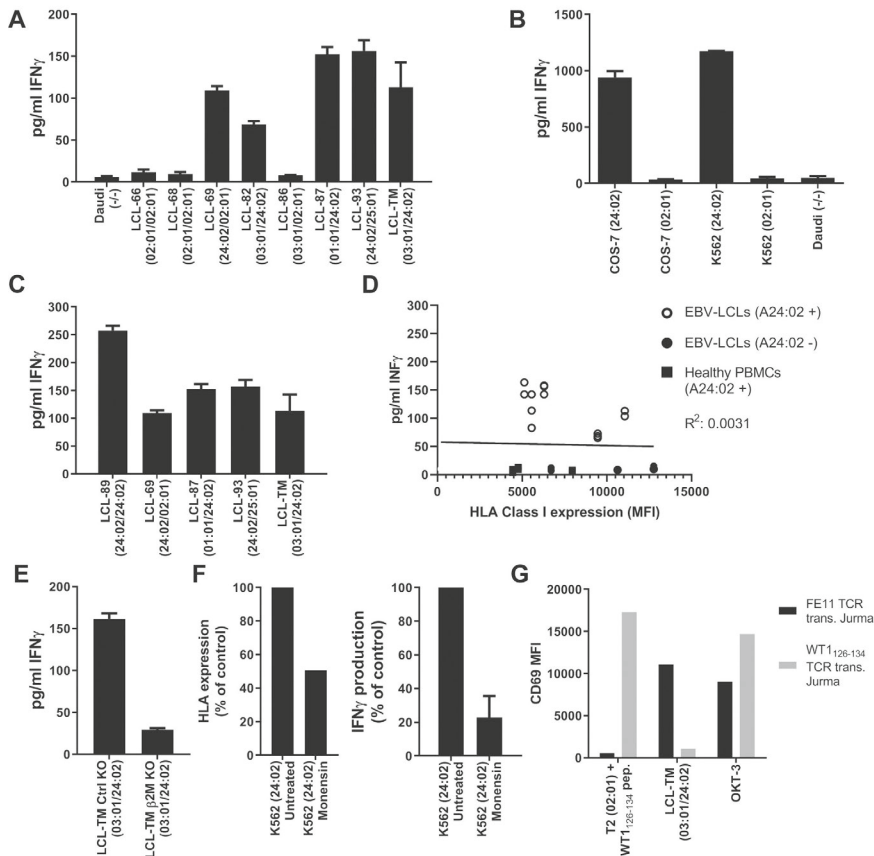

Figure 2 Activation of FE11 γδTCR transduced T-cells is dependent on expression of HLA-A*24:02. (A) Activation of T-cells, transduced with FE11 γδTCR by EBV-LCLs with different HLA genotypes. **(B)** Activation of T-cells, transduced with FE11 γδTCR by HLA-A*24:02 or HLA-A*02:01 target-cells. **(C)** Activation of T-cells, transduced with FE11 γδTCR by EBV-LCLs with different either homozygous or heterozygous HLA-A*24:02 expression. **(D)** Total HLA class I expression of HLA-A*24:02 positive and negative EBV-LCLs compared to TEG011 recognition **(E)** The effect of ß2m KO of HLA-A*24:02 target-cells on the activation of FE11 γδTCR transduced T-cells. **(F)** Activation of T-cells, transduced with FE11 γδTCR by K562 HLA-A*24:02 cells untreated or overnight monensin incubation. **(G)** Activation of Jurma cells, transduced with FE11 γδTCR or αßTCR WT1126-134 (control) by LCL-TM or A2 restricted WT1126-134 pep. loaded T2 cells. CD3 crosslinking by plate-bound α-CD3 mAb clone OKT-3 served as positive control. Recognition was assessed by measuring IFNγ secretion using ELISA. Error bars represent SD (n≥1).

Major differences in HLA expression could therefore contribute to the differential recognition between healthy cells and tumor cells. Therefore, HLA class I expression was measured of multiple HLA-A*24:02 heterozygous and negative LCLs as well as HLA-A*24:02 positive PBMC. However, no correlation was observed for small variations between the total HLA class I expression and TEG011 targeting within these LCLs indicating that only the expression levels of HLA-A*24:02 are associated with TEG011 targeting (Figure 2D). Also no substantial differences in HLA expression between PBMCs and recognized LCL have been observed. A partial CRISPR/Cas9 KO of ß2-microglobulin within recognized LCLs, reduced activation of TEG011 (Figure 2E and Supplementary Figure 2B) as expected. In addition, a substantial reduction of HLA expression on the cell membrane by monensin, a protein transport inhibitor, resulted in a decreased recognition of target-cells (Figure 2F). TEGs have been reported to lose allo-reactivity due the down regulation of the endogenous αßTCR due to dominance of the introduced γδTCR (21). However, in order to formally exclude any activity of endogenous αßTCR within the TEG format, we introduced either FE11 γδTCR or αßTCR- WT1$_{126-134}$ (as control) into the TCRß-negative Jurma cell line. The transduced Jurma cells were then co-incubated with WT1$_{126-134}$ peptide loaded T2 or LCL-TM tumor cells, and target-specific activation of Jurma cells was determined by measuring the activation marker CD69 by flow cytometry. As anticipated, FE11 γδTCR transduced Jurmas were only activated by the HLA-A*24:02 expressing LCL-TM, while the αßTCR-WT1$_{126-134}$ transduced Jurmas were only activated by WT1$_{126-134}$ loaded T2 cells (Figure 2G). In conclusion, target cell recognition by the FE11 γδTCR is critically dependent on and restricted to HLA-A*24:02.

The FE11 γδTCR selectively recognizes HLA-A*24:02 expressed in malignant but not healthy cells.

Allo-HLA reactivity is usually a phenomenon restricted to HLA on all cells of an individual (26). To assess if recognition is limited to HLA-A*24:02-positive transformed cells, we co-incubated TEG011 with healthy primary T-cells which were either positive or negative for HLA-A*24:02. In contrast to HLA-A*24:02-positive tumor cells, healthy primary cells were not recognized by TEG011, even when they were positive for HLA-A*24:02. B-cells isolated from multiple, healthy donors were not able to activate TEG011 even after being stressed by irradiation or by combination treatment of cyclophosphamide and fludarabine. Activation of these B-cells by administration of either LPS or CD40L and IL-4 also did not led to recognition by TEG011. This indicates that the expression of HLA-A*24:02 allele in combination with a malignant transformation is essential for the activation of TEG011 (Figure 3A and Supplementary Figure 3A). To further exclude recognition of healthy tissues in the absence or presence of stress or infection in epithelial tissues , HLA-A*24:02 positive fibroblasts were co-cultured with either TEG011 or T-cells transduced with the HLA-A*24:02 restricted NEF$_{134-144}$ αßTCR.[15] TEG011 did not recognize the HLA-A*24:02 fibroblast being stressed by either irradiation or administration of cyclophosphamide and fludarabine. In addition, CMV infection of these fibroblasts did not induce activation of the TEG011 while the NEF$_{134-144}$ αßTCR transduced T-cells were able to recognize the fibroblasts in all conditions (Figure 3B and Supplementary Figure 3B). To finally confirm that malignant transformation is essential for recognition by TEG011

in an autologous system, HLA-A*24:02-positive B-cells were immortalized by using EBV transformation and did activate TEG011, while the non-transformed PBMCs of the very same donor were not recognized (Figure 3C).
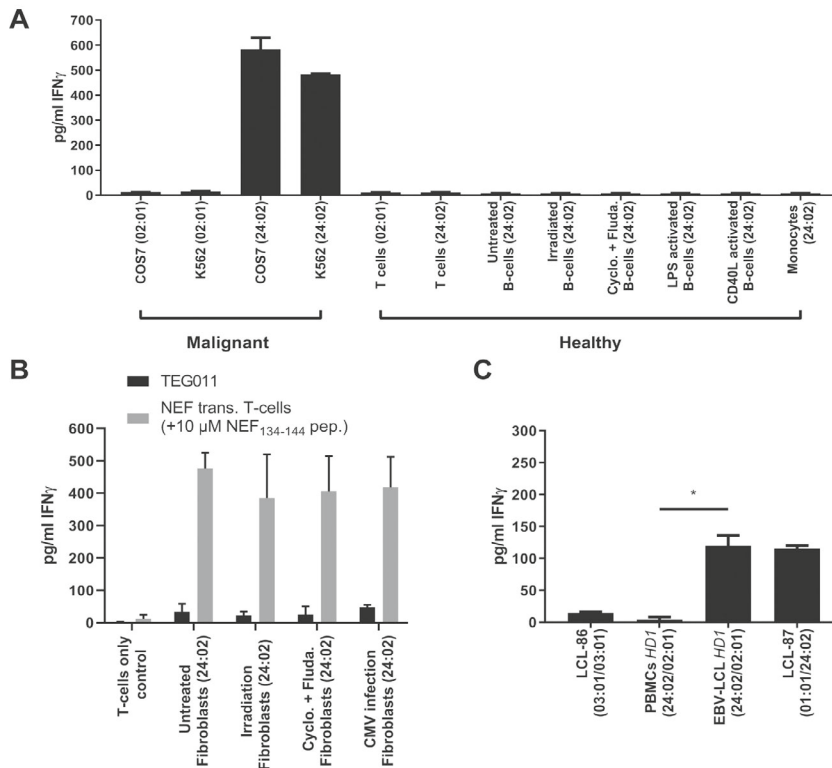

Figure 3 Activation of FE11 γδTCR-transduced T cells is limited to HLA-A*24:0⁺ malignant cells. (A) Activation of TEG011 cells by malignant and healthy hematological cells. B cells from multiple HLA-A*24:02⁺ donors were activated or stressed before the TEG011 cell coculture. **(B)** TEG011 or NEF134-144 αBTCR–engineered αß T-cell recognition after coculture with HLA-A*24:02⁺ healthy tissues. When using NEF$_{134-144}$ αBTCR–engineered αß T cells, 10 mM NEF$_{134-144}$ was added. **(C)** Healthy donor B cells (HD1) were EBV transformed and cocultured with TEG011. Recognition was assessed by measuring IFN-γ secretion using ELISA. Error bars represent the SD (n ≥ 2). *P < .05. Cyclo, cyclophosphamide; Fluda, fludarabine.
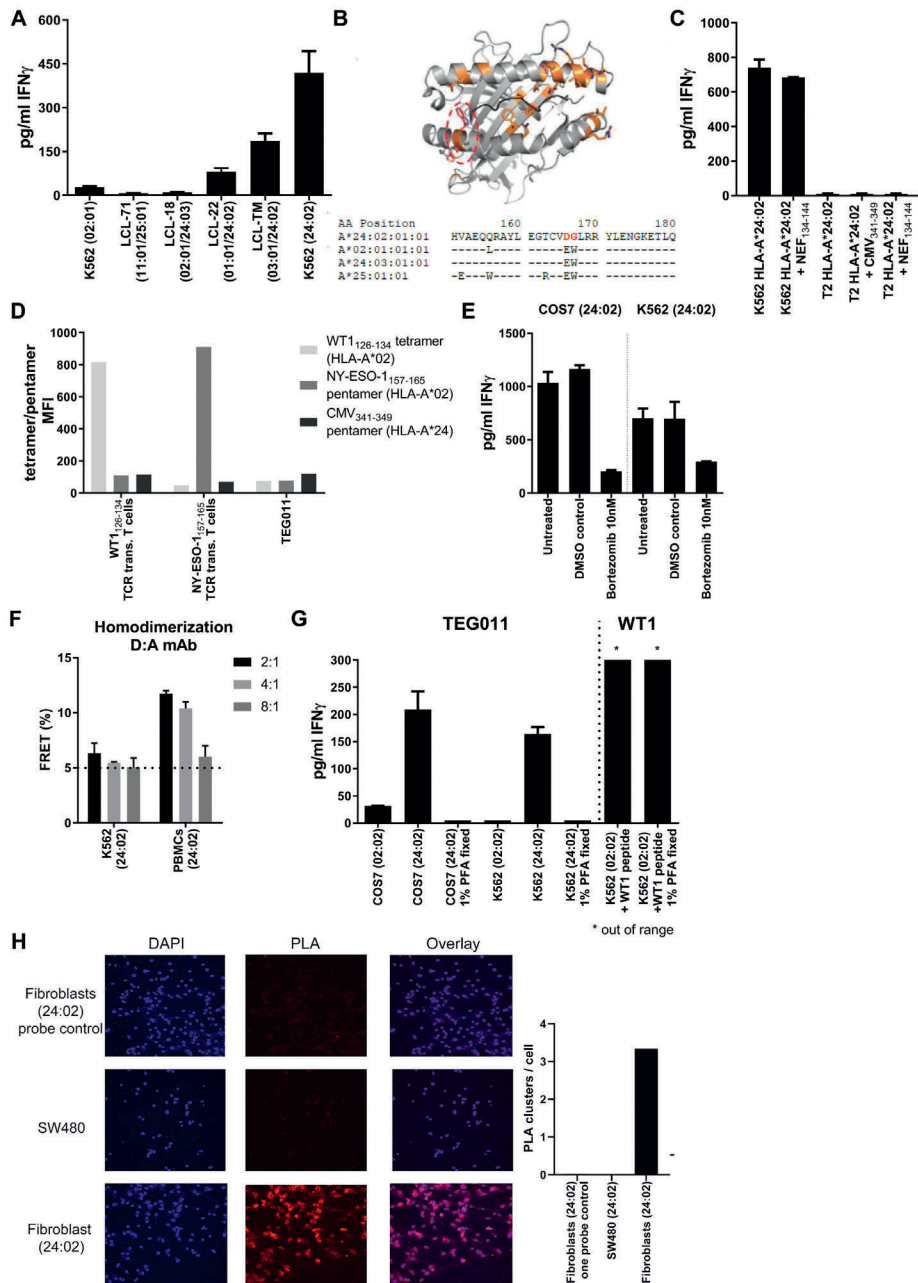
Figure 4 Activation of FE11 γδTCR-transduced T cells is dependent on the presence of a specific HLA-A*24:02-restricted peptide. (A) Activation of TEG011 by HLAA* 24:02-positive or -negative target cells. **(B)** The differences between HLA-A*02:01 and HLA-A*24:02 mapped on the structure of HLA-A*24:02 (Protein Data Bank: 3wl9), the 2 nonhomologous amino acids between HLA-A*24:02 and HLA-A*24:03 are show in the red circle (top). Alignment of HLA-A*24:02, 02:01, 24:03, and 25:01 with the 2 nonhomologous

Figure 4 *(Continued)* amino acids in red (bottom). (C) Activation of T cells, transduced with γδTCR-FE11, by HLA-A*24:02-transduced, TAP-deficient T2 cells not loaded or loaded with the A*24-restricted viral peptides NEF$_{134-144}$ or CMV$_{341-349}$ (pp65 341-349). (D) WT1$_{126-134}$ tetramer, NY-ESO1$_{157-165}$ pentamer, and CMV$_{341-349}$ pentamer binding to WT1$_{126-134}$-specific TCR, NY-ESO1$_{157-165}$-specific TCR, and FE11 TCR-transduced T cells. (E) The effect of bortezomib treatment of HLA-A*24:02-transduced target cells COS-7 (left) and K562 (right) on the activation of FE11 γδTCR-transduced T cells. (F) Homodimerization was assessed on HLA-A*24:02$^+$ cells, recognized and not recognized by flow cytometry FRET. (G) Activation of TEGs (left) or T cells transduced with the WT1$_{126-134}$-specific αβTCR (control) (right), by HLA-A*24:02-transduced COS-7 and K562 cells or HLA-A*02:01 (control). *Out of range. (H) Proximity Ligation Assay (PLA) was performed on HLA-A*24:02$^+$ fibroblasts and the SW480 cell line. Cells were stained for 4',6-diamidino-2-phenylindole and PLA signal. Where indicated, target cells were fixed before coincubation; target cells were coincubated with WT1126-134. Error bars represent the SD (n ≥ 1).

Identification of a putative binding-site of the FE11 γδTCR.

In order to further map the putative binding site of FE11, CEPH EBV-LCLs expressing HLA alleles from different supertypes were tested (i.e. HLA-A*25:01 from supertype HLA-A01 and HLA-A*02:01 from supertype HLA-A02) (27). Additionally, CEPH EBV-LCLs expressing an HLA allele within the same supertype as HLA-A*24:02 (supertype HLA-A24; HLA-A*24:03) was tested. Reactivity of TEG011 could only be observed towards the HLA-A*24:02-positive cells, not towards the strong homologous HLA-A*24:03 present on EBV-LCL-71 (Figure 4A). Sequence alignment (Figure 4B, lower part) revealed that the two amino acids on the α2 helix at position 168 and 169 (asparagine and glycine respectively) are non-homologous between HLA-A*24:02 and the non-recognized HLA alleles, indicating that these residues are key for recognition of HLA-A*24:02 by TEG011. Structural analyses of the putative binding sites at position 168 and 169 indicated a very close proximity to the peptide binding groove (Figure 4B, upper part).

Promiscuous peptides are necessary for HLA-A*24:02 recognition by γδTCR-FE11.

Due to this close proximity of the putative binding site to the peptide binding groove, we explored the role of a peptide in the recognition of HLA-A*24:02 by the FE11 γδTCR. The cell line T2, which is deficient in TAP-dependent endogenous peptide processing and presentation in HLA molecules, was transduced with HLA-A*24:02 and HLA-A*02:01 (control) and loaded with HLA-A*24:02 restricted NEF$_{134-144}$ and HLA-A*02:01 restricted WT1$_{126-134}$ peptides respectively. In order to confirm the successful loading of HLA molecules with peptides, stabilization of HLA on the surface of T2 cells was assessed by flow cytometry (Supplementary Figure 4A). HLA-A*24:02 transduced T2 cells externally loaded with NEF$_{134-144}$ or CMV$_{341-349}$ did not lead to activation of TEG011, indicating that the presence of HLA-A*24:02 alone is not sufficient when expressed on T2 cells, but that the presentation of an endogenously processed peptide could be key to establish reactivity (Figure 4C). In order to confirm this hypothesis, we co-incubated TEG011 with a CMV$_{341-349}$ HLA-A*24:02 restricted pentamer. Whereas the controls, WT1$_{126-134}$ and NY-ESO1$_{157-165}$ αβTCR-transduced T-cells with their respective tetramer or pentamer stained positive (Figure 4D), TEG011 was not stained by the HLA-A*24:02 pentamer. These data suggest that the observed recognition is not caused by classical alloreactivity and most likely involves either promiscuous peptides to stabilize the complex or a specific peptide as a critical determinant for recognition.

To further assess whether endogenously processed peptides are essential for reactivity, we interfered with the cellular peptide processing machinery by inhibiting the proteasome of recognized tumor cells by pre-treatment with Bortezomib (28). Bortezomib treatment lead to a strong decrease in recognition of both HLA-A*24:02 transduced COS-7 and K562 cells (Figure 4E) by TEG011, suggesting that peptides are at least needed for stabilization of the complex. To explore if transformation-associated peptides are involved in recognition, we selected 15 transformation-associated peptides (29-35) to load HLA-A*24:02 transduced T2 cells (Supplementary Figure 4B and Supplementary Table 2) and assessed the recognition by TEG011. None of the 15 peptides lead to activation of TEG011 (Figure 5A). Vice versa, we outcompeted the putative endogenous peptide recognized by TEG011 with NEF$_{134-144}$ WT peptide and NEF$_{134-144}$ mutants. NEF$_{134-144}$ mutants were designed by changing the four amino acids which are facing out of the HLA binding groove (Figure 5B). The four amino acids were substituted for the negatively charged amino acid glutamic acid (E), the positively charged amino acid arginine (R), and the smallest amino acid; glycine (G). At least part of these modified peptides could
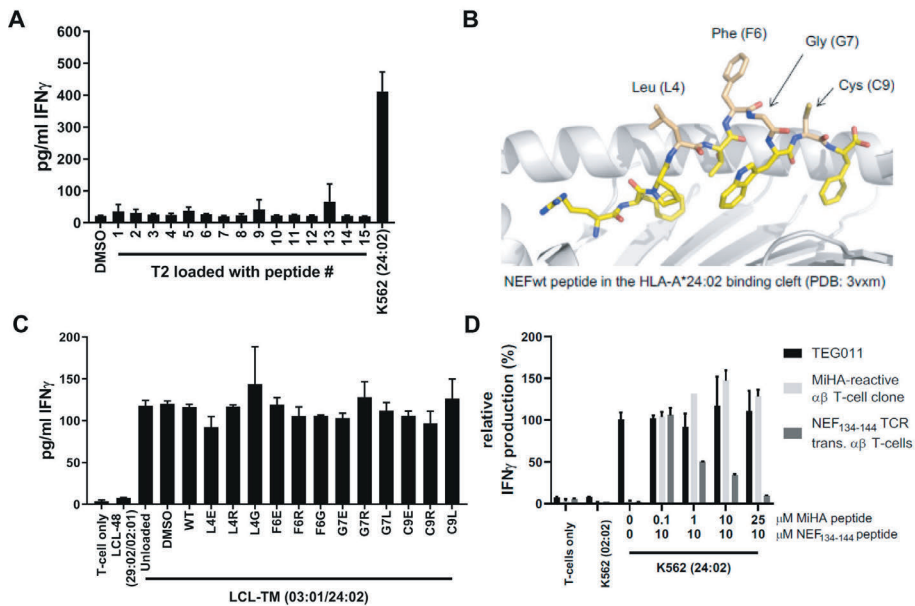
3

Figure 5 Recognition of LCL-TM cells cannot be outcompeted by peptides. (A) T2 cells were transduced with HLA-A*24:02 and loaded with 10 mM of 15 different transformation-associated peptides (supplemental Table 1), after which they were coincubated with TEG011 cells. Activation of TEG011 cells was assessed by measuring IFN-γ production. **(B)** The 4 residues of NEF$_{134-144}$ that are pointed out of the peptide binding groove of HLA-A*24:02 are indicated. **(C)** Ten micromoles of the generated NEF$_{134-144}$-derived mutant peptides were loaded on LCL-TM cells, after which they were coincubated with TEG011 cells. **(D)** HLA-A*24:02-transduced K562 cells were loaded with 10 mM NEF$_{134-144}$ before loading with increasing concentrations of an HLA-A*24:02-restricted MiHA peptide (K.F., unpublished data). The peptide-loaded loaded cells were coincubated with TEG011 cells, αβT cells engineered with an HLA-A*24:02-restricted NEF$_{134-144}$-specific TCR or a MiHA specific αβT cell clone. T-cell activation was assessed by measuring IFN-g. Error bars represent the SD (n ≥ 2).

be loaded on LCL-TM cells (Supplementary Figure 5). Next, WT NEF$_{134-144}$ peptide and all different NEF$_{134-144}$ mutants were loaded on LCL-TM after which they were co-incubated with TEG011, followed by measurement of IFNγ. None of the peptides were able to decrease the recognition, indicating that the recognition mechanism is more elaborate than a standard αßTCR peptide-HLA interaction (Figure 5C) implying that recognition is not mediated by a specific peptide, but rather promiscuous peptides are involved as stabilizer of the complex. In order to assure that peptide loading truly outcompetes HLA-A*24:02 bound peptides, HLA-A*24:02 transduced K562 cells were first loaded with WT NEF$_{134-144}$ peptide and subsequently loaded with different concentrations of an HLA-A*24:02-restricted minor histocompatibility antigen (MiHA) peptide (unpublished data, K. Fuchs). Peptide loaded cells were then co-incubated with TEG011, αßT-cells engineered with an HLA-A*24:02-restricted NEF$_{134-144}$-specific or a T cell clone expressing a defined HLA-A*24:02 restricted MiHA-specific αßTCR. With increasing concentrations of MiHA peptides, αßT-cells engineered NEF$_{134-144}$-specific TCR showed a reduced cytokine release while TEG011 activity was not affected against the very same target (Figure 5D).

Conformational change as additional distinguishing factor for recognition.

The hypothesis that promiscuous peptides are involved as stabilizer of the complex was supported by the observations that HLA-A*24:02 was also recognized within the context of another species (monkey, COS-7 cell line). In addition, as usually small amounts of endogenously processed and presented peptides are sensed by TCRs, doubling the amount of HLA in a homozygous as compared to heterozygous target should not substantially affect recognition. However, increased amounts of HLA in homozygous individuals nearly doubled functional activity of TEG011, suggesting that rather the HLA-complex than individual peptide-HLA combination was recognized. Therefore, we hypothesized that an additional key-spatial or structural conformational change in HLA-A*24:02 occurs as a result of transformation of a healthy cell into a tumor cell. To elaborate on this hypothesis we used Förster resonance energy transfer (FRET) based flow cytometry as described before (17), to determine if HLA-A*24:02 clusters in the membrane of tumor cells. In line with this assumption, FRET analysis suggested different behavior of HLA in tumor and healthy tissues with HLA-A*24:02 homodimers on PBMCs and monomers on tumor cells (Figure 4F). In order to formally test if membrane mobility of HLA-A*24:02 is key for recognition by γδTCR-HLA but not αßTCR-HLA, we assessed the effect of paraformaldehyde fixation on the sensing of target-cells. Whereas the recognition of αßTCR WT1$_{126-134}$ transduced T-cells and WT1$_{126-134}$ peptide loaded target-cells was not affected by fixation, the interaction by TEG011 cells and HLA-A*24:02 transduced target-cells was completely abolished, indicating that there are differences requirements for TCR activation (Figure 4G). Altered HLA clustering on tumor cells as compared to healthy cells was also supported by a proximity ligation assay of HLA class I molecules which showed reduced HLA clustering in SW480 cells compared to HLA-A*24:02 fibroblasts (Figure 4H). In summary, our data support the notion that malignant transformation of cells leads to alterations in HLA clustering on the cell surface, which might be an additional factor sensed by TEG011.

FE11 γδTCR critically depends on the CD8 co-receptor for tumor recognition.

To further support the idea that indeed the γδTCR-HLA interaction differs from classical HLA-αßTCR interactions, we investigated the potential role of co-receptors. One obvious candidate, due to HLA class I restriction, was CD8αα. First, we formally confirmed CD8 expression on the original clone in line with previous reports ((2) and Figure 6A). Next, we assessed whether TEG011 is dependent on the co-expression of CD8, like the original clone, by sorting TEG011 on CD4 and CD8 expression before co-culturing with SW480, LCL-TM or PBMCs (Figure 6B). In contrast to the γδT-cell clone FE11, most αßT-cells express CD8 as a heterodimer of CD8α and CD8ß for providing co-stimulation. The role of the CD8αß heterodimer on TEG011 was assessed by using blocking antibodies for either the CD8α or CD8ß chain. Not only CD8α, but also CD8ß blocking antibodies completely inhibited recognition of SW480 (Figure 6C), indicating that either CD8αα or CD8αß is essential for recognition. These data have also been confirmed by comparing CD8-positive and CD8-negative Jurma cells expressing FE11 γδTCR (Figure 6D) or αßTCR WT1$_{126-134}$ (control, Figure 6E). For co-stimulation of HLA class I-restricted αßTCRs, CD8αß can play two different roles; it serves as an adhesion molecule that stabilizes the TCR-HLA interaction and it can play an activating role by signaling via LCK (36). On the other hand, CD8αα on αßT-cells has been described as a corepressor rather than a coreceptor by competing with CD8αß for the LCK signaling molecule (37). To investigate the role of CD8αα for TEG011, we utilized a truncated variant of CD8α
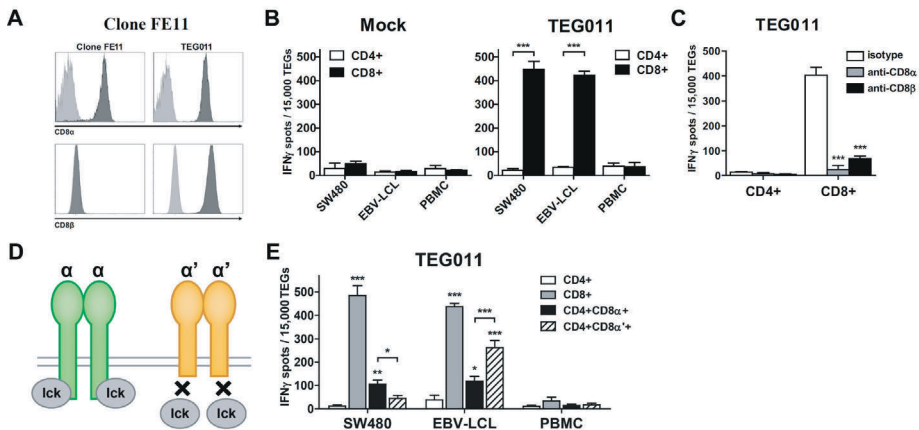
3

Figure 6 The FE11 γδTCR critically depends on the CD8 coreceptor for tumor recognition. (A) CD8α or CD8ß expression on clone FE11 cells and FE11 γδTCR-transduced αß T cells. **(B)** CD4$^+$ and CD8$^+$ αßT cells transduced with the FE11 γδTCR were sorted and cocultured with mock (left) and TEG011 (right) target cells. **(C)** TEG011 T-cell activation was assessed by IFN-γ ELISPOT. CD4$^+$ and CD8$^+$ αßT cells expressing the FE11 γδTCR were coincubated with SW480 target cells as in panel B, but in the presence of a control antibody or blocking antibodies against CD8α or CD8ß. **(D)** αßT cells were transduced with WT CD8α or α truncated, signaling-deficient CD8α variant (CD8α'), alongside the γδTCR-FE11, after which the CD4$^+$, CD8$^+$, CD4$^+$CD8α$^+$, and CD4$^+$CD8α'$^+$ T-cell populations were sorted. Recognition of healthy PBMCs and SW480 tumor target cells was assessed by measuring IFN-γ secretion using ELISPOT. Error bars represent the standard error of the mean (n ≥ 1). *P < .05; **P < .01; ***P < .001.

which is signaling deficient due to its inability to bind LCK (38). After introducing both FE11 γδTCR and truncated CD8α (CD8α') in CD4+ αßT-cells we co-cultured the TEGs with SW480. A decrease in the amount of IFNγ spots of the CD8α' variant compared to the CD8α wild type variant was observed (Figure 6F), indicating that CD8αα indeed plays a co-stimulatory role in TEG011.
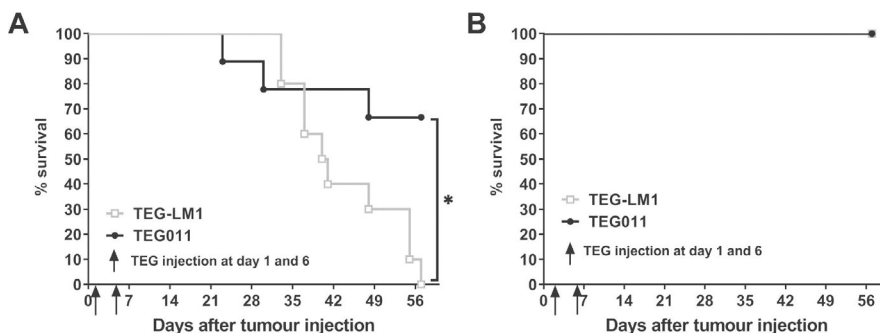

Figure 7 TEG011 treatment leads to efficient tumor control of K562-HLA*A24 tumors, whereas it shows no toxicity _in vivo_ in NSG-A24 transgenic mice. NOD.Cg-_Prkdc^scid^Il2rg^tm1Wjl_ Tg(HLA-A24)3Dvs/Sz (NSG-A24:02) mice were injected with 1×10^5 K562 HLA-A*24:02 Luciferase cells on day 0 followed by 1×10^7 TEG011 or LM1 transduced T cells on days 1 and 6 (n = 10 per group). In parallel, non-tumor–bearing mice also received 1×10^7 TEG011 or LM1 transduced T cells on days 1 and 6 (n = 5 per group). Overall survival of treated K562-HLA*A24 luciferase tumor-bearing mice for monitoring efficacy (A) and overall survival of non-tumor–bearing mice for monitoring toxicity (B) was recorded for 57 days. Data represent the mean ± SD of all mice in each group. Statistical significance was calculated by log-rank (Mantel-Cox) test; *P < .05.

Improved overall survival by TEG011

To determine safety and effectivity of TEG011 _in vivo_ we set up a humanized HLA-A*24:02 transgenic NSG mouse model for adoptive transfer of TEG011. The irradiated mice were injected with luciferase labelled HLA-A*24:02 transduced K562 and either TEG011 or LM1 transduced T-cells as control. Mice were taken out of the study when the human endpoint was reached. A significantly increased overall survival as observed in TEG011 treated group when compared to mice treated with LM1 transduced T cells (Figure 7A). TEG011 treated mice had also a significantly lower tumor burden when assessed by Bioluminescent imaging (Supplementary Figure 6). Importantly, surviving TEG011-treated tumor-bearing mice showed no further signs of discomfort. Performing pathology in three selected tumor bearing mice treated with TEG011 showed no histo-logical features of toxicity of TEG011, altogether indicating that HLA-A*24:02 positive tumor cells but not healthy cells were targeted by TEG011. Lack of toxicity of TEG011 _in vivo_ in a HLA-A*24:02 host was further substantiated by injecting non-tumor bearing mice with TEG011 and LM1 engineered transduced T cells in humanized HLA-A*24:02 transgenic NSG mice, which stayed alive during the whole observation time without showing any signs of discomfort (Figure 7B).

DISCUSSION

The major finding of the study is that we identified an allo-reactive γδTCR which is able to distinguish between healthy and tumor tissues. Furthermore, we elucidated the molecular interface of the investigated Vγ5Vδ1TCR clone FE11 and provide evidence that, although the binding site is close to the peptide binding groove of HLA-A*24:02, transformation-associated HLA peptides do not dictate recognition between healthy and cancer tissues. Most likely, other key-conformational changes within the membrane selectively occurring to HLA on tumor cells but not on healthy tissues *in vitro* and *in vivo,* are responsible for the differential recognition between tumor and healthy cells.

Allo-HLA type of recognition by γδTCRs has been suggested both for HLA-A*02 (39), HLA-A*24 (40), and B*27 (41). These data suggest that our observation reflects a broader phenomenon, however might be linked to unique γδTCR sequences as we could not find back the sequence used for TEG011 in many HLA-A*24:02 positive and negative donors (n= 7 HLA-A*24:02, total n=23, data not shown). The underlying molecular mechanism has not been defined so far, in contrast to allo-reactivity of αßTCRs (42-44). Considering this, a γδTCR selectively recognizing tumor cells in an allo-HLA context seems to be plausible, however, our data suggests that the mode of action differs between allo-reactive αßTCRs. We characterized the essential contact residues of FE11 γδTCR with HLA-A*24:02, which appeared to be in close proximity to the peptide binding groove. Our data suggests that the FE11 γδTCR is able to recognize amino acids 168 and 169 on the α2-helix of HLA-A*24:02, since these are the only non-homologous amino acids between recognized HLA-A*24:02 and non-recognized HLA-A*24:03 (45). Differences in recognition of the same peptide presented by HLA-A*24:02 and HLA-A*24:03 by CD8^{+} αßT-cells has been observed before (46). Thus, not only αßTCRs, KIRs, LILRs, and CD8 molecules (47), but also γδTCRs can bind to a specific part of HLA class I. However, our data also imply that, in contrast to recognition of HLA by an allo-peptide reactive αßTCR, promiscuous peptides are involved in mediating recognition by γδTCR-FE11. This assumption would also be an explanation for the activity of TEG011 against a very broad range of tumor cells, even though being a rare TCR sequence in humans.

Our HLA membrane topology data suggests that, instead of a defined tumor-derived peptide, another key spatial or conformational change like differences in clustering of HLA-A*24:02-molecules between tumor cells and healthy cells plays a role in mediating tumor-specificity. HLA clustering has mainly been studied within the context of HLA class II on antigen presenting cells, which does not necessarily depend on the presence of a T-cell (48). Clustering of HLA has been reported to be essential for the recognition of HLA-B*27 recognition through leukocyte immunoglobulin-like receptors B2 and killer cell immunoglobulin-like receptors 3DL2 (49, 50). HLA behavior on tumor cells has mainly been studied within the context of tumor immune escape by loss or downregulation of HLA class I expression (51). The here suggested preferential monomeric form of HLA at the cell membrane of tumor cells could be part of classical tumor escape mechanisms for αßT-cells, which can however be sensed by the here described allo-reactive γδTCR.

3

A major concern for using the allo-reactive FE11 γδTCR in a therapeutic scenario would be that, through the nature of promiscuous peptides as part of the recognition complex, safety is difficult to assess. To partially address this concern, we performed tumor control experiments in HLA-A*24:02 transgenic mice. In histological analyses we could not observe pathological evidence for auto-immunity in the investigated organs. Our observation is also supported by the clinical observation that αßT-cell depleted haplo-transplantations associate with very good tumor control and limited toxicity (52-54). Though for therapeutic scenarios the administration of TEG is more feasible because generating high numbers of TEGs for patients is superior over using expanded allo-reactive γδT cell clones, the new wave of haplo-transplantations (55) most likely benefits from a better understanding of allo-tumor reactive γδT-cell immune repertoires as described here. This knowledge would allow e.g. the development of cellular vaccines expressing tumor-HLA to boost tumor-allo-reactive γδT cell clones *in vivo*.

In summary, we report on the very interesting nature of allo-reactivity of a γδTCR which is able to distinguish between healthy and malignant cells. This observation extends the use of γδTCR for the TEG concept as next generation of CAR T as it opens an avenue to a complete new set of tumor targets seeing conformational and spatial changes at the cell membrane (8, 56). This observation emphasizes that γδT-cells, within the context of haplo-transplantation, not only possess classical antitumor reactivity but also benefit from allo-tumor reactivity (20). In addition, such γδTCR, within the context of TCR gene therapies, can be an interesting addition to tumors expressing HLA-A*24:02.

Conflict of Interest Statement

GK, DB, ZS and JK are inventors on different patents with γδTCR sequences, recognition mechanisms and isolation strategies. GK is employed by Kiadis Pharma (www.kiadis. com). JK is scientific advisor and shareholder of Gadeta (www.gadeta.nl). No potential conflicts of interest were disclosed by the other authors.

REFERENCES

1. Girardi M, Oppenheim DE, Steele CR, Lewis JM, Glusac E, Filler R, *et al*. Regulation of cutaneous malignancy by γδT cells. *Science*. 2001;294(5542):605-9.

2. Scheper W, van Dorp S, Kersting S, Pietersma F, Lindemans C, Hol S, *et al*. γδT cells elicited by CMV reactivation after allo-SCT cross-recognize CMV and leukemia. *Leukemia*. 2013;27(6):1328-38.

3. Lalor SJ, McLoughlin RM. Memory γδT Cells-Newly Appreciated Protagonists in Infection and Immunity. *Trends Immunol*. 2016;37(10):690-702.

4. Dadi S, Chhangawala S, Whitlock BM, Franklin RA, Luo CT, Oh SA, *et al*. Cancer Immunosurveillance by Tissue-Resident Innate Lymphoid Cells and Innate-like T Cells. *Cell*. 2016;164(3):365-77.

5. Hidalgo JV, Bronsert P, Orlowska-Volk M, Diaz LB, Stickeler E, Werner M, *et al*. Histological Analysis of γδT Lymphocytes Infiltrating Human Triple-Negative Breast Carcinomas. *Front Immunol*. 2014;5:632.

6. Legut M, Cole DK, Sewell AK. The promise of γδT cells and the γδT cell receptor for cancer immuno-therapy. *Cell Mol Immunol*. 2015;12(6):656-68.

7. Morita CT, Jin C, Sarikonda G, Wang H. Nonpeptide antigens, presentation mechanisms, and immuno-logical memory of human Vγ2Vδ2 T cells: discriminating friend from foe through the recognition of prenyl pyrophosphate antigens. *Immunol Rev*. 2007;215:59-76.

8. Sebestyen Z, Scheper W, Vyborova A, Gu S, Rychnavska Z, Schiffler M, *et al*. RhoB Mediates Phospho-antigen Recognition by Vγ9Vδ2 T Cell Receptor. *Cell Rep*. 2016;15(9):1973-85.

9. Willcox CR, Pitard V, Netzer S, Couzi L, Salim M, Silberzahn T, *et al*. Cytomegalovirus and tumor stress surveillance by binding of a human γδT cell antigen receptor to endothelial protein C receptor. *Nat Immunol*. 2012;13(9):872-9.

10. Groh V, Steinle A, Bauer S, Spies T. Recognition of stress-induced MHC molecules by intestinal epithelial γδT cells. *Science*. 1998;279(5357):1737-40.

11. Marlin R, Pappalardo A, Kaminski H, Willcox CR, Pitard V, Netzer S, *et al*. Sensing of cell stress by human γδTCR-dependent recognition of annexin A2. Proc Natl Acad Sci USA. 2017; 114(12): 3163-8.

12. Luoma AM, Castro CD, Mayassi T, Bembinster LA, Bai L, Picard D, *et al*. Crystal structure of Vδ1 T cell receptor in complex with CD1d-sulfatide shows MHC-like recognition of a self-lipid by human γδT cells. *Immunity*. 2013;39(6):1032-42.

13. Gu S, Sachleben JR, Boughter CT, Nawrocka WI, Borowska MT, Tarrasch JT, *et al*. Phosphoantigen-in-duced conformational change of butyrophilin 3A1 (BTN3A1) and its implication on Vγ9Vδ2 T cell activation. *Proc Natl Acad Sci USA*. 2017;114(35):E7311-E20.

14. Kuball J, Dossett ML, Wolfl M, Ho WY, Voss RH, Fowler C, *et al*. Facilitating matched pairing and ex-pression of TCR chains introduced into human T cells. *Blood*. 2007;109(6):2331-8.

15. Shimizu A, Kawana-Tachikawa A, Yamagata A, Han C, Zhu D, Sato Y, *et al*. Structure of TCR and antigen complexes at an immunodominant CTL epitope in HIV-1 infection. *Sci Rep*. 2013;3:3097.

16. Marcu-Malina V, Heijhuurs S, van Buuren M, Hartkamp L, Strand S, Sebestyen Z, *et al*. Redirect-ing αßT cells against cancer cells by transfer of a broadly tumor-reactive γδT-cell receptor. *Blood*. 2011;118(1):50-9.

17. Sebestyen Z, Nagy P, Horvath G, Vamosi G, Debets R, Gratama JW, *et al*. Long wavelength fluorophores and cell-by-cell correction for autofluorescence significantly improves the accuracy of flow cytometric energy transfer measurements on a dual-laser benchtop flow cytometer. *Cytometry*. 2002;48(3):124-35.

18. Najima Y, Tomizawa-Murasawa M, Saito Y, Watanabe T, Ono R, Ochi T, *et al*. Induction of WT1-specific human CD8^{+} T cells from human HSCs in HLA class I Tg NOD/SCID/IL2rgKO mice. *Blood*. 2016;127(6):722-34.

19. Grunder C, van Dorp S, Hol S, Drent E, Straetemans T, Heijhuurs S, *et al*. γ9 and δ2CDR3 domains regulate functional avidity of T cells harboring γ9δ2TCRs. *Blood*. 2012;120(26):5153-62.

20. Scheper W, Grunder C, Straetemans T, Sebestyen Z, Kuball J. Hunting for clinical translation with innate-like immune cells and their receptors. *Leukemia*. 2014;28(6):1181-90.

21. Straetemans T, Grunder C, Heijhuurs S, Hol S, Slaper-Cortenbach I, Bonig H, *et al*. Untouched GMP-Ready Purified Engineered Immune Cells to Treat Cancer. *Clin Cancer Res*. 2015; 21(17): 3957-68.

22. Straetemans T, Kierkels GJJ, Doorn R, Jansen K, Heijhuurs S, Dos Santos JM, *et al*. GMP-Grade Manufacturing of T Cells Engineered to Express a Defined γδTCR. *Frontiers in immunology*. 2018; 9:1062.

23. Cole DK, Gao GF. CD8: adhesion molecule, co-receptor and immuno-modulator. *Cell Mol Immunol*. 2004;1(2):81-8.

24. Pei R, Lee J, Chen T, Rojo S, Terasaki PI. Flow cytometric detection of HLA antibodies using a spectrum of microbeads. *Hum Immunol*. 1999;60(12):1293-302.

25. Dausset J, Cann H, Cohen D, Lathrop M, Lalouel JM, White R. Centre d'etude du polymorphisme humain (CEPH): collaborative genetic mapping of the human genome. *Genomics*. 1990; 6(3): 575-7.

26. Ferrara JL, Levine JE, Reddy P, Holler E. Graft-versus-host disease. *Lancet*. 2009; 373(9674): 1550-61.

27. Sidney J, Peters B, Frahm N, Brander C, Sette A. HLA class I supertypes: a revised and updated classification. *BMC Immunol*. 2008;9:1.

28. Adams J, Kauffman M. Development of the proteasome inhibitor Velcade (Bortezomib). *Cancer Invest*. 2004;22(2):304-11.

29. Kowalewski DJ, Schuster H, Backert L, Berlin C, Kahn S, Kanz L, *et al*. HLA ligandome analysis identifies the underlying specificities of spontaneous antileukemia immune responses in chronic lymphocytic leukemia (CLL). *Proc Natl Acad Sci USA*. 2015;112(2):E166-E75.

30. Lee SP, Tierney RJ, Thomas WA, Brooks JM, Rickinson AB. Conserved CTL epitopes within EBV latent membrane protein 2 - A potential target for CTL-based tumor therapy. *J Immunol*. 1997; 158(7):3325-34.

31. Pepperl S, Benninger-Doring G, Modrow S, Wolf H, Jilg W. Immediate-early transactivator Rta of Epstein-Barr virus (EBV) shows multiple epitopes recognized by EBV-specific cytotoxic T lymphocytes. *J Virol*. 1998;72(11):8644-9.

32. Rickinson AB, Moss DJ. Human cytotoxic T lymphocyte responses to Epstein-Barr virus infection. *Annu Rev Immunol*. 1997;15:405-31.

33. Sawada Y, Komori H, Tsunoda Y, Shimomura M, Takahashi M, Baba H, *et al*. Identification of HLA-A2 or HLA-A24-restricted CTL epitopes for potential HSP105-targeted immunotherapy in colorectal cancer. *Oncol Rep*. 2014;31(3):1051-8.

34. Tajima K, Demachi A, Ito Y, Nishida K, Akatsuka Y, Tsujimura K, *et al*. Identification of an epitope from the epithelial cell adhesion molecule eliciting HLA-A*2402-restricted cytotoxic T-lymphocyte responses. *Tissue Antigens*. 2004;64(6):650-9.

35. Takami A, Sugimori C, Feng XM, Wang HB, Akatsuka Y, Kuzushima K, *et al*. Identification of HLA-A*2402-restricted polymorphic peptides derived from CD62L that may mediate graft-versus-leukemia effect. *Blood*. 2003;102(11):719a-20a.

36. Veillette A, Bookman MA, Horak EM, Bolen JB. The CD4 and CD8 T cell surface antigens are associated with the internal membrane tyrosine-protein kinase p56lck. *Cell*. 1988;55(2):301-8.

37. Cheroutre H, Lambolez F. Doubting the TCR coreceptor function of CD8αα. *Immunity*. 2008; 28(2): 149-59.

38. Lyons GE, Moore T, Brasic N, Li M, Roszkowski JJ, Nishimura MI. Influence of human CD8 on antigen recognition by T-cell receptor-transduced cells. *Cancer Res*. 2006;66(23):11455-61.

39. Spits H, Paliard X, Engelhard VH, de Vries JE. Cytotoxic activity and lymphokine production of T cell receptor (TCR)-αβ+ and TCR-γδ+ cytotoxic T lymphocyte (CTL) clones recognizing HLA-A2 and HLA-A2 mutants. Recognition of TCR-γδ+ CTL clones is affected by mutations at positions 152 and 156. *J Immunol*. 1990;144(11):4156-62.

40. Ciccone E, Viale O, Pende D, Malnati M, Battista Ferrara G, Barocci S, *et al*. Specificity of human T lymphocytes expressing a γδT cell antigen receptor. Recognition of a polymorphic determinant of HLA class I molecules by a gamma/delta clone. *Eur J Immunol*. 1989;19(7):1267-71.

41. Del Porto P, D'Amato M, Fiorillo MT, Tuosto L, Piccolella E, Sorrentino R. Identification of a novel HLA-B27 subtype by restriction analysis of a cytotoxic γδT cell clone. *J Immunol*. 1994; 153(7): 3093-100.

42. Colf LA, Bankovich AJ, Hanick NA, Bowerman NA, Jones LL, Kranz DM, *et al*. How a single T cell receptor recognizes both self and foreign MHC. *Cell*. 2007;129(1):135-46.

43. Reiser JB, Darnault C, Gregoire C, Mosser T, Mazza G, Kearney A, *et al*. CDR3 loop flexibility contributes to the degeneracy of TCR recognition. *Nat Immunol*. 2003;4(3):241-7.

44. Morris EC, Stauss HJ. Optimizing T-cell receptor gene therapy for hematologic malignancies. *Blood*. 2016;127(26):3305-11.

45. Robinson J, Halliwell JA, Hayhurst JD, Flicek P, Parham P, Marsh SG. The IPD and IMGT/HLA database: allele variant databases. *Nucleic Acids Res*. 2015;43(Database issue):D423-31.

46. Burrows SR, Elkington RA, Miles JJ, Green KJ, Walker S, Haryana SM, *et al*. Promiscuous CTL recognition of viral epitopes on multiple human leukocyte antigens: biological validation of the proposed HLA-A24 supertype. *J Immunol*. 2003;171(3):1407-12.

47. Norman PJ, Hollenbach JA, Nemat-Gorgani N, Guethlein LA, Hilton HG, Pando MJ, *et al*. Co-evolution of human leukocyte antigen (HLA) class I ligands with killer-cell immunoglobulin-like receptors (KIR) in a genetically diverse population of sub-Saharan Africans. *PLoS Genet*. 2013; 9(10):e1003938.

48. Khandelwal S, Roche PA. Distinct MHC class II molecules are associated on the dendritic cell surface in cholesterol-dependent membrane microdomains. *J Biol Chem*. 2010; 285(46): 35303-10.

49. Campbell EC, Antoniou AN, Powis SJ. The multi-faceted nature of HLA class I dimer molecules. *Immunology*. 2012;136(4):380-4.

50. Kollnberger S, Bird L, Sun MY, Retiere C, Braud VM, McMichael A, *et al*. Cell-surface expression and immune receptor recognition of HLA-B27 homodimers. *Arthritis Rheum*. 2002; 46(11): 2972-82.

51. Seliger B, Cabrera T, Garrido F, Ferrone S. HLA class I antigen abnormalities and immune escape by malignant cells. *Semin Cancer Biol*. 2002;12(1):3-13.

52. Handgretinger R, Schilbach K. The potential role of γδT cells after allogeneic HCT for leukemia. *Blood*. 2018;131(10):1063-72.

53. Locatelli F, Merli P, Pagliara D, Li Pira G, Falco M, Pende D, *et al*. Outcome of children with acute leukemia given HLA-haploidentical HSCT after αβT-cell and B-cell depletion. *Blood*. 2017; 130(5):677-85.

54. Bertaina A, Zecca M, Buldini B, Sacchi N, Algeri M, Saglio F, *et al*. Unrelated donor vs HLA-haploidentical αβT-cell- and B-cell-depleted HSCT in children with acute leukemia. *Blood*. 2018; 132(24):2594-607.

55. Passweg JR, Baldomero H, Bader P, Bonini C, Duarte RF, Dufour C, *et al*. Use of haploidentical stem cell transplantation continues to increase: the 2015 European Society for Blood and Marrow Transplant activity survey report. *Bone Marrow Transplant*. 2017;52(6):811-7.

56. Bouchie A, DeFrancesco L. Nature Biotechnology's academic spinouts of 2015 (vol 34, pg 484, 2016). *Nat Biotechnol*. 2016;34(8):888.

3

SUPPLEMENTARY METHODS

Cells lines

CEPH EBV-LCL lines (CEU population panel) were a kind gift from Tuna Mutis (VU University Medical Center, Amsterdam, The Netherlands) or ordered from the Coriell Biorepository (Camden, New Jersey, USA). Daudi, K562 (WT), T2, SW480, HEK293, and Phoenix-Ampho cell lines were obtained from ATCC. HEK293FT was obtained from Thermo Fisher Scientific (Breda, The Netherlands). K562 and COS-7 (African green monkey kidney fibroblast-like) transduced with HLA-A*02:01 or HLA-A*24:02 were kindly provided by Fred Falkenburg (Leiden University Medical Centre, the Netherlands). The TCRß$^{-/-}$ Jurma cell line (a derivate of Jurkat J.RT3-T3.5 cells cells (1), was kindly provided by Hooijberg (VU Medical Center, Amsterdam, The Netherlands), OPM2-Luciferase (OPM2-Luc) was kindly provided by Anton Martens (University Medical Center Utrecht, Utrecht, the Netherlands). LCL-TM (an EBV-LCL line separate from the CEPH panel) was kindly provided by Phil Greenberg (Fred Hutchinson Cancer Research Center, Seattle, U.S.A.). All cell lines were authenticated by short tandem repeat profiling/karyotyping/isoenzyme analysis and were passaged for a maximum of 2 months, after which new seed stocks were thawed for experimental use. All cell lines were routinely verified by growth rate, morphology, and/or flow cytometry and tested negative for mycoplasma using MycoAlert Mycoplasma Kit (Lonza, Breda, The Netherlands). HLA-A*24:02 Fibroblasts, HEK293, Phoenix-Ampho, SW480, and COS-7 cells were cultured in DMEM supplemented with 1% Pen/Strep (Invitrogen) and 10% FCS (Bodinco, Alkmaar, The Netherlands). All other cell lines were cultured in RPMI with 1% Pen/Strep and 10% FCS. Primary fresh PBMCs were isolated by Ficoll-Paque (GE Healthcare, Eindhoven, The Netherlands) from buffy coats supplied by Sanquin Blood Bank (Amsterdam, The Netherlands). Monocytes and B-cells were isolated from PBMCs by MACS-sorting using CD14 and CD19-microbeads (Miltenyi Biotec) respectively, according to the manufacturers protocol.

Functional T cell assays

IFNγ ELISA and ELISPOT were performed as previously described (2, 3). Briefly; FE11 TCR-transduced, NEF$_{134-10}$ -specific αßTCR or mock-transduced T-cells and target-cells were cocultured for 18 hours in nitrocellulose-bottomed 96-well plates (Millipore) pre-coated with α-IFNγ antibody (clone 1-D1K, Mabtech). Plates were washed and incubated with a second biotinylated anti-IFNγ antibody (clone 7-B6-1, Mabtech) followed by streptavidin-HRP (Mabtech). IFNγ spots were visualized with TMB substrate (Sanquin) and the number of spots was quantified using ELISPOT Analysis Software (Aelvis). Alternatively, TEG011 and target-cells were cocultured as above in round-bottom 96-well plates, and IFNγ levels in supernatants were measured by ELISA. For testing stimulation of WT1$_{126-134}$-specific αßTCR-transduced T-cells, the HLA-A*02-positive target cells were pulsed with 10 μM WT1$_{126-134}$ (RMFPNAPYL) peptide. For testing stimulation of TEG011, HLA-A*24:02-positive target cells were pulsed with 10 μM CMV$_{341-349}$ (pp65, QYDPVAALF), NEF$_{134-10}$ (RYPLTFGWCF), NEF$_{134-144}$-derived peptide mutants, or transformation associated peptides as indicated in the supplements.

Flow cytometry

Antibodies used for flow cytometry included: γδTCR-PE (clone IMMU510, Beckman Coulter), CD4-PE-Cy7 (clone RPA-T4, BD), CD8α-APC (clone RPA-T8, BD), CD8α-Per-CP-Cy5.5 (clone RPA-T8, Biolegend), CD8α-FITC (clone G42-8, BD), CD8αβ-PE (clone 2ST8.5H7, BD), CD69-APC (Clone FN50, Sony Biotechnology) HLA-A/B/C-FITC (clone W6/32, Biolegend). NY-ESO1$_{157-165}$ (HLA-A*02:01 SLLMWITQV) R-PE labelled Pro5 MHC Pentamer (ProImmune, Oxford, United Kingdom) and CMV$_{341-349}$ (HLA-A*24:02 QYDPVAALF) R-PE labelled Pro5 MHC Pentamer (ProImmune) were used according to the manufacturer's instructions. Samples were measured with FACSCanto II and LSRFortessa cytometers (BD) and analyzed with FACSDiva software (BD) or FlowJo software (BD).

Retroviral transduction of TCRs

The Vγ5Vδ1TCR FE11, an HLA-A*02:01 restricted WT1$_{126-134}$-specific αβTCR (4) and an HLA-A*24:02 restricted NEF$_{134-10}$-specific αβTCR were transduced into αβT cells as described (2, 5). In brief, Phoenix-Ampho packaging cells were transfected with gag-pol (pHIT60), env (pCOLT-GALV) and pBullet retroviral constructs containing TCRγ/β-chain-IRES-neomycine or TCRδ/α-chain-IRES-puromycin, using Fugene-HD (Promega, Leiden, The Netherlands). PBMCs preactivated with α-CD3 (30 ng/ml) (clone OKT3, Miltenyi Biotec) and IL-2 (50 U/ml) were transduced twice with viral supernatant within 48 hours in the presence of 50 U/ml IL-2 and 4μg/ml polybrene (Sigma-Aldrich). Transduced T cells were expanded by stimulation with α-CD3/CD28 Dynabeads (0,5x10^6 beads/10^6 cells) (Invitrogen) and IL-2 (50 U/ml) and selected with 800 μg/ml geneticin (Thermo Fisher Scientific) and 5 μg/ml puromycin (Sigma-Aldrich) for one week. CD4$^+$ TCR-transduced T cells were isolated by MACS-sorting using CD4-microbeads (Miltenyi Biotec). Following transduction, transduced T cells were stimulated biweekly according to the REP protocol. Where indicated, CD4$^+$, CD8$^+$, CD4+CD8αα$^+$, CD4+CD8αβ$^+$ and CD8α' (truncated (6)) TCR-transduced T-cells were sorted using a FACSAria II (BD) flow cytometry to >99% purity. Following selection, TCR-transduced T cells were stimulated biweekly using the REP protocol. Transgenic TCR expression was routinely assessed by flow cytometry.

Target cell activation and stress induction

HLA-A*24:02 B-cells and fibroblasts were stressed by either overnight incubation with 5mM cyclophosphamide and 10μM fludarabine or 3500cGy irradiation one day prior to T cell administration. Activation of the HLA-A*24:02 B-cells was induced by administration of 20μg/ml LPS or 20ng/ml IL-4 combined with 1μg/ml CD40L 24 hours before T cell co-culture.

Generation of FE11-like mAbs

FE11-like mAbs were generated by immunization of C57BL/6 mice with SW480 and LCL-TM after which standard fusion of spleen cells was performed to generate hybridomas. Monoclonality was achieved by cloning by limiting dilution twice after which isotype determination was determined by flow cytometry using α-mIgG1 APC (Thermo Fisher Scientific), α-mIgG2b RPE (Jackson ImmunoResearch), α-mIgG2c dylight 405 (Jackson ImmunoResearch), and α-mIgG3 PerCP (Jackson ImmunoResearch). For mAb

production, hybridomas were cultured 5-8x10^5 cells/ml for 1 week in serum-free hybrid-oma medium. mAbs were purified using protein G HP SpinTrap columns (GE healthcare) following the manufacturer's instructions.

Protein separation and digestion

Samples were run on a 4-12% Bis-Tris 1D SDS-PAGE gel (BioRad) for 2.5h and stained with colloidal coomassie dye G-250 (Gel Code Blue Stain Reagent, Thermo Scientific). The lane was cut as three bands, which were treated with 6.5 mM dithiothreitol (DTT) for 1 hour at 60°C for reduction and 54 mM iodoacetamide for 30 minutes for alkylation. The proteins were digested overnight with trypsin (Promega) at 37°C. The peptides were extracted with 100% acetonitrile and dried in a vacuum concentrator.

Mass spectrometry: RP-nanoLC-MS/MS

Samples were reconstituted in 10% formic acid and analyzed by nano-LC-MS/MS on a Orbitrap Q-Exactive Plus (Thermo Fisher Scientific) coupled to an Agilent 1290 Infinity System (Agilent Technologies, Middelburg, The Netherlands) operating in reverse phase (C18) equipped with a Reprosil pur C18 (Dr. Maisch, Ammerbuch-Entringen, Germany) trap column (100µm x 2 cm, 3 µm) and a Poroshell 120 EC C18 (Agilent Technologies) analytical column (75 µm x 50 cm, 2.7 µm). After trapping with 100% solvent A (0.1% FA in H2O) for 10 min, peptides were eluted with an step gradient consisting of 35 min from 13% to 40% and, 3 min from 40% to 100% solvent B (0.1% FA, 80 % ACN). The Q-Exactive Plus was operated in data-dependent acquisition mode using the following settings: full-scan automatic gain control (AGC) target 3e6 at 35 000 resolution; scan range 375–1600 m/z; Orbitrap full-scan maximum injection time 10 ms; MS2 scan AGC target 5e4 at 17 500 resolution; maximum injection 120 ms; normalized collision energy 25; dynamic exclusion time 10s; isolation window 1.5 m/z; 10 MS2 scans per full scan.

Mass spectrometry data analysis

Raw files were processed using Proteome Discoverer 1.4 (version 1.4.1.14, Thermo Fisher Scientific). Raw files of the 3 bands per sample were combined in one search against a Uniprot database (Homo Sapiens, April 2015). The following parameters were used: carbamidomethylation of cysteines was set as a fixed modification and oxidation of methionine was set as a variable modification. Trypsin was specified as enzyme and up to two miss cleavages were allowed. A false discovery rate of 0.01 was used. Datasets processed by Proteome Discoverer were submitted to the Contaminant Repository for Affinity Purification (CRAPome) and proteins identified were sorted by Significance Analysis of INTeractome (SAINT) score, and the fold change scores FC-A or FC-B. The controls used were taken from the control immunoprecipitations performed with unspecific antibodies in each cell line. Proteins with SAINT probability greater than 0.9 were considered high-scoring interactions (7).

Proximity Ligation Assay

HLA-A*24:02$^+$ fibroblasts and SW-480 cells were grown onto coverslips and fixed in 1% Paraformaldehyde for 15 minutes. Subsequently, cells were stained using the Duolink

PLA kit (Sigma Aldrich). Briefly, the PLUS and MINUS probes were both conjugated to the HLA class I antibody clone w6/32 (Cedarlane). Cells were blocked for 60min at 37°C and washed twice with PBS. The conjugated probes were incubated for 60min at 37°C. Afterwards, cells were washed three times in PBS before detection of the probes with the in situ PLA detection kit (Duolink, Sigmaaldrich). Cells were stained with DAPI and analyzed with a 20× objective on a Zeiss confocal laser scanning microscope LSM 700. Data analysis was performed using Volocity software (PerkinElmer).

Supplementary Table 1. Immunoprecipitation with FE11- like antibodies 6 & 12 indicates that classical HLA molecules are part of the ligand. Antibodies produced by hybridoma 6 and hybridoma 12 were used for immunoprecipitation and subsequent mass spectrometry. Hits with a probability score of 1.0 are displayed.

Sample	Antibody	Accession ID	Gene
LCL-TM	12	P30498	HLA-B
LCL-TM	12	Q29963	HLA-C
LCL-TM	12	P04439	HLA-A
LCL-TM	12	P30508	HLA-C
LCL-TM	12	Q95604	HLA-C
LCL-TM	12	P30499	HLA-C
LCL-TM	12	P05534	HLA-A
LCL-TM	12	P18463	HLA-B
LCL-TM	12	P04222	HLA-C
LCL-TM	12	P01892	HLA-A
LCL-TM	12	P61769	B2M
LCL-TM	12	P30511	HLA-F
LCL-TM	6	P05534	HLA-A
LCL-TM	6	P01892	HLA-A
LCL-TM	6	P04439	HLA-A
LCL-TM	6	Q95604	HLA-C
LCL-TM	6	P30508	HLA-C
LCL-TM	6	Q29963	HLA-C
SW480	12	P05534	HLA-A
SW480	12	P01892	HLA-A
SW480	12	P10321	HLA-C
SW480	12	P01889	HLA-B
SW480	12	P18464	HLA-B
SW480	12	Q95604	HLA-C

3

Sample	Antibody	Accession ID	Gene
SW480	12	P04222	HLA-C
SW480	12	P17693	HLA-G
SW480	12	P30511	HLA-F
SW480	12	P16403	HIST1H1C
SW480	12	P10412	HIST1H1E
SW480	6	P05534	HLA-A

Supplementary Table 2. Transformation-associated peptides

| #	AA	Name	Reference
1	DYCNVLNKEF	BRLF1(EBV)	(8)
2	DYNFVKQLF	BMLF1(EBV)	(9)
3	FYTVIPHNF	PARP3 poly (ADP-ribose) polymerase family, member 3	(10)
4	IYNGKLFDL	KIF2C kinesin family member 2C	(10)
5	KFAEEFYSF	CDCA7L cell division cycle associated 7-like	(10)
6	KYPLNLYLL	TMBIM4 transmembrane BAX inhibitor motif containing 4	(10)
7	LYELHVFTF	CTDP1 CTD phosphatase, subunit 1	(10)
8	NYGIYKQDL	HSP105	(11)
9	RYQLDPKFI	EpCAM	(12)
10	RYSIFFDYM	EBNA3A (EBV)	(9)
11	TYGPVFMCL	LMP2 (EBV)	(13)
12	TYPVLEEMF	BRLF1(EBV)	(9)
13	TYSAGIVQI	EBNA3B (EBV)	(14)
14	VFTLKPLEF	HLA-DMA major histocompatibility complex, class II	(10)
15	VYKENLVDGF	NELFE negative elongation factor complex member E	(10)

Supplementary Table 3. HLA-typing of CEPH EBV-LCL lines

LCL	HLA-A		HLA-B		HLA-C	
66	A*020	A*0201	B*0702	B*0801	C*0702	C*0701
68	A*0201	A*0201	B*0801	B*1302	C*0701	C*060
69	A*2402	A*0201	B*0702	B*0702	C*0702	C*0702
82	A*0301	A*2402	B*07xx	B*55xx	C*0702	C*0702
86	A*0301	A*0201	B*-	B*-	C*0702	C*0702
87	A*0101	A*2402	B*0801	B*55xx	C*0701	C*0702
89	A*2402	A*2402	B*3701	B*35xx	C*0602	C*0401
93	A*-2402	A*-2501	B*-1801	B*-3701	C*-	C*-

SUPPLEMENTARY FIGURES
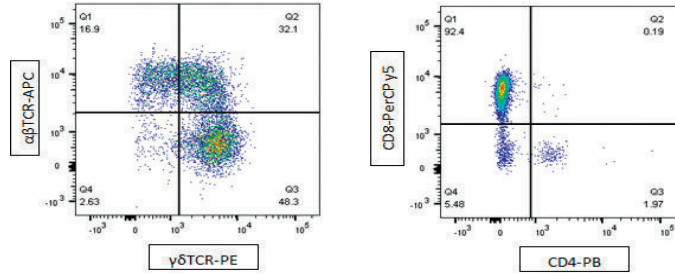
Supplementary Figure 1. A representative FACS staining of FE11 γδTCR transduced T-cells. γδTCR, αβTCR, CD4 and CD8 expression was determined by flow cytometry.
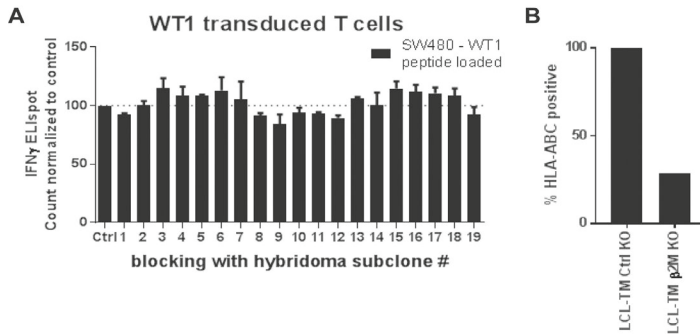
**Supplementary Figure 2. (A)** The effect of blocking with FE11 like hybridoma supernatant on the recognition of SW480 loaded with $WT1_{126-134}$ peptide by T cells transduced with a $WT1_{126-134}$-specific αβTCR transduced T cells. **(B)** LABScreen Single Antigen HLA class I beads were incubated with antibodies purified from hybridoma 6 (mAb 6) or antibodies purified from hybridoma 12 (mAb 12) and secondary α-mIgG-PE and measured using Luminex. Error bars represent SD.

3
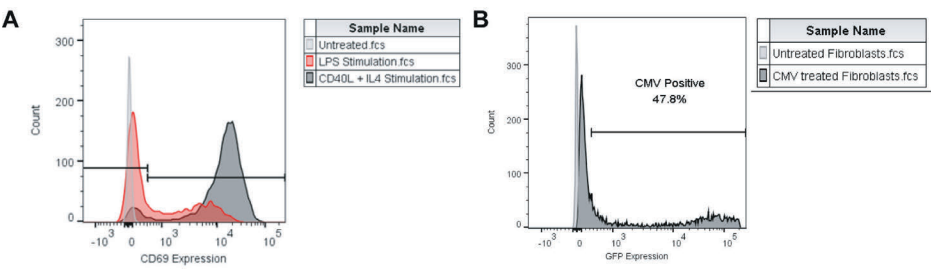
Supplementary Figure 3. (A) B-cells were isolated from HLA-A*24:02+ PBMCs of a healthy donor. Activation was achieved by either LPS administration or a combination of CD40L and IL-4. Activation was measured by CD69 expression via flow cytometry. (LPS administration: 42% CD69+, CD40L + IL-4: 92,5% CD69+ and untreated 0,01% CD69+.**(B)** HLA-A*24:02+ fibroblasts were inoculated with the TB40 HCMV-eGFP strain. CMV infection was measured by GFP expression via flow cytometry on the day of T-cell administration (6 dpi) (CMV treatment: 47,8% GFP+ and untreated 0,2% GFP+).
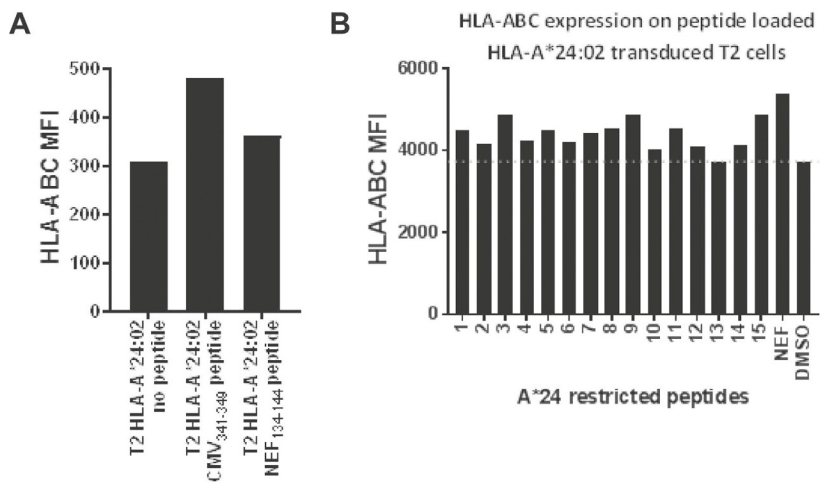

Supplementary Figure 4. (A) HLA-A*24:02-transduced T2 cells were loaded with $CMV_{341-349}$ or $NEF_{134-144}$ HLA-A*24:02-restricted peptides to assess stabilization of HLA on the surface of the T2 cells, as measured by flow cytometry. **(B)** HLA-A*24:02 transduced T2 cells were loaded with 15 HLA-A*24:02-restricted, transformation associated peptides after which stabilization of HLA on the surface of the T2 cells was measured by flow cytometry.
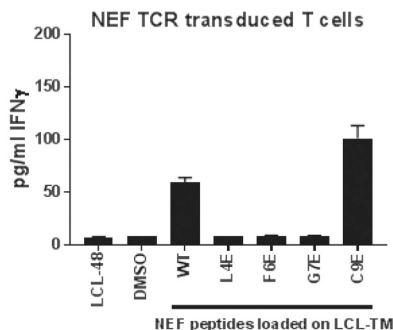
Supplementary Figure 5. LCL-TM cells were loaded with 10μM of the WT peptide and the glutamic acid (E)-modified peptides. These loaded cells were coincubated with T-cells engineered with a NEF$_{134-144}$-specific αβTCR after which activation was assessed by measuring IFNγ production.
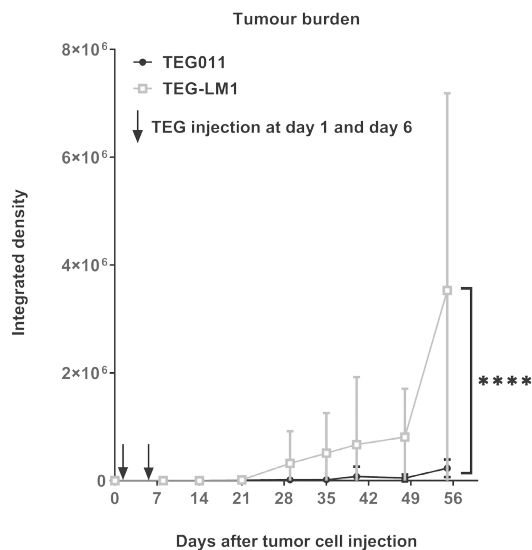
Supplementary Figure 6. *In vivo* efficacy of TEG011 against K562-HLA*A24 luciferase. Tumor burden was assessed *in vivo* by bioluminescence imaging (BLI) measuring integrated density of the entire area of mice with abdomen facing up. Data represent mean ± SD of all mice per group (n = 10). Statistical significances were calculated by a mixed-effects model with repeated measure; *, $P < 0.05$; **, $P < 0.01$; ***, $P < 0.001$; ****, $P < 0.0001$

SUPPLEMENTARY REFERENCES

1. Aarnoudse CA, Kruse M, Konopitzky R, Brouwenstijn N, Schrier PI. TCR reconstitution in Jurkat reporter cells facilitates the identification of novel tumor antigens by cDNA expression cloning. *Int J Cancer*. 2002;99(1):7-13.

2. Marcu-Malina V, Heijhuurs S, van Buuren M, Hartkamp L, Strand S, Sebestyen Z, *et al*. Redirecting αßT cells against cancer cells by transfer of a broadly tumor-reactive γδT-cell receptor. *Blood*. 2011;118(1):50-9.

3. Scheper W, van Dorp S, Kersting S, Pietersma F, Lindemans C, Hol S, *et al*. γδT cells elicited by CMV reactivation after allo-SCT cross-recognize CMV and leukemia. *Leukemia*. 2013;27(6):1328-38.

4. Kuball J, Dossett ML, Wolfl M, Ho WY, Voss RH, Fowler C, *et al*. Facilitating matched pairing and expression of TCR chains introduced into human T cells. *Blood*. 2007;109(6):2331-8.

5. Stanislawski T, Voss RH, Lotz C, Sadovnikova E, Willemsen RA, Kuball J, *et al*. Circumventing tolerance to a human MDM2-derived tumor antigen by TCR gene transfer. *Nat Immunol*. 2001;2(10):962-70.

6. Lyons GE, Moore T, Brasic N, Li M, Roszkowski JJ, Nishimura MI. Influence of human CD8 on antigen recognition by T-cell receptor-transduced cells. *Cancer Res*. 2006;66(23):11455-61.

7. Mellacheruvu D, Wright Z, Couzens AL, Lambert JP, St-Denis NA, Li T, *et al*. The CRAPome: a contaminant repository for affinity purification-mass spectrometry data. *Nat Methods*. 2013;10(8):730-6.

8. Pepperl S, Benninger-Doring G, Modrow S, Wolf H, Jilg W. Immediate-early transactivator Rta of Epstein-Barr virus (EBV) shows multiple epitopes recognized by EBV-specific cytotoxic T lymphocytes. *J Virol*. 1998;72(11):8644-9.

9. Kuzushima K, Hayashi N, Kudoh A, Akatsuka Y, Tsujimura K, Morishima Y, *et al*. Tetramer-assisted identification and characterization of epitopes recognized by HLA-A*24:02-restricted Epstein-Barr virus-specific CD8^{+} T cells. *Blood*. 2003;101(4):1460-8.

10. Kowalewski DJ, Schuster H, Backert L, Berlin C, Kahn S, Kanz L, *et al*. HLA ligandome analysis identifies the underlying specificities of spontaneous antileukemia immune responses in chronic lymphocytic leukemia (CLL). *Proc Natl Acad Sci USA*. 2015;112(2):E166-75.

11. Sawada Y, Komori H, Tsunoda Y, Shimomura M, Takahashi M, Baba H, *et al*. Identification of HLA-A2 or HLA-A24-restricted CTL epitopes for potential HSP105-targeted immunotherapy in colorectal cancer. *Oncol Rep*. 2014;31(3):1051-8.

12. Tajima K, Demachi A, Ito Y, Nishida K, Akatsuka Y, Tsujimura K, *et al*. Identification of an epitope from the epithelial cell adhesion molecule eliciting HLA-A*2402-restricted cytotoxic T-lymphocyte responses. *Tissue Antigens*. 2004;64(6):650-9.

13. Lee SP, Tierney RJ, Thomas WA, Brooks JM, Rickinson AB. Conserved CTL epitopes within EBV latent membrane protein 2: a potential target for CTL-based tumor therapy. *J Immunol*. 1997; 158(7):3325-34.

14. Rickinson AB, Moss DJ. Human cytotoxic T lymphocyte responses to Epstein-Barr virus infection. *Annu Rev Immunol*. 1997;15:405-31.

CHAPTER 4

TEG011 persistence averts extramedullary tumor growth without exerting off target toxicity against healthy tissues in a humanized HLA-A*24:02 transgenic mice

Inez Johanna[1], Patricia Hernández-López[1], Sabine Heijhuurs[1], Laura Bongiovanni[2], Alain de Bruin[2], Dennis Beringer[1], Sanne van Dooremalen[1], Leonard D. Shultz[3], Fumi-hiko Ishikawa[4], Zsolt Sebestyen[1], Trudy Straetemans[1], and Jürgen Kuball[1*]

[1] Department of Hematology and Center for Translational Immunology, University Medical Center Utrecht, Utrecht, The Netherlands
[2] Department of Pathobiology, Dutch Molecular Pathology Center, Faculty of Veterinary Medicine, Utrecht University, Utrecht, The Netherlands
[3] Department of Immunology, The Jackson Laboratory, Bar Harbor, Maine, USA
[4] Laboratory for Human Disease Models, RIKEN Center for Integrative Medical Sciences, Yokohama, Japan

ABSTRACT

γδT cells play an important role in cancer immunosurveillance and are able to distinguish malignant cells from their healthy counterparts via their γδT cell receptor (γδTCR). This characteristic makes γδT cells an attractive candidate for therapeutic application in cancer immunotherapy. Previously, we have identified a novel CD8α-dependent tumor-specific allo-HLA-A*24:02-restricted Vγ5Vδ1TCR with potential therapeutic value when used to engineer αßT cells from HLA-A*24:02 harboring individuals. αßT cells engineered to express this defined Vγ5Vδ1TCR (TEG011) have been suggested to recognize spatial changes in HLA-A*24:02 present selectively on tumor cells but not their healthy counterparts. However, *in vivo* efficacy and toxicity studies of TEG011 are still limited. Therefore, we extend the efficacy and toxicity studies as well as the dynamics of TEG011 *in vivo* in a humanized HLA-A*24:02 transgenic NSG (NSG-A24:02) mouse model to allow the preparation of a first-in-men clinical safety package for adoptive transfer of TEG011. Mice treated with TEG011 did not exhibit any GvHD-like symptoms and extensive analysis of pathologic changes in NSG-A24:02 mice did not show any off-target toxicity of TEG011. However, loss of persistence of TEG011 in tumor-bearing mice was associated with the outgrowth of extramedullary tumor masses as also observed for mock-treated mice. In conclusion, TEG011 is well-tolerated without harming HLA-A*24:02+ expressing healthy tissues, and TEG011 persistence seems to be crucial for long term tumor control *in vivo*.

INTRODUCTION

The presence of γδT cells in various tumor types suggests their essential role in cancer immunosurveillance (1-3). However, the biological mechanism and ligand recognitions for γδT cell activation remain to be elucidated. The most prevalent γδT cell subset found in human peripheral blood expresses a γ9δ2T cell receptor (TCR). γ9δ2T cells mediate antitumor reactivity against hematological and solid malignancies by sensing early metabolic changes through joint spatial and conformational changes in CD277 partially mediated by RhoB (CD277J) (4-7). On the other hand, very little is known about the antitumor properties of γδT cells harboring γδTCRs from other subfamilies (non-γ9δ2 γδT cells). One of the non-γ9δ2 γδT cell subset, Vδ1+ T cells, which mainly reside in tissues, are known to recognize stress-induced ligands, including MHC associated proteins MICA and MICB, CMV associated glycoprotein UL16, and foreign lipid antigens presented on CD1c and CD1d in classical HLA-like manner, which are often upregulated on stressed or malignant cells (8-12). Several studies have also shown the cytotoxic activity of Vδ1+ T cells against leukemia and solid tumors (13-15), thereby revealing their therapeutic potential.

4

Despite the therapeutic potential of γδT cells, their successful clinical implementation remains challenging. For examples, adoptive transfer of *in vitro* expanded γ9δ2T cell failed to show clinical responses to date (3, 16) while adoptive transfer of *ex vivo* expanded non-γ9δ2T cells (17) remain to be tested in the clinic. Major remaining hurdles encompass diversity in function and receptor expression as well as differences in products when generated from different donors (for review (3)). To partially overcome these obstacles, we introduced the concept of TEGs, αβT cells engineered to express a defined γδTCR. TEGs allow the production of αβT cells-transduced with highly tumor-reactive γδTCR from both Vδ2+ (18-20) and Vδ2- (21-23) subsets and thereby engineering strong tumor reactivity against a broad panel of malignancies. Within this context, we previously identified an allo-HLA-restricted and CD8α-dependent Vγ5Vδ1TCR. When this particular receptor was utilized for the TEG concept (later referred as TEG011), selective reactivity towards HLA-A*24:02 expressing tumor cells, but not healthy tissues was observed (24). However, safety studies have been so far very limited and also *in vivo* persistence and expansion profiles have not been assessed but are crucial before first-in-men studies. To further enrich the preclinical safety and efficacy studies needed for regulatory approval, we describe now a more detailed safety profile as well as pharmacokinetics of TEG011 after infusion in non-tumor bearing and tumor-bearing humanized HLA-A*24:02 transgenic NSG (NSG-A24:02) mice and their association with tumor control.

MATERIALS AND METHODS

Retroviral transductions of T cells
TEGs were produced as previously described (5). Briefly, Phoenix-Ampho cells were transfected with *gag-pol* (pHIT60), *env* (pCOLT-GALV), and pMP71 retroviral constructs

containing both γδTCR chains separated by a ribosomal skipping T2A sequence, using FugeneHD reagent (Promega, Leiden, The Netherlands). Human PBMCs from a healthy donor were pre-activated with 30 ng/mL anti-CD3 (Orthoclone OKT3; Janssen-Cilag, Breda, The Netherlands) and 50 IU/mL IL-2 (Proleukin, Novartis, Arnhem, The Netherlands) and subsequently transduced twice with viral supernatant within 48 hours in the presence of 50 IU/mL IL-2 and 6 µg/mL polybrene (Sigma-Aldrich, Zwijndrecht, The Netherlands). TCR-transduced T cells were expanded by stimulation with anti-CD3/CD28 Dynabeads (500,000 beads/10^6 cells; Thermo Fisher Scientific, Breda, The Netherlands) and 50 IU/mL IL-2. Thereafter, TCR-transduced T cells were depleted of the non-engineered T cells.

Depletion of non-engineered T cells

Depletion of non-engineered T cells was performed as previously described (19). Briefly, TCR-transduced T cells were incubated with a biotin-labeled anti-αßTCR antibody (clone BW242/412; Miltenyi Biotec, Leiden, The Netherlands) and incubated with an anti-biotin antibody coupled to magnetic beads (anti-biotin MicroBeads; Miltenyi Biotec). Thereafter, the cell suspension was loaded onto an LD column and αßTCR$^+$ T cells were depleted by MACS cell separation per the manufacturer's protocol (Miltenyi Biotec). After depletion, TEGs were expanded biweekly with 1µg/mL PHA-L (Sigma-Aldrich), 50U/mL IL-2, 5ng/mL IL-15 (R&D Systems), and irradiated allogeneic PBMCs, Daudi and LCL-TM cells. IL-2 and IL-15 was added twice a week as reported also for the T cell rapid expansion protocol (REP) (5).

Animal model

The NOD.Cg-*Prkdc^scid Il2rg^tm1Wjl* Tg(HLA-A24)3Dvs/Sz (NSG-A24:02) mice (25) were bred and housed in the breeding unit of the Central Animal Facility of Utrecht University as previously reported (24). Experiments were conducted under institutional guidelines after permission from the local Ethical Committee and in accordance with the current Dutch laws on Animal Experimentation. Mice were housed in sterile conditions using an individually ventilated cage (IVC) system and fed with sterile food and water. Irradiated mice were given sterile water with antibiotic ciproxin for the duration of the experiment. Mice were randomized with equal distribution by sex and divided into 5 mice/group (for non-tumor bearing model) or 9-10 mice/group (for tumor-bearing model). For the non-tumor bearing mouse model, adult NSG-A24:02 mice (8-11 weeks old) received sublethal total body irradiation (1,75 Gy) on day -1 followed by two injections of $1x10^7$ TEG011 or TEG expressing a non-functional γδTCR (TEG-LM1) (6) on day 1 and day 6. Mice were monitored at least twice a week for weight loss and graft-versus-host disease (GvHD) symptoms (scoring parameter included hunched appearance, activity, fur texture, skin integrity, and diarrhea). The GvHD scoring system is listed in Supplementary Table S1. Humane endpoint (HEP) was reached when mice experienced a 20% weight loss from the initial weight (measured on day -1) and in the case of GvHD score 2 was reached for an individual GvHD parameter or a total GvHD score of 4. For the tumor-bearing mouse model, adult NSG-A24:02 mice (8-11 weeks old) received sublethal total body irradiation (1,75 Gy) on day -1 followed by intravenous injection

of 1×10^5 K562 HLA-A*24:02 luciferase tumor cells on day 0, and received 2 injections of TEG011 and TEG-LM1 mock on day 1 and 6 as previously reported (24). All mice received $0{,}6 \times 10^6$ IU of IL-2 (Proleukin; Novartis) in 100µl incomplete Freund's adjuvant (IFA) subcutaneously together with the first TEGs injection and every 3 weeks until the end of the experiment. Mice were monitored at least twice a week for weight loss and clinical appearance scoring (scoring parameter included hunched appearance, activity, fur texture, and piloerection). The clinical appearance scoring system is listed in Supplementary Table S2. HEP was reached when mice experienced a 20% weight loss from the initial weight (measured on day -1), showed symptoms of disease (sign of paralysis, weakness, and reduced motility), extramedullary tumor masses (if any) reached 2 cm^3 in volume and in the case of clinical appearance score 2 was reached for an individual parameter or a total score of 4.

Flow cytometry analysis

The following antibodies were used for flow cytometry analysis: huCD45-PB (clone HI30; Sony Biotechnology, Surrey, UK), mCD45-APC (clone 30-F11, Sony Biotechnology), αβTCR-FITC (clone IP26; Biolegend, London, United Kingdom), pan-γδTCR-PE (clone IMMU510; Beckman-Coulter, Woerden, The Netherlands), CD8-PerCPCy5.5 (clone RPA-T8, Biolegend), CD4-PeCy7 (clone TPA-R4, Biolegend), and Vδ1-FITC (clone TS8.2, Thermo Fisher Scientific, Landsmeer, The Netherlands). To exclude non-viable cells from the analysis, Fixable Viability Dye eFluor506 was used (eBioscience, Thermo Fisher Scientific). All samples were analyzed on a BD LSRFortessa using FACSDiva Software (BD Biosciences).

Assessment for TEGs persistence

Mouse peripheral blood samples were obtained via cheek vein (max. 50-80 µl/mouse) once a week. Human cells in peripheral blood were quantified using Flow-count Fluorospheres (Beckman Coulter). Red blood cell lysis was performed for blood samples using 1X RBC lysis buffer (Biolegend) before cell staining. Blood samples were stained with a mixture of antibody panels as listed above. The persistence of TEG cells was measured in peripheral blood by quantifying for absolute cell number by flow cytometry using specific markers huCD45$^+$γδTCR$^+$CD8$^+$.

Preparation of single cell suspensions

At the end of the study, extramedullary tumor (if any) sections were isolated and processed into single cell suspensions as previously described (26). A small section of the extramedullary tumor masses was minced and passed through a 70µm cell strainer (BD); cells were washed in PBS and resuspended in RPMI media. A total of 10^6 cells were stained and analyzed for tumor burden (determined by GFP$^+$ cells) by flow cytometry analysis (BD LSRFortessa). Human cells were measured by quantifying absolute cell numbers from a total of 10^6 cells using Flow-count Fluorospheres (Beckman Coulter).

4

Histology staining and analysis

Histopathologic evaluation was performed by hematoxylin and eosin (H&E) staining for the following mouse tissues: liver, spleen, small (duodenum, jejunum, ileum) intestine, bone marrow, and extramedullary tumor masses. When present, histological lesions in major organs were semi-quantitatively evaluated based on the following criteria: 1) white pulp atrophy; 2) extramedullary hematopoiesis and cell type (including blasts, erythroid precursors, band cells, and megakaryocytes); 3) the presence of pigment and apoptotic cells. Bone marrows were evaluated based on the following criteria: 1) cellularity (percentage of hematopoietic cells relative to marrow fat); 2) ratio of the myeloid and erythroid precursors (M/E ratio); and 3) the presence of megakaryocytes. The grading system was used as follows: 0 = absent; 1 =minimal; 2 = mild; 3 =moderate; 4 = marked.

Extramedullary tumor masses were evaluated based on the following histological features: number of mitotic figures and apoptotic cells (express as a range per high-power fields (HPFs), calculated in the same, randomly selected 5 HPFs, 40X); extension of the necrotic tumor tissue and associated inflammation were graded from 0 to 4 (0: no lesions; 1: minimal; 2: mild; 3: moderate; 4: severe).

Images were taken using an Olympus BX45 microscope with the Olympus DP25 camera and analyzed using DP2-BSW (version.2.2) software.

Double immunofluorescence staining

Formalin-fixed extramedullary tumor masses were embedded in paraffin and cut into 4 µm sections. After deparaffinization and dehydration, slides were pretreated with 10 mM citrate buffer pH 6.0 for 15 min, followed by cooling at room temperature for 30 min. Immunofluorescent staining was done using anti-human Anti-Nuclei Antibody (dilution 1:100; clone 3E1.3, Merck Millipore BV, North-Holland, The Netherlands) and anti-human CD3 polyclonal antibody (dilution 1:250; Agilent Technologies, Amstelveen, The Netherlands). Slides were mounted in VECTASHIELD® Antifade Mounting Medium with DAPI (Vector Laboratories, Peterborough, United Kingdom). Images were taken using a Leica LMD7 fluorescence microscope and analyzed using LAS X (Leica Application Suite X) imaging software.

Statistical Analyses

Data were analyzed using GraphPad Prism (GraphPad Software Inc., La Jolla, CA, USA) and represented as mean ± standard deviation (SD) or standard error of mean (SEM) with * $P < 0,05$ and ** $P < 0,01$. Differences between groups were assessed using a 2-way ANOVA with repeated measures, a mixed-effects model with repeated measures, a non-parametric Mann-Whitney t-test, or Kruskal-Wallis test where indicated.

RESULTS

TEG011 do not exhibit off-target toxicity in major organs of non-tumor bearing NSG-A24:02 mice

The introduction of a novel allo-HLA-restricted and CD8α-dependent Vγ5Vδ1TCR in the concept of TEGs (αßT cells Engineered to express a defined γδTCR) (6, 19), hereby known as TEG011, has shown its efficacy against HLA-A*24:02 expressing malignant cells *in vitro* as well as *in vivo* (24). However, to date, *in vivo* efficacy and toxicity studies are limited but essential for a first-in-men study with TEG011. Therefore, we extended our *in vivo* analysis to assess in more detail the safety profile of TEG011 in a separate set of non-tumor bearing NSG mice, which express human HLA-A*24:02 (NSG-A24:02). Non-tumor bearing NSG-A24:02 mice received either two infusions of TEG011 or mock control TEG-LM1 cells. γδTCR expression for both TEG011 and TEG-LM1 mock was comparable (Supplementary Figure S1A) and most of the transduced αßT cells expressed Vδ1[+] TCR for TEG011 (Supplementary Figure S1B). Mice were subsequently monitored for T cell persistence and any possible manifestation of graft-versus-host disease (GvHD) and any other signs of toxicity (experimental outline Figure 1A).
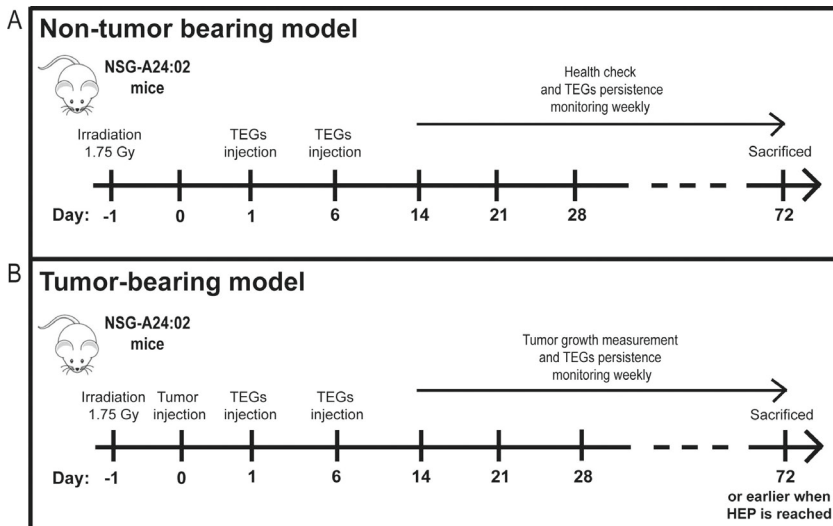
4

Figure 1 Humanized NSG-A24:02 transgenic mice models. Schematic overview of the in vivo experiment for non-tumor bearing **(A)** and K562 HLA-A*24:02 tumor-bearing mice **(B)**. Non-tumor bearing NSG-A24:02 mice were irradiated at day -1 and received 2 injections of TEG011 or TEG-LM1 mock on day 1 and 6. Irradiated tumor-bearing NSG-A24:02 mice were injected with K562 HLA-A*24:02 luciferase tumor cells on day 0 followed by received 2 injections of TEG011 or TEG-LM1 mock on day 1 and 6. Mice were monitored weekly and sacrificed at Day 72 or earlier when humane endpoint (HEP) is reached.
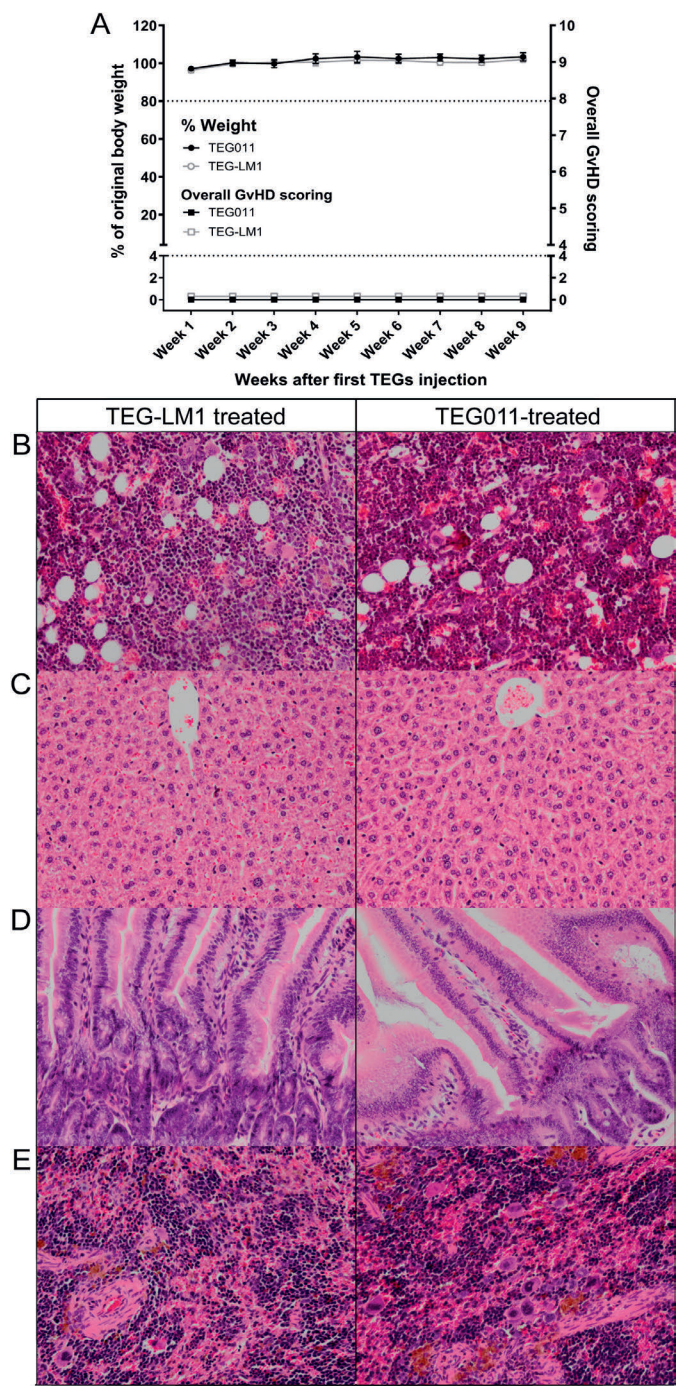
Figure 2 Weight loss, overall GvHD scoring and histopathology analysis of bone marrow and mouse vital organs (spleen, liver, intestine) of non-tumor bearing mice. (A) Percentages of weight change measured weekly during study period for non-tumor bearing mice treated with TEG011 (filled black circle) and TEG LM1 mock (open grey circle) tabulated on left Y axis. A total of 20% weight loss from initial weight measured on day -1 were considered humane endpoint (HEP) and indicated by black tick line. Overall GvHD scoring was tabulated on right Y axis for non-tumor bearing mice treated with TEG011 (filled black rectangle) and TEG-LM1 mock (open grey rectangle). Scoring was calculated based on following parameters: hunching, activity, fur texture, skin integrity, and diarrhea. Score range from 0 to 10 (see Supplementary Table S1 for detail scoring system) , where total overall score of 4 were considered HEP and indicated by black tick line. Score 0 depicts normal appearance for all GvHD parameters. Data represent mean ± SEM of all mice per group (n = 5 mice/group). **(B)** Representative photomicrographs H&E stained of mouse bone marrow from both TEG-LM1 mock (left panel) and TEG011-treated group (right panel). Magnification: 20X; **(C)** Representative photomicrographs for H&E stained of mouse liver for both TEG-LM1 mock (left) and TEG011-treated group (right) with apparent no histological lesion. Magnification: 20X; **(D)** Representative pictures for H&E staining of mouse intestine for both TEG-LM1 mock (left) and TEG011-treated group (right) with apparent no histological lesion. Magnification: 20X; **(E)** Representative photomicrographs for H&E stained of female mouse spleen for both TEG-LM1 mock (left) and TEG011-treated group (right) with a higher number of erythrocyte precursors and megakaryocytes. Magnification: 20X; Shown are representative photomicrographs from individual mice of both TEG011 and TEG-LM1 mock group (n = 5 mice/group) with no observable differences in overall histology features between treatment groups.

4

GvHD-like symptoms were monitored twice weekly for all mice using a scoring system based on hunching posture, activity, fur texture, skin integrity, and diarrhea (See Supplementary Table S1 for GvHD scoring system) ranging from 0 (normal behavior and posture), 1 (slight decreased in fitness), and 2 (moderate decreased in fitness). Score 2 of an individual parameter or an overall score of 4 was defined as humane endpoint (HEP) and mice were sacrificed. All mice did neither experience weight loss, nor any abnormality observed in relation to GvHD symptoms during the entire study duration of 72 days (Figure 2A). In addition, all mice did not exhibit any observable discomfort and survived throughout the entire study duration (24). Persistence of TEGs was assessed by measuring viable huCD45$^+$γδTCR$^+$CD8$^+$ in mouse peripheral blood by flow cytometry (Supplementary Figure S2A). In non-tumor bearing mice, T cells persisted in peripheral blood up to 48 days after infusion and had although not significant a second peak of expansion after administration of IL-2 which was more pronounced in TEG011-treated mice (Figure 3A). To evaluate in more detail possible off-target toxicity of TEG011 against human HLA-A*24:02 expressing healthy tissues, we collected bone marrow, liver, intestine, and spleen from both treatment groups of non-tumor bearing mice at the end of the study period (Day 72) for further histopathology analysis (Figure 2B). No differences were observed in terms of bone marrow cellularity (percentage of hematopoietic cells relative to marrow fat) nor in the ratio of the myeloid and erythroid precursors (M/E ratio) for both treatment group (Supplementary Table S3). Furthermore, no abnormal histological lesions were observed in liver (Figure 2C) and intestine (Figure 2D) of all mice in the study. We observed slightly increased extramedullary hematopoiesis (EMH) in the spleen of TEG011-treated female mice when compared to TEG-LM1 mock-treated mice (Figure 2E), which was determined by a higher number of erythrocyte precursors and megakaryocytes.

On the other hand, a minimal decrease of EMH was observed in the spleen of the TEG011-treated male group compared to mock-treated mice (Supplementary Table S3). Importantly, all spleen samples from both TEG011 and TEG-LM1 mock groups showed a comparable population of cells, including normal blasts, band cells, erythrocyte precursors, and megakaryocytes. Hence, these observations on spleen were deemed minimal and not associated with an evident increase of histological toxicity of TEG011. In conclusion, our data show no relevant GvHD manifestation in all mice and no histological signs of toxicity in the major organs of all healthy tissues upon TEG011 treatment. Thus, we conclude that TEG011 does not associate with off-target toxicity in an HLA-A*24:02 environment.

In vivo dynamic of TEG011 in tumor-bearing mice

Clinical data for anti-CD19 CART therapy highlight the correlation of antitumor effects with their *in vivo* persistence (27-29). To assess whether persistence of TEG011, which carries a CD8α-dependent Vγ5Vδ1TCR (24), is also key in long-term tumor control, we studied in more detail CD8$^+$ TEG persistence in tumor-bearing NSG-A24:02 mice injected with K562 HLA-A*24:02 luciferase tumor cells and subsequently treated with either TEG011 or TEG-LM1 mock cells (experimental outline Figure 1B). Thereafter, we measured viable huCD45$^+$γδTCR$^+$CD8$^+$ in mouse peripheral blood by flow cytometry (Supplementary Figure S2B). While non-functional TEG-LM1 cells diminished in all tumor-bearing control mice 29 days after infusion (Figure 3B), TEG011 cells expanded and remained detectable in peripheral blood up to 64 days. However, only 44% of TEG011-treated mice (4/9) showed significant long-term persistence of T cells until the end of the study period, while the remaining 56% of the mice (5/9) did not show long-term persistence. Therefore, we subsequently defined TEG011-treated mice into two subgroup: "persisters" and "non-persisters", respectively (Figure 3C). TEG011 "persisters" showed significantly higher TEG cell counts on Day 22 until Day 37 upon expansion compared to "non-persisters", where TEG cells were no longer detectable after Day 48 and did not recover even after IL-2 injection on Day 50. Given the fluctuating persistence profile of TEG011, we analyzed further the difference between TEG011 "persisters" and "non-persisters" by calculating area under curve (AUC) of absolute cell counts TEG011 for both "persisters" and "non-persisters" subgroup and also confirmed significant difference in T cell persistence (Figure 3C, D).
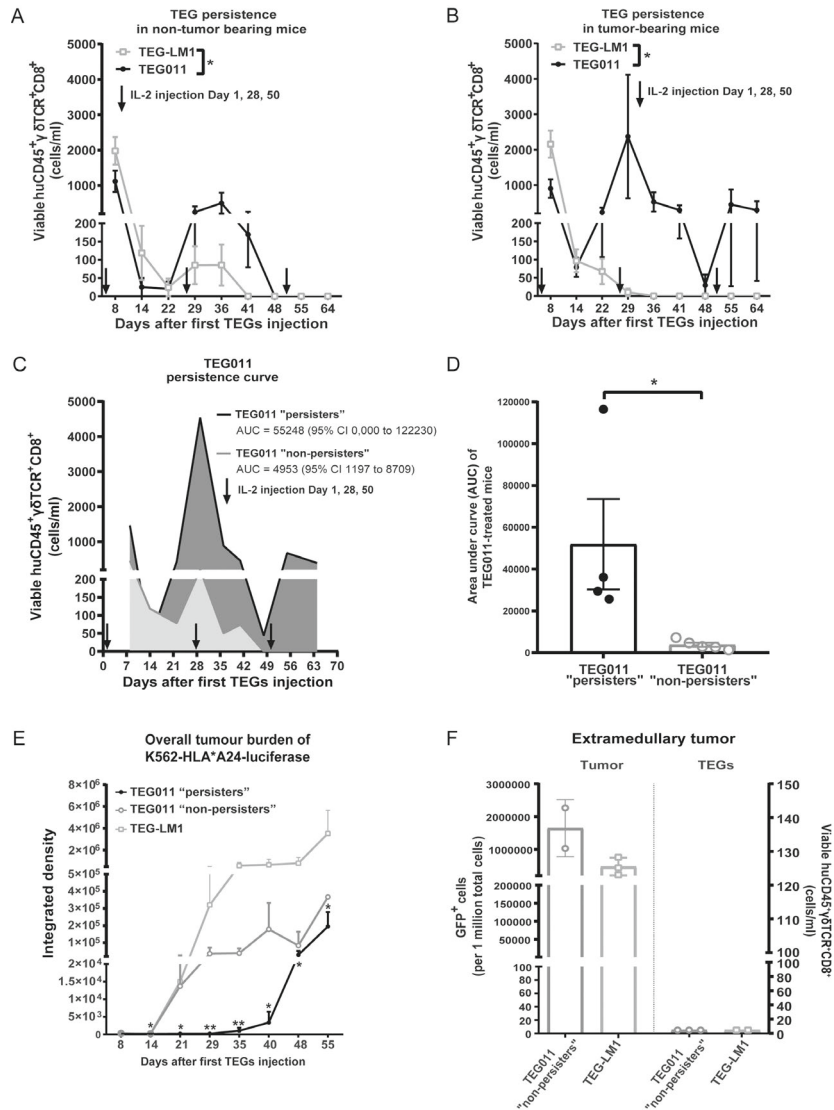
Figure 3 Long-term persistence of TEG011 cells in peripheral blood of tumor-bearing mice and its association with tumor burden. (A) TEG persistence was measured in peripheral blood by quantifying for absolute cell numbers by flow cytometry for TEG LM1 mock (open light-grey rectangle) and TEG011 (filled black circle) in non-tumor bearing mice. Data represent mean ± SEM of all mice per group (n = 5 mice). Statistical significances were calculated by mixed-effects model with repeated measures; *, P < 0.05. **(B)** TEG persistence was measured in peripheral blood by quantifying for absolute cell numbers by flow cytometry for TEG LM1 mock (open light-grey rectangle; n = 10 mice) and TEG011 (filled black circle; n = 9 mice) in tumor-bearing mice. Data represent mean ± SEM of all mice per group. Statistical significances were calculated by mixed-effects model with repeated measures; *, P < 0.05. **(C)** Area under the curve (AUC) of CD8+ TEG011 persistence were calculated for both TEG011 "persisters" (black line, dark grey area; 4/9 mice) and TEG011 "non-persisters" (grey line, light grey area; 5/9 mice) up to 64 days after infusion. Data represent mean ± SEM of all mice per group. 95% Confidence Interval (95%

Figure 3 *(Continued)* CI) were tabulated for AUC of both subgroup. **(D)** Mean AUC of CD8+ TEG011 persistence from individual mouse of both TEG011 "persisters" (filled dark grey bar; 4/9 mice) and TEG011 "non-persisters" (filled light grey bar; 5/9 mice) groups were tabulated and shown as mean ± SEM of all mice per group. Statistical significances were calculated by non-parametric Mann-Whitney t-test; *, P < 0.05. **(E)** Tumor burden for K562-HLA*A24-luciferase was assessed in vivo by bioluminescence imaging (BLI) measuring integrated density of the entire area of mice with abdomen facing up. Data shown as mean ± SD of all mice per group (TEG011 "persisters" (filled black circle; 4/9 mice), TEG011 "non-persisters" (open dark-grey circle 5/9 mice), and TEG-LM1 mock (open light-grey rectangle; n = 10 mice)). Statistical significances were calculated by non-parametric Mann-Whitney t-test in comparison to TEG-LM1 mock control; *, P < 0.05; **, P < 0.01. **(F)** Tumor burden for K562-HLA*A24-luciferase and infiltrating CD8+ TEGs were assessed from isolated extramedullary tumor masses by quantifying for absolute cell number GFP+ cells by flow cytometry. Each symbol represents an individual mouse per treatment group that developed extramedullary tumor masses. Readouts on infiltrating T cells are set to 5 cells/ml for individual mouse in the Y axis for data visualization purpose. Data represent mean ± SD of all mice per group (TEG011 "non-persisters" (open dark-grey circle; 2/5 mice) and TEG-LM1 mock (open light-grey rectangle; 3/10 mice)). FACS analyses of extramedullary tumor mass from TEG-LM1 group were only obtained from 3 out of 4 mice.

TEG011 persistence and its association with tumor control

Next, we assessed whether TEG011 persistence was associated with overall tumor control and analyzed tumor burden over time measured by bioluminescence imaging in the tumor-bearing mice injected with K562 HLA-A*24:02 luciferase tumor cells. In line with our hypothesis that the immune effector persistence is key to achieve long-term tumor control, the TEG011 "persisters" associated with a better tumor control as compared to TEG-LM1 mock group, as well as a trend of lower tumor burden in comparison to TEG011 "non-persisters" subgroup (Figure 3E). Approximately 40% of mock-treated mice (4/10) and 40% TEG011 "non-persisters" mice (2/5) developed extramedullary tumor masses, while interestingly, none of the TEG011 "persisters" mice developed any extramedullary tumor masses. Tumor burden was comparable between extramedullary tumor masses isolated from TEG011 "non-persisters" and TEG-LM1 mock-treated mice and no tumor infiltrating CD8+ TEGs could be observed in all isolated tumor masses (Figure 3F).

To measure possible discomfort due to tumor growth, all mice were monitored for weight loss and a scoring system based hunching posture, activity, fur texture, and piloerection (See Supplementary Table S2 for clinical appearance scoring system) ranging from 0 (normal behavior and posture), 1 (slight decreased in fitness), and 2 (moderate decreased in fitness). Similar to GvHD scoring system for non-tumor bearing mice, score 2 of an individual parameter or an overall score of 4 was defined as HEP and mice were sacrificed. While TEG011 treatment significantly decreased tumor progression, TEG-LM1 treated mice experienced diminished fitness and significant weight loss over time (Figure 4A). Extramedullary tumor masses were analyzed in further detail and histologically characterized by undifferentiated tumor cells of human origin, with a solid and invasive growth pattern (Figure 4B, C), consistent with a myeloid sarcoma development in line with previous reports (30, 31). We also performed immunofluorescence (IF) staining to detect any presence of human T cells within the inflammatory infiltrate associated with the multiple tumor masses observed in the xenograft mouse models. However, while we confirmed that tumor cells are of human origin, no human T cells were observed in
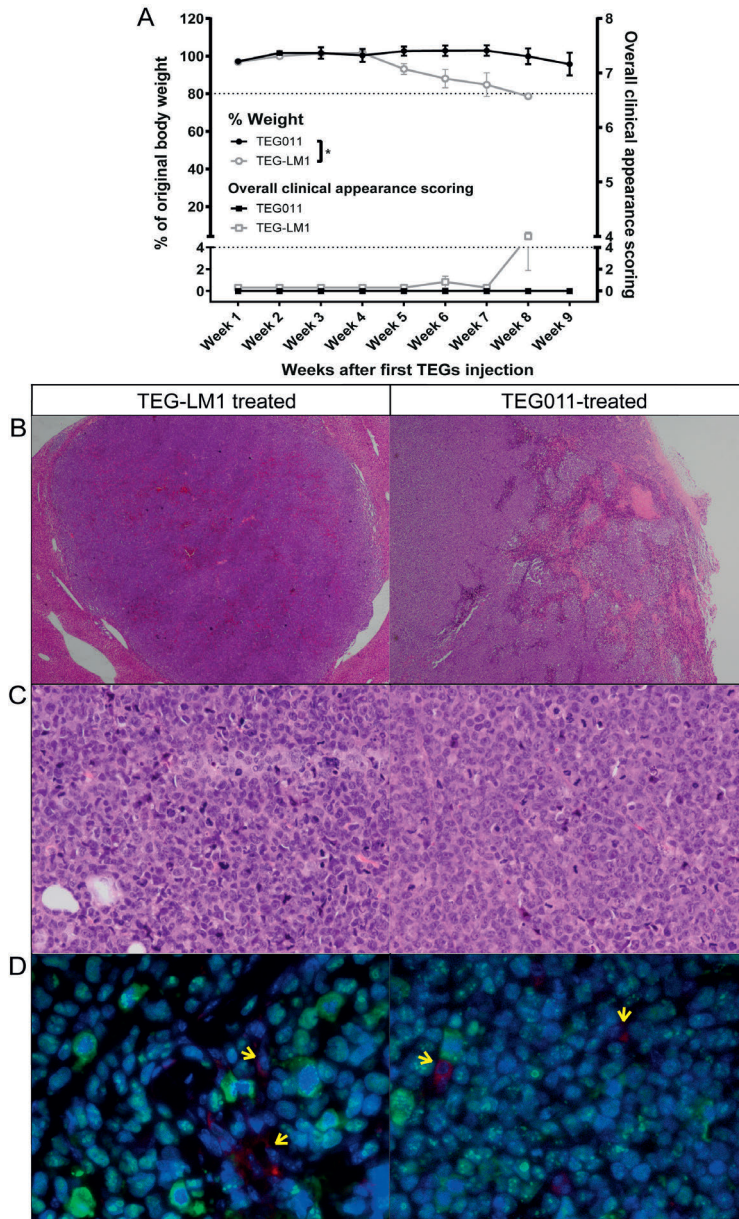
4

Figure 4 Weight loss, overall clinical appearance scoring, histopathology and immunofluorescence (IF) staining analysis of extramedullary tumor masses. (A) Percentages of weight loss measured weekly during study period for tumor-bearing mice treated with TEG011 (filled black circle; n = 9 mice) and TEG-LM1 mock (open grey circle; n = 10 mice) tabulated on left Y axis. A total of 20% weight loss from initial weight measured on day -1 were considered HEP and indicated by black tick line. Overall clinical appearance scoring was tabulated on right Y axis for tumor-bearing mice treated with TEG011 (filled black rectangle; n = 9 mice) and TEG-LM1 mock (open grey rectangle; n = 10 mice). Scoring was calcu-lated based on following parameters: hunching, activity, fur texture, and piloerection. Score range from

Figure 4 *(Continued)* 0 to 8 (see Supplementary Table S2 for detail scoring system), where total overall score of 4 were considered HEP and indicated by black tick line. Score 0 depicts normal appearance for all clinical appearance parameters. Data represent mean ± SEM of all mice per group. Statistical significances were calculated by non-parametric Mann-Whitney t-test; *, P < 0.05. **(B)** Representative photomicrographs H&E stained of multiple areas of hemorrhages and necrosis from both TEG-LM1 mock (left panel - stated as control) and TEG011-treated group (right panel). Aberrant mitotic figures were frequently observed in all samples. Magnification: 2X; **(C)** Representative photomicrographs H&E stained tissues of high mitotic rate tumor cells from both TEG-LM1 mock (left panel) and TEG011-treated group (right panel). No evident differences were observed comparing the extension of necrotic areas in the tumor tissue, associated inflammation, number of apoptotic cells and mitotic figures. Magnification: 20X. **(D)** Representative double IF staining of extramedullary tumor masses from both TEG-LM1 mock (left panel) and TEG011-treated group (right panel). Tumor mass of human origin (human nuclear antigen positive cells, green) with scattered CD3 positive cells (red; pointed by arrows) with DAPI (blue) staining for the nuclei. Magnification 63X. Shown are representative pictures from an individual mouse of both TEG-LM1 mock (n = 4 mice) and TEG011 (n = 2 mice).

all evaluated samples, as scattered positive $CD3^+$ T cells observed within the multiple tumor masses were all negative for the human nuclear antigen (Figure 4D). Thus, no TEGs could be observed by immunohistochemistry in extramedullary tumor masses as also confirmed by flow cytometry analysis (Figure 3F). Overall, our data indicate that TEG011 persistence associates with a reduced chance for developing extramedullary tumor masses *in vivo* without harming healthy compartments.

DISCUSSION

TEG011 has been reported to target HLA-A*24:02 expressing hematological tumors without harming healthy tissues (24). Within this study, we now extend previous *in vivo* analyses followed by pathological studies to further assess the efficacy-toxicity balance of TEG011 prior to clinical testing. Major findings of our study are that TEG011 treatment does not associate with any discomfort nor histopathological evidence of toxicity in an HLA-A*24:02 background. In addition, we report on an association between TEG011 persistence and lack of extramedullary tumor growth.

Toxicity studies of compounds targeting metabolic changes remain a major challenge as such changes cannot be readily studied in detail in all organs (3). Therefore, we proposed efficacy-toxicity models for TEGs targeting joint spatial and conformational changes in CD277 (later referred as CD277J) (3) through a γ9δ2TCR (TEG001) by co-incubating TEG001 with healthy and diseased tissues in an artificial 3D bone marrow niche (32) or in a mouse model where either healthy cord blood-derived $CD34^+$ progenitor or primary leukemia cells were engrafted (26). These models partially overcome the absence of the natural ligand CD277J in mice (3, 7, 33) and allowed the initiation of a first-in-men study (NTR6541) (18, 19, 34). With TEG011, we could utilize transgenic mice expressing human HLA-A*24:02 (25), allowing thereby more extensive toxicity studies of TEG011 in different tissues as compared to TEG001 (26, 32). Although we did not investigate all organs, and despite the fact that TEG011 did not persist until day 72 in the peripheral blood of all mice, we provide strong evidence that TEG011 does not

induce toxicity against human HLA-A*24:02 expressing non-tumor healthy tissues. This is also supported by our observation that tumor control in mice did not associate with any signs of toxicity against healthy tissues.

Considering the natural properties of T cells to proliferate and migrate in tissues, T cell expansion and persistence are commonly used to determine the pharmacokinetics properties of cell-based therapy (35). Our models also allowed us to investigate TEG011 kinetics in tumor-bearing mice in more detail. TEG persistence until the end of the study period was only observed in tumor-bearing mice treated with TEG011 but not TEG-LM1 cells, suggesting that antigen presence and cognate recognition through the TCR are key for long-term persistence of TEG011 in this model. Higher T cell exposure observed between day 22 to day 36 after TEG infusion correlated with superior tumor control of TEG011 ("persisters"). These data align with a recent study that showed complete response in leukemia patients that receive CART therapy when high T cell exposure has been observed in the first 48 days of infusion (36).

However, TEG011 long-term persistence was only observed in 44% of tumor-bearing mice. Within the limitation of our model, we could not identify the exact factor(s) that determine the difference between TEG011 "persisters" and "non-persisters". Most likely this is the consequence of a stochastically driven intrinsic T cell fitness and composition of the infused product. The presence of memory (stem) T cells have been reported to correlate with long-term persistence (37, 38) and complete response in patients receiving adoptive transfers of CART or antigen-specific T cells (37, 38).

Furthermore, in non-tumor bearing mice some advantage of the TEG011 product has been observed when compared to T cell bearing the non-functional receptor, though no long-term persistence has been observed. This might be the consequence of some residual TCR signal via HLA-A*24:02 which is sufficient to maintain some homeostatic proliferation but does not induce toxicity in healthy tissues. In particular, after administration of IL-2 T cell survival of cognate T cells in tumor-bearing mice has been prolonged suggesting that additional help through e.g. CD4$^+$ engineered T cells could further improve potency of TEG011. Indeed, the presence of antigen-specific TCR-engineered CD4$^+$ T cells synergistically enhances persistence and long-term tumor control when infused together with antigen-specific TCR-engineered CD8$^+$ T cells (39). Similarly, *in vivo* persistence of CD4$^+$ CART cells provides helper signal, which then increases CD8$^+$ CART cell persistence (40).

As TEG011 is CD8α-dependent and consequently in the current design lacking support by antigen-specific CD4$^+$ T cells (22, 24), equipping engineered TEG011 with CD8αα could be a strategy to further enhance T cell persistence and long-term tumor control. The precise molecular interaction between CD8αα with its specific ligand in our context remains however elusive. Possible ligands are the classical MHC-I molecule HLA-A*24:02 itself or alternative candidates such as the non-classical MHC molecule HLA-G (41, 42) and CEACAM5 (43).

Overall, we demonstrate that TEG011 does not show signs of off-target toxicity in more detailed toxicity studies. In addition, long-term persistence of TEG011 associated with lower tumor burden without harming healthy tissues, thereby highlight the potential of TEG011 for clinical application.

Conflict of Interest Disclosure

DB, ZS and JK are inventors on different patents with γδTCR sequences, recognition mechanisms and isolation strategies. JK is scientific advisor and shareholder of Gadeta (www.gadeta.nl). No potential conflicts of interest were disclosed by the other authors.

REFERENCES

1. Dadi S, Chhangawala S, Whitlock BM, Franklin RA, Luo CT, Oh SA, *et al.* Cancer Immunosurveillance by Tissue-Resident Innate Lymphoid Cells and Innate-like T Cells. *Cell*. 2016; 164(3):365-77.

2. Gentles AJ, Newman AM, Liu CL, Bratman SV, Feng W, Kim D, *et al.* The prognostic landscape of genes and infiltrating immune cells across human cancers. *Nat Med*. 2015; 21(8):938-45.

3. Sebestyen Z, Prinz I, Dechanet-Merville J, Silva-Santos B, Kuball J. Translating gammadelta (γδ) T cells and their receptors into cancer cell therapies. *Nat Rev Drug Discov*. 2019.

4. Kabelitz D, Wesch D, He W. Perspectives of γδ T cells in tumor immunology. *Cancer Res*. 2007; 67(1):5-8.

5. Marcu-Malina V, Heijhuurs S, van Buuren M, Hartkamp L, Strand S, Sebestyen Z, *et al.* Redirecting αß T cells against cancer cells by transfer of a broadly tumor-reactive γδ T-cell receptor. *Blood*. 2011; 118(1):50-9.

6. Grunder C, van Dorp S, Hol S, Drent E, Straetemans T, Heijhuurs S, *et al.* γ9 and δ2CDR3 domains regulate functional avidity of T cells harboring γ9δ2TCRs. *Blood*. 2012; 120(26):5153-62.

7. Sebestyen Z, Scheper W, Vyborova A, Gu S, Rychnavska Z, Schiffler M, *et al.* RhoB Mediates Phospho-antigen Recognition by Vγ9Vδ2 T Cell Receptor. *Cell Rep*. 2016; 15(9):1973-85.

8. Groh V, Rhinehart R, Secrist H, Bauer S, Grabstein KH, Spies T. Broad tumor-associated expression and recognition by tumor-derived γδ T cells of MICA and MICB. *Proc Natl Acad Sci USA*. 1999; 96(12):6879-84.

9. Catellani S, Poggi A, Bruzzone A, Dadati P, Ravetti JL, Gobbi M, *et al.* Expansion of Vδ1 T lymphocytes producing IL-4 in low-grade non-Hodgkin lymphomas expressing UL-16-binding proteins. *Blood*. 2007; 109(5):2078-85.

10. Poggi A, Venturino C, Catellani S, Clavio M, Miglino M, Gobbi M, *et al.* Vδ1 T lymphocytes from B-CLL patients recognize ULBP3 expressed on leukemic B cells and up-regulated by trans-retinoic acid. *Cancer Res*. 2004; 64(24):9172-9.

11. Luoma AM, Castro CD, Mayassi T, Bembinster LA, Bai L, Picard D, *et al.* Crystal structure of Vδ1 T cell receptor in complex with CD1d-sulfatide shows MHC-like recognition of a self-lipid by human γδ T cells. *Immunity*. 2013; 39(6):1032-42.

12. Zhao J, Huang J, Chen H, Cui L, He W. Vδ1 T cell receptor binds specifically to MHC I chain related A: molecular and biochemical evidences. *Biochem Biophys Res Commun*. 2006; 339(1): 232-40.

13. Schilbach K, Frommer K, Meier S, Handgretinger R, Eyrich M. Immune response of human propagated γδ-T-cells to neuroblastoma recommend the Vδ1+ subset for γδ-T-cell-based immunotherapy. *J Immunother*. 2008; 31(9):896-905.

14. Maeurer MJ, Martin D, Walter W, Liu K, Zitvogel L, Halusczcak K, *et al.* Human intestinal Vδ1+ lymphocytes recognize tumor cells of epithelial origin. *J Exp Med*. 1996; 183(4):1681-96.

15. Devaud C, Rousseau B, Netzer S, Pitard V, Paroissin C, Khairallah C, *et al.* Anti-metastatic potential of human Vδ1+ γδ T cells in an orthotopic mouse xenograft model of colon carcinoma. *Cancer Immunol Immunother*. 2013; 62(7):1199-210.

16. Deniger DC, Moyes JS, Cooper LJ. Clinical applications of γδ T cells with multivalent immunity. *Front Immunol*. 2014; 5:636.

17. Siegers GM, Lamb LS, Jr. Cytotoxic and regulatory properties of circulating Vδ1+ γδ T cells: a new player on the cell therapy field? *Mol Ther*. 2014; 22(8):1416-22.

18. Straetemans T, Kierkels GJJ, Doorn R, Jansen K, Heijhuurs S, Dos Santos JM, *et al.* GMP-Grade Manufacturing of T Cells Engineered to Express a Defined γδTCR. *Front Immunol*. 2018; 9:1062.

4

19. Straetemans T, Grunder C, Heijhuurs S, Hol S, Slaper-Cortenbach I, Bonig H, *et al*. Untouched GMP-Ready Purified Engineered Immune Cells to Treat Cancer. *Clin Cancer Res*. 2015; 21(17): 3957-68.

20. Straetemans T, Janssen A, Jansen K, Doorn R, Aarts T, van Muyden ADD, *et al*. TEG001 Insert Integrity from Vector Producer Cells until Medicinal Product. *Mol Ther*. 2019.

21. Scheper W, Sebestyen Z, Kuball J. Cancer Immunotherapy Using γδT Cells: Dealing with Diversity. *Front Immunol*. 2014; 5:601.

22. Scheper W, van Dorp S, Kersting S, Pietersma F, Lindemans C, Hol S, *et al*. γδT cells elicited by CMV reactivation after allo-SCT cross-recognize CMV and leukemia. *Leukemia*. 2013; 27(6):1328-38.

23. Scheper W, Grunder C, Straetemans T, Sebestyen Z, Kuball J. Hunting for clinical translation with innate-like immune cells and their receptors. *Leukemia*. 2014; 28(6):1181-90.

24. Kierkels GJJ, Scheper W, Meringa AD, Johanna I, Beringer DX, Janssen A, *et al*. Identification of a tumor-specific allo-HLA-restricted γδTCR. *Blood Adv*. 2019; 3(19):2870-82.

25. Najima Y, Tomizawa-Murasawa M, Saito Y, Watanabe T, Ono R, Ochi T, *et al*. Induction of WT1-specific human CD8+ T cells from human HSCs in HLA class I Tg NOD/SCID/IL2rgKO mice. *Blood*. 2016; 127(6):722-34.

26. Johanna I, Straetemans T, Heijhuurs S, Aarts-Riemens T, Norell H, Bongiovanni L, *et al*. Evaluating *in vivo* efficacy - toxicity profile of TEG001 in humanized mice xenografts against primary human AML disease and healthy hematopoietic cells. *J Immunother Cancer*. 2019; 7(1):69.

27. Porter DL, Hwang WT, Frey NV, Lacey SF, Shaw PA, Loren AW, *et al*. Chimeric antigen receptor T cells persist and induce sustained remissions in relapsed refractory chronic lymphocytic leukemia. *Sci Transl Med*. 2015; 7(303):303ra139.

28. Brentjens RJ, Riviere I, Park JH, Davila ML, Wang X, Stefanski J, *et al*. Safety and persistence of adoptively transferred autologous CD19-targeted T cells in patients with relapsed or chemotherapy refractory B-cell leukemias. *Blood*. 2011; 118(18):4817-28.

29. Kochenderfer JN, Dudley ME, Feldman SA, Wilson WH, Spaner DE, Maric I, *et al*. B-cell depletion and remissions of malignancy along with cytokine-associated toxicity in a clinical trial of anti-CD19 chimeric-antigen-receptor-transduced T cells. *Blood*. 2012; 119(12):2709-20.

30. Lozzio BB, Lozzi CB, Machado E. Human myelogenous (Ph+) leukemia cell line: transplantation into athymic mice. *J Natl Cancer Inst*. 1976; 56(3):627-9.

31. Caretto P, Forni M, d'Orazi G, Scarpa S, Feraiorni P, Jemma C, *et al*. Xenotransplantation in immuno-suppressed nude mice of human solid tumors and acute leukemias directly from patients or *in vitro* cell lines. *Ric Clin Lab*. 1989; 19(3):231-43.

32. Braham MVJ, Minnema MC, Aarts T, Sebestyen Z, Straetemans T, Vyborova A, *et al*. Cellular immuno-therapy on primary multiple myeloma expanded in a 3D bone marrow niche model. *Oncoimmunology*. 2018; 7(6):e1434465.

33. Harly C, Guillaume Y, Nedellec S, Peigne CM, Monkkonen H, Monkkonen J, *et al*. Key implication of CD277/butyrophilin-3 (BTN3A) in cellular stress sensing by a major human γδ T-cell subset. *Blood*. 2012; 120(11):2269-79.

34. Kierkels GJ, Straetemans T, de Witte MA, Kuball J. The next step toward GMP-grade production of engineered immune cells. *Oncoimmunology*. 2016; 5(2):e1076608.

35. Kakkanaiah VN, Lang KR, Bennett PK. Flow cytometry in cell-based pharmacokinetics or cellular kinetics in adoptive cell therapy. *Bioanalysis*. 2018; 10(18):1457-9.

36. Mueller KT, Maude SL, Porter DL, Frey N, Wood P, Han X, *et al*. Cellular kinetics of CTL019 in relapsed/refractory B-cell acute lymphoblastic leukemia and chronic lymphocytic leukemia. *Blood*. 2017; 130(21):2317-25.

37. Xu Y, Zhang M, Ramos CA, Durett A, Liu E, Dakhova O, *et al*. Closely related T-memory stem cells correlate with in vivo expansion of CAR.CD19-T cells and are preserved by IL-7 and IL-15. *Blood*. 2014; 123(24):3750-9.

38. Louis CU, Savoldo B, Dotti G, Pule M, Yvon E, Myers GD, *et al*. Antitumor activity and long-term fate of chimeric antigen receptor-positive T cells in patients with neuroblastoma. *Blood*. 2011; 118(23):6050-6.

39. Morris EC, Tsallios A, Bendle GM, Xue SA, Stauss HJ. A critical role of T cell antigen receptor-transduced MHC class I-restricted helper T cells in tumor protection. *Proc Natl Acad Sci USA*. 2005; 102(22):7934-9.

40. Guedan S, Posey AD, Jr., Shaw C, Wing A, Da T, Patel PR, *et al*. Enhancing CAR T cell persistence through ICOS and 4-1BB costimulation. *JCI Insight*. 2018; 3(1).

41. Sanders SK, Giblin PA, Kavathas P. Cell-cell adhesion mediated by CD8 and human histocompatibility leukocyte antigen G, a nonclassical major histocompatibility complex class 1 molecule on cytotrophoblasts. *J Exp Med*. 1991; 174(3):737-40.

42. Hofmeister V, Weiss EH. HLA-G modulates immune responses by diverse receptor interactions. *Semin Cancer Biol*. 2003; 13(5):317-23.

43. Roda G, Jianyu X, Park MS, DeMarte L, Hovhannisyan Z, Couri R, *et al*. Characterizing CEACAM5 interaction with CD8α and CD1d in intestinal homeostasis. *Mucosal Immunol*. 2014; 7(3):615-24.
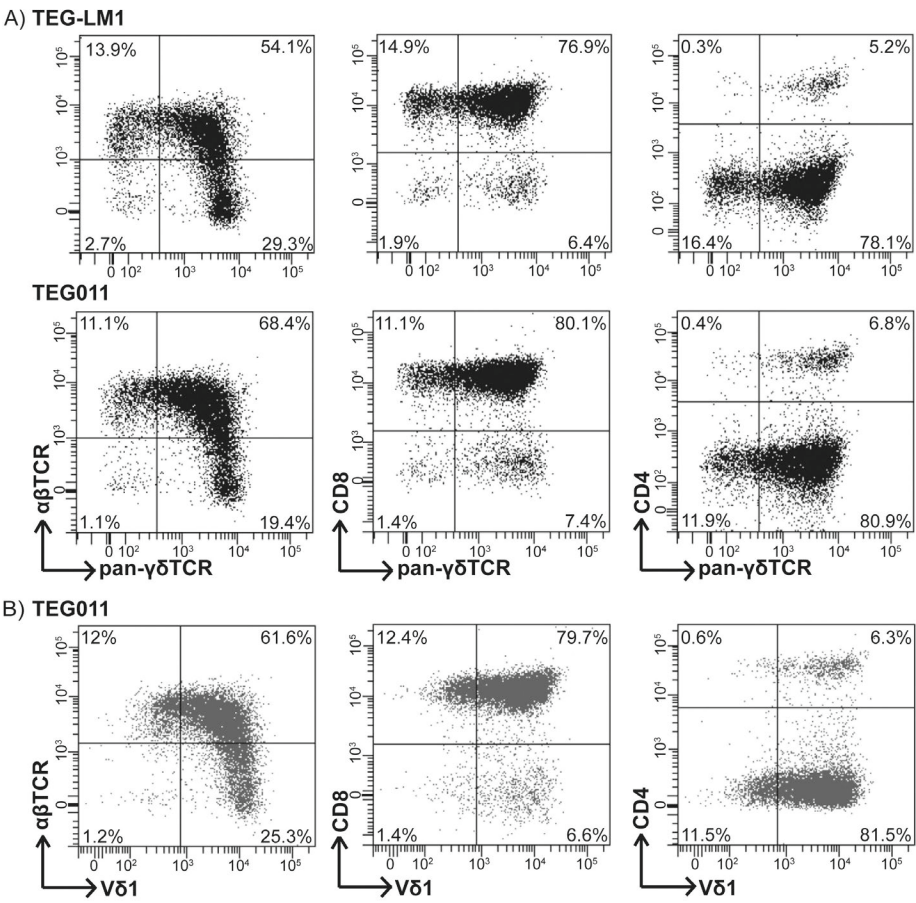
4

SUPPLEMENTARY FIGURES

Figure S1 γδTCR expression of TEG011 and TEG-LM1 mock. (A) Representative flow cytometry plots for γδTCR expression of TEG-LM1 mock (top panel) and TEG011 (bottom panel) prior to infusion into mice after 2 weeks expansion. **(B)** A representative flow cytometry plot for Vδ1 TCR expression of TEG011 as quality control for flow cytometry panel using pan-γδTCR monoclonal antibody.
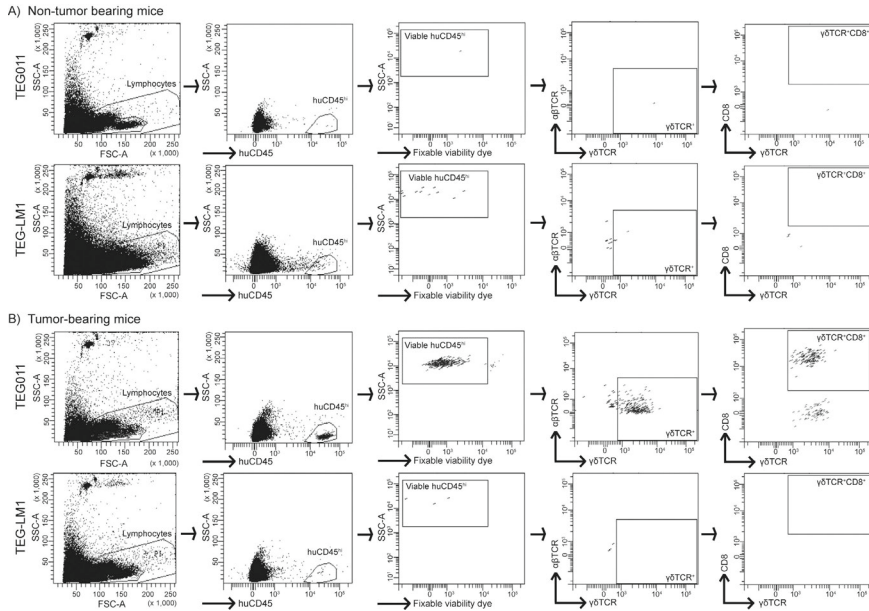
Figure S2 Gating strategy for flow cytometry analysis of TEGs persistence in peripheral blood. (A) Representative flow cytometry plots of peripheral blood in non-tumor bearing mice model on Day 29. TEG persistence was measured by quantifying absolute cell number of viable huCD45+γδTCR+CD8+ for TEG011 and TEG-LM1 mock group. **(B)** Representative flow cytometry plots of peripheral blood in tumor-bearing mice model Day 29. TEG persistence was measured by quantifying absolute cell number of viable huCD45+γδTCR+CD8+ for TEG011 and TEG-LM1 mock group.
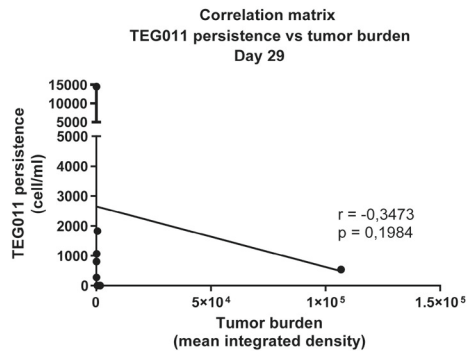
4

Figure S3 Correlation between tumor burden and TEG011 persistence overtime. Tumor burden for K562-HLA*A24-luciferase was assessed in vivo by bioluminescence imaging (BLI) measuring integrated density of the entire area of mice with abdomen facing up. TEG persistence was measured in peripheral blood by quantifying for absolute cell numbers by flow cytometry for TEG011 in tumor-bearing mice. Each dot representing paired tumor burden vs. TEG011 persistence for individual mouse at any given time points up to Day 56 (n = 63 data pairs). The best-fit regression line, Pearson's correlation coefficient and p-value are provided within the graph.

Supplementary Table S1. GvHD symptom scoring for non-tumor bearing mice

Treatment	Mouse ID	Hunching Week 1	2	3	4	5	6	7	8	9	Activity Week 1	2	3	4	5	6	7	8	9	Fur texture Week 1	2	3	4	5	6	7	8	9	Skin integrity Week 1	2	3	4	5	6	7	8	9	Diarrhea Week 1	2	3	4	5	6	7	8	9	Overall scoring
TEG-LM1	A1	0	0	0	0	0	0	0	0	0	0	0	0	0	0	0	0	0	0	0	0	0	0	0	0	0	0	0	0	0	0	0	0	0	0	0	0	0	0	0	0	0	0	0	0	0	0
TEG-LM1	A2	0	0	0	0	0	0	0	0	0	0	0	0	0	0	0	0	0	0	0	0	0	0	0	0	0	0	0	0	0	0	0	0	0	0	0	0	0	0	0	0	0	0	0	0	0	0
TEG-LM1	A3	0	0	0	0	0	0	0	0	0	0	0	0	0	0	0	0	0	0	0	0	0	0	0	0	0	0	0	0	0	0	0	0	0	0	0	0	0	0	0	0	0	0	0	0	0	0
TEG-LM1	B1	0	0	0	0	0	0	0	0	0	0	0	0	0	0	0	0	0	0	0	0	0	0	0	0	0	0	0	0	0	0	0	0	0	0	0	0	0	0	0	0	0	0	0	0	0	0
TEG-LM1	B2	0	0	0	0	0	0	0	0	0	0	0	0	0	0	0	0	0	0	0	0	0	0	0	0	0	0	0	0	0	0	0	0	0	0	0	0	0	0	0	0	0	0	0	0	0	0
TEG011	C1	0	0	0	0	0	0	0	0	0	0	0	0	0	0	0	0	0	0	0	0	0	0	0	0	0	0	0	0	0	0	0	0	0	0	0	0	0	0	0	0	0	0	0	0	0	0
TEG011	C2	0	0	0	0	0	0	0	0	0	0	0	0	0	0	0	0	0	0	0	0	0	0	0	0	0	0	0	0	0	0	0	0	0	0	0	0	0	0	0	0	0	0	0	0	0	0
TEG011	D1	0	0	0	0	0	0	0	0	0	0	0	0	0	0	0	0	0	0	0	0	0	0	0	0	0	0	0	0	0	0	0	0	0	0	0	0	0	0	0	0	0	0	0	0	0	0
TEG011	D2	0	0	0	0	0	0	0	0	0	0	0	0	0	0	0	0	0	0	0	0	0	0	0	0	0	0	0	0	0	0	0	0	0	0	0	0	0	0	0	0	0	0	0	0	0	0
TEG011	D3	0	0	0	0	0	0	0	0	0	0	0	0	0	0	0	0	0	0	0	0	0	0	0	0	0	0	0	0	0	0	0	0	0	0	0	0	0	0	0	0	0	0	0	0	0	0

Score legend:

Hunching
0 Normal
1 Only at rest
2 Severe and impaired movement

Activity
0 Normal
1 Mild to moderate decreased
2 Stationary unless stimulated

Fur texture
0 Normal
1 Mild to moderate ruffling
2 Severe ruffling or poor grooming

Skin integrity
0 Normal
1 Scaling of paws and tail
2 Obvious areas of denuded skin

Diarrhea
0 Normal
1 Green or yellow droppings
2 Excrement sticking around anus

Supplementary Table S2. Clinical appearance scoring for tumor-bearing mice

Clinical appearance parameter and scoring. Weeks 1–9 for each parameter (Hunching, Activity, Fur texture, Piloerection), with Overall scoring.

Treatment	Mouse ID	Hunching (Week 1–9)	Activity (Week 1–9)	Fur texture (Week 1–9)	Piloerection (Week 1–9)	Overall scoring
TEG-LM1	E1	0 0 0 0 0 0 0 0 -	0 0 0 0 0 0 0 0 -	0 0 0 0 0 0 0 0 -	0 0 0 0 0 0 0 0 -	0*
TEG-LM1	E2	0 0 0 0 0 1 - - -	0 0 0 0 0 1 - - -	0 0 0 0 0 1 - - -	0 0 0 0 0 1 - - -	4
TEG-LM1	F1	0 0 0 0 0 - - - -	0 0 0 0 0 - - - -	0 0 0 0 0 - - - -	0 0 0 0 0 - - - -	0**
TEG-LM1	F2	0 0 0 0 0 0 0 0 0	0 0 0 0 0 0 0 0 0	0 0 0 0 0 0 0 0 0	0 0 0 0 0 0 0 0 0	0**
TEG-LM1	F3	0 0 0 0 0 0 0 2 -	0 0 0 0 0 0 0 2 -	0 0 0 0 0 0 0 2 -	0 0 0 0 0 0 0 2 -	8
TEG-LM1	G1	0 0 0 0 0 0 0 1 -	0 0 0 0 0 0 0 1 -	0 0 0 0 0 0 0 1 -	0 0 0 0 0 0 0 1 -	4
TEG-LM1	G2	0 0 0 0 0 - - - -	0 0 0 0 0 - - - -	0 0 0 0 0 - - - -	0 0 0 0 0 - - - -	0*
TEG-LM1	G3	0 0 0 0 0 - - - -	0 0 0 0 0 - - - -	0 0 0 0 0 - - - -	0 0 0 0 0 - - - -	0***
TEG-LM1	G4	0 0 0 0 0 0 - 0 -	0 0 0 0 0 0 - 0 -	0 0 0 0 0 0 - 0 -	0 0 0 0 0 0 - 0 -	0*
TEG-LM1	G5	0 0 0 0 0 0 - - -	0 0 0 0 0 0 - - -	0 0 0 0 0 0 - - -	0 0 0 0 0 0 - - -	0*
TEG-LM1	H1††	0 0 0 0 0 0 0 - -	0 0 0 0 0 0 0 - -	0 0 0 0 0 0 0 - -	0 0 0 0 0 0 0 - -	0***
TEG011	H2†	0 0 0 0 0 0 0 0 0	0 0 0 0 0 0 0 0 0	0 0 0 0 0 0 0 0 0	0 0 0 0 0 0 0 0 0	0
TEG011	I1†	0 0 0 0 0 0 0 0 0	0 0 0 0 0 0 0 0 0	0 0 0 0 0 0 0 0 0	0 0 0 0 0 0 0 0 0	0
TEG011	I2†	0 0 0 0 0 0 0 0 0	0 0 0 0 0 0 0 0 0	0 0 0 0 0 0 0 0 0	0 0 0 0 0 0 0 0 0	0
TEG011	J1†	0 0 0 0 0 0 0 0 0	0 0 0 0 0 0 0 0 0	0 0 0 0 0 0 0 0 0	0 0 0 0 0 0 0 0 0	0
TEG011	J2††	0 0 0 0 - - - - -	0 0 0 0 - - - - -	0 0 0 0 - - - - -	0 0 0 0 - - - - -	0*
TEG011	J3††	0 0 0 0 - - - - -	0 0 0 0 - - - - -	0 0 0 0 - - - - -	0 0 0 0 - - - - -	0*
TEG011	J4††	0 0 0 0 0 0 0 0 0	0 0 0 0 0 0 0 0 0	0 0 0 0 0 0 0 0 0	0 0 0 0 0 0 0 0 0	0
TEG011	J5††	0 0 0 0 0 0 0 0 0	0 0 0 0 0 0 0 0 0	0 0 0 0 0 0 0 0 0	0 0 0 0 0 0 0 0 0	0

Scoring legend:

Hunching
0 Normal
1 Only at rest
2 Severe and impaired movement

Activity
0 Normal
1 Mild to moderate decreased
2 Stationary unless stimulated

Fur texture
0 Normal
1 Mild to moderate ruffling
2 Severe ruffling or poor grooming

Piloerection
0 Normal
1 Partial
2 marked-staring coat

* Mice were sacrificed due to 20% weight loss
** Mice were sacrificed due to paralysis
*** Mice were sacrificed due to extramedullary tumor growth
† Mice were classified into TEG011 "persisters" subgroup (highlighted in green)
†† Mice were classified into TEG011 "non-persisters" subgroup

4

Supplementary Table S3. Detailed histopathology analysis of bone marrow and mouse vital organs (spleen, liver, intestine) of non-tumor bearing mice

| Treatment | Mouse ID | Sex | Spleen | | Cell type presence | Bone marrow | | | Liver [4] | Intestine [4] |
			Extramedullary hematopoiesis grading (EMH)	EMH grading average for each sex		Cellularity [1,3]	M/E ratio [2,3]	Presence of megakaryocytes		
TEG-LM1	A1	M	2	2	Blast, erythroid precursors, band cells, megakaryocytes	Normal	Normal	Normal	None	None
	A2	M	2		Blast, erythroid precursors, band cells, megakaryocytes	Normal	Normal	Normal	None	None
	A3	M	2		Blast, erythroid precursors, band cells, megakaryocytes	Normal	Minimal decreased	Minimal increased	None	None
	B1	F	3	2.5	Blast, erythroid precursors, band cells, megakaryocytes	Normal	Normal	Normal	None	None
	B2	F	2		Blast, erythroid precursors, band cells (minimal increased in numbers), megakaryocytes	Normal	Normal	Normal	None	None
TEG011	C1	M	1	1.5	Blast, erythroid precursors, band cells, megakaryocytes	Minimal decreased	Normal	Normal	None	None
	C2	M	2		Blast, erythroid precursors, band cells, megakaryocytes	Normal	Normal	Normal	None	None
	D1	F	3	3	Blast, erythroid precursors (minimal increased in numbers), band cells, megakaryocytes (minimal increased in numbers)	Normal	Normal	Normal	None	None
	D2	F	3		Blast, erythroid precursors (minimal increased in numbers), band cells, megakaryocytes (minimal increased in numbers)	Normal	Normal	Normal	None	None
	D3	F	3		Blast, erythroid precursors (minimal increased in numbers), band cells, megakaryocytes (minimal increased in numbers)	Normal	Normal	Normal	None	None

Grading system extramedullary hematopoiesis spleen:

0 = None
1 = Mild
2 = Moderate
3 = Severe
4 = Marked

[1] Bone marrow cellularity is determined by percentage of hematopoietic cells relative to marrow fat
[2] M:E ratio is determined by ratio of myeloid and erythroid precursors
[3] BM cellularity and M/E ratio are qualitatively analyzed by comparing to naïve NSG-A24 mice as control for each sex and classified into normal, increased or decreased.
[4] No abnormal histological lesions observed

CHAPTER 5

Adding help to a HLA-A*24:02 tumor-reactive γδTCR increases tumor control

Inez Johanna[1‡], Patricia Hernández-López[1‡], Sabine Heijhuurs[1], Wouter Scheper[1], Laura Bongiovanni[3], Alain de Bruin[3,4], Dennis X Beringer[1], Rimke Oostvogels[2], Trudy Straetemans[1,2], Zsolt Sebestyen[1], and Jürgen Kuball[1,2*]

[1] Center for Translational Immunology, University Medical Center Utrecht, Utrecht, The Netherlands
[2] Department of Hematology, University Medical Center Utrecht, Utrecht, The Netherlands
[3] Department of Biomolecular Health Sciences, Dutch Molecular Pathology Center, Faculty of Veterinary Medicine, Utrecht University, Utrecht, The Netherlands
[4] Department of Pediatrics, University Medical Center Groningen, University of Groningen, Groningen, The Netherlands

[‡] IJ and PH contributed equally to this work
[*] corresponding author

ABSTRACT

γδT cell receptors (γδTCRs) recognize a broad range of malignantly-transformed cells in mainly a major histocompatibility complex (MHC)-independent manner, making them valuable additions to the engineered immune effector cell therapy that currently focuses primarily on αßTCRs and chimeric antigen receptors (CARs). As an exception to the rule, we have previously identified a γδTCR, which exerts antitumor reactivity against HLA-A*24:02-expressing malignant cells, however without the need for defined HLA-restricted peptides, and without exhibiting any sign of off-target toxicity in humanized HLA-A*24:02 transgenic NSG (NSG-A24:02) mouse models. This particular tumor-HLA-A*24:02-specific Vγ5Vδ1TCR required CD8αα co-receptor for its tumor reactive capacity when introduced into αßT cells engineered to express a defined γδTCR (TEG), referred to as TEG011, thus it was only active in CD8$^+$ TEG011. We subsequently explored the concept of additional redirection of CD4$^+$ T cells through co-expression of the human CD8α gene into CD4$^+$ and CD8$^+$ TEG011 cells, later referred as TEG011_CD8α. Adoptive transfer of TEG011_CD8α cells in humanized HLA-A*24:02 transgenic NSG (NSG-A24:02) mice injected with tumor HLA-A*24:02$^+$ cells showed superior tumor control in comparison to TEG011, and to mock control groups. The total number of functional TEG011_CD8α cells persisted significantly longer in mice peripheral blood up to 4 weeks after TEG infusion, mainly due to a dominance of CD4$^+$CD8$^+$ double positive TEG011_CD8α which resulted in higher total counts of functional T cells in spleen and bone marrow. We observed that tumor clearance in the bone marrow of TEG011_CD8α-treated mice associated with better human T cell infiltration, which was not observed in the TEG011-treated group. Overall, introduction of transgenic human CD8α receptor on TEG011 improves antitumor reactivity against HLA-A*24:02$^+$ tumor cells, and further enhances in vivo tumor control.

Keywords: cancer immunotherapy, TEGs, mouse model, preclinical, TCR engineering, human leukocyte antigens, persistence, efficacy

INTRODUCTION

γδT cells share the properties of both innate and adaptive immunity and play an essential role in cancer immunosurveillance (1, 2). Unlike conventional αβT cells, γδT cells recognize their cognate antigens in an MHC-unrestricted manner, targeting stress-induced and malignantly-transformed self-antigens (3, 4). As such, γδT cells represent an attractive cell subset to substantiate T cell-based immunotherapeutic strategies that still mainly focus on αβT cells.

Based on their TCRδ chain repertoire, γδT cells can be distinguished into two major subsets: Vδ2+ and Vδ2- cells. Vδ2+ cells mainly reside in human peripheral blood, representing up to 5% of total circulating T cells, and sense metabolic changes in tumor cells with intracellular accumulation of phosphoantigens (pAgs) level. Vδ2+ T cell recognition is facilitated by butyrophilin (BTN) family molecules, including BTN2A1 and BTN3A1 (5-10). On the other hand, Vδ2- cells mainly localize in mucosal and epithelial tissues, but their antitumor properties are scarcely known (4). Vδ2- cells recognize broad range of stress-induced ligands, such as the MHC-associated proteins MICA and MICB, foreign lipid antigens presented on CD1c/d molecules in classical HLA-like manner, and CMV-associated UL16-binding protein (ULBP) family members, that are upregulated in stressed or malignant cells (11-15).

Vδ1+ T cells, one of the major Vδ2- subsets, have been shown to exert antitumor reactivity against leukemia and solid tumors (16-21), indicating their potential in cancer immunotherapy. Adoptive transfer of in vitro expanded Vδ2+ cells only showed marginal clinical responses to date (4, 22), while adoptive transfer of Vδ2- cells is yet to be tested in the clinic (23). Translational efforts using γδT cells and their receptors outside the context of allogeneic stem cell transplantation (24, 25) face substantial hurdles, due to their limited proliferative capacity, underestimated diversity in co-receptors expression and function, as well as scarce information on how γδTCRs interact with their targets.

To bypass these major drawbacks of translating γδT cells-based immune therapies into clinical practice, we developed the concept of TEGs: αβT cells engineered to express a defined γδTCR, allowing the introduction of highly tumor-reactive γδTCR, both Vδ2+ (26, 27) or Vδ2- (28, 29) subsets, into proliferatively-proficient αβT cells (27, 30, 31). We previously identified an allo-HLA-restricted and tumor-specific Vγ5Vδ1TCR, introduced in TEG concept as TEG011, which was, although not dependent on a defined peptide, selectively targeting HLA-A*24:02+ tumor cells without impairing the healthy tissues (32). Within this scope, we also highlighted the function of CD8α as costimulatory receptor required for antitumor reactivity of FE11 γδTCR and showed that both CD8αα on the original clone FE11 and CD8αβ on transduced αβT cells are capable of providing co-stimulation to the FE11 γδTCR (32).

Human CD8 is a membrane glycoprotein classified in an immunoglobulin-like super family consisting of hetero- or homodimer of α and β chains, making up for the CD8αβ

5

or CD8αα co-receptor on the cell surface. CD8αβ predominantly expressed on αβT cells, while CD8αα mainly expressed on the cell membrane of innate immune cells, including macrophages, dendritic cells, natural killer (NK) cells, and γδT cells (33). Within this context, we addressed the implication of CD8αα-dependency of FE11 γδTCR in relation to its tumor immunity. Importantly, we demonstrate that introduction of transgenic human CD8α co-receptor into CD4+ TEG011 cells successfully enhanced its antitumor efficacy in vitro and in vivo, and thus did not require CD8β. Furthermore, we show that the co-expression of CD8α in CD4+ TEG011 provides additional survival signal and facilitates better T cell persistence and infiltration in vivo, both of which are essential to sustain long-term tumor control of adoptively transferred TCR-based immunotherapy.

MATERIALS AND METHODS

Cell lines

Daudi, SW480, and Phoenix-Ampho cell lines were obtained from ATCC. K562 with HLA-A*24:02-transduced cell line was kindly provided by Fred Falkenburg (Leiden University Medical Centre, the Netherlands) and subsequently transduced with luciferase for *in vivo* imaging purposes. EBV-LCL was kindly provided by Phil Greenberg (Seattle, WA). Phoenix-Ampho and SW480 cells were cultured in DMEM supplemented with 1% Pen/Strep (Invitrogen) and 10% FCS (Bodinco), whereas all other cell lines in RPMI with 1% Pen/Strep and 10% FCS. All cell lines were authenticated by short tandem repeat profiling/karyotyping/iso-enzyme analysis and were passaged for a maximum of 2 months, after which new cell line stocks were thawed for experimental use. Furthermore, all cell lines were routinely verified by growth rate, morphology, and/or flow cytometry and tested negative for mycoplasma using MycoAlert Mycoplasma Kit (Lonza, Breda, The Netherlands). Peripheral blood mononuclear cells (PBMCs) from healthy donors were isolated by Ficoll-Paque (GE Healthcare, Eindhoven, The Netherlands) from buffy coats supplied by Sanquin Blood Bank (Amsterdam, The Netherlands).

Cloning of TEG011_CD8α and TEGLM1_CD8α

Clone FE11 was generated as previously described (28). FE11 and LM1 (non-functional γ9δ2TCR with length mutation on the complementary determining region 3 (CDR3) of the δ2-chain (31)) γδTCRs were subcloned to pMP71 retroviral vectors containing both γTCR and δTCR chains, separated by a ribosomal skipping T2A sequence. pU57 constructs containing a ribosomal skipping P2A sequence, followed by full-length human CD8α were purchased from Baseclear (Leiden, The Netherlands). Thereafter, CD8α was subcloned into pMP71 vector using *Xho*I and *Hind*III restriction sites downstream of γ115TCR-T2A-δ115_LM1 sequence to generate a TEGLM1_CD8α construct that contained *Nco*I and *Xho*I restriction sites up- and downstream of LM1 γδTCR chains. *Nco*I and *Xho*I restriction sites were then inserted up- and downstream of FE11 γδTCR sequences by site-directed mutagenesis PCR, after which this sequence was ligated to P2A-CD8α sequence in pMP71 vector using the introduced *Nco*I and *Xho*I sites, generating a TEG011_CD8α construct (Supplementary Table 1). Where indicated, CD4+, CD8+, CD4+CD8αα+ and

CD4⁺CD8αβ⁺ TCR-transduced T-cells were sorted using a FACSAria II (BD) flow cytometry to >99% purity. Expression levels of CD8α mutants were measured by flow cytometry using anti-CD8α antibody (clones RPA-T8).

Functional T cell assays

IFNγ ELISPOT was performed using anti-human IFNγ mAb1-D1K (I) and mAb7-B6–1 (II) (Mabtech) per the manufacturer's protocol. 15,000 TEG cells (TEG011, TEGLM1, TEG011_CD8α, or TEGLM1_CD8α) were co-incubated with 50,000 target cells (E:T ratio 1:3) for 18-24 hours in nitrocellulose-bottomed 96-well plates (Millipore). IFNγ spots were visualized with TMB substrate (Sanquin) and subsequently the number of spots was quantified using ELISPOT Analysis Software (Aelvis). Where indicated, blocking of CD8α was performed using 10 µg/ml anti-CD8α antibody clone OKT8 (eBioscience) and blocking of CD8ß with 10 µg/ml anti-CD8ß clone 2ST8.5H7 (Abcam).

Retroviral transductions of T cells

TEGs were generated as previously described (30). Briefly, Phoenix-Ampho packaging cells were transfected with gag-pol (pHIT60), env (pCOLT-GALV), and pMP71 retroviral constructs containing both γTCR and δTCR chains separated by a ribosomal skipping T2A sequence and followed by CD8α sequence separated by P2A sequence where applicable, using FugeneHD reagent (Promega, Leiden, The Netherlands). PBMCs from a healthy donor pre-activated with 30 ng/mL anti-CD3 (clone OKT3, Miltenyi Biotec) and 50 IU/mL IL-2 (Proleukin, Novartis, Arnhem, The Netherlands) were transduced twice with viral supernatant within 48 hours, in the presence of 50 IU/mL IL-2 and 6 µg/mL polybrene (Sigma-Aldrich, Zwijndrecht, The Netherlands). TCR-transduced T cells were expanded by stimulation with anti-CD3/CD28 Dynabeads (500,000 beads/10^6 cells; Thermo Fisher Scientific, Breda, The Netherlands) and 50 IU/mL IL-2. Thereafter, transduced T cells were depleted of the non-engineered T cells.

Depletion of non-engineered T cells

Non-engineered T cells was depleted as previously described (27). In brief, transduced T cells were incubated with a biotin-labeled anti-αßTCR antibody (clone BW242/412; Miltenyi Biotec, Leiden, The Netherlands) and then incubated with an anti-biotin antibody coupled to magnetic beads (anti-biotin MicroBeads; Miltenyi Biotec). Thereafter, the cell suspension was loaded onto an LD column, and αßTCR⁺ T cells were depleted by MACS cell separation per the manufacturer's protocol (Miltenyi Biotec). After depletion, TEGs were expanded using a T cell rapid expansion protocol (REP) (30).

Separation of CD4⁺ subsets of TEGs

The separation of CD4⁺ TEGs was performed using CD4 Microbeads (Miltenyi Biotech) as per manufacturer's instructions. Briefly, TEGs were incubated with magnetic microbeads cells and loaded into LS column for MACS cell separation. Thereafter, CD4⁺ selected or bulk (with CD4:CD8 ratio 50:50) TEGs were expanded separately using REP. TEG expression was monitored prior to functional assays or *in vivo* infusion by flow cytometry using anti-αßTCR-APC (clone IP26, eBioscience), anti-pan-γδTCR-PE (clone IMMU510, Beckman

5

Coulter), anti-CD8-PerCP-Cy5.5 (clone RPA-T8, Biolegend), anti-CD4-PeCy7 (clone TPA-R4, Biolegend), anti-CD4-FITC (clone TPA-R4, Biolegend), and Vδ1-FITC (clone TS8.2, Thermo Fisher Scientific) antibodies.

Animal model

The NOD.Cg-*Prkdc*^{scid}*Il2rg*^{tm1Wjl}Tg(HLA-A24)3Dvs/Sz (NSG-A24:02) mice (34) were bred and housed in the breeding unit of the Central Animal Facility of Utrecht University. Experiments were conducted per institutional guidelines after obtaining permission from the local Ethical Committee, and performed in accordance with the current Dutch laws on Animal Experimentation. Mice were housed in individually ventilated cage (IVC) system to maintain sterile conditions and fed with sterile food and water. After irradiation, mice were given the antibiotic ciproxin in the sterile water for the duration of the experiment. Both male and female mice were randomized with equal distribution among the different groups, based on age and initial weight (measure on Day -1) into 10 mice/group. Adult NSG-A24:02 mice (11-20 weeks old) received sub-lethal total body irradiation (1,75 Gy) on day -1 followed by intravenous injection of 1x10^5 K562-HLA-A*24:02 luciferase tumor cells on day 0, and received 2 intravenous injections of TEG011, TEG011_CD8α or TEGLM1_CD8α cells on day 1 and 6 as previously reported (32). Together with the first TEGs injection, all mice received 0,6 × 10^6 IU of IL-2 (Proleukin; Novartis) in 100μl incomplete Freund's adjuvant (IFA) subcutaneously and subsequently administered every 3 weeks until the end of the experiment. Mice were monitored at least twice a week for any symptoms of disease (sign of paralysis, weakness, and reduced motility), weight loss, and clinical appearance scoring (scoring parameter included hunched appearance, activity, fur texture, and piloerection). The humane endpoint was reached when mice showed aforementioned symptoms of disease, experienced a 20% weight loss from the initial weight (measured on day -1), developed extramedullary solid tumor masses (if any) reached 2 cm^3 in volume and when clinical appearance score 2 was reached for an individual parameter or a total score of 4.

Flow cytometry analysis

The following antibodies were used for flow cytometry analysis: huCD45-PB (clone HI30; Sony Biotechnology), pan-γδTCR-PE (clone IMMU510; Beckman-Coulter), mCD45-APC (clone 30-F11, Sony Biotechnology), αβTCR-FITC (clone IP26; Biolegend), CD4-PeCy7 (clone RPA-T4, Biolegend), CD8-PerCPCy5.5 (clone RPA-T8, Biolegend), PD-1-BV711 (clone EH12.2H7, Biolegend), and TIM3-BV650 (clone F38-2E2, Biolegend). To exclude non-viable cells from the analysis, Fixable Viability Dye eFluor506 was used (eBioscience). All samples were analyzed on a BD LSRFortessa using FACSDiva Software (BD Biosciences).

Assessment for TEGs persistence

Mouse peripheral blood samples were obtained via cheek vein (max. 50-70 μl/mouse) once a week. Red blood cell was lysed using 1X RBC lysis buffer (Biolegend) and were then stained with a mixture of antibody panels as listed above. The persistence of TEG cells were counted as absolute cell number of huCD45$^+$γδTCR$^+$CD8$^+$ population in mouse

peripheral blood using Flow-count Fluorospheres (Beckman Coulter) measured by flow cytometry.

Preparation of single cell suspensions

At the end of the study period, bone marrow (mixed from tibia and femur) and spleen sections were isolated and processed into single cell suspension. Femur and tibia from the hind legs were collected; bone marrow cells were collected by centrifugation of the bones at 10,000 rpm for 15 seconds and resuspension of the cells in phosphate buffer saline (PBS).

A small section of the spleen was minced and filtered through a 70µm cell strainer (BD); incubated with 1X RBC lysis buffer cells for maximum 4 minutes, and subsequently cells were washed and resuspended in PBS.

Absolute cell number of TEG cells were quantified using Flow-count Fluorospheres and measured from a total of 10^6 cells stained for the presence of TEG cells in spleen and bone marrow by flow cytometry analysis (BD LSRFortessa).

Histology staining and analysis

Formalin-fixed femur for bone marrow sections were embedded in paraffin and cut into 4µm sections. Hematoxylin and eosin (H&E) staining was performed for the femur, for bone marrow section. Tissue sections were evaluated to assess for any differences in the presence, distribution and extension of neoplastic foci indicating tumor tissue. Tissue sections of the femur were evaluated for quantification of tumor tissue by dividing the area covered by the tumor cells by the total area of bone marrow tissue visible in the section using the ImageJ analysis system software (NHI, Bethesda, Maryland, USA) and expressed as a percentage. Images were taken using an Olympus BX45 microscope with the Olympus DP25 camera and analyzed using DP2-BSW (version 2.2) or ImageJ softwares.

Statistical Analyses

Experimental data were analyzed using GraphPad Prism (GraphPad Software Inc., La Jolla, CA, USA) and shown as mean ± standard deviation (SD) or standard error of mean (SEM) with *P < 0.05; **P < 0.01; ***P < 0.001; and ****P < 0.0001. Statistical significances between groups were assessed using a non-parametric Kruskal-Wallis test, a two-way ANOVA, and a mixed-effects model with repeated measures where indicated.

RESULTS

Co-transfer of transgenic CD8α receptor is sufficient to re-establish tumor reactivity of CD4+ TEG011 cells

We previously identified an allo-restricted CD8α-dependent Vγ5Vδ1TCR clone FE11 (28), which showed *in vitro* antitumor reactivity against HLA-A*24:02-expressing tumor cells

(32). We therefore investigated whether introduction of CD8αα or CD8αß along with Vγ5Vδ1TCR derived from clone FE11 could re-establish antitumor reactivity of not only CD8^{+}, but also CD4^{+} TEG011 cells. Hence, we co-transduced T cells with the FE11 γδTCR, and with either CD8α alone or CD8α together with CD8ß (Figure S1). Subsequently, we sorted separate sets of CD4^{+} TEG011 cells that co-expressed either exogenous CD8αα (CD4^{+}CD8α^{+}) or CD8αß (CD4^{+}CD8αß^{+}) as well as TEG011 cells expressing only endogenous CD4 and CD8 as negative and positive controls for tumor recognition, respectively (Figure 1A). Thereafter, TEG cells were co-cultured with SW480 and EBV-LCL target cells or healthy PBMCs as mock control. Both CD4^{+}CD8α^{+} and CD4^{+}CD8αß^{+} TEG011 cells secreted significantly higher levels of IFNγ upon exposure to tumor targets than CD4^{+} TEG011 cells. The acquired antitumor reactivity of CD4^{+}CD8α^{+} and CD4^{+}CD8αß^{+} TEG011 cells could be blocked by CD8α and CD8ß blocking antibodies (Figure 1B), confirming the strict dependence of FE11 γδTCR on introduced CD8 molecules. Taken together, we showed that introduction of CD8α alone is sufficient to re-establish antitumor reactivity of CD4^{+} T cells expressing FE11 γδTCR. Introduction of CD8ß did not further enhance tumor recognition, but was functionally involved in the molecular interaction with its target when present.

For clinical administration, co-expression of both CD8α and the γδTCR in one vector is preferred to allow reproducible and cost-effective production processes (26, 27, 35). Moreover, co-expressing both CD8α and the γδTCR in one vector can also overcome the difference in transduction efficiency when they were transduced separately. Therefore, we generated new retroviral constructs carrying either FE11 γδTCR or a non-functional length mutant clone LM1 γδTCR ((31); served as mock control) followed by full-length human CD8α receptor sequences (TEG011_CD8α and TEGLM1_CD8α, Figure 1C). To elucidate whether introduction of transgenic CD8α receptor adequately rescues TEG011 reactivity in CD4-transduced cells once delivered by the very same vector, we co-cultured tumor target HLA-A*24:02-transduced K562, SW480, and EBV-LVL cells with either CD4^{+} TEG011_CD8α, CD4^{+} TEGLM1_CD8α, or CD4^{+} TEG011 (without introduction of the CD8α receptor). Healthy T cells and TEG011 bulk cells (with CD4:CD8 1:1 ratio) were used as the untransformed mock target and positive effector control, respectively (Figure 1D). CD4^{+} TEG011_CD8α cells produced a significantly higher IFNγ level compared to CD4^{+} TEG011, which was equivalent to those of TEG011 bulk cells against all tumor targets, without affecting healthy cells. Importantly, enhanced tumor recognition was strictly restricted to TEG011_CD8α cells and not TEGLM1_CD8α mock cells, highlighting the specific role of CD8α as co-stimulation for the introduced FE11 γδTCR. We concluded that introduction of transgenic CD8α receptor in combination with Vγ5Vδ1TCR derived from clone FE11 allowed reprogramming of CD4^{+} T cells towards HLA-A*24:02-expressing tumor cells *in vitro*.
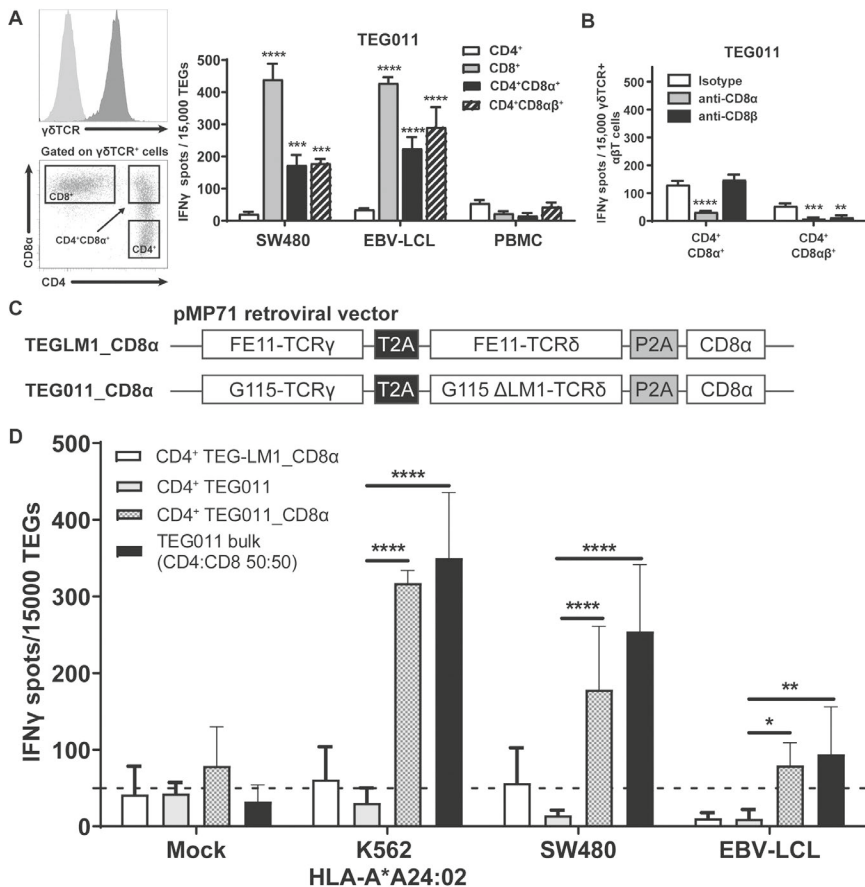
Figure 1 Introduction of transgenic CD8α receptor on TEG011 improves T cell activation. (A) TEG011 were retrovirally transduced with either CD8α alone or CD8α in combination with CD8ß. CD4+, CD8+, CD4+CD8α+ and CD4+CD8αß+ subsets of T cells were subsequently sorted (left panel is a representative sorting plot for CD4+, CD8+ and CD4+CD8α+ cells; CD4+CD8αß+ cells were sorted in a similar manner) and tested for recognition of SW480 and EBV-LCL target cells by IFNγ ELISPOT (right panel). Healthy PBMCs were included as untransformed mock control target cells. Data are of representative of four independent experiments and error bars represent mean ± SEM (**P < 0.01; ***P < 0.001) calculated by two-way ANOVA. **(B)** CD8α and CD8ß blocking on CD4+ T cells were transduced with the FE11 γδTCR and CD8α alone, or CD8α with CD8ß. TEG011 was co-incubated with SW480 target cells in the presence of a control antibody, or CD8α or CD8ß blocking antibodies. IFNγ production was measured by ELISPOT. Data represent mean ± SD of replicates for each effector (**P < 0.01; ***P < 0.001; ****P < 0.0001) calculated by two-way ANOVA. **(C)** Schematic diagram of pMP71 retroviral vector constructs containing codon-optimized human γδTCR sequences from either clone FE11 (referred as TEG011_CD8α) or non-functional LM1 chains (referred as TEGLM1_CD8α) in combination with full length of human CD8α receptor (top panel). Within the transgene cassettes, individual γTCR and δTCR chains have been linked with a self-cleaving thosea asigna virus 2A (T2A; black box) ribosomal skipping sequence, while the CD8α sequence was connected with a porcine teschovirus-1-derived 2A (P2A; grey box) ribosomal skipping sequence. **(D)** CD4+ αßT cells were transduced with either TEGLM1_CD8α, TEG011, or TEG011_CD8α γδTCR (as effector cells) and subsequently co-cultured with HLA-A*24:02-expressing target cell lines or healthy T cells (E:T ratio is 1:3) for 18-24 h. TEG011 bulk population with 50:50 ratio of both CD4+ and CD8+ TEGs and T cells from healthy donor were used as

TEG011_CD8α improves *in vivo* tumor control and associates with higher persistence of functional T cells

In previous studies, we have shown TEG011 efficacy against HLA-A*24:02-expressing tumor cells *in vitro* and an extended *in vivo* safety profile as well as peripheral persistence of TEG011, where long-term persistence of TEG associated with reduced probability for developing extramedullary solid tumor masses *in vivo* (32, 36). To assess the consequence of the additional expression of TEG011_CD8α, NSG transgenic mice expressing human HLA-A*24:02 (NSG-A24:02) were irradiated, received luciferase-labeled HLA-A*24:02-transduced CML tumor cells (K562) and subsequently obtained two infusions of either mock control TEGLM1_CD8α, TEG011_CD8α, or TEG011 cells. All infused TEG variants showed comparable γδTCR expression, where the transduced αßT cells expressed Vδ1+ TCR for TEG011 and TEG011_CD8α (Figure S2). Mice were monitored for tumor burden assessed by bioluminescent imaging, T cell persistence and infiltration, as well as any other signs of discomfort. Mice were sacrificed when the humane endpoints were reached (experimental outline Figure 2A). TEG011_CD8α-treated mice had a significantly lower tumor burden over time compared to the mock control TEGLM1_CD8α and TEG011-treated groups (Figure 2B), indicating superior tumor control *in vivo* by TEG011_CD8α.

Next, we assessed CD8-expressing TEG cell product properties and persistence by measuring viable huCD45+γδTCR+CD8+ single positive and huCD45+γδTCR+CD4+CD8+ double positive cells (present in mock TEGLM1_CD8α and TEG011_CD8α only) in mouse peripheral blood using flow cytometry. TEG cells persisted up to 4 weeks after infusion in the mouse peripheral blood (Figure 2C). Despite some repeated measure; (*P < 0.05; **P < 0.01). **(C)** TEG cells were measured in peripheral blood using flow cytometry by quantifying the absolute cell numbers of TEGLM1_CD8α mock (open light gray rectangle), TEG011 (open black circle), and TEG011_CD8α (open black triangle) in tumor-bearing mice. TEG cells are distinguished into different cellular compartments: CD8+ single positive (SP; white stacked bar), CD4+ single positive (SP; grey stacked bar), and CD4+CD8+ double positive (DP; grey dotted stacked bar). Black arrows indicate higher or lower T cell counts observed. Data are shown as mean ± SEM of all mice per group (n = 10 mice). Statistical significances were calculated by a mixed-effects model with repeated measures (*P < 0.05; ****P < 0.0001). **(D)** Functional CD8-expressing TEG cells was assessed in spleen and bone marrow by quantifying the total viable cells of huCD45+γδTCR+CD8+ and huCD45+γδTCR+CD4+CD8+ per one million single cell suspension by flow cytometry. Cell counts of individual mouse per treatment group are represented by each symbol. Functional TEG011 cells consist of two different cellular compartments: CD8+ single positive (SP; white stacked bar) and CD4+CD8+ double positive (DP; grey dotted stacked bar). Data are shown as mean ± SEM (*P < 0.05; **P < 0.01) calculated by a mixed-effects model with repeated measures.
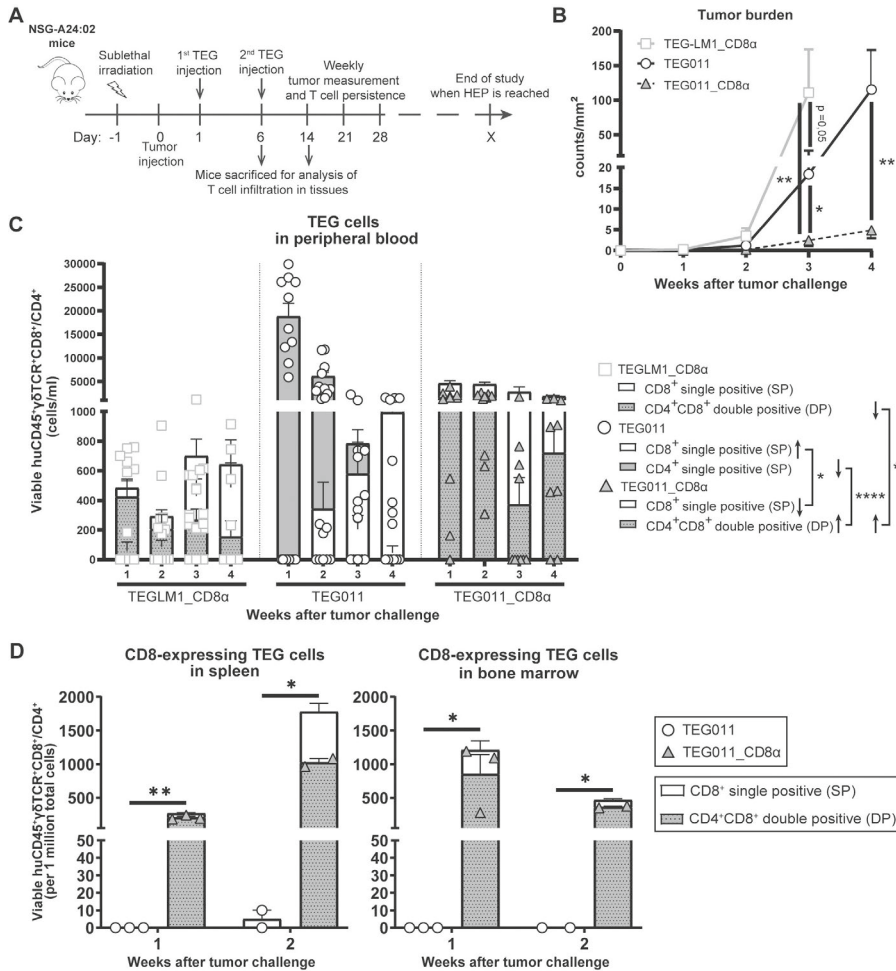
Figure 2 TEG011_CD8α improves *in vivo* tumor control against HLA-A*24:02⁺ tumor cells and enhances TEG persistence and infiltration. (A) Schematic overview of the *in vivo* experiment for NSG-A24:02 tumor-bearing mice. Irradiated mice were intravenously injected with K562-HLA*A24:02-luciferase tumor cells on day 0 followed by two infusions of TEG011, TEG011_CD8α or TEGLM1_CD8α mock cells on days 1 and 6. Mice were monitored regularly and sacrificed when the humane endpoint (HEP) was reached. **(B)** Tumor burden for K562-HLA*A24:02-luciferase was assessed *in vivo* by measuring integrated signal density per total surface area (count/mm²) using bioluminescence imaging (BLI) with the mouse abdomen facing up. Data are shown only up to week 3 for the TEGLM1_CD8α mock-treated group (open light gray rectangle) due to subsequent mouse dropout >50%, while data for TEG011 (open black circle) and TEG011_CD8α (open black triangle) are shown up to week 4. Data are shown as mean ± SEM of all mice per group (n = 10). Statistical significances were calculated by a mixed-effects model with imbalance in the CD4:CD8 ratio with lower numbers for CD8⁺ TEG011 infused (Figure S2), more CD8⁺ TEG011 persisted over time when compared to CD8⁺ single positive TEG011_CD8α. Vice versa, endogenous CD4 T cells for TEG011_CD8α were lower before infusion when compared to TEG011 prior to infusion, while CD4⁺CD8⁺ double positive TEG011_CD8α were higher in numbers over time when compared to both non-functional CD4⁺CD8⁺ TEGLM1_CD8α and non-functional CD4⁺ TEG011 cells (Figure 2C). As a net effect, we observed more functional CD8-expressing T cells for TEG011_CD8α cells when compared to TEG011 (Figure 2C and S3). Next, we investigated the expression of PD1 and TIM3 on CD8⁺ single positive cells and CD4⁺ single

Thereafter, we investigated infiltration of TEG cells into spleen and bone marrow on weeks 1 and 2 after infusion. Specifically, we compared the TEG011 and TEG011_CD8α groups to elucidate the contribution of transgenic CD8α co-expression in TEG011 infiltration *in vivo,* and focused on the total sum of functional CD8-expressing TEG011 cells. We detected a significantly higher number of functional TEG cells infiltrating in the spleen and bone marrow of TEG011_CD8α-treated mice at both time points (Figure 2D). Importantly, we did not observe rapid clearance of functional TEG011_CD8α cells in these tissues within these time points, whereas TEG011 cells were barely detected. Thus, we conclude that CD8α co-stimulation with TEG011 improves overall *in vivo* tumor control, T cell persistence and infiltration.
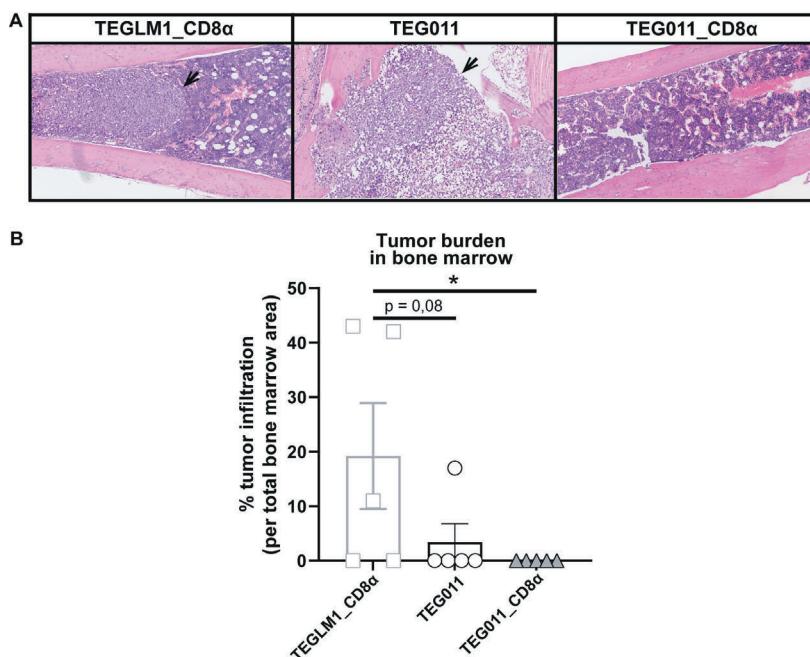
Figure 3 TEG011_CD8α effectively cleared tumor cells in bone marrow, without a significant difference in tumor infiltration observed in other major organs. (A) Representative pictures H&E stained of mouse bone marrow from where no neoplastic cells (black arrow) observed only in TEG011_CD8a treated group for each individual mouse. Magnification:10×; Shown are representative pictures from individual mice of each treatment group (n = 5mice/group); **(B)** Percentage cases of tumor infiltration in mouse bone marrow for each treatment group (n = 5mice/group). Calculation was performed by dividing the area covered by the tumor cells per the total area of bone marrow tissue visible in the section using ImageJ. Data are shown as mean ± SEM (*P < 0.05) calculated by non-parametric Kruskal-Wallis test.

TEG011_CD8α enhanced T cell infiltration and effectively cleared tumor cells in bone marrow

We previously reported an extensive *in vivo* safety profile of TEG011 against healthy tissues that express HLA-A*24:02 molecules, in which no significant histological lesions were observed in major organs, including liver, spleen, and intestine (36). For histopathology analysis, we collected a femur bone marrow section from each treatment group at the end of the study period to further evaluate antitumor efficacy of the new TEG011_CD8α cells (Figure 3A). Tissue sections were assessed for the presence and extension of the neoplastic foci. The mock control TEGLM1_CD8α-treated group showed evident 19,2% neoplastic infiltration, whereas the TEG011-treated group showed up to 3,4% neoplastic infiltration of a homogeneous population of neoplastic cells in the bone marrow. Interestingly, we did not observe any neoplastic infiltration in the bone marrow of mice in the TEG011_CD8α group and the appearance of bone marrow cell composition and cellularity were normal (Figure 3B). In conclusion, here we report that TEG011_CD8α effectively cleared tumor cells in bone marrow, emphasizing the role of CD8α co-stimulation for better *in vivo* tumor control of TEG011 cells. Overall, our data indicate that introduction of transgenic CD8α on TEG011 cells effectively improves *in vivo* tumor control and better T cell infiltration into bone marrow.

5

DISCUSSION

TEG011 has been reported to specifically recognize HLA-A*24:02$^+$ malignant cells while sparing the HLA-A*24:02-expressing healthy tissues with the requirement of CD8α co-stimulation (32, 36). While TEG011 has shown a favorable efficacy profile *in vivo*, we only observed in 44% of the mice long-term persistence of functional TEG011 cells, which could be due to the lack of support by antigen-specific CD4$^+$ T cells (29, 36). To further improve the antitumor efficacy of TEG011, we introduced transgenic CD8α co-receptor together with TEG011 cells. In this study, we reported on the capacity of the introduced CD8α co-receptor to successfully redirect non-reactive CD4$^+$ TEG011 cells *in vivo* and *in vitro* against tumor targets that express HLA-A*24:02 molecules. Furthermore, TEG011_CD8α cells showed higher T cell counts and stable peripheral persistence *in vivo*, which was, however, mainly a consequence of the persistence of CD4$^+$CD8$^+$ double positive TEG011_CD8α and not an improved persistence of CD8$^+$ single positive TEG011_CD8α. Regardless of the precise underlying molecular mechanism, for the first time we observed tumor clearance in the bone marrow by TEG011_CD8α, but not by TEG011 alone.

Reprogramming CD4$^+$ T cells by genetic engineering has been reported to clinically impact efficacy and toxicity by high affinity receptors, like CARs (37). Vγ9Vδ2TCR (30) and CD8αβ independent αβTCRs (38) have been also reported to reprogram CD4$^+$ T cells which have the not only the ability to exert tumor cell killing but also induce maturation of professional antigen presenting cells. Transfer of CD8αβ in combination with intermediate affinity tumor reactive αβTCR has been reported to support tumor control *in*

vitro and *in vivo* (39, 40) and for high affinity αßTCR with artificial signaling domains adding CD8α alone has been shown to reprogram CD4⁺ T cells (41). Within this context, our data show that CD8αα in combination with a natural γδTCR functions serves as co-stimulatory receptor, as opposed to the well-described inhibitory function of CD8αα on αßT cells within the context of a natural αßTCR. Expression of that CD8αα on activated CD4⁺ and CD8αß⁺ αßT cells has been reported to act as corepressor by competing with CD8αß⁺ cells for p56^{lck} signaling molecule (42). Though we investigated the role of CD8αα in the TEG concept, our data support the notion that CD8αα in combination with a γδTCR are synergistic on natural γδT cells, as activated CD8αα⁺ γδT cells were reported in supporting control of HIV infection (43). We have also previously reported significant increases in circulating CD8αα⁺ γδT cells in CMV-positive population (28). Thus, CD8αα appears to have opposing functions on innate and adaptive immune cells, where it acts as co-stimulatory receptor in the context of a γδTCR.

Using humanized transgenic mice expressing human HLA-A*24:02, we could study the implication of CD8α introduction to TEG011, referred to as TEG011_CD8α, elucidating their improved efficacy *in vivo*. We provide evidence that TEG011_CD8α effectively cleared tumor cells in bone marrow and elicited better tumor control against human HLA-A*24:02-expressing tumor cells. We cannot entirely exclude that superior tumor control in TEG011_CD8α may have been caused initially by more CD8 single positive cells in the TEG011_CD8α product compared to TEG011 product, as CD4⁺/CD8⁺ ratios could not be entirely controlled in the experimental set up prior to infusion. However, our mouse model also allowed us to investigate TEG011_CD8α kinetics in the presence of tumor cells; and we observed sustained long-term TEG persistence mainly for γδTCR⁺CD4⁺CD8⁺ double positive and a decline in γδTCR⁺CD8⁺ single positive TEG011_CD8α cells. Importantly, the sustained peripheral TEG persistence was only observed for TEG011_CD8α but not TEGLM1_CD8α, highlighting the key role of a functional tumor-reactive γδTCR. This observation rather argues against the classical helper function of γδTCR⁺CD4⁺CD8⁺ double positive TEG011_CD8α cells within the context of TEG011_CD8α. Hence, the concurrent expression of CD4⁺ and CD8⁺ co-receptor most likely provided additional survival signal for tumor-specific CD4⁺ T cells, which did not, however, translate into classical helper functions towards CD8⁺ T cells (36, 44, 45). CD4⁺ T cells have been reported to avoid expression of inhibitory receptors on CD8⁺ T cells (46) and as an important cell subset to induce memory T cell formation (47). Along this line we observed over time reduced expression of TIM3 in CD8⁺ single positive TEG011_CD8α cells compared to mock and TEG011 group. CD4⁺CD8⁺ double positive TEG011_CD8α cells had lower levels of TIM3 when compared to CD8⁺ single positive TEG011_CD8α cells. These data remain difficult to interpret, and most likely simply reflect different regulation and activation of functional and non-functional CD4⁺ and CD8⁺ TEG cells. We also acknowledge that xenograft mouse models do not allow to completely mimic all potential helper roles of human CD4⁺ T cells, due to the lack of human professional antigen presenting cells.

The precise molecular interaction between CD8αα and its specific ligand in our context remains yet to be unraveled. The CD8αα receptor has been shown to bind to MHC

Class I molecules, including HLA-A*02:01, HLA-A*11:01, HLA-B*35:01, HLA-C*07:02, via protruding α3 domain loop of MHC molecules with lower affinity than the binding of a TCR-pMHC complex (48-51). Polymorphisms in the MHC α3 domain contributes to a binding variation of CD8αα to different HLA molecules, such as HLA-A*24:02. In this context, HLA-A*24:02 is one of the possible ligands for CD8αα on TEG011, in line with an earlier study that reported CD8αα interaction with HLA-A*24:02 in a similar way with HLA-A*02:01, involving binding to the α2 and α3 domains, as well as to the ß2m domain of pMHC complex, but with different conformation that suggests CD8αα plasticity (52). The non-classical MHC molecules are also reported to interact with CD8α, such as HLA-G and HLA-E (53). HLA-G is a known ligand for CD8αα, which is expressed on some colorectal cancer (54-56), while HLA-E is mainly expressed in human endothelial cells and is highly expressed in tumor cells (53). Other studies also demonstrated the interaction between CD8 and CEACAM5, which support the possibility of CEACAM5 as CD8α ligands (57). Overall, we demonstrate that TEG011 equipped with human CD8α co-receptor elicits superior tumor control and long-term persistence, which mainly impacted numbers of functional γδTCR^{+}CD4^{+}CD8^{+} double positive TEG011_CD8α cells, and associated with better T cell infiltration. In addition, TEG011_CD8α cells successfully cleared tumor cells in the bone marrow, which highlights its potential for further clinical application.

Conflict of Interest Disclosure

Author Contributions

IJ, TS, ZS and JK conceptualized, designed and developed the *in vivo* models. IJ, PH, WS and SH performed the *in vitro* and *in vivo* experiments. LB and AB performed the histopathology examination of the mouse tissues. DB and RO contributed vital components. IJ analyzed all *in vitro* and *in vivo* data and was a major contributor in writing the manuscript. IJ, ZS, and JK interpret all *in vitro* and *in vivo* data. IJ and JK wrote the manuscript; all authors read, review and approved the final manuscript.

Funding

Acknowledgments

5

REFERENCES

1.   Dadi S, Chhangawala S, Whitlock BM, Franklin RA, Luo CT, Oh SA, *et al*. Cancer Immunosurveillance by Tissue-Resident Innate Lymphoid Cells and Innate-like T Cells. *Cell*. 2016; 164(3):365-77.

2.   Melandri D, Zlatareva I, Chaleil RAG, Dart RJ, Chancellor A, Nussbaumer O, *et al*. The γδTCR combines innate immunity with adaptive immunity by utilizing spatially distinct regions for agonist selection and antigen responsiveness. *Nat Immunol*. 2018;19(12):1352-65.

3.   Muro R, Takayanagi H, Nitta T. T cell receptor signaling for γδT cell development. *Inflamm Regen*. 2019;39:6.

4.   Sebestyen Z, Prinz I, Dechanet-Merville J, Silva-Santos B, Kuball J. Translating gammadelta (γδ) T cells and their receptors into cancer cell therapies. *Nat Rev Drug Discov*. 2020;19(3):169-84.

5.   Sandstrom A, Peigne CM, Leger A, Crooks JE, Konczak F, Gesnel MC, *et al*. The intracellular B30.2 domain of butyrophilin 3A1 binds phosphoantigens to mediate activation of human Vγ9Vδ2 T cells. *Immunity*. 2014;40(4):490-500.

6.   Sebestyen Z, Scheper W, Vyborova A, Gu S, Rychnavska Z, Schiffler M, *et al*. RhoB Mediates Phospho-antigen Recognition by Vγ9Vδ2 T Cell Receptor. *Cell Rep*. 2016;15(9):1973-85.

7.   Karunakaran MM, Willcox CR, Salim M, Paletta D, Fichtner AS, Noll A, *et al*. Butyrophilin-2A1 Directly Binds Germline-Encoded Regions of the Vγ9Vδ2 TCR and Is Essential for Phosphoantigen Sensing. *Immunity*. 2020;52(3):487-98 e6.

8.   Rigau M, Ostrouska S, Fulford TS, Johnson DN, Woods K, Ruan Z, *et al*. Butyrophilin 2A1 is essential for phosphoantigen reactivity by γδT cells. Science. 2020;367(6478).

9.   Vyborova A, Beringer DX, Fasci D, Karaiskaki F, van Diest E, Kramer L, *et al*. γ9δ2T cell diversity and the receptor interface with tumor cells. *J Clin Invest*. 2020;130(9):4637-51.

10. Cano CE, Pasero C, De Gassart A, Kerneur C, Gabriac M, Fullana M, *et al*. BTN2A1, an immune check-point targeting Vγ9Vδ2 T cell cytotoxicity against malignant cells. *Cell Rep*. 2021; 36(2): 109359.

11. Groh V, Rhinehart R, Secrist H, Bauer S, Grabstein KH, Spies T. Broad tumor-associated expression and recognition by tumor-derived γδT cells of MICA and MICB. *Proc Natl Acad Sci USA*. 1999;96(12):6879-84.

12. Catellani S, Poggi A, Bruzzone A, Dadati P, Ravetti JL, Gobbi M, *et al*. Expansion of Vδ1 T lympho-cytes producing IL-4 in low-grade non-Hodgkin lymphomas expressing UL-16-binding proteins. *Blood*. 2007;109(5):2078-85.

13. Poggi A, Venturino C, Catellani S, Clavio M, Miglino M, Gobbi M, *et al*. Vδ1 T lymphocytes from B-CLL patients recognize ULBP3 expressed on leukemic B cells and up-regulated by trans-retinoic acid. *Cancer Res*. 2004;64(24):9172-9.

14. Luoma AM, Castro CD, Mayassi T, Bembinster LA, Bai L, Picard D, *et al*. Crystal structure of Vδ1 T cell receptor in complex with CD1d-sulfatide shows MHC-like recognition of a self-lipid by human γδT cells. *Immunity*. 2013;39(6):1032-42.

15. Zhao J, Huang J, Chen H, Cui L, He W. Vδ1 T cell receptor binds specifically to MHC I chain related A: molecular and biochemical evidences. *Biochem Biophys Res Commun*. 2006; 339(1): 232-40.

16. Schilbach K, Frommer K, Meier S, Handgretinger R, Eyrich M. Immune response of human propagat-ed γδ-T-cells to neuroblastoma recommend the Vδ1[+] subset for γδ-T-cell-based immunotherapy. *J Immunother*. 2008;31(9):896-905.

17. Devaud C, Rousseau B, Netzer S, Pitard V, Paroissin C, Khairallah C, *et al*. Anti-metastatic potential of human Vδ1^{+} γδT cells in an orthotopic mouse xenograft model of colon carcinoma. *Cancer Immunol Immunother*. 2013;62(7):1199-210.

18. Almeida AR, Correia DV, Fernandes-Platzgummer A, da Silva CL, da Silva MG, Anjos DR, *et al*. Delta One T Cells for Immunotherapy of Chronic Lymphocytic Leukemia: Clinical-Grade Expansion/Differentiation and Preclinical Proof of Concept. *Clin Cancer Res*. 2016;22(23):5795-804.

19. Di Lorenzo B, Ravens S, Silva-Santos B. High-throughput analysis of the human thymic Vδ1+ T cell receptor repertoire. *Sci Data*. 2019;6(1):115.

20. Janssen A, Villacorta Hidalgo J, Beringer DX, van Dooremalen S, Fernando F, van Diest E, *et al*. γδT-cell Receptors Derived from Breast Cancer-Infiltrating T Lymphocytes Mediate Antitumor Reactivity. *Cancer Immunol Res*. 2020;8(4):530-43.

21. Harly C, Joyce SP, Domblides C, Bachelet T, Pitard V, Mannat C, *et al*. Human γδT cell sensing of AMPK-dependent metabolic tumor reprogramming through TCR recognition of EphA2. *Sci Immunol*. 2021;6(61).

22. Deniger DC, Moyes JS, Cooper LJ. Clinical applications of γδT cells with multivalent immunity. *Front Immunol*. 2014;5:636.

23. Siegers GM, Lamb LS, Jr. Cytotoxic and regulatory properties of circulating Vδ1+ γδT cells: a new player on the cell therapy field? *Mol Ther*. 2014;22(8):1416-22.

24. de Witte MA, Janssen A, Nijssen K, Karaiskaki F, Swanenberg L, van Rhenen A, *et al*. αβT-cell graft depletion for allogeneic HSCT in adults with hematological malignancies. *Blood Adv*. 2021; 5(1):240-9.

25. de Witte M, Daenen LGM, van der Wagen L, van Rhenen A, Raymakers R, Westinga K, *et al*. Allogeneic Stem Cell Transplantation Platforms With *Ex Vivo* and *In Vivo* Immune Manipulations: Count and Adjust. *Hemasphere*. 2021;5(6):e580.

26. Straetemans T, Kierkels GJJ, Doorn R, Jansen K, Heijhuurs S, Dos Santos JM, *et al*. GMP-Grade Manufacturing of T Cells Engineered to Express a Defined γδTCR. *Front Immunol*. 2018;9:1062.

27. Straetemans T, Grunder C, Heijhuurs S, Hol S, Slaper-Cortenbach I, Bonig H, *et al*. Untouched GMP-Ready Purified Engineered Immune Cells to Treat Cancer. *Clin Cancer Res*. 2015; 21(17): 3957-68.

28. Scheper W, van Dorp S, Kersting S, Pietersma F, Lindemans C, Hol S, *et al*. γδT cells elicited by CMV reactivation after allo-SCT cross-recognize CMV and leukemia. *Leukemia*. 2013;27(6):1328-38.

29. Scheper W, Grunder C, Straetemans T, Sebestyen Z, Kuball J. Hunting for clinical translation with innate-like immune cells and their receptors. *Leukemia*. 2014;28(6):1181-90.

30. Marcu-Malina V, Heijhuurs S, van Buuren M, Hartkamp L, Strand S, Sebestyen Z, *et al*. Redirecting αβT cells against cancer cells by transfer of a broadly tumor-reactive γδT-cell receptor. *Blood*. 2011;118(1):50-9.

31. Grunder C, van Dorp S, Hol S, Drent E, Straetemans T, Heijhuurs S, *et al*. γ9 and δ2CDR3 domains regulate functional avidity of T cells harboring γ9δ2TCRs. *Blood*. 2012;120(26):5153-62.

32. Kierkels GJJ, Scheper W, Meringa AD, Johanna I, Beringer DX, Janssen A, *et al*. Identification of a tumor-specific allo-HLA-restricted γδTCR. *Blood Adv*. 2019;3(19):2870-82.

33. Gibbings D, Befus AD. CD4 and CD8: an inside-out coreceptor model for innate immune cells. *J Leukoc Biol*. 2009;86(2):251-9.

34. Najima Y, Tomizawa-Murasawa M, Saito Y, Watanabe T, Ono R, Ochi T, *et al*. Induction of WT1-specific human CD8+ T cells from human HSCs in HLA class I Tg NOD/SCID/IL2rgKO mice. *Blood*. 2016;127(6):722-34.

35. Straetemans T, Janssen A, Jansen K, Doorn R, Aarts T, van Muyden ADD, *et al*. TEG001 Insert Integrity from Vector Producer Cells until Medicinal Product. *Mol Ther*. 2020;28(2):561-71.

36. Johanna I, Hernandez-Lopez P, Heijhuurs S, Bongiovanni L, de Bruin A, Beringer D, *et al*. TEG011 persistence averts extramedullary tumor growth without exerting off-target toxicity against healthy tissues in a humanized HLA-A*24:02 transgenic mice. *J Leukoc Biol*. 2020;107(6):1069-79.

5

37. Shah NN, Highfill SL, Shalabi H, Yates B, Jin J, Wolters PL, *et al*. CD4/CD8 T-Cell Selection Affects Chimeric Antigen Receptor (CAR) T-Cell Potency and Toxicity: Updated Results From a Phase I Anti-CD22 CAR T-Cell Trial. *J Clin Oncol*. 2020;38(17):1938-50.

38. Kuball J, Schmitz FW, Voss RH, Ferreira EA, Engel R, Guillaume P, *et al*. Cooperation of human tumor-reactive CD4^{+} and CD8^{+} T cells after redirection of their specificity by a high-affinity p53A2.1-specific TCR. *Immunity*. 2005;22(1):117-29.

39. Bajwa G, Lanz I, Cardenas M, Brenner MK, Arber C. Transgenic CD8αß co-receptor rescues endogenous TCR function in TCR-transgenic virus-specific T cells. *J Immunother Cancer*. 2020; 8(2).

40. Yachi PP, Ampudia J, Zal T, Gascoigne NR. Altered peptide ligands induce delayed CD8-T cell receptor interaction-a role for CD8 in distinguishing antigen quality. *Immunity*. 2006;25(2):203-11.

41. Willemsen R, Ronteltap C, Heuveling M, Debets R, Bolhuis R. Redirecting human CD4^{+} T lymphocytes to the MHC class I-restricted melanoma antigen MAGE-A1 by TCR αß gene transfer requires CD8α. *Gene Ther*. 2005;12(2):140-6.

42. Cheroutre H, Lambolez F. Doubting the TCR coreceptor function of CD8αα. *Immunity*. 2008; 28(2):149-59.

43. Omi K, Shimizu M, Watanabe E, Matsumura J, Takaku C, Shinya E, *et al*. Inhibition of R5-tropic HIV type-1 replication in CD4^{+} natural killer T cells by γδT lymphocytes. *Immunology*. 2014; 141(4):596-608.

44. Morris EC, Tsallios A, Bendle GM, Xue SA, Stauss HJ. A critical role of T cell antigen receptor-transduced MHC class I-restricted helper T cells in tumor protection. *Proc Natl Acad Sci USA*. 2005;102(22):7934-9.

45. Willemsen RA, Sebestyen Z, Ronteltap C, Berrevoets C, Drexhage J, Debets R. CD8α coreceptor to improve TCR gene transfer to treat melanoma: down-regulation of tumor-specific production of IL-4, IL-5, and IL-10. *J Immunol*. 2006;177(2):991-8.

46. Ahrends T, Spanjaard A, Pilzecker B, Babala N, Bovens A, Xiao Y, *et al*. CD4^{+} T Cell Help Confers a Cytotoxic T Cell Effector Program Including Coinhibitory Receptor Downregulation and Increased Tissue Invasiveness. *Immunity*. 2017;47(5):848-61 e5.

47. Shedlock DJ, Shen H. Requirement for CD4 T cell help in generating functional CD8 T cell memory. *Science*. 2003;300(5617):337-9.

48. Gao GF, Willcox BE, Wyer JR, Boulter JM, O'Callaghan CA, Maenaka K, *et al*. Classical and nonclassical class I major histocompatibility complex molecules exhibit subtle conformational differences that affect binding to CD8αα. *J Biol Chem*. 2000;275(20):15232-8.

49. Witte T, Spoerl R, *Chang* HC. The CD8ß ectodomain contributes to the augmented coreceptor function of CD8αß heterodimers relative to CD8αα homodimers. *Cell Immunol*. 1999; 191(2):90-6.

50. Chang HC, Tan K, Hsu YM. CD8αß has two distinct binding modes of interaction with peptide-major histocompatibility complex class I. *J Biol Chem*. 2006;281(38):28090-6.

51. Huang J, Edwards LJ, Evavold BD, Zhu C. Kinetics of MHC-CD8 interaction at the T cell membrane. *J Immunol*. 2007;179(11):7653-62.

52. Shi Y, Qi J, Iwamoto A, Gao GF. Plasticity of human CD8αα binding to peptide-HLA-A*24:02. *Mol Immunol*. 2011;48(15-16):2198-202.

53. Gavlovsky PJ, Tonnerre P, Guitton C, Charreau B. Expression of MHC class I-related molecules MICA, HLA-E and EPCR shape endothelial cells with unique functions in innate and adaptive immunity. *Hum Immunol*. 2016;77(11):1084-91.

54. Yie SM, Yang H, Ye SR, Li K, Dong DD, Lin XM. Expression of human leukocyte antigen G (HLA-G) correlates with poor prognosis in gastric carcinoma. *Ann Surg Oncol*. 2007;14(10):2721-9.

55. Sanders SK, Giblin PA, Kavathas P. Cell-cell adhesion mediated by CD8 and human histocompatibility leukocyte antigen G, a nonclassical major histocompatibility complex class 1 molecule on cytotrophoblasts. *J Exp Med*. 1991;174(3):737-40.

56. Hofmeister V, Weiss EH. HLA-G modulates immune responses by diverse receptor interactions. *Semin Cancer Biol*. 2003;13(5):317-23.

57. Roda G, Jianyu X, Park MS, DeMarte L, Hovhannisyan Z, Couri R, *et al*. Characterizing CEACAM5 interaction with CD8α and CD1d in intestinal homeostasis. *Mucosal Immunol*. 2014;7(3):615-24.

5

SUPPLEMENTARY FIGURES
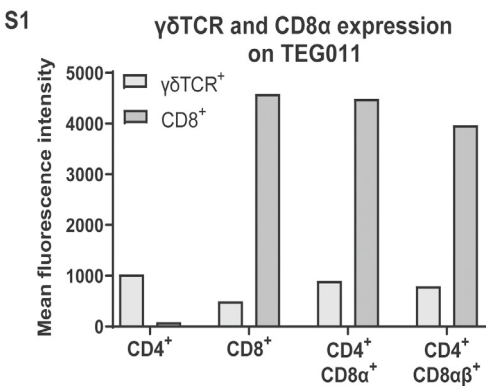
Figure S1 Transgene expression levels on T cells transduced with the FE11 γδTCR in combination with CD8α alone or CD8α and CD8ß. αßT cells were transduced with the FE11 γδTCR, and with either CD8α alone or CD8α combined with CD8ß. Thereafter, CD4+, CD8+, CD4+CD8α+ and CD4+CD8αß+ TEG011 cells were sorted, and the expression of γδTCR and CD8α was measured by flow cytometry.
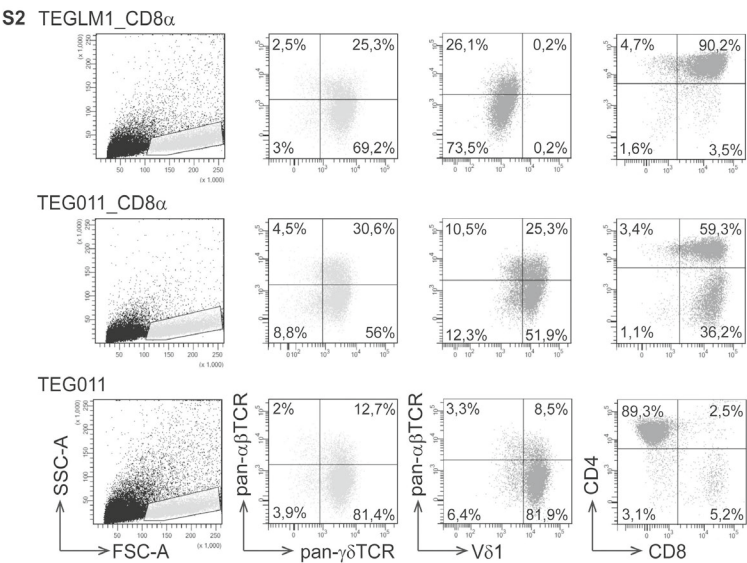
Figure S2 γδTCR expression of TEG011, TEG011_CD8α, and TEGLM1_CD8α mock. Representative flow cytometry plots for γδTCR expression of TEGLM1_CD8α (top panel), TEG011_CD8α (middle panel), and TEG011 (bottom panel) prior to infusion into mice after 2 weeks expansion. Representative plots for Vδ1 TCR expression of TEG011 and TEG011_CD8α were included as quality control for flow cytometry panel using pan-γδTCR monoclonal antibody.
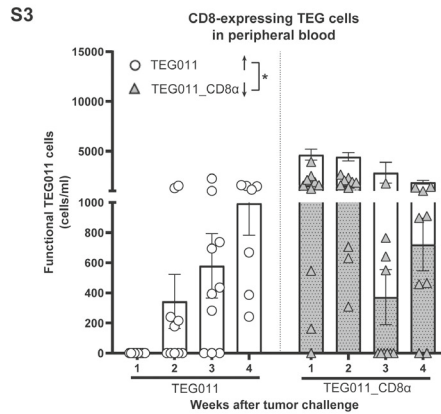
Figure S3 Overall functional TEG011 cells in periphery. Absolute number of CD8-expressing TEG011 cells were measured in peripheral blood by flow cytometry for TEG011 (open black circle) and TEG011_CD8α (open black triangle) in tumor-bearing mice. TEG cells are distinguished into two different cellular compartments: CD8+ single positive (SP; white stacked bar) and CD4+CD8+ double positive (DP; grey dotted stacked bar). Black arrows indicate higher or lower T cell counts observed. Data represent mean ± SEM of all mice per group (n = 10 mice). Statistical significances were calculated by a mixed-effects model with repeated measures (*P < 0.05).

5
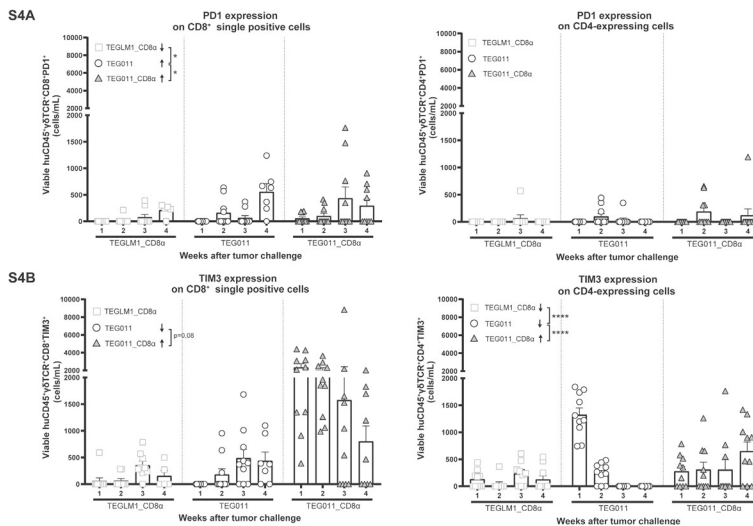
Figure S4 PD1 and TIM3 expression on CD4+ and CD8+ TEGs. Absolute cell counts of PD1-expressing **(A)** and TIM3-expressing **(B)** huCD45+γδTCR+CD8+ single positive cells (left panel) and huCD45+γδTCR+CD4+ single positive or CD4+CD8+ double positive cells (right panel) were measured by flow cytometry for TEGLM1_CD8α mock (open light gray rectangle), TEG011 (open black circle), and TEG011_CD8α (grey triangle). Black arrows indicate higher or lower T cell counts observed. Data represent mean ± SEM of all mice per group (n = 10 mice). Statistical significances were calculated by a mixed-effects model with repeated measures (*P < 0.05; ****P < 0.0001).

Supplementary Table 1. Complete sequence of TEG011_CD8α

(pMP71-TCR_FE11g-T2A-FE11d_P2A-CD8a)

```
                                        >>--TCR FE11γ-->
1081   gctcacttac aggcggccac gcgtggatcc gaattcacca tgggatgggc tctgctggtg
       >--------------------------------TCR FE11γ----------------------------->
1141   ctgctggcct ttctgtctcc tgccagccag aagtccagca acctggaagg cggcaccaa
       >--------------------------------TCR FE11γ----------------------------->
1201   agcgtgacca gacctacaag aagcagcgcc gagatcacct gtgacctgac cgtgatcaac
       >--------------------------------TCR FE11γ----------------------------->
1261   gccttctaca tccactggta tctgcaccaa gaaggcaagg cccctcagcg gctgctgtac
       >--------------------------------TCR FE11γ----------------------------->
1321   tacgatgtgt ccaacagcaa ggacgtgctg gaaagcggac tgagccccgg caagtactac
       >--------------------------------TCR FE11γ----------------------------->
1381   acccacacac ctagacggtg gtcctggatc ctgatcctgc ggaacctgat cgagaacgac
       >--------------------------------TCR FE11γ----------------------------->
1441   tccggcgtgt actactgcgc cacctgggat agacccgaga tctactataa gaagctgttc
       >--------------------------------TCR FE11γ----------------------------->
1501   ggcagcggca ccacactggt ggtcacagac aaacagctgg acgccgacgt gtcccctaa
       >--------------------------------TCR FE11γ----------------------------->
1561   cctaccatct tcctgccttc tatcgccgag acaaagctgc agaaggccgg cacctacct
       >--------------------------------TCR FE11γ----------------------------->
1621   tgcctgctgg aaaagttctt cccagacgtg atcaagatcc actgggaaga gaagaagtcc
       >--------------------------------TCR FE11γ------------------------------>
1681   aacaccatcc tgggcagcca agagggcaac accatgaaga ccaacgacac ctacatgaa
       >--------------------------------TCR FE11γ----------------------------->
1741   ttcagctggc tgaccgtgcc tgagaagtcc ctggacaaag aacaccggtg catcgtgcg
       >--------------------------------TCR FE11γ----------------------------->
1801   cacgagaaca acaagaacgg cgtggaccaa gagatcatct tcccacctat caagaccgac
       >--------------------------------TCR FE11γ----------------------------->
1861   gtcatcacaa tggaccccaa ggacaactgc tccaaggacg ccaacgatac cctgctgct
       >--------------------------------TCR FE11γ----------------------------->
1921   cagctgacaa acaccagcgc ctactacatg tatttgctgc tgttgctgaa gtccgtggt
       >--------------------------------TCR FE11γ----------------------------->
1981   tacttcgcca tcatcacatg ctgcctgctg cggagaaccg ccttctgctg caatggcga
       ----->>------------------------------T2A linker-----------------------------
2041   aaaagcgtcg acagcggctc tggcagatct ggctctggcg aaggcagagg ctctctgct
       -------------------------T2A linker---------------------->>----------------
2101   acatgtggcg acgtggaaga gaaccccgga cctcgcttaa ttaacatggt gttcagcagc
       >--------------------------------TCR FE11δ----------------------------->
2161   ctgctgtgcg tgttcgtggc ctttagctac agcggaagca gcgtggccca gaaagtgaca
       >--------------------------------TCR FE11δ----------------------------->
2221   caggcccagt cctccgtgtc tatgcctgtg cggaaagccg tgacactgaa ctgcctgtac
       >--------------------------------TCR FE11δ----------------------------->
2281   gagacaagct ggtggtctta ctacatcttc tggtacaagc agctgcccag caaagagat
       >--------------------------------TCR FE11δ----------------------------->
2341   atctttctga tccggcaggg cagcgacgag cagaatgcca agagcggcag atactccgt
       >--------------------------------TCR FE11δ----------------------------->
2401   aacttcaaga aagccgccaa gtctgtggcc ctgaccatct ctgctctgca actggaagat
       >--------------------------------TCR FE11δ----------------------------->
```

2461   agcgccaagt acttctgcgc cctgggcgat tcttatggcg gcggacctct gtacaccgac
        >-------------------------------TCR FE11δ----------------------------->

2521   aagctgatct tcggcaaggg caccagagtg accgtggaac ctagaagcca gcctcacacc
        >-------------------------------TCR FE11δ----------------------------->

2581   aagccttccg tgtttgtgat gaagaacggc accaacgtgg cctgcctggt caaagagttc
        >-------------------------------TCR FE11δ----------------------------->

2641   taccctaagg acatccggat caacctggtg tccagcaaga agatcaccga gttcgacccc
        >-------------------------------TCR FE11δ----------------------------->

2701   gccatcgtga tcagccctag cggcaagtat aacgccgtga agctggggaa gtacgaggac
        >-------------------------------TCR FE11δ----------------------------->

2761   agcaatagcg tgacctgcag cgtgcagcat gataacaaga ccgtgcacag caccgatttc
        >-------------------------------TCR FE11δ-------------------------------->

2821   gaagtgaaaa ccgactccac cgaccacgtg aagcccaaag agacagagaa caccaagca
        >-------------------------------TCR FE11δ----------------------------->

2881   cccagcaagt cctgccacaa gcctaaggcc atcgtgcaca ccgagaaagt gaacatgat
        >-------------------------------TCR FE11δ----------------------------->

2941   agcctgacag tgctgggcct gagaatgctg ttcgccaaga cagtggccgt gaatttcct
        >-------TCR FE11δ------->>-----------------P2A linker----------------

3001   ctgaccgcca agctgttctt tctgctcgag ggcagcggcg ccacaaattt cagcctgct
        ----------------P2A linker--------------------->>---------------------------

3061   aaacaggccg gcgacgtcga agaaaatcct ggaccaatgg ccttaccagt gaccgcctt
        >-------------------------------CD8α------------------------------------->

3121   ctcctgccgc tggccttgct gctccacgcc gccaggccga gccagttccg ggtgtcgcc
        >-------------------------------CD8α------------------------------------->

3181   ctggatcgga cctggaacct gggcgagaca gtggagctga agtgccaggt gctgctgtcc
        >-------------------------------CD8α-------------------------------------->

3241   aacccgacgt cgggctgctc gtggctcttc cagccgcgcg gcgccgccgc cagtcccacc
        >-------------------------------CD8α------------------------------------->

3301   ttcctcctat acctctccca aaacaagccc aaggcggccg aggggctgga cacccagcg
        >-------------------------------CD8α------------------------------------->

3361   ttctcgggca agaggttggg ggacaccttc gtcctcaccc tgagcgactt ccgccgaga
        >-------------------------------CD8α-------------------------------->

3421   aacgagggct actatttctg ctcggccctg agcaactcca tcatgtactt cagccacttc
        >-------------------------------CD8α------------------------------------->

3481   gtgccggtct tcctgccagc gaagcccacc acgacgccag cgccgcgacc accaacacc
        -------------------------------CD8α--------------------------------------

3541   gcgcccacca tcgcgtcgca gcccctgtcc ctgcgcccag aggcgtgccg gccagcggc
        >-------------------------------CD8α------------------------------------->

3601   gggggcgcag tgcacacgag ggggctggac ttcgcctgtg atatctacat ctgggcgccc
        >-------------------------------CD8α-------------------------------->

3661   ctggccggga cttgtggggt ccttctcctg tcactggtta tcacccttta ctgcaaccac
        >-------------------------------CD8α------------------------------------->

3721   aggaaccgaa gacgtgtttg caaatgtccc cggcctgtgg tcaaatcggg agacaagccc
        >-----------CD8α----------->>

3781   agcctttcgg cgagatacgt ctgatat**ga**a aagcttaaca cgagccatag atagaataaa

Supplementary Table 2. Complete sequence of TEGLM1_CD8α

(pMP71-TCRG115γ-T2A-TCRG115δ_LM1_P2A-CD8a)

                                                              >>--TCR G115γ-->

1081   gctcacttac aggcggccac gcgtggatcc gaattcacc**a tg**gtgtccct gctgcacgcc
        >-------------------------------TCR G115γ-------------------------------->

1141   agcaccctgg ccgtgctggg cgccctgtgc gtgtatggcc ccggacacct ggaacagccc
        >-------------------------------TCR G115γ-------------------------------->

1201   cagatcagca gcaccaagac cctgagcaag accgccaggc tggaatgcgt ggtgtccggc
        >-------------------------------TCR G115γ-------------------------------->

1261   atcaccatca gcgccacctc cgtgtactgg tacagagaga gacccggcga ggtcatcca
        >-------------------------------TCR G115γ-------------------------------->

1321   ttcctggtgt ccatcagcta cgacggcacc gtgcggaaag agagcggcat ccccagcggc
        >-------------------------------TCR G115γ-------------------------------->

1381   aagttcgagg tggacagaat ccccgagacc agcacctcca ccctgaccat ccacaacgt
        >-------------------------------TCR G115γ--------------------------------->

1441   gagaagcagg acatcgccac ctactactgc gccctgtggg aggcccagca ggaactgggc
        >-------------------------------TCR G115γ-------------------------------->

1501   aagaaaatca aggtgttcgg ccctggcacc aagctgatca tcaccgacaa gcagctggac
        >-------------------------------TCR G115γ-------------------------------->

1561   gccgacgtga gccccaagcc taccatcttc ctgcccagca tcgccgagac caagctgca
        >-------------------------------TCR G115γ-------------------------------->

1621   aaggccggca cctacctgtg cctgctggaa aagttcttcc ccgacgtgat caagatccac
        >-------------------------------TCR G115γ--------------------------------->

1681   tgggaggaaa agaagagcaa caccatcctg ggcagccagg aaggcaatac catgaaaacc
        >-------------------------------TCR G115γ-------------------------------->

1741   aacgacacct acatgaagtt cagctggctg accgtgcccg agaagagcct ggacaaaga
        >-------------------------------TCR G115γ-------------------------------->

1801   cacagatgca tcgtccggca cgagaacaac aagaacggcg tggaccagga aatcatcttc
        >-------------------------------TCR G115γ-------------------------------->

1861   cccccccatca agaccgatgt gatcacaatg gaccccaagg acaactgcag caaggacgcc
        >-----------------------------TCR G115γ------------------------------->

1921   aacgataccc tgctgctgca gctgaccaac accagcgcct actacatgta tctcctgct
        >-------------------------------TCR G115γ---------------------------->

1981   ctgctgaaga gcgtggtgta cttcgccatc atcacctgct gtctgctgcg gcggaccgcc
        >------TCR G115γ-------->>---------------------T2A linker-------------------

2041   ttctgctgca acggcgagaa gagcgtcgac agcggcagcg ggcgcagcgg cagcggcgaa
        -------------------------------------T2A linker--------------------------------

2101   ggccgcggca gcctgctgac ctgcggcgat gtggaagaaa accctggccc gcgcttaatt
        ---->>---------------------TCR G115δ_LM1------------------->

2161   aacatggagc ggatcagcag cctgatccac ctgagcctgt tctgggccgg agtgatgagc
        >----------------------------TCR G115δ_LM1---------------------------->

2221   gccatcgagc tggtgcccga gcaccagacc gtgcccgtga gcatcggcgt gcccgccacc
        >----------------------------TCR G115δ_LM1---------------------------->

2281   ctgcggtgca gcatgaaggg cgaggccatc ggcaactact acatcaactg gtacagaaa
            >---------------------------TCR G115δ_LM1--------------------------->

2341   acccagggca acaccatgac cttcatctac cgggagaagg acatctacgg ccctggcttc
            >---------------------------TCR G115δ_LM1--------------------------->

2401   aaggacaact tccagggcga catcgacatc gccaagaacc tggccgtgct gaagatcct
            >---------------------------TCR G115δ_LM1--------------------------->

2461   gcccccagcg agagggacga gggcagctac tactgcgcct gcgacaccct ggccaccgac
            >---------------------------TCR G115δ_LM1--------------------------->

2521   aagctgatct tcggcaaggg cacccgggtg accgtggagc ccagaagcca gccccacacc
            >---------------------------TCR G115δ_LM1--------------------------->

2581   aagcccagcg tgttcgtgat gaagaacggc accaacgtgg cctgcctggt gaaagagttc
            >---------------------------TCR G115δ_LM1--------------------------->

2641   taccccaagg acatccggat caacctggtg tccagcaaga agatcaccga gttcgacccc
            >---------------------------TCR G115δ_LM1--------------------------->

2701   gccatcgtga tcagccccag cggcaagtac aacgccgtga agctgggcaa gtacgaggac
            >---------------------------TCR G115δ_LM1--------------------------->

2761   agcaacagcg tgacctgcag cgtgcagcac gacaacaaga ccgtgcacac caccgacttc
            >---------------------------TCR G115δ_LM1--------------------------->

2821   gaggtgaaaa ccgactccac cgaccacgtg aagcccaaag agaccgagaa caccaagca
            >---------------------------TCR G115δ_LM1--------------------------->

2881   cccagcaaga gctgccacaa gcccaaggcc atcgtgcaca ccgagaaggt gaacatgat
            >---------------------------TCR G115δ_LM1--------------------------->

2941   agcctgaccg tgctgggcct gcggatgctg ttcgccaaga cagtggccgt gaacttcct
            >----TCR G115δ_LM1--->>----------------P2A linker----------------

3001   ctgaccgcca agctgttctt cctgctcgag ggcagcggcg ccacaaattt cagcctgct
            -------------------P2A linker------------------->>----------CD8α---------->

3061   aaacaggccg gcgacgtcga agaaaatcct ggaccaatgg ccttaccagt gaccgcctt
            >-----------------------------------CD8α----------------------------------->

3121   ctcctgccgc tggccttgct gctccacgcc gccaggccga gccagttccg ggtgtcgcc
            >-----------------------------------CD8α----------------------------------->

3181   ctggatcgga cctggaacct gggcgagaca gtggagctga agtgccaggt gctgctgtcc
            >-----------------------------------CD8α----------------------------------->

3241   aacccgacgt cgggctgctc gtggctcttc cagccgcgcg gcgccgccgc cagtcccacc
            >-----------------------------------CD8α----------------------------------->

3301   ttcctcctat acctctccca aaacaagccc aaggcggccg aggggctgga cacccagcg
            >-----------------------------------CD8α----------------------------------->

3361   ttctcgggca agaggttggg ggacaccttc gtcctcaccc tgagcgactt ccgccgaga
            >-----------------------------------CD8α----------------------------------->

3421   aacgagggct actatttctg ctcggccctg agcaactcca tcatgtactt cagccacttc
            >-----------------------------------CD8α----------------------------------->

3481   gtgccggtct tcctgccagc gaagcccacc acgacgccag cgccgcgacc accaacacc
            >-----------------------------------CD8α----------------------------------->

3541   gcgcccacca tcgcgtcgca gcccctgtcc ctgcgcccag aggcgtgccg gccagcggc
            >-----------------------------------CD8α----------------------------------->

5

3601   gggggcgcag tgcacacgag ggggctggac ttcgcctgtg atatctacat ctgggcgccc
           >--------------------------------CD8α-------------------------------->

3661   ctggccggga cttgtggggt ccttctcctg tcactggtta tcacccttta ctgcaaccac
           >-----------------------------------CD8α---------------------------------->

3721   aggaaccgaa gacgtgtttg caaatgtccc cggcctgtgg tcaaatcggg agacaagccc
           >------------CD8α---------->>

3781   agcctttcgg cgagatacgt ctgata**tga**a aagcttaaca cgagccatag atagaataaa

CHAPTER 6

General discussion

Despite the surmounting clinical responses from immunotherapy against cancer, only some cancer patient populations benefit from the treatment (1). This is the consequence of our rather limited understanding of how to better engineer a balance between the targeted killing of malignant cells while protecting their healthy counterparts. Within this context, T cells are a major player which facilitates cellular immunity against different foreign proteins, including malignantly-transformed cells. If this delicate balance of cancer immunosurveillance failed, multiple reasons are accountable for tumor development. Reasons for immune escape are as follows, e.g., loss of antigens, because tumor-reactive T cells became anergic or deleted, or immune cells are kept outside the established immunosuppressive tumor microenvironment (1). To overcome these hurdles, better understanding of the interplay between the immune system, cancer cells, and healthy tissues is crucial for developing effective cancer immunotherapy options to offer better outcome for patients. With this perspective, multiple cancer immunotherapies have been developed in laboratories, as described in **Chapter 1** (2, 3). However, a critical step in clinical translation is to substantially reduce the gap between laboratory findings and clinical exploration of novel therapeutic candidates. This thesis focuses on bridging the path from the laboratory findings to first-in-men studies by studying the efficacy and safety balance of two novel therapeutic candidates of cancer immunotherapy, namely αßT cells Engineered to express a defined γδTCR (TEG), expressing two distinct γδTCRs: a tumor-reactive γ9δ2TCR (TEG001) and a tumor-reactive γ5δ1TCR (TEG011). In this chapter, I will summarize my findings related to TEG-based therapies in the broader perspective of cellular therapy with respect to current literature.

6

Strength and weakness of TIL, αßTCR-engineering, CART-, and TEG-based therapies
The field of adoptive immunotherapies started by exploring the potential benefit of autologous *ex vivo* expanded tumor-infiltrating lymphocytes (TILs). Despite their initial clinical success, TILs are hindered by their scarce numbers of infiltrating T cells that can be isolated from cancer patients for a broader clinical administration. Moreover, clinical outcomes of adoptive T cell therapy (ACT) using TILs has shown only occasional efficacy in a small percentage of the patients (3, 4), which could be due to low tumor mutational load (5) or the effect of immunosuppressive tumor microenvironment impeding immune infiltration (1).

To partially override the aforementioned drawbacks, αßTCR-engineered αßT cell and chimeric antigen receptor (CAR) therapies were introduced. αßT cells recognize specific tumor antigens presented in major histocompatibility complex (MHC) molecules. αßTCR-engineered αßT cell therapy is performed by isolating tumor-specific αßTCR and genetically transfer them into polyclonal αßT cells, and thus redirecting their tumor specificity and broadening the applicability for larger patient populations (6). Using this approach, tumor-specific αßT cells expressing αßTCR with high avidity αßTCR could be generated bypassing the central tolerance mechanism. However, this approach is still impeded by the requirement of human leukocytes antigens (HLA)-matching donors that are vital to avoid possible graft-versus-host-disease (GvHD) manifestation (7). Moreover, it is challenging to identify tumor antigens that are exclusively restricted to

tumor cells, contributing to significant off-target or on-target off-tumor toxicities (8). Therefore, targeting neoantigens with tumor-specific αßTCR is heavily explored, but clinical logistics to identify a defined αßTCR and engineer αßT cells under GMP-grade conditions with individual receptors for each patient are major logistical and regulatory hurdles yet to overcome (9).

CAR T cells have been explored side by side with the aforementioned strategies and are to date the "winner" immunotherapeutic strategy, resulting in a clinically approved and reimbursed drug (10). CAR T cells carry a synthetic receptor with antibody-like specificity and CD3 signaling domain that allow tumor recognition in an MHC-independent manner and, therefore, not only applicable for a particular patient population with specific HLA alleles (11, 12). Based on the promising clinical results, CAR T cells directed towards CD19 antigen have been approved by FDA and EMA (13) to target B cells malignancies, including acute lymphoblastic leukemia (14) and diffuse large B cell lymphoma (15). Inspired by this groundbreaking success that resulted in the introduction of living drugs as one of the standard-of-care arsenal to cancer patients across the globe, many additional clinical studies have been initiated for CAR T cells with different target antigens across different type of malignancies (16, 17). However, CAR T cells only recognize surface antigens, unlike TCR-engineered T cells that could recognize both surface and intracellular antigens presented on MHC molecules (18). As CAR T cells recognition is determined on tumor antigen expression, it also contributes to their on-target off-tumor toxicity where target antigens may be expressed on healthy cells in low density (19). Moreover, tumor cells downregulate or shed their targeted tumor antigens as a tumor escape mechanism and promote therapy resistance (20).

A recent novel cancer immunotherapy strategy arose by observing that enrichment of γδT cells in tumors was associated with improved clinical outcomes (21). This observation inspired the usage of unmodified γδT cells and engineering strategy, including TEGs, as further explored in detail in this thesis.

Strength and weakness of γδT cell-based versus TEG-based therapies
γδT cells recognize their targets mainly independent of MHC-restriction and thus target a broad range of malignancies, including cancer cells with a low mutational burden (22, 23). γδTCR can differentiate between healthy and malignant cells mainly by recognizing stress-induced ligands or metabolic alterations, which are not restricted by one specific tumor antigen. Whether the antitumor property of γδT cell-based immunotherapy arises from the γδTCR (24, 25), other natural killer (NK)-types of receptors (26), or both, remains debatable. Clinical studies which aimed to harvest the antitumor reactivity of both γδTCR and NK receptors by harnessing autologous unmodified γδT cells showed rather disappointing clinical responses (27).

The lack of success of autologous unmodified γδT cell-based therapy could be contributed by the limited proliferative capacity and rapid clearance of circulating γδT cells in cancer patients, even in the presence of aminobisphosphonate and IL-2 (28-34) or

their underestimated diversity (35). Furthermore, some studies also observed scarce infiltration of γδT cells in target tissues (36). Nevertheless, these clinical studies showed a favorable safety profile of γδT cell-based therapy, including the absence of GvHDs in MHC mismatch background (37). However, without a well-defined antitumor efficacy, this lack of toxicity property is clinically not very meaningful. Therefore, careful selection of optimal tumor-reactive γδT cells, e.g., expanded γδT cells with defined cytokine cocktails (38) or extraction and expression of individual receptors, might be a critical parameter in designing γδTCR-based cancer immunotherapy (27).

Strong evidence that the γδTCR itself is a key for antitumor reactivity and thus can be used for clinical therapeutic concepts is shown in my thesis. Antitumor reactivity of TEG cells expressing a γ9δ2TCR sense joint conformational and spatial changes of target ligands on the surface of tumor cells, which does not occur on healthy cells (35, 39, 40). Introduction of γδTCR into αβT cells do not cause TCR mispairing or promote alloreactivity, which might occur in antigen-specific αβTCR transfer or CAR T cells (24, 41). Hence, this approach allowed studying tumor control efficacy in different models within the TEG concept as described in **Chapters 2** to **5** (39, 42, 43).

However, the major limitation of γδTCR-based therapeutic is the frequently inadequate characterization of specific ligands involved in γδTCR tumor recognition, which obscures the assessment of their efficacy and safety profiles prior to first-in-men studies (27). With the TEG concept, we redirect αβTCR antitumor response using highly tumor-reactive γδTCR and override the requirement of HLA-restriction while retaining the proliferative capacity (24, 41, 44). We also uncoupled innate-like receptors from the tolerance mechanism and mitigated the highly diverse γδTCR repertoire and their functions (27, 45). Using the TEG concept, we could retain both CD4$^+$ and CD8$^+$ effector cell functions while exerting the antitumor reactivity from γδTCR, either from Vδ2$^+$ or Vδ2$^-$ subsets.

Bridging the gap towards first-in-men studies: efficacy-safety balance of TEG001

The main focus of my research was the assessment of therapeutic efficacy and safety of novel cell-based therapy, which is classified as advanced therapy medicinal products (ATMP) consisting of 'living' medicinal products that are heterogeneous and far more complex than other biological products. Due to this characteristic, therapeutic assessment of cell-based therapeutic can frequently not follow the established procedure for conventional drugs. Hence, ATMP products require distinct assessments involving advanced technology transfer from laboratory-grade processes into the implementation of Good Manufacturing Practices (GMP) for production processes (46, 47). Moreover, separate pharmacological and toxicological data are needed considering the desired interaction of the cellular product with surrounding normal tissues and cancer cells (48, 49), as well as pharmacokinetics properties measured by biodistribution of the medicinal product itself, i.e., cell viability, growth, persistence, and migration (50, 51).

Due to these prerequisites, selecting suitable preclinical models to assess the nonclinical efficacy and safety studies is rather challenging, taking into account the dissimilar

6

microenvironment and relevant receptors involved in the reactivity of the cell-based therapeutics (51). Moreover, the activity of cell-based therapy products in animal models may be limited or even absent due to the unrelated immunogenicity due to artificial immune reactivity against human cells, and therefore it has to be carefully considered (52-54).

In this manner, assessment of efficacy-safety balance for TEG001 adds further complexity as a result of its underestimated diversity in functions, receptors, and the nature of its targets, as outlined above. However, despite this complexity, the development of relevant preclinical models remains critical to enhance efficacy and minimize the risk of off- and on-target off-tumor toxicity (55, 56). To assess the efficacy and safety of TEG-based therapies, we developed different models where healthy and tumor cells are sequentially or simultaneously present *in vitro* and *in vivo*. Within this context, we first explored in **Chapter 2** *in vitro* activity of TEG001 against several primary leukemic cell blasts and healthy tissues. Our data showed that induction of cellular stress, either by irradiation or exposure to inflammatory cytokines, and the presence of chemotherapy agents do not induce TEG001 off-target toxicity, even in the presence of monocytes as a physiological target of γ9δ2TCRs. However, the number of healthy tissues to be tested has been limited due to the scarce healthy tissues that can be isolated and tested in the laboratory. Also, the physiological environment does not entirely mimic the bone marrow niche. To overcome this shortcoming, we also simultaneously tested the efficacy and toxicity of TEG001 in a 3D model, which allowed additional stroma of the bone marrow niche. This model also enabled us to assess the effect of TEG001 antitumor activity against autologous stroma and tumor targets as described that seem otherwise impossible to test because of their low numbers, as only limited numbers of immune cells and tumor cells are needed in this autologous system (57). Yet, also 3D models do not mimic the complete hematopoietic niche and all counter-attacks of a tumor.

To partially overcome the limitations of *in vitro* 2D and 3D efficacy and toxicity models, we next moved to an *in vivo* model and explored TEG001 efficacy and toxicity in mice. However, as immunocompetent mice have different γδT cell subsets (58, 59), they are also devoid of the natural ligands CD277 in the context of γ9δ2TCR and TEG001 (27, 40, 60). This created the need to work with immunodeficient NSG mice transplanted with human tumor cells or healthy tissues followed by infusion of TEG cells. I report in **Chapter 2** on the therapeutic efficacy profile of TEG001 towards primary AML blast. We established a patient-derived xenograft (PDX) model by inoculating primary patient materials to better mimic human tumor characteristics and complexity, as well as maintain biological and histological features of the original tumor, including their intra-tumoral and inter-tumoral heterogeneity (61, 62). The major limitations of this model are the limited availability of primary patient materials and poor engraftment rates (63). In addition, donor variation influences the treatment outcome of the PDX tumor due to allogeneic response. Autologous PDX models would have been a more favorable tool to assess the efficacy and safety of immunotherapeutic agents; however, harvesting a sufficient amount of tumor cells and immune cells from one patient remains challeng-

ing, particularly when requiring repetitions for statistics. Despite these restrictions, our PDX model allowed us to confirm a reduction of the leukemic burden by TEG001 in these rather more complex models and served as a positive control for toxicity tests, which were performed in a different set of mice. The toxicity of TEG001 against healthy hematopoietic compartments was explored after engrafting NSG mice with healthy cord-blood derived CD34^{+} hematopoietic stem cells (HD-X). Our data showed that TEG001 treatment does not impair the reconstitution of healthy hematopoietic compartments in the periphery, spleen, and bone marrow, even in the presence of physiological target of γ9δ2TCRs, such as monocytes, which were still detectable *in vivo* after TEG001 treatment. Using humanized mouse models, we are able to perform a detailed evaluation of the therapeutic efficacy of immunotherapy. Nevertheless, careful evaluation for further translation into the clinics remains critical as these models may not fully represent human immune responses as seen in patients.

Bridging the gap towards first-in-men studies: efficacy-safety balance of TEG011

In the next set of chapters, I worked on the further drug development of TEG011. As described in **Chapter 3**, in contrast to classical γδTCR and peptide-MHC recognition for alloreactive αβTCRs, TEG011 recognizes spatial changes and alteration of HLA-A*24:02 clustering on tumor cells irrespective of the specific peptide presented and thus contributing to their broad range reactivity against tumor cells. TEG011 follows an unconventional recognition pattern compared to the previously known tumor antigen recognition via classical HLA molecules (64), whereby it recognizes target cells in an alloreactive-MHC class I-restricted fashion to discriminate healthy and tumor cells. Moreover, the contribution of HLA molecules expressed on tumor cells is mainly studied in relation to tumor escape mechanism from antigen-specific αβTCRs by downregulation or loss of Class I MHC expression (65). The differential HLA clustering on tumor cells in monomeric form suggests the possibility of a tumor escape mechanism from αβT cells, yet still targetable by an alloreactive γδTCR, including the identified FE11 γδTCR. Previous studies have suggested allo-HLA reactivity of γδT cells as a general occurrence and not limited to malignantly-transformed cells (66, 67). However, it is noteworthy to acknowledge that these studies did not investigate the γδTCR reactivity against healthy and tumor cells in detail.

The ability of TEG011 to differentiate healthy and malignant cells by sensing distinct spatial and conformational changes of HLA-A*24:02 molecules pose a very intriguing nature of alloreactive-γδTCR. Nevertheless, due to their mode-of-action, it is rather difficult to assess the safety profile of TEG011 properly. To mitigate this limitation, I evaluated the efficacy-safety balance of TEG011 in tumor-bearing and non-tumor bearing transgenic NSG mice expressing human HLA-A*24:02 (NSG-A24:02) as shown in **Chapter 3**. Despite the advantages of the primary leukemic PDX mouse model as shown for the abovementioned efficacy-safety studies for TEG001, it is rather difficult to obtain primary patient materials with HLA-A*24:02-expressing tumors sufficient for *in vivo* studies due to their infrequent allele occurrence. Hence, I utilized HLA-A*24:02-transduced chronic myeloid leukemia (K562) cell line and developed a cell line-derived xenograft

6

(CDX) model. This model has been well-established, easy to control, and frequently used for efficacy study of therapeutic agents (68). Using cancer cell lines, we can generate tumor models that partially recapitulate the molecular and genetic diversity of cancer cells *in vivo* (69). However, we acknowledge the limitation of this model, in which they do not fully represent the stromal complexity and heterogeneity of human tumors (70). Despite these shortcomings, we observed a significant reduction of tumor progression and prolonged overall survival of tumor-bearing mice treated with TEG011 cells. Separately, we could also evaluate TEG011 toxicity in different tissues more extensively compared to TEG001. As shown in **Chapter 4**, we did not observe any histopathological evidence of toxicity against the investigated healthy tissues. All non-tumor bearing mice did not show decreased in physical fitness throughout the study period, suggesting the absence of autoimmunity or GvHDs development against healthy tissues.

Alongside the aforementioned efficacy and safety evaluations, our mouse models allowed the extensive pharmacokinetics assessment of TEG011 expansion and persistence *in vivo*. As previously described, T cell persistence can be used to measure the pharmacokinetics of cell-based therapy. Furthermore, short-term T cell persistence in patients receiving TCR-engineered therapies has been shown to limit their antitumor activity (71). In **Chapter 2**, I showed that TEG001 persisted in mouse peripheral blood up to 4 weeks after infusion, while in **Chapter 4,** I unexpectedly observed 44% of mice that showed the presence of TEG011 "persister" up to 9 weeks after infusion, which was then associated with the absence of extramedullary solid tumor growth in these mice. The difference between TEG001 and TEG011 persistence is most likely a consequence of the HLA-A*24:02 background when using TEG011, which could have provided tonic signaling, while no binding at all was possible to TEG001 as both BTN2A1 and BTN3A1 are absent in mice (58, 60, 72).

Based on the observation of different TEG persistence *in vivo*, I was interested in investigating which factor(s) influenced the long-term TEG persistence *in vivo*. The presence of both tumor-specific CD4$^+$ and CD8$^+$ αßT cells has been reported to significantly improved clinical responses compared to tumor-specific CD8$^+$ αßT cells alone (73). Therefore, I further investigated the contribution of each αßT cell subset for *in vivo* persistence and antitumor reactivity of TEG011, which selectively redirected CD8$^+$ αßT cells. The introduction of transgenic CD8α co-receptor in TEG011, referred to as TEG011_CD8α, successfully redirected non-reactive CD4$^+$ TEG011 cell *in vitro* and *in vivo* against tumor targets. Interestingly, for the first time, we observed tumor clearance in mouse bone marrow after treatment of TEG011_CD8α, but not TEG011 alone. Also, TEG011_CD8α stably persisted with higher T cell counts consisting of mainly CD4$^+$CD8$^+$ double-positive T cells. This observation supports the notion that simultaneous expression of CD4$^+$ and CD8$^+$ co-receptor provides additional survival for tumor-specific CD4$^+$ T cells. This finding is in line with clinical studies for CAR T cells directed against CD19 have shown that a mixture of both CD4$^+$ and CD8$^+$ T cells with 1:1 ratio facilitated better tumor remission in B-ALL patients that could be due to increasing T cell survival by CD4$^+$ T cells that not only enhanced their own persistence but simultaneously improved CD8$^+$ T cells persistence

(74, 75). Moreover, it has been indicated that CD4^{+} T cells are less prone to exhaustion and AICDs (76-79), leading to robust antitumor capacity than CD8^{+} T cells. While T cell persistence may indicate the biodistribution and longevity of cell-based therapeutics, it is important to acknowledge that the circulating compartment of T cells detected in the periphery neither accurately reflects the presence of T cells at the primary tumor or metastasis sites, nor does it indicates T cell dynamic and tumor trafficking.

CONCLUSION

In conclusion, a careful choice of relevant preclinical models and appropriate study designs are pivotal to assess the efficacy-safety balance to support the successful translation of cell-based immunotherapy into the clinic. Within this context, I bridged the gap from preclinical development of different TEG formats to first-in-men studies. While 2D and 3D models provided some hints for efficacy and lack of toxicity, *in vivo* models are very valuable in studying the impact on the complete human hematopoietic compartment and studying important parameters that impact persistence, even in the absence of the appropriate target molecule. Within the limitation of our preclinical mouse models, we could proficiently assess the efficacy-safety profile of both TEG001 and TEG011 against hematological malignancies and hereby provide sufficient nonclinical evidence prior to first-in-men studies, in which TEG-based therapy may have beneficial effects for cancer patients. As a result, TEG001 is currently tested in a first-in-men study (clinical trial registration NTR6541).

6

REFERENCES

1. Ribas A. Adaptive Immune Resistance: How Cancer Protects from Immune Attack. *Cancer Discov*. 2015; 5(9):915-9.

2. Chandran SS, Klebanoff CA. T cell receptor-based cancer immunotherapy: Emerging efficacy and pathways of resistance. *Immunol Rev*. 2019; 290(1):127-47.

3. Bonini C, Mondino A. Adoptive T-cell therapy for cancer: The era of engineered T cells. *Eur J Immunol*. 2015; 45(9):2457-69.

4. Creelan BC, Wang C, Teer JK, Toloza EM, Yao J, Kim S, *et al*. Tumor-infiltrating lymphocyte treatment for anti-PD-1-resistant metastatic lung cancer: a phase 1 trial. *Nat Med*. 2021; 27(8):1410-8.

5. Van Allen EM, Miao D, Schilling B, Shukla SA, Blank C, Zimmer L, *et al*. Genomic correlates of response to CTLA-4 blockade in metastatic melanoma. *Science*. 2015; 350(6257):207-11.

6. Clay TM, Custer MC, Sachs J, Hwu P, Rosenberg SA, Nishimura MI. Efficient transfer of a tumor antigen-reactive TCR to human peripheral blood lymphocytes confers anti-tumor reactivity. *J Immunol*. 1999; 163(1):507-13.

7. Bendle GM, Linnemann C, Hooijkaas AI, Bies L, de Witte MA, Jorritsma A, *et al*. Lethal graft-versus-host disease in mouse models of T cell receptor gene therapy. *Nat Med*. 2010; 16(5):565-70, 1p following 70.

8. Schmitt TM, Stromnes IM, Chapuis AG, Greenberg PD. New Strategies in Engineering T-cell Receptor Gene-Modified T cells to More Effectively Target Malignancies. *Clin Cancer Res*. 2015; 21(23):5191-7.

9. Arnaud M, Bobisse S, Chiffelle J, Harari A. The Promise of Personalized TCR-Based Cellular Immunotherapy for Cancer Patients. *Front Immunol*. 2021; 12:701636.

10. Chabannon C, Kuball J, McGrath E, Bader P, Dufour C, Lankester A, *et al*. CAR-T cells: the narrow path between hope and bankruptcy? *Bone Marrow Transplant*. 2017; 52(12):1588-9.

11. Lee JB, Chen B, Vasic D, Law AD, Zhang L. Cellular immunotherapy for acute myeloid leukemia: How specific should it be? *Blood Rev*. 2019; 35:18-31.

12. June CH, O'Connor RS, Kawalekar OU, Ghassemi S, Milone MC. CAR T cell immunotherapy for human cancer. *Science*. 2018; 359(6382):1361-5.

13. de Witte MA, Kierkels GJ, Straetemans T, Britten CM, Kuball J. Orchestrating an immune response against cancer with engineered immune cells expressing αßTCRs, CARs, and innate immune receptors: an immunological and regulatory challenge. *Cancer Immunol Immunother*. 2015; 64(7):893-902.

14. Maude SL, Laetsch TW, Buechner J, Rives S, Boyer M, Bittencourt H, *et al*. Tisagenlecleucel in Children and Young Adults with B-Cell Lymphoblastic Leukemia. *N Engl J Med*. 2018; 378(5):439-48.

15. Schuster SJ, Bishop MR, Tam CS, Waller EK, Borchmann P, McGuirk JP, *et al*. Tisagenlecleucel in Adult Relapsed or Refractory Diffuse Large B-Cell Lymphoma. *N Engl J Med*. 2019; 380(1):45-56.

16. D'Aloia MM, Zizzari IG, Sacchetti B, Pierelli L, Alimandi M. CAR-T cells: the long and winding road to solid tumors. *Cell Death Dis*. 2018; 9(3):282.

17. Abken H. Adoptive therapy with CAR redirected T cells: the challenges in targeting solid tumors. *Immunotherapy*. 2015; 7(5):535-44.

18. Eisenberg V, Hoogi S, Shamul A, Barliya T, Cohen CJ. T-cells "a la CAR-T(e)" - Genetically engineering T-cell response against cancer. *Adv Drug Deliv Rev*. 2019; 141:23-40.

19. Castellarin M, Sands C, Da T, Scholler J, Graham K, Buza E, *et al*. A rational mouse model to detect on-target, off-tumor CAR T cell toxicity. *JCI Insight*. 2020; 5(14).

20. Debets R, Donnadieu E, Chouaib S, Coukos G. TCR-engineered T cells to treat tumors: Seeing but not touching? *Semin Immunol*. 2016; 28(1):10-21.

21. Gentles AJ, Newman AM, Liu CL, Bratman SV, Feng W, Kim D, *et al*. The prognostic landscape of genes and infiltrating immune cells across human cancers. *Nat Med*. 2015; 21(8):938-45.

22. Melandri D, Zlatareva I, Chaleil RAG, Dart RJ, Chancellor A, Nussbaumer O, *et al*. The γδTCR combines innate immunity with adaptive immunity by utilizing spatially distinct regions for agonist selection and antigen responsiveness. *Nat Immunol*. 2018; 19(12):1352-65.

23. Muro R, Takayanagi H, Nitta T. T cell receptor signaling for γδT cell development. *Inflamm Regen*. 2019; 39:6.

24. Grunder C, van Dorp S, Hol S, Drent E, Straetemans T, Heijhuurs S, *et al*. γ9 and δ2CDR3 domains regulate functional avidity of T cells harboring γ9δ2TCRs. *Blood*. 2012; 120(26):5153-62.

25. Janssen A, Villacorta Hidalgo J, Beringer DX, van Dooremalen S, Fernando F, van Diest E, *et al*. γδT-cell Receptors Derived from Breast Cancer-Infiltrating T Lymphocytes Mediate Antitumor Reactivity. *Cancer Immunol Res*. 2020; 8(4):530-43.

26. Wu Y, Kyle-Cezar F, Woolf RT, Naceur-Lombardelli C, Owen J, Biswas D, *et al*. An innate-like Vdelta1^{+} γδT cell compartment in the human breast is associated with remission in triple-negative breast cancer. *Sci Transl Med*. 2019; 11(513).

27. Sebestyen Z, Prinz I, Dechanet-Merville J, Silva-Santos B, Kuball J. Translating gammadelta (γδ) T cells and their receptors into cancer cell therapies. *Nat Rev Drug Discov*. 2020; 19(3):169-84.

28. Kunzmann V, Bauer E, Feurle J, Weissinger F, Tony HP, Wilhelm M. Stimulation of γδT cells by aminobisphosphonates and induction of antiplasma cell activity in multiple myeloma. *Blood*. 2000; 96(2):384-92.

29. Nicol AJ, Tokuyama H, Mattarollo SR, Hagi T, Suzuki K, Yokokawa K, *et al*. Clinical evaluation of autologous γδT cell-based immunotherapy for metastatic solid tumours. *Br J Cancer*. 2011; 105(6):778-86.

30. Kobayashi H, Tanaka Y, Yagi J, Minato N, Tanabe K. Phase I/II study of adoptive transfer of γδT cells in combination with zoledronic acid and IL-2 to patients with advanced renal cell carcinoma. *Cancer Immunol Immunother*. 2011; 60(8):1075-84.

31. Sakamoto M, Nakajima J, Murakawa T, Fukami T, Yoshida Y, Murayama T, *et al*. Adoptive immunotherapy for advanced non-small cell lung cancer using zoledronate-expanded γδTcells: a phase I clinical study. *Journal of immunotherapy*. 2011; 34(2):202-11.

32. Dieli F, Vermijlen D, Fulfaro F, Caccamo N, Meraviglia S, Cicero G, *et al*. Targeting human γδT cells with zoledronate and interleukin-2 for immunotherapy of hormone-refractory prostate cancer. *Cancer Res*. 2007; 67(15):7450-7.

33. Meraviglia S, Eberl M, Vermijlen D, Todaro M, Buccheri S, Cicero G, *et al*. *In vivo* manipulation of Vγ9Vδ2 T cells with zoledronate and low-dose interleukin-2 for immunotherapy of advanced breast cancer patients. *Clin Exp Immunol*. 2010; 161(2):290-7.

34. Bennouna J, Levy V, Sicard H, Senellart H, Audrain M, Hiret S, *et al*. Phase I study of bromohydrin pyrophosphate (BrHPP, IPH 1101), a Vγ9Vδ2 T lymphocyte agonist in patients with solid tumors. *Cancer Immunol Immunother*. 2010; 59(10):1521-30.

35. Vyborova A, Beringer DX, Fasci D, Karaiskaki F, van Diest E, Kramer L, *et al*. γ9δ2T cell diversity and the receptor interface with tumor cells. *J Clin Invest*. 2020; 130(9):4637-51.

36. Payne KK, Mine JA, Biswas S, Chaurio RA, Perales-Puchalt A, Anadon CM, *et al*. BTN3A1 governs antitumor responses by coordinating αß and γδT cells. *Science*. 2020; 369(6506):942-9.

37. Godder KT, Henslee-Downey PJ, Mehta J, Park BS, Chiang KY, Abhyankar S, *et al*. Long term disease-free survival in acute leukemia patients recovering with increased γδT cells after partially mismatched related donor bone marrow transplantation. *Bone Marrow Transplant*. 2007; 39(12):751-7.

6

38. Almeida AR, Correia DV, Fernandes-Platzgummer A, da Silva CL, da Silva MG, Anjos DR, *et al*. Delta One T Cells for Immunotherapy of Chronic Lymphocytic Leukemia: Clinical-Grade Expansion/Differentiation and Preclinical Proof of Concept. *Clin Cancer Res*. 2016; 22(23):5795-804.

39. Kierkels GJJ, Scheper W, Meringa AD, Johanna I, Beringer DX, Janssen A, *et al*. Identification of a tumor-specific allo-HLA-restricted γδTCR. *Blood Adv*. 2019; 3(19):2870-82.

40. Sebestyen Z, Scheper W, Vyborova A, Gu S, Rychnavska Z, Schiffler M, *et al*. RhoB Mediates Phosphoantigen Recognition by Vγ9Vδ2 T Cell Receptor. *Cell Rep*. 2016; 15(9):1973-85.

41. Marcu-Malina V, Heijhuurs S, van Buuren M, Hartkamp L, Strand S, Sebestyen Z, *et al*. Redirecting αßT cells against cancer cells by transfer of a broadly tumor-reactive γδT-cell receptor. *Blood*. 2011; 118(1):50-9.

42. Johanna I, Straetemans T, Heijhuurs S, Aarts-Riemens T, Norell H, Bongiovanni L, *et al*. Evaluating *in vivo* efficacy - toxicity profile of TEG001 in humanized mice xenografts against primary human AML disease and healthy hematopoietic cells. *J Immunother Cancer*. 2019; 7(1):69.

43. Johanna I, Hernandez-Lopez P, Heijhuurs S, Bongiovanni L, de Bruin A, Beringer D, *et al*. TEG011 persistence averts extramedullary tumor growth without exerting off-target toxicity against healthy tissues in a humanized HLA-A*24:02 transgenic mice. *J Leukoc Biol*. 2020; 107(6):1069-79.

44. Straetemans T, Grunder C, Heijhuurs S, Hol S, Slaper-Cortenbach I, Bonig H, *et al*. Untouched GMP-Ready Purified Engineered Immune Cells to Treat Cancer. *Clin Cancer Res*. 2015; 21(17): 3957-68.

45. Scheper W, Grunder C, Straetemans T, Sebestyen Z, Kuball J. Hunting for clinical translation with innate-like immune cells and their receptors. *Leukemia*. 2014; 28(6):1181-90.

46. de Wilde S, Veltrop-Duits L, Hoozemans-Strik M, Ras T, Blom-Veenman J, Guchelaar HJ, *et al*. Hurdles in clinical implementation of academic advanced therapy medicinal products: A national evaluation. *Cytotherapy*. 2016; 18(6):797-805.

47. Coppens DGM, De Bruin ML, Leufkens HGM, Hoekman J. Global Regulatory Differences for Gene- and Cell-Based Therapies: Consequences and Implications for Patient Access and Therapeutic Innovation. *Clin Pharmacol Ther*. 2018; 103(1):120-7.

48. Johnson LA, Morgan RA, Dudley ME, Cassard L, Yang JC, Hughes MS, *et al*. Gene therapy with human and mouse T-cell receptors mediates cancer regression and targets normal tissues expressing cognate antigen. *Blood*. 2009; 114(3):535-46.

49. Abou-El-Enein M, Romhild A, Kaiser D, Beier C, Bauer G, Volk HD, *et al*. Good Manufacturing Practices (GMP) manufacturing of advanced therapy medicinal products: a novel tailored model for optimizing performance and estimating costs. *Cytotherapy*. 2013; 15(3):362-83.

50. Committee for Advanced T, Secretariat CATS, Schneider CK, Salmikangas P, Jilma B, Flamion B, *et al*. Challenges with advanced therapy medicinal products and how to meet them. *Nat Rev Drug Discov*. 2010; 9(3):195-201.

51. Silva Lima B, Videira MA. Toxicology and Biodistribution: The Clinical Value of Animal Biodistribution Studies. *Mol Ther Methods Clin Dev*. 2018; 8:183-97.

52. Kochenderfer JN, Yu Z, Frasheri D, Restifo NP, Rosenberg SA. Adoptive transfer of syngeneic T cells transduced with a chimeric antigen receptor that recognizes murine CD19 can eradicate lymphoma and normal B cells. *Blood*. 2010; 116(19):3875-86.

53. Alcantar-Orozco EM, Gornall H, Baldan V, Hawkins RE, Gilham DE. Potential limitations of the NSG humanized mouse as a model system to optimize engineered human T cell therapy for cancer. *Hum Gene Ther Methods*. 2013; 24(5):310-20.

54. Gattinoni L, Klebanoff CA, Palmer DC, Wrzesinski C, Kerstann K, Yu Z, *et al*. Acquisition of full effector function *in vitro* paradoxically impairs the *in vivo* antitumor efficacy of adoptively transferred CD8^{+} T cells. *J Clin Invest*. 2005; 115(6):1616-26.

55. Neelapu SS, Tummala S, Kebriaei P, Wierda W, Gutierrez C, Locke FL, *et al*. Chimeric antigen receptor T-cell therapy - assessment and management of toxicities. *Nat Rev Clin Oncol*. 2018; 15(1):47-62.

56. Linette GP, Stadtmauer EA, Maus MV, Rapoport AP, Levine BL, Emery L, *et al*. Cardiovascular toxicity and titin cross-reactivity of affinity-enhanced T cells in myeloma and melanoma. *Blood*. 2013; 122(6):863-71.

57. Braham MVJ, Minnema MC, Aarts T, Sebestyen Z, Straetemans T, Vyborova A, *et al*. Cellular immunotherapy on primary multiple myeloma expanded in a 3D bone marrow niche model. *Oncoimmunology*. 2018; 7(6):e1434465.

58. Blazquez JL, Benyamine A, Pasero C, Olive D. New Insights Into the Regulation of γδT Cells by BTN3A and Other BTN/BTNL in Tumor Immunity. *Front Immunol*. 2018; 9:1601.

59. Raverdeau M, Cunningham SP, Harmon C, Lynch L. γδT cells in cancer: a small population of lymphocytes with big implications. *Clin Transl Immunology*. 2019; 8(10):e01080.

60. Harly C, Guillaume Y, Nedellec S, Peigne CM, Monkkonen H, Monkkonen J, *et al*. Key implication of CD277/butyrophilin-3 (BTN3A) in cellular stress sensing by a major human γδT-cell subset. *Blood*. 2012; 120(11):2269-79.

61. Izumchenko E, Paz K, Ciznadija D, Sloma I, Katz A, Vasquez-Dunddel D, *et al*. Patient-derived xenografts effectively capture responses to oncology therapy in a heterogeneous cohort of patients with solid tumors. *Ann Oncol*. 2017; 28(10):2595-605.

62. Byrne AT, Alferez DG, Amant F, Annibali D, Arribas J, Biankin AV, *et al*. Interrogating open issues in cancer precision medicine with patient-derived xenografts. *Nat Rev Cancer*. 2017; 17(4):254-68.

63. Bareham B, Georgakopoulos N, Matas-Cespedes A, Curran M, Saeb-Parsy K. Modeling human tumor-immune environments *in vivo* for the preclinical assessment of immunotherapies. *Cancer Immunol Immunother*. 2021.

64. Benveniste PM, Roy S, Nakatsugawa M, Chen ELY, Nguyen L, Millar DG, *et al*. Generation and molecular recognition of melanoma-associated antigen-specific human γδT cells. *Sci Immunol*. 2018; 3(30).

65. Seliger B, Cabrera T, Garrido F, Ferrone S. HLA class I antigen abnormalities and immune escape by malignant cells. *Semin Cancer Biol*. 2002; 12(1):3-13.

66. Ciccone E, Viale O, Pende D, Malnati M, Battista Ferrara G, Barocci S, *et al*. Specificity of human T lymphocytes expressing a gamma/delta T cell antigen receptor. Recognition of a polymorphic determinant of HLA class I molecules by a γδ clone. *Eur J Immunol*. 1989; 19(7):1267-71.

67. Spits H, Paliard X, Engelhard VH, de Vries JE. Cytotoxic activity and lymphokine production of T cell receptor (TCR)-αβ+ and TCR-γδ+ cytotoxic T lymphocyte (CTL) clones recognizing HLA-A2 and HLA-A2 mutants. Recognition of TCR-γδ+ CTL clones is affected by mutations at positions 152 and 156. *J Immunol*. 1990; 144(11):4156-62.

68. Saito R, Kobayashi T, Kashima S, Matsumoto K, Ogawa O. Faithful preclinical mouse models for better translation to bedside in the field of immuno-oncology. *Int J Clin Oncol*. 2020; 25(5):831-41.

69. Frese KK, Tuveson DA. Maximizing mouse cancer models. *Nat Rev Cancer*. 2007;7(9):645-58.

70. Sulaiman A, Wang L. Bridging the divide: preclinical research discrepancies between triple-negative breast cancer cell lines and patient tumors. *Oncotarget*. 2017; 8(68):113269-81.

71. Govers C, Sebestyen Z, Roszik J, van Brakel M, Berrevoets C, Szoor A, *et al*. TCRs genetically linked to CD28 and CD3ε do not mispair with endogenous TCR chains and mediate enhanced T cell persistence and anti-melanoma activity. *J Immunol*. 2014; 193(10):5315-26.

72. Karunakaran MM, Gobel TW, Starick L, Walter L, Herrmann T. Vγ9 and Vδ2 T cell antigen receptor genes and butyrophilin 3 (BTN3) emerged with placental mammals and are concomitantly preserved in selected species like alpaca (*Vicugna pacos*). *Immunogenetics*. 2014; 66(4):243-54.

6

73. Rosenberg SA, Dudley ME. Cancer regression in patients with metastatic melanoma after the transfer of autologous antitumor lymphocytes. *Proc Natl Acad Sci U S A*. 2004; 101 Suppl 2:14639-45.

74. Turtle CJ, Hanafi LA, Berger C, Gooley TA, Cherian S, Hudecek M, *et al*. CD19 CAR-T cells of defined CD4^{+}:CD8^{+} composition in adult B cell ALL patients. *J Clin Invest*. 2016; 126(6):2123-38.

75. Guedan S, Posey AD, Jr., Shaw C, Wing A, Da T, Patel PR, *et al*. Enhancing CAR T cell persistence through ICOS and 4-1BB costimulation. *JCI Insight*. 2018; 3(1).

76. Wang D, Aguilar B, Starr R, Alizadeh D, Brito A, Sarkissian A, *et al*. Glioblastoma-targeted CD4^{+} CAR T cells mediate superior antitumor activity. *JCI Insight*. 2018; 3(10).

77. Adusumilli PS, Cherkassky L, Villena-Vargas J, Colovos C, Servais E, Plotkin J, *et al*. Regional delivery of mesothelin-targeted CAR T cell therapy generates potent and long-lasting CD4-dependent tumor immunity. *Sci Transl Med*. 2014; 6(261):261ra151.

78. Liadi I, Singh H, Romain G, Rey-Villamizar N, Merouane A, Adolacion JR, *et al*. Individual Motile CD4^{+} T Cells Can Participate in Efficient Multikilling through Conjugation to Multiple Tumor Cells. *Cancer Immunol Res*. 2015; 3(5):473-82.

79. Agarwal S, Hanauer JDS, Frank AM, Riechert V, Thalheimer FB, Buchholz CJ. *In vivo* Generation of CAR T Cells Selectively in Human CD4^{+} Lymphocytes. *Mol Ther*. 2020; 28(8):1783-94.

APPENDICES

SUMMARY

Conventional treatment options for cancer, including surgery, chemotherapy, radiotherapy, and targeted therapy, can successfully eliminate cancer cells. To date, there are still significant relapses in cancer patients after these treatments. In addition, there are still substantial unwanted side effects that cause damage to the healthy tissues and reduce the quality of life over many years, even after the treatment has been completed. Thus, other treatment alternatives are needed. To overcome these limitations, cancer immunotherapy has been explored as one of the therapeutic options against different malignancies and implemented, due to its efficacy in safety profile into many daily treatment concepts. This strategy was based on the observation that the human immune system protects not only from infection but also has been shown to recognize and target malignantly transformed cells and prevent further developments of cancer cells.

Chapter 1 provides an overview on how cancer immunotherapy aims to stimulate antitumor response without harming healthy tissues by using the patients' own immune system to eliminate cancer cells. Furthermore, we elaborate on different immunotherapy options and focus on differences between conventional αßT cells and unconventional γδT cells. We emphasize that αßT cells recognize specific tumor peptides represented on Human Leukocytes Antigens (HLA) molecules and eventually eliminate the tumor cells. On the other hand, γδT cells express γδ T cell receptor (TCR) on the cell surface and recognize infected and tumor cells by sensing metabolic changes in these cells without the need of specific peptide representation on HLA molecules, making them applicable for a broader patient population compared to αßT cells. Our research group specifically interested in γδT cells for their ability to target cancer cells and without harming healthy cells, and thus focusing on the development of a new cancer immunotherapy approach based on potent antitumor reactivity of γδT cells. Furthermore, in this chapter we introduce alternative treatment concepts based on the observation that despite their promising potential, clinical responses of adoptive transfer of *ex vivo* expanded unmodified γδT cells are relatively marginal. We propose to focus on new insights into γδT cell biology which uncovered the underestimated diversity in T cell functions and molecular activation modes. Considering these obstacles, we introduce the concept of TEGs: αßT cells engineered to express a defined γδTCR, where highly-tumor reactive γδTCR is introduced into αßT cell with superior proliferative capacity in cancer patients. Careful considerations of the efficacy-safety balance of cell-based therapeutic modalities against cancer are critical prior to clinical implementation. Hence, this thesis mainly focuses on evaluating the efficacy-safety balance of our TEG-based cellular therapy in preclinical mouse models.

In **Chapter 2**, the efficacy-safety balance of TEG001 were evaluated against primary tumor tissues and primary healthy cells, respectively. TEG001 has been selected as the first clinical candidate of TEG-based therapy based on its ability to target a broad range of hematological malignancies *in vitro* and has previously shown *in vivo* to control tumor growth in mouse model injected with tumor cell lines. Here, I assessed for the first

time the efficacy of TEG001 treatment in clinically relevant model of leukemic mouse model that injected with primary AML blast derived from a patient. In parallel, I also assessed the safety of TEG001 treatment by injecting mice with cord blood-derived stem cells that reconstituted into complete healthy hematological cell subsets. In this way, I studied the effect of TEG001 treatment for any potential toxicity against these healthy cells. Overall, we showed that TEG001 effectively suppress the growth of primary AML blast without any indicative side effects against healthy cells *in vivo*. Thus, within the limitation of the current models, there are no data indicating increased safety risk for TEG001.

Chapter 3 focuses on the identification of the ligand for tumor-specific γδTCR that have been identified previously. Unlike αβT cells, γδT cells do not require antigen presentation via Human Leukocytes Antigen (HLA) molecules on the infected or ma-lignantly-transformed cells. Here, we attempt to identify specific ligand for this FE11 γδTCR and its recognition mechanism against tumor cells. We identified HLA-A*24:02 molecule as ligand of tumor-specific FE11 γδTCR. We also uncovered the mode-of-action of this particular γδTCR that recognizes alteration in HLA-A*24:02 clustering on the cell surface of tumor cells, independent of a specific tumor peptide. When introduced into TEG format, subsequently named as TEG011, the antitumor reactivity of FE11 γδTCR was retained and thus able to differentiate healthy and malignant cells expressing HLA-A*24:02 molecules. I specifically focused on the assessment of therapeutic efficacy of TEG011 in humanized transgenic NSG mouse model expressing human HLA-A*24:02 molecules. I reported an improved overall survival of tumor-bearing mice treated with TEG011. Since TEG011 is able to target many different HLA-A*24:02-expressing tumor cells, it is attractive to eventually use this γδTCR as immunotherapy. The sequence of FE11 and its potential applications have been patented by our group.

Chapter 4 describes further the efficacy-safety balance of TEG011 assessed in tu-mor-bearing and non-tumor bearing NSG-A24:02 mice. I showed that TEG011 treat-ment does not associate with any discomfort nor any clear evidence of toxicity in HLA-A*24:02-expressing non-tumor healthy tissues. I reported that no relevant graft-versus-host disease (GvHD) manifestation in all mice and no signs of toxicity in the major organs of all healthy tissues upon TEG011 treatment. The pharmacokinetics properties of cell-based therapy can be determined by *in vivo* T cell expansion and persistence in the cancer patients. I also reported long-term persistence of TEG011 in approximately 44% of the TEG011-treated mice, which were associated with the absence of solid tumor growth outside of the bone marrow, emphasizing the crucial aspect of T cell persistence to sustain long-term efficacy.

In **Chapter 5**, I extended the biological mechanism of TEG011 that is CD8α-dependent and investigated further their functions as coreceptor for FE11 γδTCR. Introduction of transgenic CD8α receptor on TEG011 cells is considered an additional strategy to further enhance T cell persistence and long-term tumor control. The new construct design is subsequently referred to as TEG011_CD8α. I showed that non-reactive CD4^{+}

TEG011 cells can be redirected to target HLA-A*24:02-expressing tumor targets after genetic introduction of human CD8α gene. In transgenic NSG-A24:02 mice engrafted with HLA-A*24:02-expressing tumor cells, TEG011_CD8α treatment showed stable peripheral persistence with higher T cell counts in comparison with TEG011 cells alone. Moreover, I showed that TEG011 equipped with human CD8α co-receptor elicits better tumor control, promotes long-term T cell persistence and associated with better T cell infiltration. In addition, I observed for the first time that TEG011_CD8α treatment successfully cleared tumor cells in bone marrow and thus further highlight its potential clinical application.

In the last chapter, **Chapter 6**, earlier findings in the afore-mentioned chapters were put in broader perspective of preclinical model development within the context of TEG-based therapy and in relation to current literatures.

NEDERLANDSE SAMENVATTING

Conventionele behandelingen voor kanker zoals operatie, chemotherapie, radiotherapie en doelgerichte therapie kunnen kankercellen succesvol opruimen. Helaas keert de ziekte na deze behandelingen tot op heden nog steeds bij een aanzienlijk deel van de kankerpatiënten terug. Daarnaast treden er vaak ook ongewenste bijwerkingen op die schade toebrengen aan gezonde weefsels en de kwaliteit van leven gedurende vele jaren verminderen, zelfs nadat de behandeling is beëindigd. Er zijn dus nog andere behandelopties nodig.

Immunotherapie is onderzocht als een van de verbeterde therapeutische opties tegen verschillende soorten kanker. Tegenwoordig is het al geïmplementeerd in vele dagelijkse behandelplannen vanwege zijn werkzaamheid en veiligheid. Immunotherapie is gebaseerd op het vermogen van het immuunsysteem van de mens om niet alleen te beschermen tegen infecties maar ook om kwaadaardige cellen in een vroeg stadium te herkennen en op te ruimen en zo de verdere ontwikkeling van kanker te voorkomen.

Hoofdstuk 1 geeft een overzicht over hoe immunotherapie het eigen immuunsysteem van een patiënt tracht te stimuleren om kanker te bestrijden, zonder gezonde weefsels te beschadigen. Verder gaan we dieper in op verschillende vormen van immunotherapie en we richten ons op de verschillen tussen conventionele αβT cellen en de onconventionele γδT cellen. We benadrukken dat αβT cellen specifieke tumor eiwitten herkennen die gepresenteerd worden door zogenaamde Humane Leukocyten Antigenen (HLA) moleculen, waarna de αβT cel de tumorcellen zal opruimen. Anders dan αβT cellen, brengen γδT cellen een γδT cel receptor (TCR) tot expressie, waarmee ze subtiele veranderingen herkennen in het metabolisme van tumorcellen, die vaak vroeg in de transformatie van een gezonde- naar een tumorcel ontstaan. Deze herkenning is onafhankelijk van de expressie van specifieke HLA moleculen, waardoor γδT cellen geschikt zijn voor een bredere patiëntenpopulatie dan αβT cellen. Onze onderzoeksgroep is voornamelijk geïnteresseerd in γδT cellen om hun unieke vermogen om tumorcellen te kunnen onderscheiden van gezonde cellen, en concentreert zich daarom op de ontwikkeling van immunotherapie tegen kanker gebaseerd op de antitumor activiteit van γδT cellen. Helaas is de klinische effectiviteit van kankertherapieën waarbij ex vivo geëxpandeerde en ongemodificeerde γδT cellen worden gebruikt tot nu toe gering gebleken. Om dit te verbeteren, introduceren we in dit hoofdstuk andere mogelijke behandelconcepten gebaseerd op γδT cellen. We richten ons op nieuwe inzichten in de biologie van γδT cellen die de onderschatte diversiteit in T cel functies, en moleculaire activeringsmodi onthullen. Onze groep heeft het concept van genetisch gemodificeerde cellen ontwikkeld, ook wel TEGs genoemd. Deze afkorting staat voor het Engelse "αβT cells engineered to express a defined γδTCR", waarbij een geselecteerde hoge affiniteit tumor reactieve γδTCR geïntroduceerd wordt in een αβT cel die een hoge groeisnelheid heeft in kankerpatiënten. Een zorgvuldige overweging van de balans tussen werkzaamheid en veiligheid van cellulaire therapieën tegen kanker is van cruciaal belang voorafgaand aan de klinische implementatie. Daarom richt dit proefschrift zich met name op de

evaluatie van de balans tussen werkzaamheid en veiligheid van onze TEG-therapie in preklinische muismodellen.

In **hoofdstuk 2** bespreken we de balans tussen werkzaamheid en veiligheid van TEG001 tegen primaire tumorweefsels en primaire gezonde hematologische cellen. TEG001 is geselecteerd als eerste klinische kandidaat van TEG-therapie vanwege zijn hoge reactiviteit tegen verschillende hematologische tumoren in vitro en verminderde tumorgroei in muizen geïnjecteerd met tumor cellijnen. In dit hoofdstuk laat ik voor de eerste keer de therapeutische werkzaamheid van TEG001 zien, getest in een klinisch relevant leukemisch muismodel, waarbij de uitgroei van leukemische cellen van een patiënt in de muizen wordt gevolgd na behandeling met TEG001- of mock cellen. Tegelijkertijd heb ik ook de veiligheid van TEG001 behandeling beoordeeld door muizen te injecteren met stamcellen uit navelstrengbloed waaruit vervolgens de volledige gezonde hematologische cel subsets uitgroeiden. Op deze manier heb ik de mogelijke toxiciteit van TEG001 tegen deze gezonde cellen onderzocht. Kortom, we hebben laten zien dat TEG001 de groei van primaire AML blasten effectief inhibeert, zonder enige aanwijzing van bijwerkingen tegen gezonde cellen in vivo. Dus, ondanks de beperking van de huidige muismodellen, zijn er geen data die wijzen op een verhoogd veiligheidsrisico door TEG001.

Hoofdstuk 3 beschrijft de zoektocht naar het ligand van een van de tumor-specifieke γδTCRs die we eerder hebben geïdentificeerd. In tegenstelling tot αßT cellen, zijn γδT cellen niet afhankelijk van de expressie van specifieke HLA moleculen voor herkenning en activatie. In dit hoofdstuk hebben we echter wel een HLA-A*24:02 molecuul geïdentificeerd als ligand van de tumor-specifieke FE11 γδTCR. We laten zien dat deze FE11 γδTCR een verandering in de clustering van het HLA-A*24:02 molecuul op kwaadaardige cellen herkent, onafhankelijk van de presentatie van specifiek peptide. Als TEG, in het vervolg TEG011 genoemd, bleef de antitumor reactiviteit van FE11 γδTCR behouden. TEG011 is dus in staat gezonde en kwaadaardige cellen van elkaar te onderscheiden op basis van de clustering van HLA-A*24:02. Ik heb mij specifiek gericht op de beoordeling van de therapeutische werkzaamheid van TEG011 in een gehumaniseerd transgeen NSG muismodel dat HLA-A*24:02 (NSG-A24:02) tot expressie brengt, waarbij we een verlenging van de levensduur hebben aangetoond voor muizen met tumor die behandeld werden met TEG011. Aangezien TEG011 in staat is om veel verschillende tumoren die HLA-A*24:02 tot expressie brengen te herkennen, is het een veelbelovende kandidaat om uiteindelijk als immunotherapie te gebruiken. De sequentie van FE11 en de mogelijke toepassingen zijn door onze groep gepatenteerd.

Hoofdstuk 4 beschrijft de balans tussen werkzaamheid en veiligheid van TEG011, onderzocht in NSG-A24:02 muizen die al dan niet geïnjecteerd werden met HLA-A*24:02+ tumorcellen. Ik heb laten zien dat TEG011 behandeling niet gepaard gaat met enig ongerief voor de muizen, en ik vond geen bewijs van toxiciteit in gezonde weefsels die HLA-A*24:02 tot expressie brengen. Na TEG011 behandeling zag ik in geen enkele muis tekenen van graft-vs-host ziekte (GvHD), en ook geen toxiciteit in weefsels van de belangrijke organen. Verder rapporteer ik langdurige persistentie van TEG011 in 44% van

de met TEG011 behandelde muizen, wat geassocieerd is met de afwezigheid van groei van solide tumoren buiten het beenmerg. Dit benadrukt dat T cel persistentie belangrijk is voor langdurige werkzaamheid van de therapie.

In **Hoofdstuk 5** heb ik mij verder verdiept in het biologische activerings mechanisme van TEG011, specifiek in de rol die CD8α speelt als co-receptor voor de FE11 γδTCR. De introductie van de CD8α receptor op TEG011 cellen kan leiden tot verbeterde T cel persistentie en tumorcontrole. Het nieuwe construct wordt in het vervolg TEG011_CD8a genoemd. Ik laat zien dat niet-reactieve CD4+ TEG011 cellen na genetische introductie van het humane CD8α-gen, tumorcellen die HLA-A*24:02 tot expressie brengen kunnen herkennen. In transgene NSG-A24:02 muizen met een HLA-A*24:02⁺ tumor zag ik na be-handeling met TEG011_CD8α, een stabiele perifere persistentie van T cellen, met hogere cel aantallen in vergelijking tot TEG011. Verder heb ik aangetoond dat TEG011_CD8α zorgt voor een betere tumorcontrole, de T cel persistentie voor lange tijd bevordert, en zorgt voor een betere T cel infiltratie. Daarnaast heb ik voor de eerste keer gezien dat behandeling met TEG011_CD8α succesvol tumorcellen opruimt in het beenmerg. Dit benadrukt de potentiële klinische toepassing van deze behandeling.

In het laatste hoofdstuk, **Hoofdstuk 6**, worden de hierboven beschreven resultaten in een breder perspectief geplaatst en vergeleken met de resultaten die momenteel in de literatuur bekend zijn.

ACKNOWLEDGMENTS

This thesis would not be possible without the input and support of various people who cheering and accompany my PhD journey in the last years. I would like to thank every single one of you immensely for this!

My promoter Prof. dr. Jürgen Kuball, dear **Jürgen**, I always amaze how do you divide your time to still invest on research of the group, seeing patients, and family time. You are super busy and yet super approachable whenever I need to discuss something. Thank you for all your input in my projects and for being my debate partners during meetings. And I was proud for a moment I can be 20% exception of student to be right against your approach! Most of all, thank you for all your support during my difficult time and understanding with my situations. If I ever decide to pursue my career in academia, you are definitely my role model as a great mentor. I hope we will have the opportunity to work together again in the future and I wish all the best with everything you do.

My co-promoter Dr. Zsolt Sebestyén, dear **Zsolt**, there are so many things I could say about you, a paragraph may not be enough! From the first meeting, I already feel that you're very nice and helpful. Over time, I got to learn that you're very easy-going and social. I enjoyed so much all our discussion, both scientific and all about random stuffs. Thank you for your patience to entertain all my hard-headedness and listened to all my rambling and frustrations in the past 5 years. I will always give you food recommendations, anytime. And please stop with the rumor about me as model! I hope we could keep in contact and probably work together again in future. Till then, I wish you all the best including to make a reservation at Sea Palace, Amsterdam! ;)

Dear **Trudy**, thanks for all your input for all the experiments and also to train me with mice work at the beginning. Although sometimes we didn't really see eye-to-eye, I enjoyed working together with you and all the discussions we had. I wish you all the best for the upcoming projects!

Dear **Sabine**, I am happy to say that we work together very well from the beginning. We started the mice team with only two of us, until finally Patricia joined us. I could not ask for a more solid team to work together! I love all our chitchat and coffee time. We went through all kinds of difficulty together and yet we still worked it out! Also I love all our rambling time together, knowing I am not crazy alone :P Thanks for all your help during my PhD, translating all my documents to Dutch when needed and always give a good input. And of course, to be my paranymph and helping me with all the defense stuffs. I really enjoyed working together and hope to keep in contact!

Dear **Patricia**, who made our mice team complete! I had such great time working and being stress together with you ;P We went through working only the 2 of us when COVID lockdown first happened and still got out of it without killing each other! It's a good sign! ;) Thanks for all your help with the experiments, especially when you came over

the weekend to take care of my mice. I also enjoy all our hangouts outside of work and glad I have a friend in not liking beer too much. And of course, thanks a lot to help me as paranymph. I hope the rest of your PhD time will go smooth!

All other (past and present) Kuball group members: **Sanne** thanks for your help with Illustrator for my paper. **Guido**, meeting with Jurgen and you is never a dull one! **Marleen**, thanks for all the help at the beginning at my PhD and to keep the friendship outside of work, I enjoy all our hangout times! **Febi** and **Alberto**, thank you for all your help with all my statistical questions. **Koen** and **Ruud**, who never fails to greet me any time and thanks for all the fun coffee times. **Lovro**, though we didn't really work together for a project, I enjoyed the time you were in the group and always nice to hang out with. Hopefully one day I can come to Slovenia and we can have a short catchup! **Anna**, although you are quite busy but I enjoyed all our corridor conversation to just update each other about work and life in general. All the best for the training to be hematologist, I am sure you will be a great one!

Anke, thank you for the help with my first paper and I enjoyed our time in Keystone together. All the best with your time in the clinic and also finishing the thesis and of course enjoy the motherhood!

Esther, really nice to have you in a group for a short period, and I enjoyed our short meetup again in Madrid and Utrecht. My student **Willemijn**, thank you for your contribution to my project. I had a great time being your supervisor, from all the discussion about the project and all other fun borrel we had. Wish you all the best for the future! **Domenico**, I enjoyed the time when you're part of the group. All your snappy, funny stories and comments when we were both busy in ML-2. I wish all the best with the current job and hopefully our path cross again in the future. **Luuk**, too bad I only found out you are also wine person during your farewell picnic! I will give you a nudge when I'm in Nijmegen for a wine time ;) Thanks for all the help with FACS phenotype panel and hope you enjoy the new job! **Annet**, nice to have you in the group and all the best for you! **Moniek**, although we don't really interact much, I appreciate your input to my projects and also enjoyed our conversations during Kuball outjes. **Monique**, thank you for your help arranging meeting with Jurgen and also other administrative work you done during my PhD. **Froso** my twin in pulling Dr. Zsolt's leg, you are always helpful whenever I have questions no matter how busy your day was. Hope we can keep in touch outside of work for some drinks and chitchat. Congrats again for your recent wedding and keep loving each other every day. I hope you enjoy the new job also! **Tineke** thanks for always helping every time I have (stupid) questions, what would the Kuball group do without you! **Astrid**, it's nice working together with you for and also our ranting sessions together and all the best for the remaining of your PhD! **Eline**, my buddy since Day 1, I will always remember all the frustration we had to make GABs model works and we still need celebration now it's working! All the best for the thesis and the next chapter of your career. Do keep in touch! **Angelo**, the shadow personnel of our mice team, I enjoyed the time we have to do some in vivo experiments together and also the morning

meetings that we both struggle with. Good luck with your PhD and looking forward to more borrels and trips together with the others. Do report yourself to Dr. Zsolt, else he will always look for you! **Mara**, **Lucrezia**, and **Konstantinos**, happy to have you join the group and also get close during the short period I have left. Enjoy your PhD period and I look forward to our mischiefs together ;)

Jeroen and **Pien**, thank you for all the help with FACS setup. I appreciate all the brainstorm session to make our in vivo panel works fine. Hopefully we will cross path again in future.

My office roommates: **Kim**, I enjoyed all our chitchat together that keep me sane during busy period. **Ingrid**, another PhD buddy, thanks for all the gezelligheid as my next desk partner and to figure stuff together about the PhD program. I look forward for your defense! **Anna**, I enjoyed our dinner out together during the PhD and I wish you all the best for the postdoc position! **All other CTI colleagues**, I may not mention one by one, but thank you for making me feel welcomed and enjoyed my PhD time in the department.

Dear **Elsbeth**, **Saskia**, **Laura**, thank you for all the help and collaboration with all the pathology samples and analysis. I appreciate all the communication, arrangement, and training to accommodate our studies. Dear **Jarno**, **Kai, SangHo, Florijn** and **Heggert**, thank you for the collaboration with some of the projects that we managed to do together and also to facilitate the cells for in vivo experiments.

Dear besties, I could never make it without you all. **Anna**, I always looking forward to all our coffee break/getaway and to listen to all my rambling. Hopefully your thesis will be done soon and you get a position that you enjoy this time. My super smart girl **Lorenita**, thank for all our group therapy sessions ;) even though we are apart but you always checking up on me. My best man **Andrea**, you are way too far sometimes, but always close at heart. Thank you for all the video calls at strange times and hopefully we can see each other again soon! Try to reply our texts promptly! My lovely **Sarita**, I love all the voice notes we sent each other, all the random conversations. I couldn't wait to enjoy some holiday with you again soon and all the best for your PhD! My thanksgiving buddies **Adri**, **Aniko**, **Nik**, **Emilie**, **Marti** and **Ziva**, I always look forward for our fun tradition every year. Although the last couple of years we can't manage to get together, I hope we can get back on track soon! So many places we still need to explore in a short friendsgiving weekend. **Rianne** and **Melissa**, I always love all our dinner and weekend sleepover with all the heart-to-heart conversations we have. Although your calendar usually fully booked, we still have our catchup moments and feels like we talk to each other every day, which were always fun! Hopefully we can hangout more often! I love you, all!

Oom Bing, **Oom Thijs**, **Elske** who supports my journey from the first time I stepped foot in The Netherlands. Thank you for all your input and advise in my career as well as in everyday life. I am happy to have a family here that I know I can count on. **Mama**, **Mia**,

and **all my family members in Jakarta** who always be my motivator to keep going and pursue what I want to do in life and supports me in everything. I love you all.

Dearest **Michael**, no words are enough to show how grateful I am to have you. My personal walking encyclopedia, who helped me win Kuball Pubquiz. You always have my back, always support me when I feel stress about work, always listen to all my frustrations in a calm way, always push me forward and who keep me sane during all the crazy times and never forget to hold my hand in every step of the way. You never failed to bring smile on my face, always. I look forward to our future days together, till we're old, smelly, and senile. I love you, through good fa*** and (unfortunately) also bad ones.

LIST OF PUBLICATIONS

This thesis

1. Johanna I*, Straetemans T*, Heijhuurs S, Aarts-Riemens T, Norell H, Bongiovanni L, *et al*. Evaluating *in vivo* efficacy - toxicity profile of TEG001 in humanized mice xenografts against primary human AML disease and healthy hematopoietic cells. J Immunother Cancer. 2019;7(1):69.

2. Kierkels GJJ*, Scheper W*, Meringa AD*, Johanna I*, Beringer DX, Janssen A, *et al*. Identification of a tumor-specific allo-HLA-restricted gammadeltaTCR. Blood Adv. 2019;3(19):2870-82.

3. Johanna I, Hernández-López P, Heijhuurs S, Bongiovanni L, de Bruin A, Beringer D, *et al*. TEG011 persistence averts extramedullary tumor growth without exerting off-target toxicity against healthy tissues in a humanized HLA-A*24:02 transgenic mice. Journal of leukocyte biology. 2020;107(6):1069-79.

4. Johanna I*, Hernández-López P*, Heijhuurs S, Scheper W, Bongiovanni L, de Bruin A, Beringer DX, *et al*. Adding help to a HLA-A*24:02 tumor-reactive γδTCR increases tumor control. Front. Immunol. 2021; 12:752699.

Others

1. van Gils MJ*, van den Kerkhof TL*, Ozorowski G, Cottrell CA, Sok D, Pauthner M, Pallesen J, de Val N, Yasmeen A, de Taeye SW, Schorcht A, Gumbs S, Johanna I, *et al*. An HIV-1 antibody from an elite neutralizer implicates the fusion peptide as a site of vulnerability. Nat Microbiol. 2016; 2:16199

2. Dekkers JF*, Alieva M, Cleven A, Keramati F, Brazda P, Rebel HG, Wezenaar AKL, Puschhof J, Buchholz M, Román MB, Johanna I, Meringa AD, *et al*. Behavioral-transcriptomic landscape of engineered T cells targeting human cancer organoids. *Manuscript in revision 2021.* Preprint doi: https://doi.org/10.1101/2021.05.05.442764

3. van Diest E*, Hernández-López P*, Meringa AD, Vyborova A, Karaiskaki E, van Dooremalen S, Johanna I, *et al*. Gamma delta TCR Anti-CD3 Bispecific molecules (GABs) as novel immunotherapeutic compounds. J Immunother Cancer. *Manuscript accepted 2021.*

4. Hernández-López P*, van Diest E*, Johanna I, Meringa AD, Heijhuurs S, Karaiskaki E, *et al*. Enhancing the therapeutic potential of γ9δ2TEG cancer targeting through modified NKG2D co-stimulation. *Manuscript in preparation 2021.*

5. Cleven A, Fasci D, Johanna I, Beringer DX, Mizutani T, Lim S, Bernink J, *et al*. BTN3A1-linked novel protein network already present at very early malignant transformation events regulates tumor cell recognition by Vγ9Vδ2 TCR T cells. *Manuscript in preparation 2021.*

* These authors contributed equally

CURRICULUM VITAE

Inez Johanna Gan was born on October 10th 1988 in Jakarta, Indonesia. In 2006 she started with a bachelor's degree in Biology at Atma Jaya Catholic University of Indonesia and graduated at 2010 as top 5% honor student of her class. During her bachelor's program, she obtained work experience as laboratory assistant for practical subjects of basic biochemistry and animal cell culture. Thereafter, she started internship program abroad as research officer at System Biology lab, Genome Institute of Singapore. After this internship, she started working at contract manufacturing facility at Lonza Biologics Tuas Pte Ltd, Singapore where she worked as Validation Specialist for several costumer projects in production active pharmaceutical ingredients (API). She mainly responsible for development, execution and documentation of Cleaning and Autoclaves Qualifications, including supporting site discrepancies and deviations investigation/closure. In this position, she also actively involved in FDA/EMA audits as subject matter expert (SME) for Cleaning and Autoclaves Qualification. In 2014 Inez decided to pursue a master's degree in Infection and Immunity at Universiteit van Amsterdam. Her master's literature thesis titled "The Degree of Off-Target Effects Associated with CRISPR/Cas9 as Gene Editing Tool and the Implications for Future Applications" was written at Netherlands Cancer Institute (NKI) under supervision of Dr. Roderick Beijersbergen. After completing her master's degree, Inez pursued her cancer immunotherapy interest and started her PhD at the Center for Translational Immunology (CTI), Utrecht University Medical Center, under supervision of Prof. Jürgen Kuball and Dr. Zsolt Sebestyén. Here, she focused on development of preclinical mouse model to test efficacy-safety balance of engineered γδTCR-based cellular therapy against cancer. The results of Inez' work are described in this thesis.